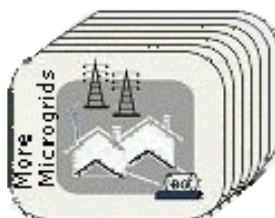




A European Project Supported by the European Commission within the
Sixth Framework Programme for RTD



Advanced Architectures and Control Concepts for More Microgrids

Contract No: SES6-019864

WORK PACKAGE G

**DG3. Report on the technical, social, economic, and
environmental benefits provided by Microgrids on power
system operation**

**Annex 4 – Reliability Impact of DER and Microgrids
on Low Voltage Grids**

December 30th 2009

**Final Version
PUBLIC**

Coordination:	C. Schwaegerl	christine.schwaegerl@siemens.com
Authors:	L. Tao	liang.tao@siemens.com
	C. Schwaegerl	christine.schwaegerl@siemens.com

Content

List of Figures	5
List of Tables.....	7
Abbreviations and Indices.....	9
Executive Summary	10
1 Introduction.....	11
2 Power System Reliability Simulation.....	11
2.1 Power System Reliability.....	11
2.1.1 Introduction to Power System Reliability	11
2.1.2 Methods for Reliability Calculation	13
2.2 Simulation Tool PSS@SINCAL/ZUBER Module.....	15
2.2.1 Program description.....	15
2.2.2 Reliability indices.....	17
2.2.3 Modelling of Failure Events -- Failure Models	18
2.2.4 Modelling of Remedial Measures – Restoration Model	19
2.3 Reliability Calculation for Microgrids supplied by local time-varying micro-sources.....	21
3 Basic Reliability Impact investigated with Conventional Analytical Reliability Analysis.....	21
3.1 Introduction of the Basic Test Network (Base Case).....	21
3.1.1 Reliability Simulation of Simple Network.....	22
3.1.2 Protection Device	27
3.2 Simple Network Analysis – Impact of DG with Constant Operation.....	28
3.2.1 Introduction of Base Case with Micro-source Penetration (Scenario I).....	28
3.2.2 Impact of Micro-source with Constant Operation.....	30
3.3 Simple Network Analysis – Time-dependency of Generation and Load Profiles	45
3.3.1 General Introduction	45
3.3.2 Probability distribution of Fully Supplied Hours	50
3.4 Impact of Single DG Technology	51
3.4.1 Impact of PV (Scenario II).....	51
3.4.2 Impact of WT (Scenario III).....	52
3.4.3 Impact of CHP (Scenario IV)	53
3.4.4 Consideration of Intermittency with reduced DG availability	55
3.4.5 Comparison of Reliability Impact of Different DG Types	56
3.5 Reliability Impact of Demand Side Management.....	58
3.6 Impact of DG Allocation.....	60
3.6.1 General Allocation Options – 100% Penetration Level.....	60
3.6.2 DG is Islanded Operation in Comparison with Grid Connection	61

3.6.3	Summary	63
3.7	Conclusions of Simple Network Analysis	64
4	Analytical reliability analysis directly considering reliability contribution of micro-sources	67
4.1	Stochastic load demand and DG generation modelling.....	67
4.1.1	Decorrelation of interdependent loads and DGs.....	68
4.2	Comparison of net power PDF based on CGCE model and discrete model	71
4.3	Analysis part.....	73
4.3.1	Input of analysis part.....	73
4.3.2	Reliability indices computation	74
4.4	Case Study	80
4.4.1	Italy Rural network	81
4.4.2	German urban LV network.....	84
5	Time Sequential Monte-Carlo Simulation for Reliability Analysis in Networks with Micro-sources	84
5.1	Monte-Carlo Simulation Procedure	85
5.1.1	Step 1: Failure event list generation.....	87
5.1.2	Step 2: Network State Analysis.....	88
5.1.3	Step 3: Load State Analysis	92
5.1.4	Step 4: Restoration and repair process	93
5.2	Case study- Italy rural network.....	94
5.2.1	Convergence progress of system reliability after applying micro-sources	94
5.2.2	Comparison between Monte-Carlo simulation and analytical method.....	95
5.2.3	Comparison of probability distribution of reliability indices	97
5.3	Battery Modelling.....	98
5.3.1	Battery charging and discharging modelling.....	98
5.3.2	Battery impact on reliability performance	100
5.4	Impact of Microgrid Control on Reliability.....	104
5.5	Comparison of Sequential Monte-Carlo Simulation and Analytical Method	104
6	Optimum micro-source planning strategy considering their impact on reliability	105
6.1	Optimum micro-source planning strategy for technical reliability improvement	105
6.1.1	Micro-source location.....	105
6.1.2	Micro-source operation.....	110
6.2	Optimal planning strategy considering economic benefit	111
6.2.1	Economic benefit model of micro-sources	112
6.2.2	German LV network optimisation.....	113
6.3	Optimum battery planning strategy	119

6.4	Conclusions.....	122
7	European Network Simulation.....	122
7.1	German urban LV network.....	123
7.2	Italy rural network.....	123
7.3	Italy urban network.....	124
7.4	Portugal urban network.....	128
7.5	Portugal rural network.....	131
7.6	The Netherlands network.....	134
7.7	Germany MV network.....	135
7.8	Comparison of simulation results on European Level.....	136
	References.....	139
	Appendix.....	143
A.1	General Scenario Overview.....	143
A.2	Homogeneous Markov Process.....	144
	A2.1 General Description.....	144
	A3.2 Consideration of Microsource Availability.....	145
A.3	Node Result and Network Result of Simple Network.....	147
A.4	Probability Distributions of Reliability Indices.....	149
	A4.1 General Description.....	149
	A4.1 Poisson Distribution for Frequency of Supply Interruptions.....	150
	A4.2 Weibull Distribution of Other Indices.....	150
A.5	Capacity Factor and Availability Factor.....	153
A.6	Probability Distribution of Power Balance Provided by DG.....	154
	A6.1 Power Balance of Different Loads and Generation Units.....	154
	A6.2 Theory of Probability Distributions.....	154
	A6.3 Probability Distributions with Power Limits.....	156
	A6.4 Calculation with Normal Distribution.....	157
	A 6.5 Calculation with Adapted Normal Distribution.....	159
	A6.6 Calculation the Power Balance by Convolution of Probability Functions.....	160
	A6.7 Comparison of the Variants.....	162
	A6.8 Application for Calculation of Fully Supplied Hours.....	163
A.7	Gram-Charlier expansion.....	168
A.8	Load settings for European network simulation.....	170
	A8.1 Load setting of German urban LV network.....	170
	A8.2 Load setting of Italian urban LV network.....	171
	A8.3 Settings of Italian rural network.....	172
	A8.4 Setting of Portuguese rural network.....	172
	A8.4 Settings of the Netherlands rural network.....	172
	A8.4 Settings of German MV network.....	173

List of Figures

Figure 2-1 Cost Optimum for Reliability	12
Figure 2-2 Heterogeneous Power Quality and Reliability [5]	12
Figure 2-3 Schematic Sequence of a Probabilistic Reliability Analysis [11].....	14
Figure 2-4 Flow Chart Reliability Calculation	14
Figure 2-5 Structure of the ZUBER Module	16
Figure 2-6 Independent Single Failure of Line L2	18
Figure 2-7 Temporal Sequence of Fault Recovery	20
Figure 3-1 Basic Test Network without any DG Units (<i>Base Case</i>)	21
Figure 3-2 Load Modelling Approaches of Testing and Household Load	23
Figure 3-3 Network Reliability Comparison by Different Load Modelling	24
Figure 3-4 Poisson distribution of frequency of supply interruption of the Simple Network ..	26
Figure 3-5 Weibull Distribution of Other Reliability Indices of the Simple Network	27
Figure 3-6 Base Case: Simple Network with one DG unit (<i>Scenario I</i>)	28
Figure 3-7 Power allocation models.....	29
Figure 3-8 Load ADC for the Impact of Penetration Level (four durations).....	31
Figure 3-9 Frequency of supply interruption depending on DG Penetration without LP	31
Figure 3-10 Unavailability depending on DG Penetration without LP	32
Figure 3-11 Frequency of supply interruption depending on DG Penetration with LP	33
Figure 3-12 Unavailability depending on DG Penetration with LP	34
Figure 3-13 Interrupted Power in Pessimistic Mode	35
Figure 3-14 Network Interrupted Power depending on Power Allocation Mode	36
Figure 3-15 Probability Distributions depending on DG Penetration (Pessimistic Mode)	38
Figure 3-16 Reliability Indices with Different Numbers of DG Units.....	40
Figure 3-17 Reliability Indices depending on Different DG Location.....	41
Figure 3-18 Two state DG model	43
Figure 3-19 Reliability Indices depending on DG reliability.....	44
Figure 3-20 Hourly Household Load and PV Generation Profiles.....	47
Figure 3-21 ADC of PV and the Household Load	47
Figure 3-22 Hourly Household Load and WT Generation Profiles.....	48
Figure 3-23 ADC of WT and the Household Load	48
Figure 3-24 Hourly Household Load and CHP Generation Profiles.....	49
Figure 3-25 ADC of CHP and the Household Load	49
Figure 3-26 Probability of Power Balance $p_L - p_G$ (DER with Household Load)	50
Figure 3-27 Input load ADC for PVs Option (Scenario II)	51
Figure 3-28 Input load ADC for WT Option (Scenario III)	52
Figure 3-29 Input load ADC for CHP Option (Scenario IV)	54
Figure 3-30 Reliability Comparison Concerning Different Simulation Modes	56
Figure 3-31 Reliability Indices depending on Different DG Types	57
Figure 3-32 Reliability Improvement by Each DG Option Concerning Different Indices	58
Figure 3-33 Load ADC of Scenario III and Scenario LM.....	59
Figure 3-34 Reliability Comparison between Scenario III and Scenario LM	59
Figure 3-35 ADC of Household Industry and Commercial Load Profile.....	60
Figure 3-36 Probability of DG Fully Supplying Loads by Different Penetration Level	63
Figure 3-37 Recommendations for Reliability Improvement	66
Figure 4-1 Correlation coefficient of German loads and various micro-sources	68
Figure 4-2 PV output power and load demand variation.....	68
Figure 4-3 Covariance coefficients of DGs and Load	71
Figure 4-4 Different orders CGCE and real curve comparison	73
Figure 4-5 PDF of adapted and original CHP unit.....	76
Figure 4-6 Comparison of discrete model and adapted model	76
Figure 4-7 Italy rural network topology.....	80
Figure 4-8 German urban LV network topology	81
Figure 4-9 Simulation result of scenario 2100-2105	82

Figure 4-10 Impact of DG unavailability on network reliability	83
Figure 4-11 Simulation result of German urban LV scenario 2400-2405	84
Figure 5-1 Flow chart of time-sequential Monte-Carlo simulation	86
Figure 5-2 Terminal positions in the network	89
Figure 5-3 Islanding topology of Italy rural network	91
Figure 5-4 Flow chart of restoration process	93
Figure 5-5 Convergence process of system reliability	95
Figure 5-6 Reliability indices comparison for CHP scenario	95
Figure 5-7 System reliability indices comparison for WT scenario	96
Figure 5-8 System reliability indices comparison of scenario 4120	96
Figure 5-9 Cumulative distribution function (CDF) for Italian rural network with CHP penetration	97
Figure 5-10 Probability density function (PDF) for Italian rural network with CHP penetration	98
Figure 5-11 Operation state of battery	100
Figure 5-12 Location of battery storage in Italian rural network	101
Figure 5-13 PDF system reliability improvement by battery	101
Figure 5-14 CDF System reliability improvement by battery	102
Figure 5-15 CDF System reliability indices with battery and different micro-sources	103
Figure 5-16 Comparison of micro-source technology impact on reliability	103
Figure 5-17 Battery storage capacity influence to system reliability	103
Figure 5-18 Battery storage capacity influence to system reliability	104
Figure 5-19 Probability distribution of technology dependent reliability indices	104
Figure 6-1 Reliability depending on CHP location neglecting HV and MV influence	106
Figure 6-2 Reliability depending on CHP location considering HV and MV influence	106
Figure 6-3 Reliability depending on number of micro-sources neglecting HV/ MV influence	107
Figure 6-4 Reliability depending on number of micro-sources considering HV and MV influence	108
Figure 6-5 Reliability depending on load size neglecting MV and HV influence	109
Figure 6-6 Reliability depending on load size considering MV and HV influence	109
Figure 6-7 Interruption costs depending on location of CHP units close to loads with different priority	110
Figure 6-8 CHP reliability indices improvement with the increase of CHP penetration level	111
Figure 6-9 Simplified topology of German LV network	114
Figure 6-10 Impact on economic cost regarding DG unit and reliability	115
Figure 6-11 Economic cost regarding DG unit and reliability in case of maximum outage costs	116
Figure 6-12 Economic cost regarding DG unit and reliability in case of minimum outage costs	117
Figure 6-13 Economic benefit depending on outage costs	117
Figure 6-14 Optimised DG penetration based on maximal DG rated power per unit	118
Figure 6-15 Cost impact of micro-source availability with average outage cost model	119
Figure 6-16 System reliability indices regarding CHP capacity and battery capacity	120
Figure 6-17 System reliability indices regarding WT capacity and battery capacity	121
Figure 6-18 System reliability indices regarding PV capacity and battery capacity	121
Figure 7-1 Italy urban network topology	124
Figure 7-2 Economic cost regarding reliability	127
Figure 7-3 Economic cost of scenario regarding unavailability	127
Figure 7-4 Portugal urban network	128
Figure 7-5 Economic cost of Portugal urban network after DG penetration with different cost models	130
Figure 7-6 Portugal rural network topology	131

Figure 7-7 Economic cost of Portugal rural network after DG penetration with different cost model	133
Figure 7-8 Holland network topology	134
Figure 7-9 German MV network topology	135
Figure 7-10 Economic benefit comparison of Microgrids on European Level.....	136
Figure 7-11 System unavailability comparison of different countries	137
Figure 7-12 Optimised penetration level regarding interruption frequency without micro-sources.....	138
Figure A-1 State Transition Diagram.....	145
Figure A-2 Poisson Distribution of Frequency of Supply Interruption	150
Figure A-3 Weibull Distribution of Unavailability (min/a)	151
Figure A-4 Weibull Distribution of Interrupted Power (MVA/a).....	152
Figure A-5 Weibull Distribution of Energy Not Supplied (MVAh/a)	152
Figure A-6 Probability Distributions of Normalized Generation and Load.....	154
Figure A-7 Distribution of Step Function	155
Figure A-8 Probability Density and Probability Function with Given Power Limits.....	157
Figure A-9 Comparison of Truncated and Adapted Normal Distribution.....	160
Figure A-10 Example for Limited Power Distribution	162
Figure A-11 Comparison of Probability Density Functions.....	163
Figure A-12 Comparison of Probability Functions.....	163
Figure A-13 Comparison of Probability Functions of Generation.....	164
Figure A-14 Comparison of Probability Functions of Load.....	164
Figure A-15 Truncated and Adapted Normal Distribution for Commercial Load.....	165
Figure A-16 Truncated and Adapted Normal Distribution for WT Generation.....	165
Figure A-17 Truncated and Adapted Normal Distribution for PV Generation	165
Figure A-18 Distributions of Power Balance between PV/WT and Household	167
Figure A-19 Distributions of Power Balance between CHP and Household.....	167

List of Tables

Table 2-1 Reliability Indices in ZUBER	17
Table 2-2 Component Reliability Input Data Used in Test Simple Network.....	19
Table 3-1 Input Data of 2 States Load Modelling in PSS TM SINCAL.....	23
Table 3-2 Reliability Indices of the Base Case T	24
Table 3-3 Indices Comparison of Base Case T and Scenario I -T.....	29
Table 3-4 Power range for reliability improvements.....	32
Table 3-5 Indices depending on PL without LP (Pessimistic Mode)	38
Table 3-6 Indices depending on PL with LP (Pessimistic Mode)	38
Table 3-7 Indices depending on number of DG Units.....	40
Table 3-8 Indices Comparison by Different DG Location.....	42
Table 3-9 DG Reliability Input Data with constant failure rate.....	43
Table 3-10 DG Reliability Input Data with constant down time	44
Table 3-11 Indices Comparison Concerning DG Availability	45
Table 3-12 Reliability Indices of PV Option.....	52
Table 3-13 Network Indices Comparison between PV Option and Base Case H.....	52
Table 3-14 Reliability Indices of WT Option	53
Table 3-15 Indices Comparison between WT Option and Base Case H	53
Table 3-16 Reliability Indices of CHP Option (100 % available)	54
Table 3-17 Reliability Indices of CHP Option (90% available)	55
Table 3-18 Indices Comparison between CHP Option and Base Case H	55
Table 3-19 Input data of highly unavailable DG Units.....	55
Table 3-20 Reliability Improvement by different DG Options, Base Case H and Scenario I-H	57
Table 3-21 Maximum Possible Fully Supplied Hours of DG Options.....	61

Table 3-22 Equivalent Reliability Contribution between DG Island Mode and Grid Connection	62
Table 4-1 Load setting of a example to demonstrate indices computation by SAM	74
Table 4-2 DG settings of an example to demonstrate indices computation by SAM	74
Table 4-3 Reliability setting of LV.....	81
Table 4-4 Scenario 2100-2105.....	82
Table 5-1 Terminal information required for Monte-Carlo simulation	89
Table 5-2 Infeeder information required for Monte-Carlo simulation.....	89
Table 5-3 Busbar information required for Monte-Carlo simulation	90
Table 5-4 Line information required for Monte-Carlo simulation	90
Table 5-5 Transformer information required for Monte-Carlo simulation	90
Table 5-6 Load information required for Monte-Carlo simulation	90
Table 5-7 Island categorization for network topology analysis.....	91
Table 5-8 Comparison of Monte-Carlo method and analytical method.....	105
Table 6-1 Interruption cost of different types of load.....	109
Table 6-2 Specific control unit cost	113
Table 6-3 DG setting of scenarios for German LV network	115
Table 6-4 Economic cost in case of maximum outage costs	116
Table 6-5 Economic cost in case of minimum outage costs	117
Table 6-6 Optimised DG penetration based on maximum DG output power.....	118
Table 7-1 HV and MV Reliability setting of European network	122
Table 7-2 Italy rural network reliability indices of different DG penetration	123
Table 7-3 Simulation result with average outage costs.....	123
Table 7-4 Simulation result with maximum outage costs	123
Table 7-5 Simulation result with minimum	124
Table 7-6 Optimised DG penetration of Italy rural network considering economic benefit .	124
Table 7-7 Italy network reliability indices of different DG penetration	125
Table 7-8 Simulation result with maximum outage cost model	125
Table 7-9 Simulation result with minimum cost model.....	126
Table 7-10 Simulation result with average cost model.....	126
Table 7-11 Optimised DG penetration of Italy rural network considering economic benefit	128
Table 7-12 Technical optimised result of Portugal urban network	128
Table 7-13 Simulation result with average cost model.....	129
Table 7-14 Simulation result with maximum cost model.....	129
Table 7-15 Simulation result with minimum cost model.....	129
Table 7-16 Optimised DG penetration of Portugal urban network considering economic benefit	130
Table 7-17 Portugal rural network reliability indices of different DG penetration	131
Table 7-18 Simulation result for average outage cost model.....	132
Table 7-19 Simulation result for maximum cost model	132
Table 7-20 Simulation result for minimum cost model	132
Table 7-21 Optimised DG penetration of Portugal rural network considering economic benefit	133
Table 7-22 Holland network reliability indices of different DG penetration.....	134
Table 7-23 Reliability indices for average cost model.....	134
Table 7-24 Reliability indices for maximum cost model	134
Table 7-25 Reliability indices for minimum cost model	134
Table 7-26 Simulation result of scenario 6700 and 6701	136
Table A -1 Descriptions of Scenarios analysed in this report.....	143
Table A-2 Failure Combinations of Multiple Faults	147
Table A-3 Failure Combinations in the Original Simple Network	147
Table A-4 Power Limits of Load and DER Generation Profiles.....	164
Table A-5 Distribution Parameters from Different Methods (WT Option).....	166
Table A-6 Distribution Parameters from Different Methods (PV Option).....	166
Table A-7 Distribution Parameters from Different Methods (CHP Option).....	166

Abbreviations and Indices

ADC	Annual Duration Curve
AGC	Annual Generation Curve
ALC	Annual Load Curve
ASAI	Average System Availability Index
C	Cost
CAIDI	Customer Average Interruption Duration Index
CB	Circuit Breakers
CDF	Cumulative Density Function
CGCE	Combined Gram-Charlier and Cumulant Expansion
CHP	Combined Heat and Power
CIREED	Congrès International des Réseaux Electriques de Distribution
DER	Distributed Energy Resource
DG	Distributed Generator
EPRI	Electric Power Research Institute
EU	European Union
GHG	Green House Gas
Hu	Interruption Frequency
HV	High Voltage
ISF	Independent Single Failure
LF	Load Factor
LP	Load Priority
LV	Low Voltage
MV	Medium Voltage
NERC	North American Electric Reliability Council
PDF	Probability Density Function
PL	Penetration Level
PQR	Power Quality and Reliability
Pu	Interrupted Power
PV	Photovoltaic
Qu	Unavailability
RES	Renewable Energy Sources
SAIDI	System Average Interruption Duration Index
SAIFI	System Average Interruption Frequency Index
SAM	Stochastic Analytical Method
SINCAL	SIEMENS Network Calculations
UPO	Unnecessary Protection Operation
WT	Wind Turbine
Wu	Interrupted Energy

Executive Summary

This Annex provides an evaluation of reliability contribution of different micro-sources such as intermittent renewable and dispersed generation units.

New stochastic evaluation tools have been required that take into account the limited time-varying availability of these units. Different calculation methods based on analytical method and on Monte-Carlo simulation have been developed and are presented in this Annex. While the analytical method is faster, the simulation of battery behaviour is only possible with Monte-Carlo-simulation. Monte-Carlo provides quasi accurate results with and without micro-sources. By nature of this method also probability distributions of the reliability indices can be calculated. The analytical method produces errors due to micro-source modelling with PDF.

The Microgrid approach allows operation of a local MV or LV supply area with different micro-sources such as generation and storage units also in islanded mode in case of failures in upstream network.

An improvement of the reliability of supply is possible also with dispersed generation (DG) such as CHP units that are normally operated in a heat driven mode as well as by intermittent renewable generation units. Economic benefits from reliability improvement under Microgrid operation were evaluated on regional, national and European level.

In general, intermittency of generation needs to be considered, otherwise the results are too good. Renewable and non-controllable generation units contribute to reliability only if their intermittent output power is higher than simultaneous demand. The reliability improvement increases with increasing full load generation hours of DG (highest for CHP, lowest for PV with $PV < WT < CHP < \text{Controlled CHP}$ (from heat-driven to electricity-driven mode)

Additionally to the impact of intermittency the DG availability itself needs to be considered. Battery storage units increase reliability indices up to certain value.

There is a linear correlation between DG availability and overall reliability. Examples for the impact of a battery and of Microgrid control on reliability improvement are given.

Economic benefits due to Microgrid operation concerning reliability strongly increase with increasing customer outage costs; especially for commercial and industrial customer segments. There are minimum total reliability costs when interruption cost and investment cost arrive at an optimized reliability index.

An immediate transition to island mode mainly improves frequency dependent reliability indices

The optimum DG penetration level (installed capacity compared to maximum load) to achieve highest reliability improvement depends on system interruption frequency before DG penetration. The optimum level increases with raising interruption costs.

1 Introduction

One of the important technical benefits of Microgrids operation is the possibility to enhance reliability locally due to the islanding possibility.

Renewable generation units only contribute to reliability if the intermittent output power is higher than the simultaneous load demand. This topic is normally not taken into account and thus not covered in literature so far; evaluations are normally done with fixed operating point of the micro-generation. This Annex aims therefore to study also scenarios considering the synergy of time-dependent load profile and intermittent generation profiles and then to compare the results between these generation modelling approaches.

2 Power System Reliability Simulation

2.1 Power System Reliability

2.1.1 Introduction to Power System Reliability

The function of an electrical power system is to provide electricity through the transmission and distribution network with maximum efficiency to consumers at acceptable voltages, frequency and reliability. The term of reliability has a broad meaning. A useful definition that illustrates the different dimensions of the reliability concept is:

Reliability is the probability of a device or system performing its function adequately, for the period of time intended, under the operating conditions intended [1].

A reasonable subdivision of reliability can be presented as two basic aspects of a power system: *system adequacy* and *system security* [2].

- *System adequacy* relates to sufficiency in providing electricity to customers which includes sufficient generating capacity, transmission and distribution systems. This concept only considers static systems conditions which do not consider any disturbances that can cause insufficient energy supply to customers.
- *System security* relates to the ability of the system to sustain any disturbances within the system. It can be associated with the dynamic response of the system to whatever perturbation it is subjected to.

Power system reliability evaluation put the primary emphasis on the optimization of the balance between economic and reliability constrains (see Figure 2-1). The utilities have to minimise the operating costs as much as possible, and at the same time sustain the acceptable system quality. The resulting economic and reliability impacts can lead to difficult management decisions in both the planning and operating phases [4].

Since the deregulation and liberalization of the electricity market, the reliability, which is directly seen by end-customers, becomes a more critical issue in competition. For example, a sustained interruption can cost certain customers hundreds of thousands of dollars per hour. Even a momentary interruption can cause computer systems to crash and industrial processes

to be ruined [3]. The homogeneous quality of service (Figure 2-1) in distribution network is replaced progressively by heterogeneous reliability service (Figure 2-2). Up to now, still little analysis and data collection has been done to configure the parameter of the pyramid, as well as the consequences of disaggregating the loads on various groups of varying power quality and reliability (PQR) and the corresponding costs caused by varying PQR requirements are poorly understood currently [5]. It is necessary to develop new system planning approaches which allow a more differentiated analysis and assessment of required network configurations.

Figure 2-1 conceptually shows the qualitative relationship between homogeneous power quality and reliability and the costs with a range of minimum total social costs. With increasing requirements of PQR, invest costs could be potentially increased consequently. Power quality consists of service quality, supply reliability and voltage quality. Costs comprise two components: the costs of providing reliability and the costs of residual unreliability.

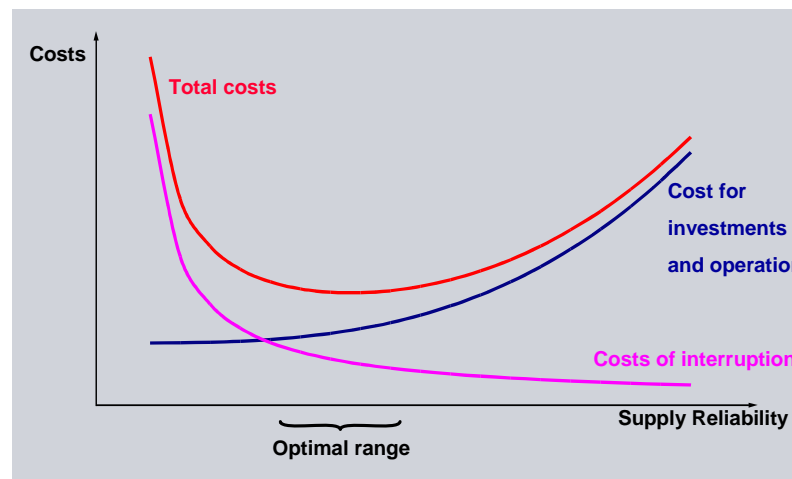


Figure 2-1 Cost Optimum for Reliability

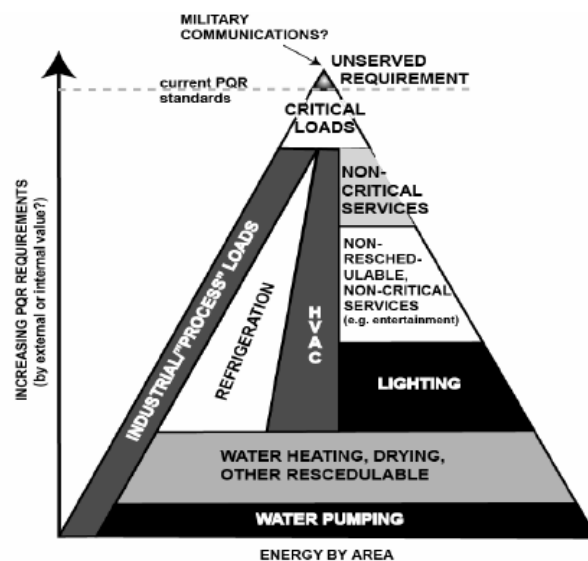


Figure 2-2 Heterogeneous Power Quality and Reliability [5]

1.1.2 Methods for Reliability Calculation

Most popular used strategies to evaluate power system reliability are the 'N-1 criterion' or probabilistic methods.

N-1 criterion means that the outage of any single contingency will not cause any system limitation. The well-known N-1 criterion provides a rapid overview of the whole system reliability and has been widely used in the system planning. It is especially apt for the fundamental qualitative evaluation of the whole system reliability. However, with this method it is not possible to quantify the system reliability; therefore comparison of different N-1 strategies is not possible. Additionally single system operation component reliability is not considered in the evaluation and the evaluation of detailed failure modes of the system is not possible with this method.

Probabilistic methods quantify the future system reliability based on the past observed component reliability data. These methods allow all failure modes and system states to be generated and evaluated automatically with component statistic reliability parameters. It provides concrete system reliability information. Probabilistic methods can provide quantifiable values to customers and more meaningful information to be used in design and resource in planning and allocation. Two techniques - analytical method and Monte-Carlo simulation – can be distinguished.

Analytical Method

The analytical Method represents the system by a mathematical model and evaluates the reliability indices from this model using direct numerical solutions. It mainly provides the expected value of final evaluation indices. The advantage of this method is the fast computation speed and accurate evaluation result when the evaluated system is not too complex. This method is already applied to power system reliability analysis successfully [30], [31], [32]. However, when the complexity of power system increases, assumptions, that may cause errors, are required to produce a mathematical model. Another disadvantage of the analytical method is that it can not reflect time-dependent models, such as stochastic load demand, power generation and maintenance process.

The *homogeneous Markov Process* is one of the most widely used analytical methods for stochastic system description and simulation. It can describe the random behaviour of a system that can reach different states over time. There are two prerequisites for this method:

- transition rates constant with time;
- ‘‘memory less’’ distribution [17].

Markov Process uses the complete mapping for every state change, and generates the transition matrix quantified with the precise transition rates. Then the frequency of occurrence and the probability of each component, which will be summated to determine the system reliability afterwards, are calculated by expression of steady state frequency and probability. However, Markov Processes are unable to describe a system subject to changes and modernization. After each network modification it is necessary to repeat states mapping and transition rates quantification [16].

Monte-Carlo Simulation

The Monte-Carlo Simulation method estimates the reliability indices by simulating the actual operation process and random behaviour of the system. A simplification is not required and it is able to simulate all contingencies and aspects inherent of the planning system.

Two basic techniques are utilized in Monte-Carlo applications to power system reliability evaluation. These are known as the sequential and non-sequential method. In the non-sequential method [33], the states of all components are sampled and a non-chronological system state is obtained. In the sequential approach [34], [35], [36], the up and down cycles of all components are simulated and a system operating cycle is obtained by combining all the components cycles. Chronological issues of system operation are taken into account by sequential Monte-Carlo simulation and probability distribution of reliability indices can be calculated. However this method requires large computation times [37].

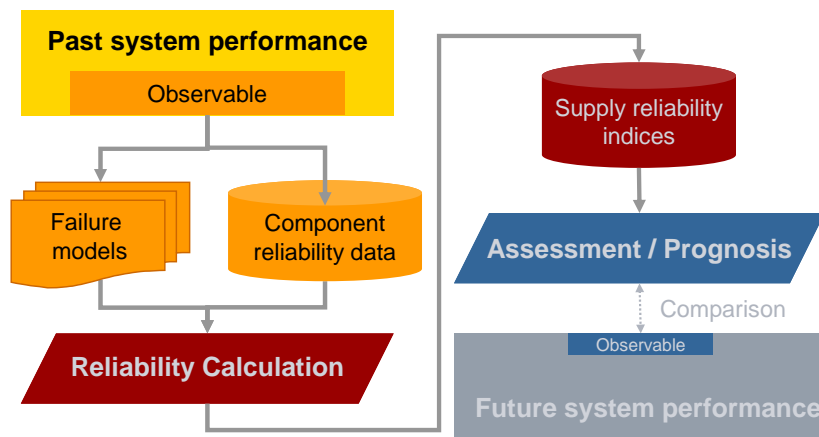


Figure 2-3 Schematic Sequence of a Probabilistic Reliability Analysis [11]

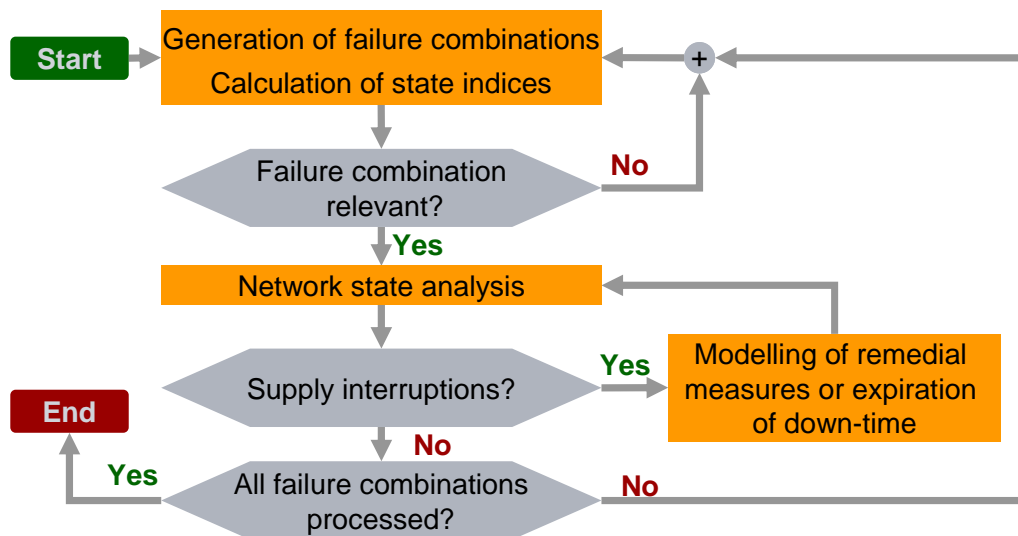


Figure 2-4 Flow Chart Reliability Calculation

Monte Carlo simulation estimates reliability indices by simulating the actual random behaviour of the system. Starting with an originating state, points in time for failure events and restoration of failed elements are determined out of the distributions of up-times and down-times caused by failures with the help of random numbers [12].

The advantage of Monte Carlo simulation is that any distribution function for the component reliability data can be considered. Thus, apart from the expected or average values of reliability indices which the analytical method can provide, the distribution functions of the calculated reliability indices can also be specified. The disadvantage of the simulative method is the high computation time required as each event is separately calculated. Another problem of the simulative approach is to determine the error with which the results are always afflicted [12].

1.2 Simulation Tool PSS®SINCAL/ZUBER Module

1.2.1 Program description

PSS®SINCAL (SIEMENS Network Calculations) is a family of calculation programs for electricity and flow networks. With a graphical user interface and an appropriate database, the program provides direct-viewing planning structures and simulation results. A number of modules, such as load flow, motor starting, harmonics, ripple control, distance protection, stability, reliability, etc, are included in PSS™SINCAL calculation and evaluation programs.

ZUBER is the module for reliability simulation, which can be used for any network structure and voltage level. It applies the analytic approach (homogeneous Markov process) to run the simulation, with which each contingency state is calculated only once for the main advantage of shorter computation time. And the calculated probabilistic indices represent the expected value, which only present the average performance of the network under the observation of certain infinite time period (normally the period defaulted in ZUBER module is an annual year), even without probability distributions. Consequently, the forecast uncertainty is inevitable as it is caused by stochastic properties of the process (like e.g. various nature characteristic and third-part damage in different periods), and not related to any approximations or errors in calculation or input data. Nevertheless, both the expected value and variance of each index (except interruption cost and reimbursements) can be given by ZUBER [11], which are the basic parameters for modelling the distribution functions by using analytical method.

Based on network data and appropriate reliability setting, possible failure combinations within the framework of reliability calculation are generated as well as the subsequent state analysis is performed by homogeneous Markov process. Then the responsible component failure combinations are selected to analyze the contribution to either system or nodes, and the related failure combinations are summated to form the final results, which are shown in ZUBER results files. This is the analysis part of the program. The main structure of ZUBER module is shown in Figure 2-5.

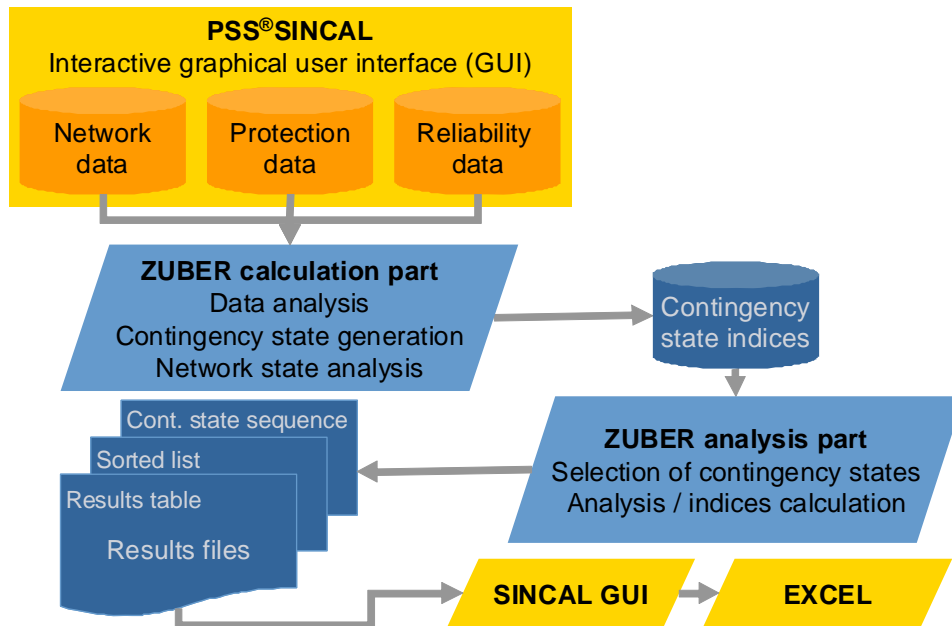


Figure 2-5 Structure of the ZUBER Module

Two separate parts of ZUBER make the structure clearer and the evaluation easier. The calculation part creates component failure combinations and models their sequence until the normal supply, while the analytic part assesses the results of calculation part in detail. The calculation will take quite amount of time but it is normally done once for each reliability analysis and the results are stored in ZUBER database, which can be analyzed in different ways in short time to save computation time.

There are three different result lists provided by the analysis part:

- (1) Results Table: The selected failure combinations are accumulated to each load node, and then the reliability indices are given to both the separate customers and the complete power system respectively. In this table, the weak points of the system can be identified.
- (2) Listed Sequence of Individual Component Failure Combinations: The selected component failure combinations by chosen criteria are listed in detail temporal sequence. Both failure-affected equipments and elements in the same tripping area, which are disconnected commonly, are specified. Besides, the indices can be differentiated according to the separate failure models. Furthermore, the supply restrictions and afterwards the remedial measures such as switching operations are also listed.
- (3) Sorted List: The failure combinations are listed sorted according to a fixed reliability index, which declared in the control parameters. It is important to analyze the main reason of supply interruptions as easy-identification of the failure combinations which have the greatest effect on the supply reliability.

1.2.2 Reliability indices

To analyze the results, ZUBER uses several reliability indices to show quantifiable values, corresponding to the standard reliability indices. Generally, the reliability can not be sufficiently represented by any single index; it is a combined view of different aspects to evaluate the reliability. Table 2-1 is an overview of the basic indices provided by ZUBER.

Symbol	Name	Unit
H_u	Frequency of supply interruptions, also known as	1/a
T_u	Mean duration of supply interruptions	h or min
Q_u	Unavailability/Probability of supply interruption	1 (common: min/a)
P_u	(Cumulated) interrupted power	MVA/a
W_u	(Cumulated) energy not supplied in time	MVAh/a

Table 2-1 Reliability Indices in ZUBER

- H_u describes the number of interruptions under the period considered. This index contains no information on the effect or the duration of an interruption.
- T_u specifies the mean time span ranging from the start to the end of a supply interruption on a load node or the system respectively. A supply interruption is eliminated as soon as the undersupplied load can be fully re-supplied by means of switching operations, etc.
- Q_u describes the possibility of power system or a single load node which is in the state of supply interruption on a randomly given point in time. It is the product of H_u and T_u , without unit. For better representation, it commonly uses the unit min/a.
- P_u indicates the sum of interrupted power under considered period. The interrupted power depends on H_u and the sum of interrupted power of each affected load, but independent from T_u . And it gives an indication on the magnitude of the interruption.
- W_u is the sum of the energy that can not be delivered to a load or to all the loads in a system in the period under consideration, related to the period under consideration. In addition to the influence coefficients listed above for the interrupted power, the energy not supplied also depends on the duration of the interruption.

These indices correspond to the following well known system indices, defined by IEEE:

- System Average Interruption Duration Index (SAIFI), corresponding to H

$$SAIFI = \frac{\text{Total Number of Customer Interruptions}}{\text{Total Number of Customer Served}}$$

- System Average Interruption Duration Index (SAIDI), corresponding to Q

$$SAIDI = \frac{\sum \text{Customer Interruption Durations}}{\text{Total Number of Customer Served}}$$

- Customer Average Interruption Duration Index (CAIDI), corresponding to T

$$CAIDI = \frac{\sum \text{Customer Interruption Durations}}{\text{Total Number of Customer Interruption}}$$

In contrast of SAIDI, SAIFI and CAIDI system reliability indices SCIFI, SCIEI, SCICI are system cumulative values to evaluate the system power loss, energy loss as well as interruption cost during failure period

- System cumulative interruption power index (SCIFI), corresponding to P_u

$$SCIFI = \sum \text{Customer Interruption Power}$$

- System cumulative interruption energy index (SCIEI), corresponding to W_u

$$SCIEI = \sum \text{Customer Interruption Energy}$$

- System cumulative interruption cost index (SCICI)

$$SCICI = k_p * SCIFI + k_w * SCIEI$$

where k_p is power specific cost and k_w is energy specific cost.

1.2.3 Modelling of Failure Events -- Failure Models

To analyze the system reliability, it is important to model the failures occurring in power system operation as precise as possible.

Independent Single Failure

It is the failure of one unique component which is independent from any other incident or failure that may occur at the same time. An example is shown in Figure 2-6. The Line L2 is disconnected due to the protection devices tripping after a failure detected. No other disconnection occurs by this event. The failure rate and down time of independent single failure can be declared by H_u and T_u .

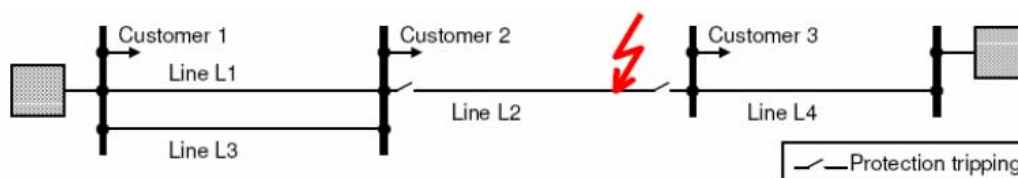


Figure 2-6 Independent Single Failure of Line L2

Independent single failures may be overlapping. But each failure that overlapped is a stochastic case without any casual relationship between them, although they happen at the same time.

It is the most important failure model that is considered in this report as most significant failure combinations are caused by it.

Unnecessary Protection Operation of Multiple Outages

It occurs only as a succeeding failure within the scope of an extension of the primary incident – independent single failure - due to unnecessary disconnecting further protection area in contrary to the normal protection concept. The down time is the reconnection time of the unnecessary disconnected elements.

The component reliability input data of different failure models is summarized in Table 2-2.

Failure model	Network Component	$H (1/a^*)$	$T (h)$	p^{**}
Independent Single Failure (ISF)	Cable	0,0189	15	
	Distribution Substation	0,006	6,5	
	Primary Substation	0,0052	5,5	
	Busbar-side Switchbay	0,0001	3,2	
	Switchbay for Finishing	0,0002	3,2	
Unnecessary Protection Operation (UPO)			0,5	0,0049

* in $1/(km a)$ for overhead lines and cables

H Frequency of occurrence/failure rate

** in $1/km$ for overhead lines and cables

T Down time

p Conditional probability

Table 2-2 Component Reliability Input Data Used in Test Simple Network

Modelling of further failures

There are much more failure models known for simulation of transmission network reliability which can affect the system and cause its deficit. Main scope of this report is low voltage levels and thus fuses are applied for the protection devices. Consequently, some of the failure models are not necessary to take into account while considering the reliability simulation. For example, malfunction of protection device probably does not happen due to the characteristic of the fuses applied in distribution networks; multiple earth faults are practically not in existence as the low voltage system is normally isolated or directly earthed, etc. Therefore, only independent single failure and unnecessary protection operation are considered here. It is assumed that unnecessary protection operation can be neglected due to the minor effect to reliability results as generally independent single failure takes the most part of the results

1.2.4 Modelling of Remedial Measures – Restoration Model

The reliability component index T (down time) is the provisional time for repair or replacement of that defected equipment unit, which is the internal characteristic of the components and independent from the network structures. However, the reliability index T_u (mean duration of supply interruptions) is mainly dependent on the remedial measures, which can possibly reduce or eliminate the interruptions before the failed element is repaired and reconnected. Also the index W_u is strongly dependent on these remedial measures.

These measures are classified into two parameters:

- Quasi-continuous parameters e.g. include:
 - Control of the power flow by transformer taps,
 - Alteration of the reactive and active power injection of power stations
- Discrete parameters
 - Connection of circuits disconnected in normal operation state,
 - Coupling with neighbouring system areas,
 - Coupling of multiple busbars disconnected in normal operation state,
 - Unlocking of failure affected elements and reconnection of intact elements of disconnected protection tripping areas,
 - Bus transfer,
 - Start-up of injection units,
 - Connection after maintenance abort,
 - Load relocation.

Switching operations are conducted in the sequence of the state analysis. In case that a supply interruption on one or several load nodes is detected, the program chooses the switching operation leading to partial or complete restoration of supply. If several switching operations are necessary, the program proceeds chronologically. Additionally, the sequence of the switching operations is influenced by the respective priority of switching operations. The switching duration can be given individually for each operation. Switching operations are mostly more effective than quasi-continuous measures.

The action of the system management in the fault recovery can be schematized according to Figure 2-7.

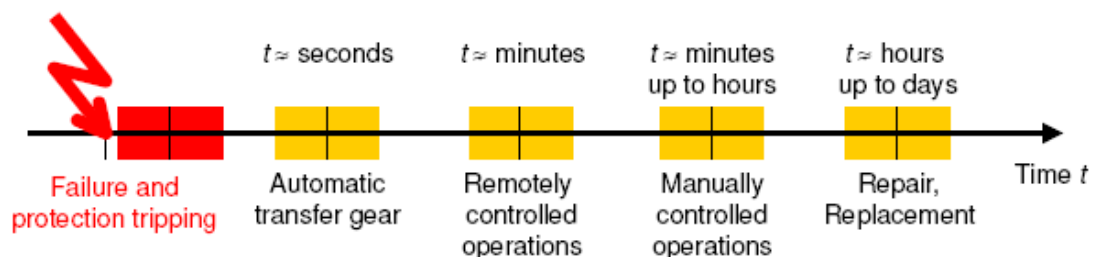


Figure 2-7 Temporal Sequence of Fault Recovery

The system state after applicable protection tripping and automatic transfer gear, which is assumed by steady-state calculation, is the basic for the modelling of fault recovery. At first, remotely controlled operations are tried to be achieved and completed after 10 to 20 minutes. In case the remotely controlled operations are not accessible or unable to eliminate the interruptions, manually controlled operations is necessary by sending personnel to the fault location for the transaction of remedial measures, which typically requires up to several hours time. If there are still interrupted customers after these measures, complete supply can only be restored by (provisional) repair or replacement of the defected equipment units. This may take up to several days. In the last resort, any supply interruptions will finally be ended by the reconnection of the failed components after their down-time has expired.

1.3 Reliability Calculation for Microgrids supplied by local time-varying micro-sources

Within the project 3 different simulation methods were developed to take into account the reliability contribution by intermittent micro-sources due to islanding:

- Conventional analytical reliability analysis with subsequent evaluation of local impact: In this case results from ZUBER Analysis part are taken for further evaluation (Chapter 3)
- Analytical reliability analysis directly considering reliability contribution of micro-sources: Based on failure combination database after ZUBER calculation part corresponding reliability indices are manually calculated (Chapter 4)
- Monte-Carlo-Simulation (Chapter 5)

Each method has its advantages and drawbacks especially concerning computation time and accuracy.

All three of them are applied in this report when appropriate to demonstrate certain reliability aspects; they are described in detail in the following three chapters.

3 Basic Reliability Impact investigated with Conventional Analytical Reliability Analysis

1.4 Introduction of the Basic Test Network (Base Case)

In order to observe the reliability improvement by DG units located in Microgrids, a simple test network (Figure 3-1) is taken as an example for reliability evaluation, which is considered as the base case without any DG units (*Base Case*); it serves as a reference to value any improvements that are achieved with further studies of DG penetration.

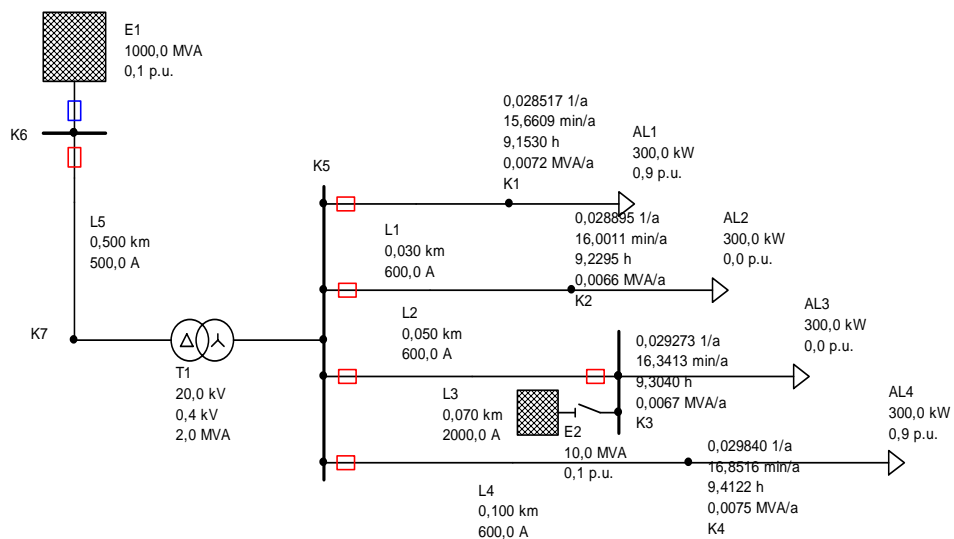


Figure 3-1 Basic Test Network without any DG Units (*Base Case*)

On 20 kV network level there are: Network infeasible E1; Busbar K6; Line L5; Node K7; Transformer: T1; while on 0.4 kV level there are Busbar K5; 4 parallel Lines L1, L2, L3 and L4; 4 Nodes K1, K2, K3 and K4; (disconnected DG E2); 4 Loads AL1, AL2, AL3 and AL4.

Assumption and Simplification

- All the network components, nodes and loads mentioned above, except network infeasible (100% reliable by setting), may suffer from outages during network operation;
- Only the failure model 'Independent Single Failure' is considered for simulation.

Input Data and Reliability Setting

- Reliability input data of the network components is according to Table 2-2, while the system input data of each component can be seen in Figure 3-1 (The rated power of total loads in this simple network equals 1.267 MVA and the load profile is identical for all four loads);
- The unavailability threshold is set to E-10 (failure combinations with lower probability are not considered in analytical reliability simulation);
- The failure order component is between 1 and 5 (min. 1 and max. 5 components may suffer from outages at the same time);
- Power allocation mode is pessimistic with defaulted value (the interrupted power equals the total load in this mode; see further details in section 1.5.1).

1.4.1 Reliability Simulation of Simple Network

1.4.1.1 Load Modelling

The load flow situation depending on actual load and generation has significant influence on the power related indices such as interrupted power P_u and energy not supplied W_u .

Load profiles are taken according to German standard load profiles that were identified as typical daily profiles for household, commercial, and industrial consumer segments. However, only the annual duration curve (ADC) is evaluated by ZUBER module as the use of standardized daily load curves is only possible with Monte-Carlo simulation. Using sorted and standardized annual load duration curves neglects the temporal correlation between separate customers. It is not possible to regard the fact that separate power system parts as well as generation of units and simultaneous demand of the load may reach their peak at different times. Ways to overcome this problem are discussed in chapter 1.6.

No DG units are connected in this chapter and infeasible E1 is considered as slack node. The load is modelled by a discrete ADC. Necessary parameters are:

- Load Factor (LF): The ratio of the average load over a designated period of time to the peak load occurring in that period;
- Demand Ratio $p = P_L / P_{Lmax} = P_L / P_{Lr}$; P_L is the actual load demand, while P_{Lr} is the rated power of the load. It is always assumed that $P_{Lmax} = P_{Lr}$.

A testing load with $LF = 0.758$ and a household load with $LF = 0.535$ are used for simulation with the simple network, each modelled either by 10 states or by 2 states as demonstrated in Figure 3-2.

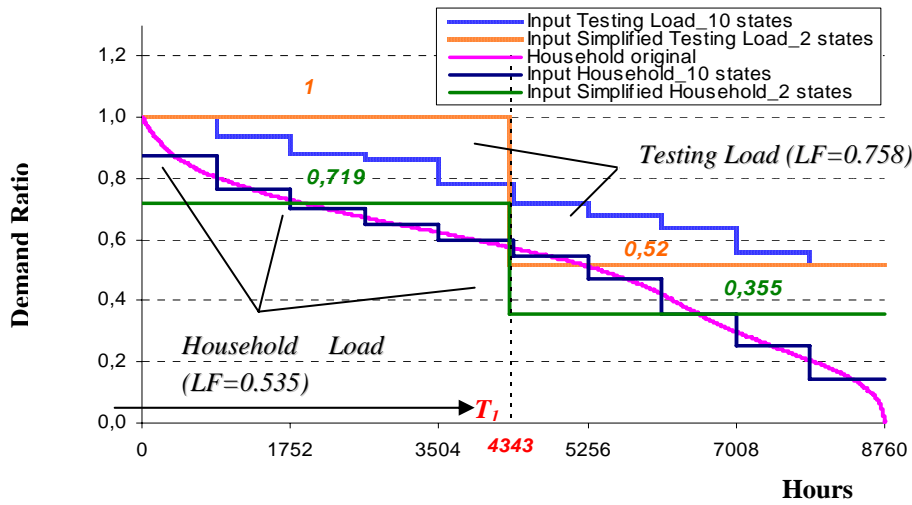


Figure 3-2 Load Modelling Approaches of Testing and Household Load

$$LF \cdot 8760 = \sum_i^{n-1} (p_{Li} \cdot T_i) + p_{Ln} \cdot (8760 - \sum_i^{n-1} T_i)$$

with T_i : each considered duration

p_{Li} : demand ratio during the duration T_i

n : total number of considered discrete durations

$$2 \text{ states by simplification } \frac{T_1}{8760} = \frac{LF - p_{L2}}{p_{L1} - p_{L2}} \quad (p_{L1} > p_{L2})$$

Equation 3-1

10 states input load ADC is generated by 10 even durations ($8760 \times 10 = 8760h$), which is derived from the original ADC, while 2 states input load ADC can be determined from Equation 3-1. With the same load profile, both 10 states and 2 states load ADC have the same LF. Table 3-1 provides the example input data of 2 states load modelling in PSS[®]SINCAL. The left side indicates the duration for maximum and minimum of the test load; the demand ratio of the household load is determined to have equal duration for each step as for the testing load. It could also be described by two values with demand ratio 1 and 0 with duration of 4687 h and 4073 h respectively.

	Duration/h	Demand Ratio		Duration/h	Demand Ratio
Testing Load	4343	1.00	Household Load	4343	0.719
	4417	0.52		4417	0.355
	LF	0.758		LF	0.535

Table 3-1 Input Data of 2 States Load Modelling in PSS[™]SINCAL

The simulation results are plotted in Figure 3-3, where the network reliability indices H_u, Q_u, P_u and W_u are compared between both load profiles.

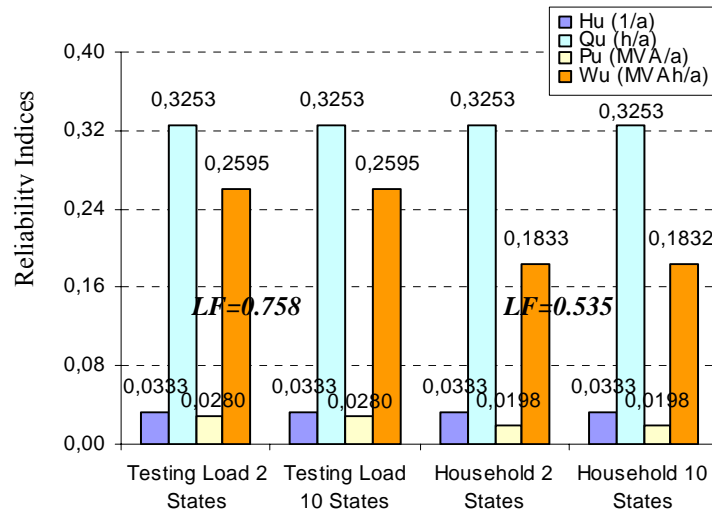


Figure 3-3 Network Reliability Comparison by Different Load Modelling

Two observations can be drawn from the diagram:

- Non-power related indices H_u and Q_u are independent from the behaviour of load demand in the case without DG, while power related indices P_u and W_u vary with different LF. Both interrupted power P_u and energy not supplied W_u enlarge with increasing load.
- With the same load profile, there is no difference between 10 states and 2 states load modelling according to the calculation method in ZUBER.

Therefore, the input load ADC is adopted by 2 states load modelling for simplification in the following studies, the Testing Load as *Base Case T* used in chapter 3 and chapter 4, the Household Load as *Base Case H* for chapter 5.

1.4.1.2 Node Result and Network Result

Table 3-2 shows the reliability indices for both network and each end-customer node k in *Base Case T*; a description of the failure combinations as well as the calculation of the reliability indices is attached in A.3).

Node	H_u [1/a]	Q_u [min/a]	T_u [h]	P_u [MVA/a]	W_u [MVAh/a]
K1	0,028517	15,6609	9,152962	0,007205328	0,06595009
K2	0,028895	16,0011	9,229451	0,006570724	0,06064417
K3	0,029273	16,3413	9,303966	0,006656681	0,06193352
K4	0,029840	16,8516	9,412198	0,007539608	0,07096428
Network	0,033275	19,5183	9,776258	0,027972340	0,25949210

Table 3-2 Reliability Indices of the Base Case T

Similar to the category of *customer-oriented indices* and *system-oriented indices*, in Table 3-2, node result and network result are reported. Node indices of K1, K2, K3 and K4 reflect

the individual customer experiences, which are specialized to each end-customer k . On the other hand, network result is an overview of the performance of the whole network.

- Node result for frequency of supply interruption is the summation of failure combinations (frequency) of the responsible component failures leading to that node in supply interruptions. Considering node K3, failure combinations of K6, T1, L5, K5 and L3 may contribute to the reliability results. In other words, if there is any fault occurring in any of these five components, node K3 will be affected. The calculation of all indices is according to Equation A -7 in appendix A.3.
- Network result for frequency of supply interruption is the sum of the maximum failure combinations (frequency) of the relevant component failures that have contributions to any of the end-customer in supply interruptions. It can be understood by an example: if failure combination i leads to a supply interruption of more than one customer k , the network result considers this failure combination only once with the maximum $H_{u,jk}$, due to available power and load demand, as well as the maximum $T_{u,jk}$, due to the restoration model (attached in A.3, Equation A -8).

1.4.1.3 Probability Distributions of Reliability Indices

As introduced previously, both *expected value* (denoted $E(x)$) and *relative variance* (denoted

$\sigma_r(x)$ with $\sigma_r = \frac{\sqrt{\sigma^2(x)}}{E(x)}$ [11]) of each index, except interruption cost and reimbursements,

can be provided by ZUBER module. With the knowledge of probability theory and statistics (detailed information of probability distributions can be found in appendix A.4), the probability distributions of each index, which are the prerequisite for further risk assessment providing confidence interval of the reliability indices, rather than only the expected value, under a certain observation period, could be determined with one or two parameters estimated from expected value and variance.

It should be noticed that the relative variance $\sigma_r(x)$ used for parameter estimation is not the exact value calculated by ZUBER, but following the modification $\sigma_r(x)/\sqrt{10}$. ZUBER considers only one year for calculating this variance, but year and year variation due to e.g. nature, weather or third-part damage may be very large. As such a short observation period very possibly induces an exaggerating deviation from the expected value it is thus practically replaced by an observation period of 10 years.

Mean Duration of Supply Interruptions

The mean duration of supply interruptions, in fact, is in most cases dependent on the duration of the restoration measures, such as switching actions, rather than the outage duration of the failure affected component, which can be calculated from the statistics. The identification of distribution functions of this index is not easily possible [9] and is not provided in this report.

Frequency of Supply Interruptions

As probabilistic reliability calculation is modelling ON and OFF state of network components with constant transition rate in time, the probability of the failure frequency of a system component can be described by a Poisson distribution [10]. As the reliability index frequency of supply interruptions is the summarized value of the relevant component failures leading to supply interruptions, the Poisson distribution is also appropriate for it [20].

The distribution of the network index frequency of supply interruption of Base Case T (blue curve) is plotted in Figure 3-4. It shows that the network frequency of supply interruption is less than 0.1 1/a with 72 % probability, and less than 0.2 1/a with 95 % probability, with respect to the expected value $E(x) = 0.331/a$.

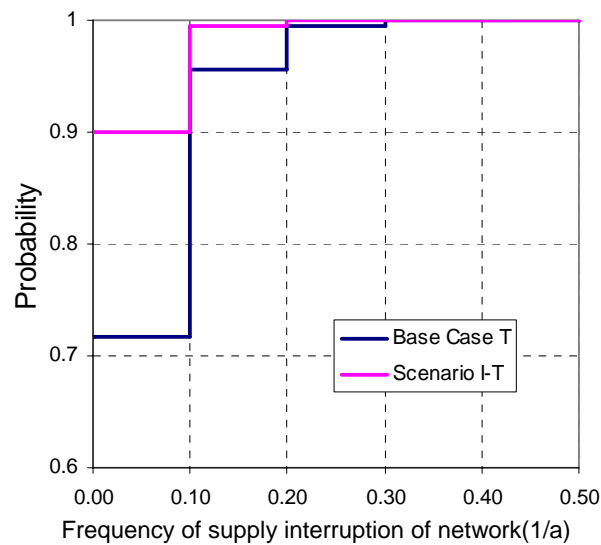


Figure 3-4 Poisson distribution of frequency of supply interruption of the Simple Network

Remaining Indices

The probability distributions of the remaining indices – unavailability Q_u , interrupted power P_u and energy not supplied W_u – can be assumed to fit the Weibull distribution (characterized by two parameters a and b) with good accuracy [9] as this distribution has no specific characteristic shape [10].

The distributions of the remaining indices of the original simple network without DG are plotted in Figure 3-5 (blue curves). The plots show the network reliability indices expressed with a 90% confidence interval, e.g. network unavailability is between 0 and 52 min/a with respect to $E(x) = 19.518 \text{ min/a}$; network interrupted power is between 0 and 0.075 MVA/a with respect to $E(x) = 0.028 \text{ MVA/a}$; network energy not supplied varies between 0 and 0.69 MVAh/a with respect to $E(x) = 0.02598 \text{ MVAh/a}$.

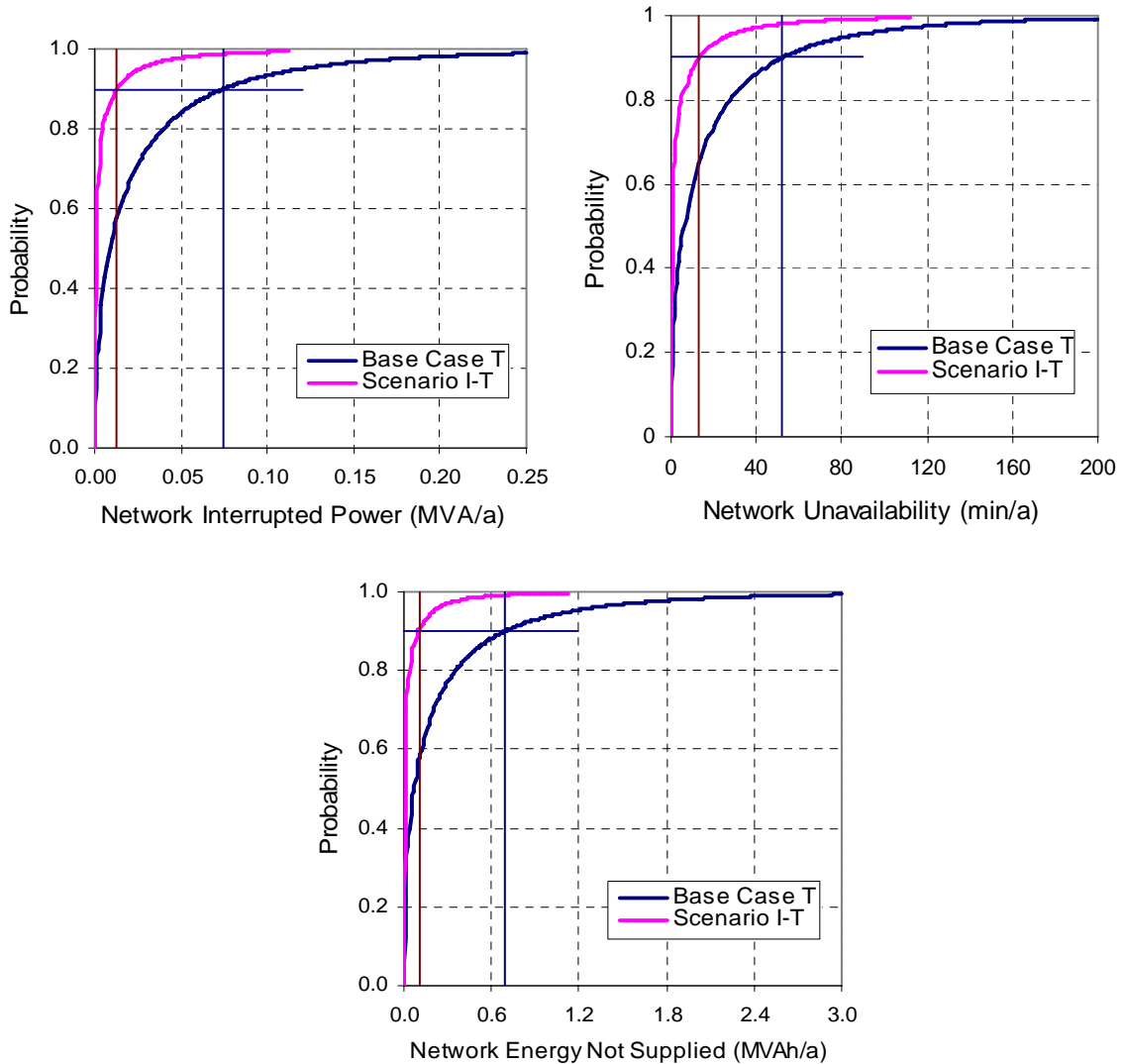


Figure 3-5 Weibull Distribution of Other Reliability Indices of the Simple Network

1.4.2 Protection Device

In reliability analysis, another very important component is the protection device. Before running the reliability simulation, the first work is to deploy the protection devices into the network with appropriate criteria. The device position, protection direction as well as the device characteristic should be well-considered to selected protection criteria such as defined tripping areas and so on.

In a radial feeder, protection devices are only expected to detect the unidirectional flow of current, coordinated via time lags [13]. On the other hand, in a DG-enhanced feeder, power flow is not unidirectional and conventional protection logic must be altered in order for the fault-detecting devices to successfully perform their function [14]. In low voltage network practice, normally certain circuit breakers (CB) (blue rectangle in Figure 3-1) and fuses (red rectangle) are used as the protection devices. Fuses are single-phase devices that trip the fault current flow after a predetermined time delay; Breakers may also be single-phase or three-phase devices, commonly with reclosing capability.

Busbar K5 in the test network will be affected if there is no fuse implemented at any of the lines in 0.4 kV level. In that case, failure combinations of lines other than the responsible one should be taken into account to the final result, which makes the reliability of this node much worse. Furthermore, due to the supplement of protection devices, the affect of failures occurring in protection devices can not be disregarded under reliability consideration.

To keep both voltage and frequency within acceptable ranges during micro-source islanded operating mode, it requires significant coordination of micro-sources with feeder protection devices, which is out of the scope of this report.

1.5 Simple Network Analysis – Impact of DG with Constant Operation

1.5.1 Introduction of Base Case with Micro-source Penetration (Scenario I)

This part analyses several aspects of their impact on reliability are analysed, such as micro-source size, micro-source allocation, micro-source location, and micro-source outages. Figure 3-6 demonstrates scenario I: one micro-source unit is connected to node K3 with output power equal to the rated power of the total load (100% penetration level (PL)) and without outages (100% reliability). With Testing load profile, it is designated as Scenario I-T; with Household load profile, it is designated as Scenario I-H.

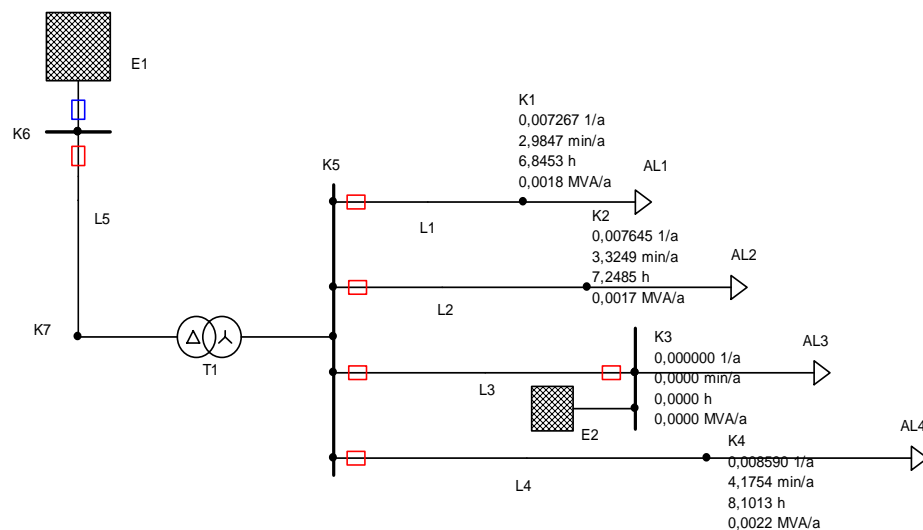


Figure 3-6 Base Case: Simple Network with one DG unit (Scenario I)

The previous setting of the simple network as in Base Case is still adopted. Apart from this additional assumptions are:

- One or more DG components are considered (in this chapter, each aspect is based on the Scenario I-T of Figure 3-6, and separately observed from other aspects);
- The Islanded Operating Mode of the DG units is always allowed when the main supply is interrupted, furthermore, DG can provide power without delay after supply interruption;
- Power Allocation Mode is pessimistic as default value; during this study, another optimistic mode is implemented to observe the variation of the results as well.

Power Allocation Modes

Pessimistic power allocation mode means that customers are not able to adopt the restricted available power and therefore interrupted power equals total demand. In contrary, optimistic power allocation mode means the customers are able to adopt the restricted available power and thus the interrupted power is the difference between actual demand and available power [12]. The determination of this parameter directly affects the reliability indices P_u and W_u when only the restricted power is available in the network (here due to the penetration of DG). The effect is illustrated in the section 1.5.2.1.

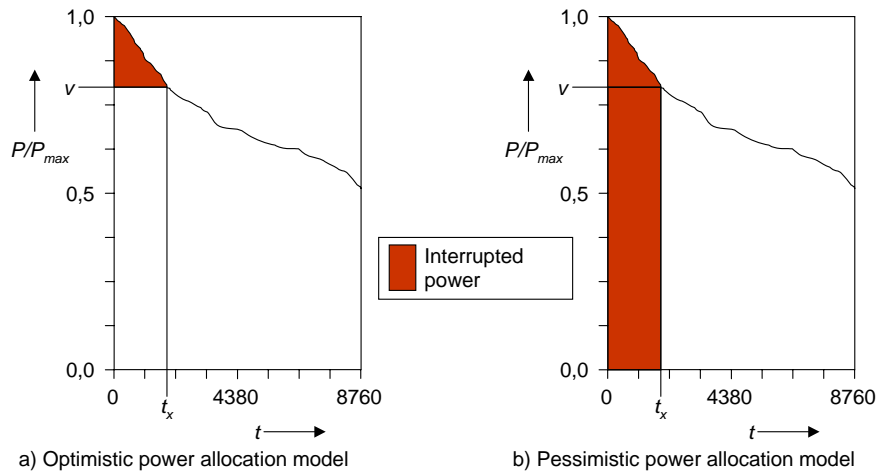


Figure 3-7 Power allocation models

Probability Distributions of the Reliability Indices

The probability distributions for both, *Base Case T* with *Scenario I-T*, are plotted in Figure 3-4 and Figure 3-5 for indices H_u , Q_u , P_u and W_u of the network.

The results of both, expected value $E(x)$ and extreme values according to the probability distribution with a considered confidence interval 90 % are listed in Table 3-3. The index H_u is compared with the probability that the frequency of supply interruptions is less than 0.1 1/a.

90% Confidence Interval	H_u (1/a)		Q_u (min/a)		P_u (MVA/a)		W_u (MVAh/a)	
	$E(x)$	Probability	$E(x)$	Probability	$E(x)$	Probability	$E(x)$	Probability
<i>Base Case T</i>	0.0333	(72%) <0.1	19.5183	0-52	0.0280	0-0.075	0.2595	0-0.69
<i>Scenario I-T</i>	0.0105	(90%) <0.1	5.6130	0-13	0.0057	0-0.013	0.0428	0-0.11
<i>Improvement related to Base Case T</i>	68.4%		71.2%	0%-75%	79.5%	0%-83%	83.5%	0%-84%

Table 3-3 Indices Comparison of Base Case T and Scenario I-T

Micro-source operation in this chapter is assumed to be constant at rated output power, without considering micro-source generation curve or generation schedule. Consequently, the

results can not represent the actual reliability improvement achieved by micro-source units, especially not with intermittent generation units such as PV or WT with relatively long periods of unavailability. Nevertheless, the studies explicate the fundamentals of a possible reliability improvement after micro-source penetration by providing comparable results for different aspects.

1.5.2 Impact of Micro-source with Constant Operation

1.5.2.1 Impact of Penetration Level

The penetration level PL is the proportion of installed micro-source capacity and the total customer demand in a given supply area. It also explicates the balance between the micro-source generation and demand, which is particularly critical in islanded operating mode.

Here micro-source output power P_G is kept constant always equal to its rated power P_{Gr} . Therefore, 100 % PL is described as $P_G = P_{Lr} = P_{GLmax}$, which means micro-source can always fully supply the total load (only for studies, possibly not practical in reality).

In general, the contribution of micro-source to reliability improvement can be divided into two categories:

- 1) To all loads in micro-source's supply area ($AL1$, $AL2$, $AL3$ and $AL4$); the micro-source unit can provide power to all these nodes through $L3$ and $K5$ in case the failure occurs in 20 kV network level ($K6$, $L5$ and $T1$) – micro-source and the 4 loads are operated in island mode – and hence the reliabilities of all these nodes can be improved.
- 2) To the load directly supplied by the micro-source unit as it is connected in same node ($AL3$); the micro-source unit can improve the reliability of this node further as $AL3$ is still supplied by micro-source in case the failure occurs in $K5$ or $L3^*$ – micro-source and $AL3$ are operated in island mode – while the other loads will suffer from interruptions (*:micro-source power is not accessible to other loads except $AL3$ while failures occurring in $K5$ or in $L1$, $L2$, $L3$ and $L4$).

In reality, the capacity of the DG unit varies, also depending on interests of unit or network operator. The effect of the different penetration levels on reliability is simulated for the simple network in the following section. Two cases, with and without load priority (LP), are studied.

As the load state may have a significant influence on the reliability results, the two-state load modelling is not sufficient in order to observe the effect of LP. Therefore, the Testing load ADC is simplified to an approximated equivalent four-duration curve with the same LF as Testing load (Figure 3-8).

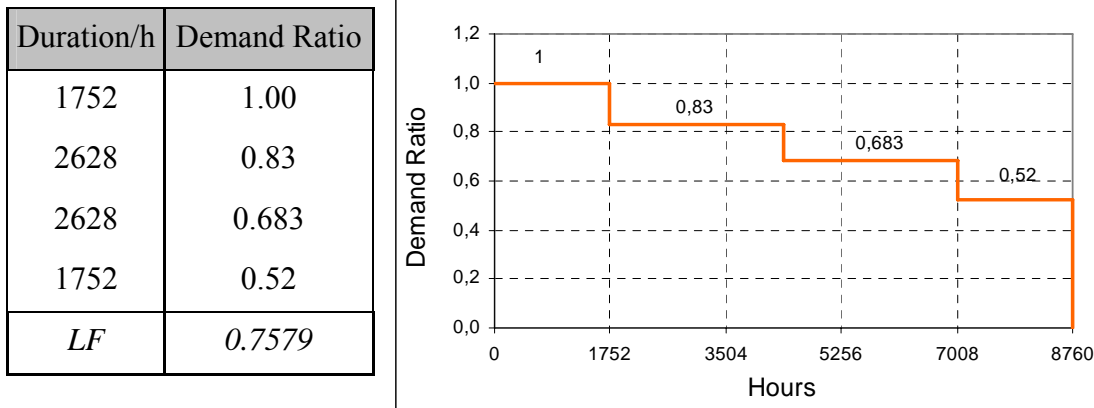


Figure 3-8 Load ADC for the Impact of Penetration Level (four durations)

Without Load Priority

In the case without load priority, no sensitive loads are in the network, and thus all the loads share the same priority to be supplied in island mode. The reliability indices are calculated according to the analytical approach based on the load ADC and different PL schemes. The reliability indices frequency of supply interruption H_u and unavailability Q_u relevant to different PL are shown in Figure 3-9 and Figure 3-10 (the values shown in Figure are for K3 and Network).

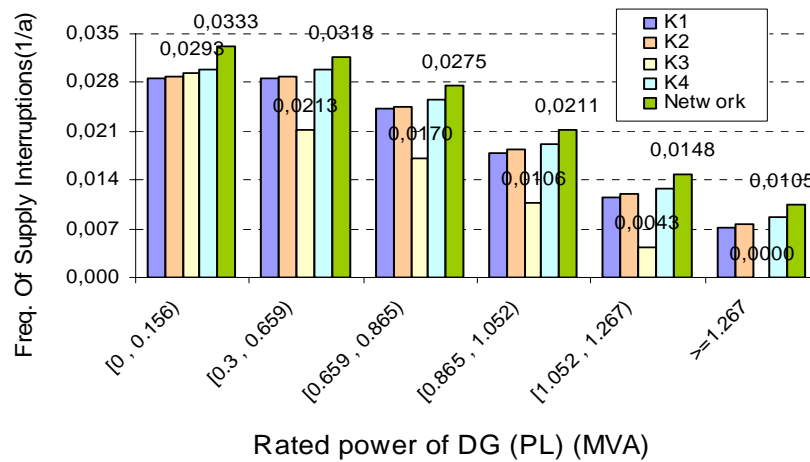


Figure 3-9 Frequency of supply interruption depending on DG Penetration without LP

The impact of PL on reliability indices shows discrete characteristics. The reason depends on the load ADC. Generally, if the power available is higher than the demand, it doesn't cause supply interruptions during that time; the frequency of supply interruption and the unavailability decrease.

With the given network structure and assumptions, such as no interconnecting lines, micro-source units reacting without delay, considering only ISF, the switching actions with respect to the outage duration can be disregarded. Therefore, Equation 3-2 is the simplified formula for this simple network derived from Equation A -7 and Equation A -8 with the conditional

interruption probability $p_{z,jk}$ (see A.3) – the ratio of the duration, when the demand is higher than the available power.

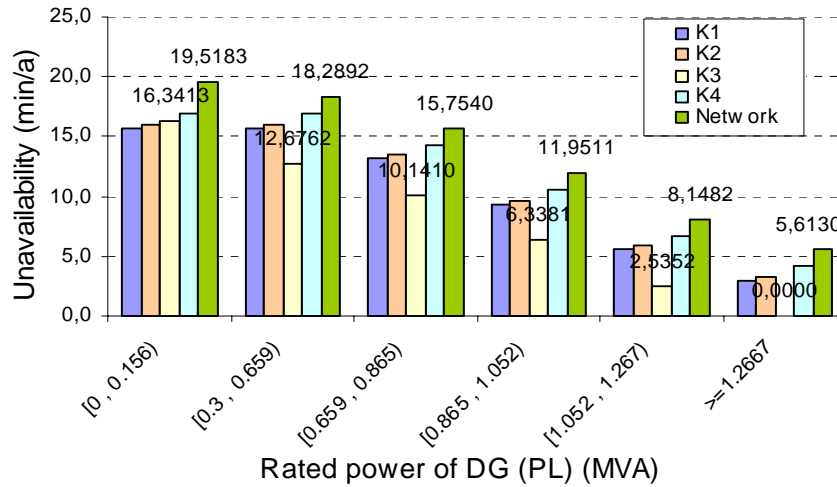


Figure 3-10 Unavailability depending on DG Penetration without LP

$$Node : H_{u,k} = \sum_i H_{u,ik} = \sum_i (p_{z,ik} \cdot H_{z,i}) \quad Q_{u,k} = \sum_i Q_{u,ik} = \sum_i [(p_{z,ik} \cdot H_{z,i}) \cdot T_{u,ik}]$$

$$Network : H_u = \sum_i \text{Max}_k (H_{u,ik}) \quad Q_u = \sum_i \text{Max}_k (Q_{u,ik})$$

Equation 3-2

Improvements in reliability are achieved either if a certain share of the total load can be covered by the total capacity of DG according to their ADC (see category 1) or if a certain share of local load can be covered with increasing PL (category 2).

With increasing PL from 0% to 100% (Figure 3-9) there is a stepwise reliability improvement according to 7 schemes that can be derived from the power thresholds of the ADC in Table 3-4.

Demand Ratio	P_G that supplies system (MVA)	P_G that supplies AL3 (MVA)
1.00	1.267	0.3
0.83	1.051	0.249
0.683	0.865	0.205
0.52	0.659	0.156

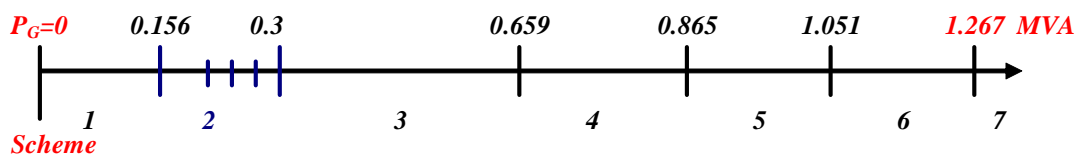


Table 3-4 Power range for reliability improvements

As the 2nd scheme with $P_G \in [0.156, 0.3)MVA$ doesn't show a constant value due to an increasing share of power that can be covered locally according to category 2) it is not included in the plots.

In the first 3 schemes, $P_G < 0.659MVA$ ($0.52 \times 1.267MVA$), the available power from micro-source unit is less than the base demand of the total load. This means, there is no reliability improvement by the 1) category, i.e. a failure in K6, L5 and T1 has no possibility to be balanced. However, the 2) category, the reliability of K3 can be improved by the decreased $H_{u,i3}$ ($P_G \geq 0.156MVA$ ($0.52 \times 0.3MVA$)) in failure combination i of K5 and L3 when only micro-source and AL3 are in island mode, according to the load ADC of AL3.

From the 4th to the 6th scheme, $P_G \in [0.659, 1.267)MVA$, apart from the additional reliability improvement of K3 by the 2) category, reliability of all the 4 loads is improved by same degree due to the same LP by the 1) category step by step, according to the four-duration load ADC (Figure 3-8) and the calculated value of $\rho_{z,ik}$ with respect to PL. With $P_G = 1.267MVA$, the 7th scheme, the reliability improvement achieves the maximum level as the total load is fully supplied by DG.

With Load Priority

In this case, the loads are set to different load priorities. From up to down, Load AL1 is set to the highest, and load AL4 is set to the lowest. If the system can fully supply the demand of the total load, the load priority has no further impact on reliability results. On the other hand, if only part of the loads can be satisfied with available power, the load priority affects the power allocation to each load and hence influences the reliability of both the individual nodes and the whole network.

Since DG power is unevenly allocated to the individual nodes in island mode due to the varied LP, it is much more complicated to determine each maximum power of the PL schemes in this case, which needs to consider the load ADC of each load. Thus only the indices of some specific PL are plotted in Figure 3-11, and Figure 3-12 for indices H_u and Q_u respectively (the values shown are for K3 and the network).

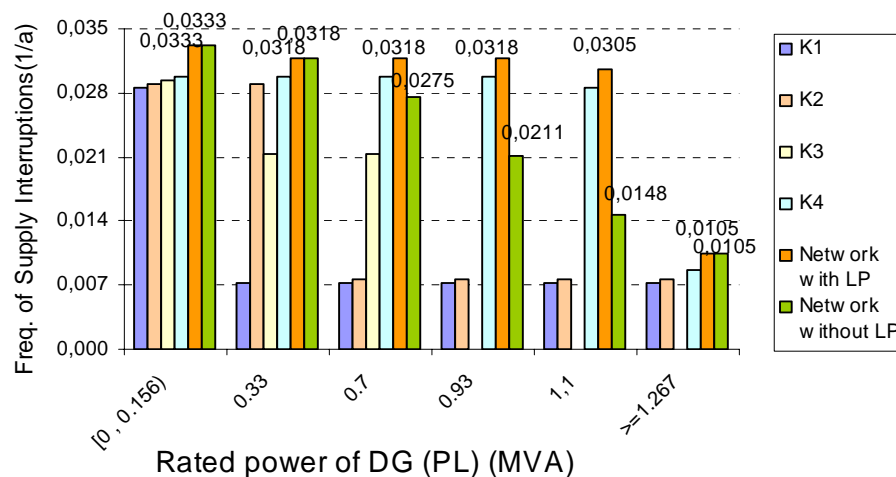


Figure 3-11 Frequency of supply interruption depending on DG Penetration with LP

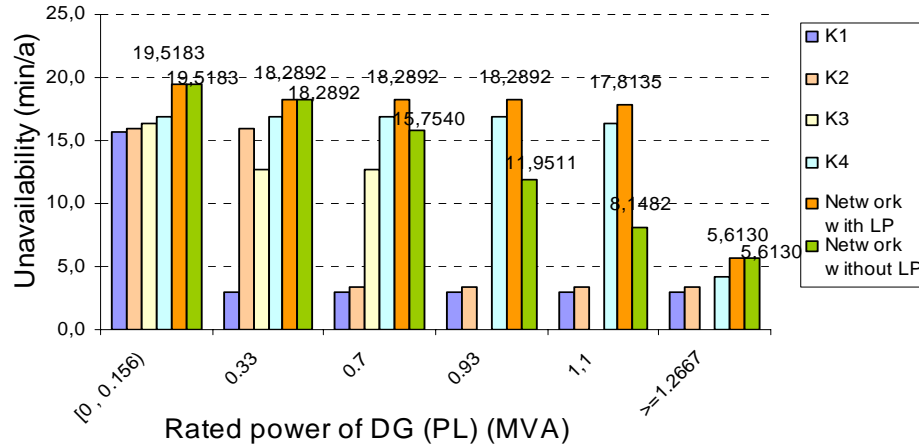


Figure 3-12 Unavailability depending on DG Penetration with LP

Node Result

The loads with higher LP get power allocated from micro-source, which means a reliability improvement as long as $P_G \geq P_{Lmin}$. As load AL1 in K1 shares the highest load priority, the micro-source unit delivers as much power as possible primarily to satisfy the demand of node AL1 when the network is in islanded operating mode; if the rated power of micro-source is higher than the peak demand of the first-class priority load, the residual power serves to supply the secondary-class priority load (AL2), and by analogy to other nodes.

Network Result

Comparing the network result with and without LP demonstrates that network reliability with LP is not improved until the reliability in K4 (with lowest LP) is improved. It can be explained with Equation 3-2, with $Hu = \sum_i \text{Max}_k(H_{u,ik})$. In the case without LP, the frequency of supply interruption of each end-customer k in failure combination i of K6, L5 or T1 is the same, i.e. $H_{u,iK1} = H_{u,iK2} = H_{u,iK3} = H_{u,iK4}$; on the other hand, in the case with LP, the value is varied, e.g. $H_{u,iK1} \neq H_{u,iK4}$, therefore, the calculation will take these $\text{Max}_k(H_{u,ik}) = H_{u,iK4}$ in these failure combinations, which are kept constant before the reliability in K4 increases.

Power Interrupted in both cases, with and without LP

Different from frequency and unavailability, the indices of interrupted power and energy not supplied are cumulative values. Without considering remedial measures due to the structure and assumption of the simple network, the simplified formula of interrupted power and energy not supplied can be expressed as in Equation 3-3 (detailed symbol descriptions are attached in Annex A.3):

Node Result:

with pessimistic power allocation mode :

$$S_{u,k} = \sum_i S_{u,ik} \quad \text{with } S_{u,ik} = H_{Z,i} \cdot S_{Z,ik} \quad \text{and } S_{Z,ik} = \sum_d p_d \cdot S_{kd}$$

with optimistic power allocation mode :

$$S_{u,k} = \sum_i S_{u,ik} \quad \text{with } S_{u,ik} = H_{Z,i} \cdot S_{Z,ik} \quad \text{and } S_{Z,ik} = \sum_d p_d \cdot (S_{kd} - S_{ik})$$

$$W_{u,k} = \sum_i W_{u,ik} \quad \text{with } W_{u,ik} = H_{Z,i} \cdot T_{u,ik} \cdot S_{Z,ik}$$

Network Result:

$$S_u = \sum_k S_{u,k} \quad W_u = \sum_k W_{u,k}$$

d : the step from ADC with $S_{kd} > S_{ik}$

p_d : probability of step d in 1 year from ADC

S_{kd} : demand of end – customer k in step d

S_{ik} : available power on end – customer k in failure combination i

Equation 3-3

Figure 3-13 shows the interrupted power in both cases. The node result can be explained in the same way as H_u and Q_u , nevertheless, the network result is different. From Equation 3-3, it can be seen that the network's interrupted power is a summarised value of each end-customer's index $S_{u,k}$, thus it will be improved as long as any of the end-customer's $S_{u,k}$ increases. Consequently, the improvement of S_u in the case with LP is faster than in the case without LP, what can be seen in Figure 3-13.

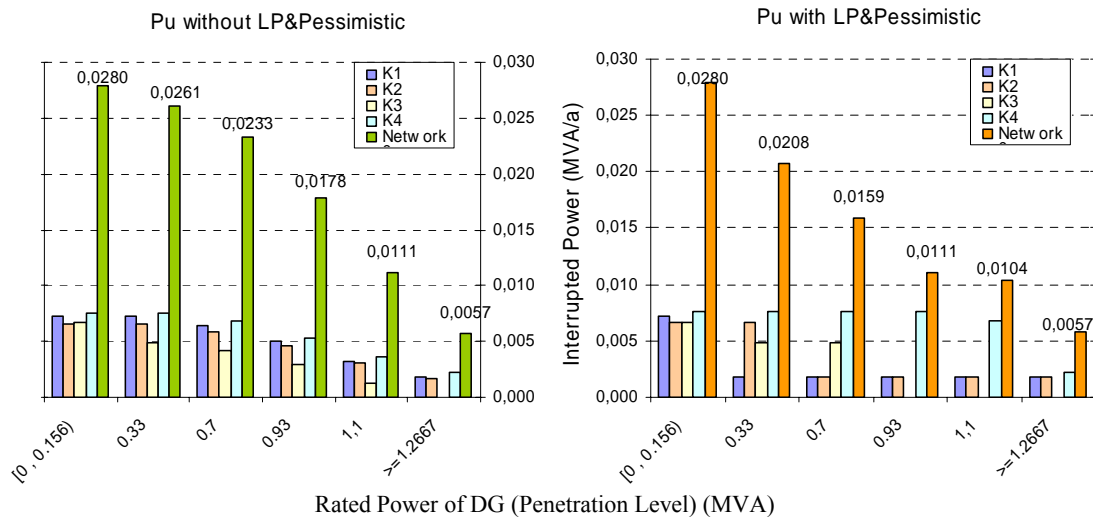


Figure 3-13 Interrupted Power in Pessimistic Mode

Furthermore, Figure 3-14 demonstrates the effects of a variation of power allocation mode (Figure 3-7), which has the influence on power related indices, on interrupted power P_u (network result). The blue curves are with pessimistic mode (discrete characteristic) while

the red ones are from optimistic mode, which display continuous characteristic and show higher reliability improvement.

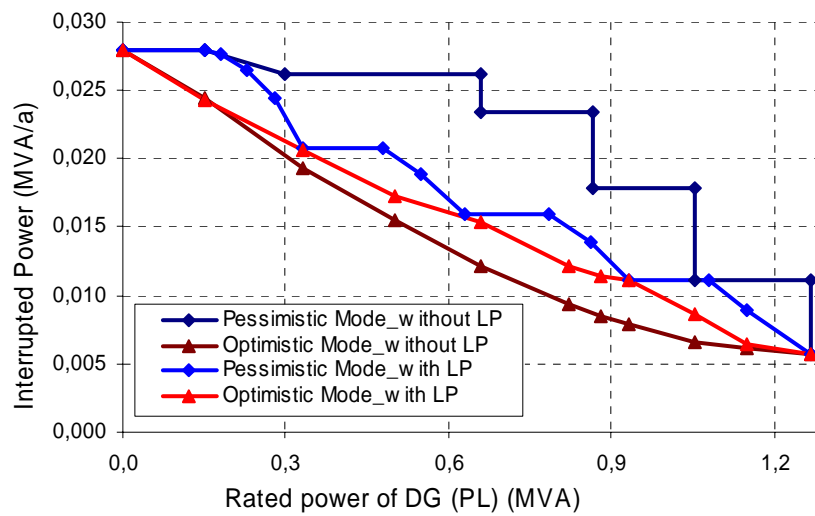


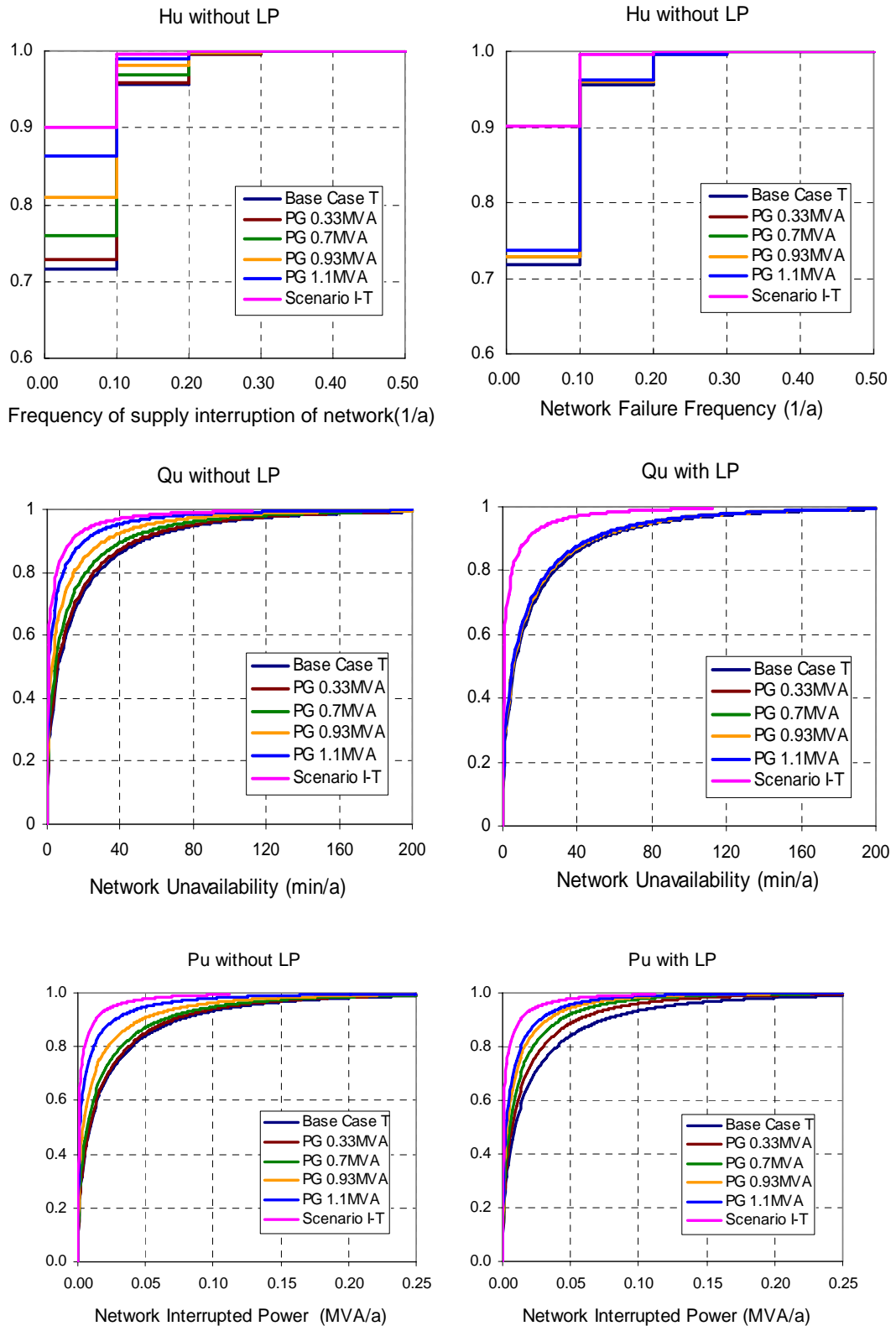
Figure 3-14 Network Interrupted Power depending on Power Allocation Mode

Three observations can be derived from Figure 3-14:

- The light blue curve is the case of pessimistic mode with LP. It can be divided into 4 sections, with each section displaying the same shaped but proportionally shrunk curve as the dark blue one (the case of pessimistic mode without LP) due to the unique load profile and the various LP of each load.
- The light red curve presents the case of optimistic mode with LP. Compared with the dark red curve (optimistic without LP), the network interrupted power decreases once the injected DG power is higher than zero (continuous characteristic) in both cases; but the value of light red curve is little bit higher than the dark red one, which is caused by the characteristic of the adopted load ADC (critical index $S_{Z,k}$ in Equation 3-3). It may also happen that the value of dark red curve is higher than the light red one when the load profile of ADC changes, especially possible for the load profile with lower LF.
- It is interesting to see that the difference between two modes in the case with LP is much smaller than the one in the case without LP, because the individual $S_{u,k}$ is easier improved in the case with LP.

According to the observations, one conclusion can be drawn. If the pessimistic mode is considered, in term of interrupted power, the case with LP should be chosen for better reliability indices while in optimistic mode the better case depends on the adopted load ADC.

Probability Distributions of the Reliability Indices



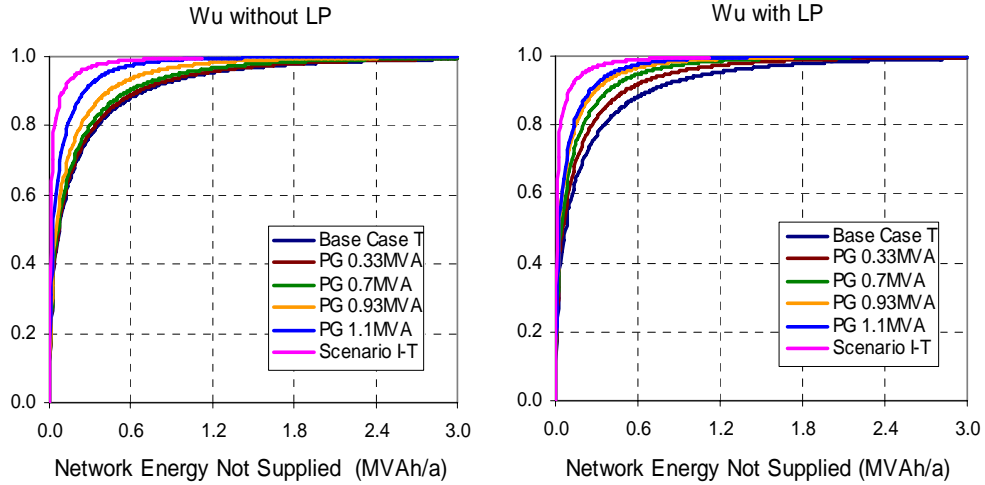


Figure 3-15 Probability Distributions depending on DG Penetration (Pessimistic Mode)

With a considered confidence interval of 90 %, the indices are compared for both cases without and with LP in Table 3-5 and Table 3-6 respectively.

90% Confidence Interval	Hu (1/a)		Qu (min/a)		Pu (MVA/a)		Wu (MVAh/a)	
	<i>E(x)</i>	<i>Probability</i>	<i>E(x)</i>	<i>Probability</i>	<i>E(x)</i>	<i>Probability</i>	<i>E(x)</i>	<i>Probability</i>
Base Case T	0,0333	(72%) <0.1	19,5183	0-52	0,0280	0-0.075	0,2595	0-0.69
<i>P_G</i> =0.33MVA	0,0318	(73%) <0.1	18,2892	0-49	0,0261	0-0.07	0,2456	0-0.66
<i>P_G</i> =0.7MVA	0,0275	(76%) <0.1	15,7540	0-42	0,0233	0-0.063	0,2177	0-0.58
<i>P_G</i> =0.93MVA	0,0211	(81%) <0.1	11,9511	0-31	0,0178	0-0.047	0,1629	0-0.44
<i>P_G</i> =1.1 MVA	0,0148	(86%) <0.1	8,1482	0-21	0,0111	0-0.027	0,0963	0-0.26
Scenario I-T	0,0105	(90%) <0.1	5,6130	0-13	0,0057	0-0.013	0,0428	0-0.11

Table 3-5 Indices depending on PL without LP (Pessimistic Mode)

90% Confidence Interval	Hu (1/a)		Qu (min/a)		Pu (MVA/a)		Wu (MVAh/a)	
	<i>E(x)</i>	<i>Probability</i>	<i>E(x)</i>	<i>Probability</i>	<i>E(x)</i>	<i>Probability</i>	<i>E(x)</i>	<i>Probability</i>
Base Case T	0,0333	(72%) <0.1	19,5183	0-52	0,0280	0-0.075	0,2595	0-0.69
<i>P_G</i> =0.33MVA	0,0318	(72%) <0.1	18,2892	0-49	0,0208	0-0.055	0,1922	0-0.51
<i>P_G</i> =0.7MVA	0,0318	(72%) <0.1	18,2892	0-49	0,0159	0-0.043	0,1442	0-0.39
<i>P_G</i> =0.93MVA	0,0318	(72%) <0.1	18,2892	0-49	0,0111	0-0.033	0,0961	0-0.29
<i>P_G</i> =1.1 MVA	0,0305	(74%) <0.1	17,8135	0-48	0,0104	0-0.028	0,0947	0-0.25
Scenario I-T	0,0105	(90%) <0.1	5,6130	0-13	0,0057	0-0.013	0,0427	0-0.11

Table 3-6 Indices depending on PL with LP (Pessimistic Mode)

Summary

The penetration level – the ratio between rated power of DG units and total load in a supply area – has significant impact on reliability results.

Without LP, after PL reaching the base power demand of total loads during one year, the increasing PL has an even accreting positive impact discretely step by step on both node and network reliability indices. On the other hand, with LP, DG supplies node one after another according to the different levels of LP, which leads to the conclusion that, nodes with higher LP could receive reliability improvements under a low PL value while nodes with lower LP cannot receive reliability enhancements until PL value is sufficiently large. PL impact on reliability performance for separate nodes is the same as the case without LP. And the network reliability indices H_u and Q_u can not be improved until the reliability of the node with lowest priority is improved.

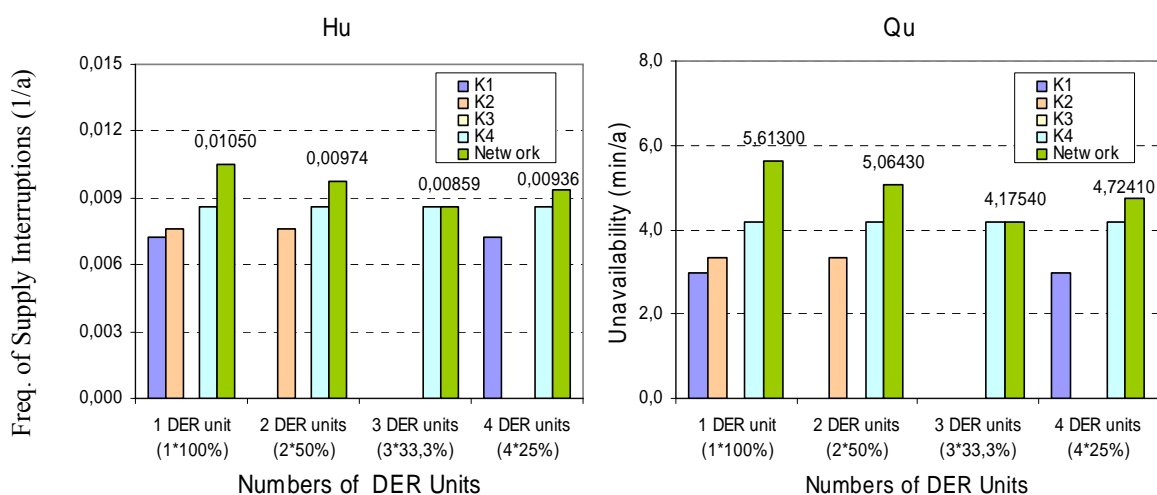
Network indices P_u and W_u improve as long as any of the individual customer’s $P_{u,k}$ and $W_{u,k}$ decreases. With pessimistic power allocation mode, the improvement of P_u and W_u is discrete while with optimal power allocation mode, their improvement is continuous.

1.5.2.2 Impact of the Numbers of DG Units

Under the same PL, the number of DG units may also have impacts on node and network reliability. Thus 4 schemes based on *Scenario I-T* are analysed in this section. All DG units share the same power factor.

- Scheme 1 (*Scenario I-T*): 1 DG unit (100% PL) is connected to K3
- Scheme 2: 2 DG units (2*50% PL) are connected to K3 and K1
- Scheme 3: 3 DG units (3*33.3% PL) are connected to K3, K1 and K2
- Scheme 4: 4 DG units (4*25% PL) are connected to K3, K1, K2 and K4

The reliability indices are compared in Figure 3-16.



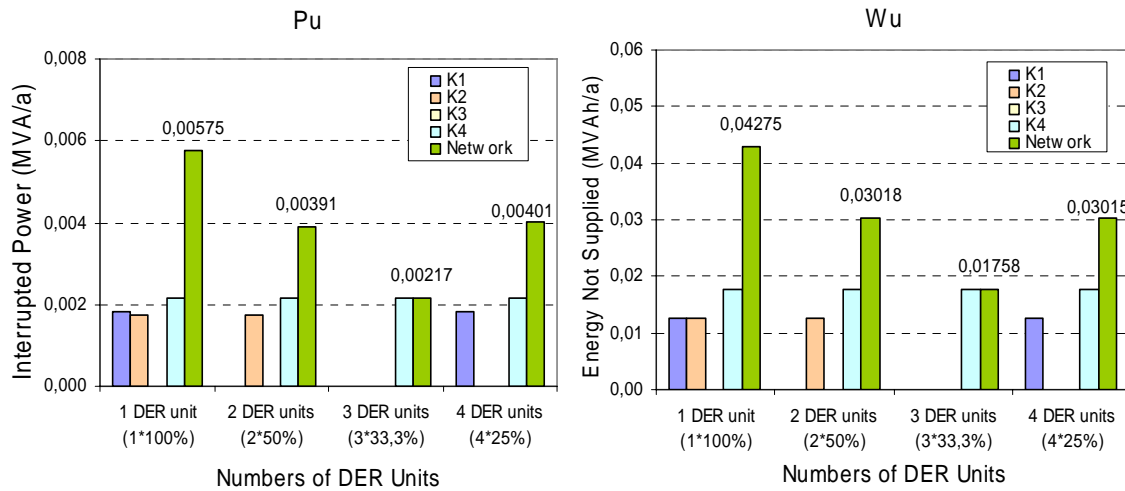


Figure 3-16 Reliability Indices with Different Numbers of DG Units

The indices can be explained in two categories as well:

- To the 1) category (for global influence):
Since the PL for total DG units is the same in 4 schemes, for the integrated single node system, $H_{u,K6j}$, $H_{u,L5j}$ and $H_{u,T1j}$ always keep constant during scheme variation.
- To the 2) category (for local influence):
Since more individual end-customer nodes are deployed DG units, the failure combinations $H_{u,K5j}$, $H_{u,L1j}$, $H_{u,L2j}$, $H_{u,L3j}$ and $H_{u,L4j}$ may decrease dependent on the output power and location of each DG unit.

Therefore, the best reliability indices are achieved by a DG allocation scheme where most of the end-customers are fully supplied by DG units. In this section, the best scheme is scheme 3 in which K1, K2 and K3 are fully supplied by 33.3 % PL DG units; on the other hand, in scheme 4 only K2 and K3 are fully supplied by the connected DG unit (25% PL) although 4 DG units are connected to the individual nodes respectively.

With a considered confidence interval of 90 %, the indices are compared in Table 3-7.

90% Confidence Interval	Hu (1/a)		Qu (min/a)		Pu (MVA/a)		Wu (MVAh/a)	
	$E(x)$	Probability	$E(x)$	Probability	$E(x)$	Probability	$E(x)$	Probability
Base Case T	0.0333	(72%) <0.1	19.5183	0-52	0.0280	0-0.075	0.2595	0-0.69
Scenario I -T	0.0105	(90%) <0.1	5.6130	0-13	0.0057	0-0.013	0.0428	0-0.11
2 DG Units	0,0097	(91%) <0.1	5,0643	0-12	0,0039	0-0.009	0,0302	0-0.07
3 DG Units	0,0086	(92%) <0.1	4,1754	0-9	0,0022	0-0.005	0,0176	0-0.04
4 DG Units	0,0094	(91%) <0.1	4,7241	0-11	0,0040	0-0.009	0,0302	0-0.07

Table 3-7 Indices depending on number of DG Units

Summary

It is necessary to consider the number of DG units, their distribution in the network as well as their ability to cover demand to evaluate the impact of a certain DG penetration level for given network areas.

Generally, more DG units which are connected to different nodes could possibly result in better reliability performance than using a single DG unit with same total installed capacity. Highest reliability is achieved when most of the end-customers are fully supplied by DG units directly connected to the loads.

1.5.2.3 Impact of DG Location

In this simple network, three options of DG location (*K3 – Scenario I-T, K5 and K7*) are chosen to evaluate the impact of DG location on reliability (Figure 3-17, the values shown correspond to K3, K4 and Network).

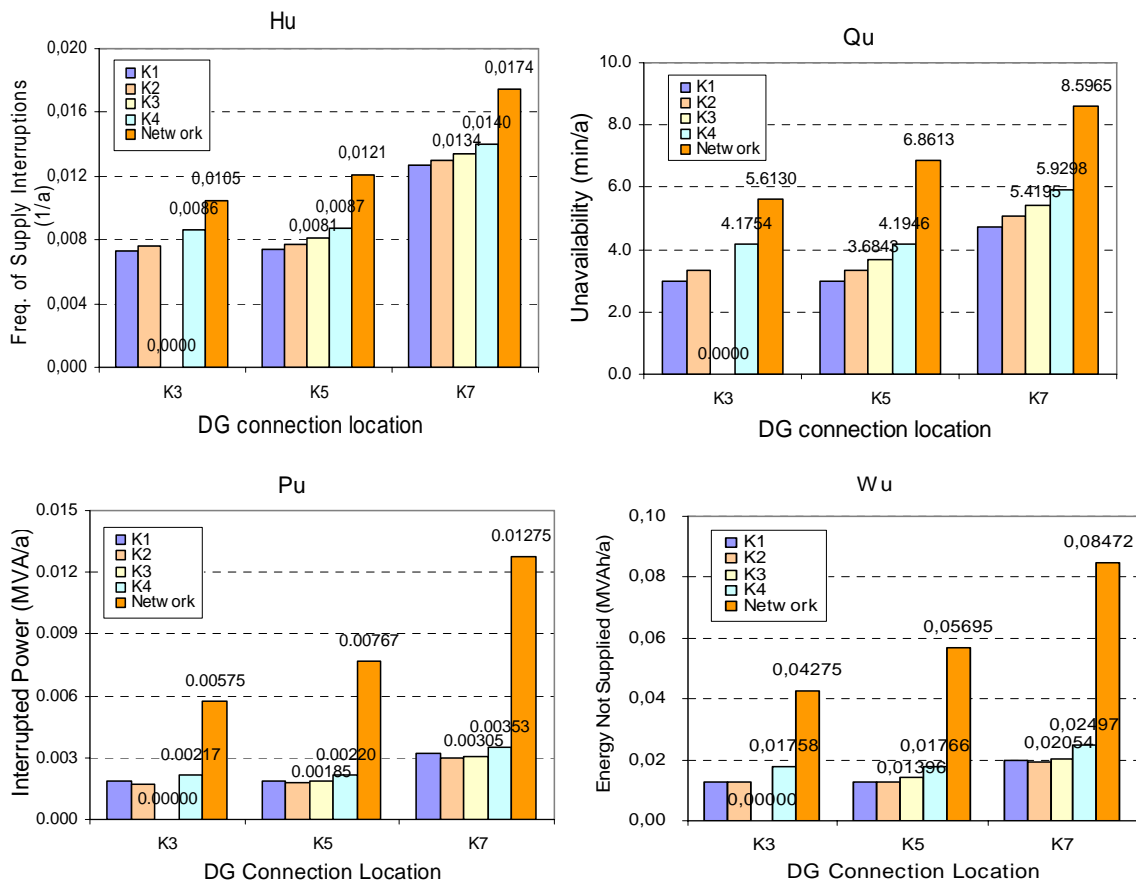


Figure 3-17 Reliability Indices depending on Different DG Location

From Figure 3-17, especially by observing the node result of *K3*, which is directly connected to DG in the first option, it can be seen that $H_{u,K3}$, $Q_{u,K3}$, $P_{u,K3}$ and $W_{u,K3}$ are growing with increasing distance of the DG unit location from *K3* (from the connection node *K3* to *K5* and then to *K7*). In other words, the DG unit improves the node reliability most in these nodes with shortest distance.

Both node and network reliability are worst for the option that DG is connected to K7 due to the contribution of additional failure combinations of the transformer T1. In case of failures in T1, only DG unit connected to K5 or more downstream can reduce the impact of the outage.

By analogy, a higher reliability of the network is shown by a DG location in K3 instead of K5, which is caused by the eliminated failure combination of Line L3 (for reliability of node K3, the result difference is caused by the failure combinations of both L3 and K5; and for reliability of other nodes, there is actually no difference between the location of K3 and K5 as L3 is not the responsible component for reliability of other nodes except K3). Consequently, it can be generally concluded that the reliability improves when the DG moves downstream.

It should be noted that, as the 4 loads are connected in parallel to the busbar K5 indirectly with lines of different-length, which can be considered as an integrated load of single-node system, the node K1 (AL1), K2 (AL2), K3 (AL3) and K4 (AL4) are at the same ‘‘downstream level’’. According to the conclusions above, if the DG is connected to K1, K2, K3 and K4 respectively (4 cases), two points in term of reliability variation can be derived.

- Node result: only the nodes that change the situation from not being connected to being directly connected with DG or vice versa have the reliability variation while the case is changed. And in each case, the node which is directly connected to DG displays the highest improvement of reliability.
- Network result: the reliability is slightly changed among these 4 cases, which is caused by the different lengths of L1, L2, L3 and L4. The best case is the one in which the DG unit is connected to K4, as line L4 has the longest length and hence the largest failure combination among L1, L2, L3 and L4, which can be eliminated due to the penetration of DG.

With a considered confidence interval or 90 %, the indices are compared in Table 3-8.

90% Confidence Interval	Hu (1/a)		Qu (min/a)		Pu (MVA/a)		Wu (MVAh/a)	
	$E(x)$	Probability	$E(x)$	Probability	$E(x)$	Probability	$E(x)$	Probability
<i>Base Case T</i>	0.0333	(72%) <0.1	19.5183	0-52	0.0280	0-0.075	0.2595	0-0.69
<i>DG at K7</i>	0,0174	(84%) <0.1	8,5965	0-22	0,0128	0-0.034	0,0847	0-0.22
<i>DG at K5</i>	0,0121	(88%) <0.1	6,8613	0-17	0,0077	0-0.018	0,0570	0-0.14
<i>Scenario I-T</i>	0.0105	(90%) <0.1	5.6130	0-13	0.0057	0-0.013	0.0428	0-0.11

Table 3-8 Indices Comparison by Different DG Location

Summary

DG units can reduce the impact of outages in upstream networks of the DG location if the remaining network is able to be operated in island mode. In this point of view, the optimum location to connect DG units among three analysed locations is the node K3, which is located

most downstream. But it should be noted that, the most downstream location might not be the optimal choice in practice when the DG unit produces large reserved power flow to the system, which causes significant power losses in scope of the whole network.

Furthermore, the example here is a very simple network, with one transformer feeding only one busbar. Once there are more transformers and busbars connected to node K7, the last option (DG is connected to K7) becomes more advantages especially when the DG unit is operated in island mode. In other words, with the second option (DG is connected to K5) during islanded operation, the reliability indices of end-customer nodes except K3 will increase significantly due to the long path of power flow that is supplied by the most downstream DG unit, which is normally not a worthwhile trade-off.

In reality, the situation is much more complicated; the optimum location of the DG units depends on multiple-considered conditions, such as the type of load (where is the sensitive load that must not be interrupted), the capacity of DG units (how many loads can be supplied), the types of the DG (PV, WT, CHP or in combinations), territorial restrictions, etc.

1.5.2.4 Impact of DG Availability

Both the electrical networks, and also the generation systems, have impacts on power quality and reliability. Outages in the generation system do not only have technical influences on power quality, but also significant economical consequences [18].

Outages of DG units (the reliability of power generation units from upstream network is out of scope here) are simulated by the easiest way using a two state model where the components only have an ‘‘ON’’ and an ‘‘OFF’’ state.

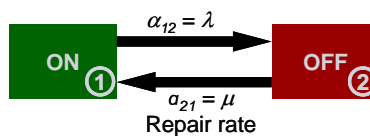


Figure 3-18 Two state DG model

Failure rate and down time of the independent single failure are predefined as the reliability input data in PSSTMSINCAL/ZUBER. This study assumes several DG availability schemes - independent from the DG technologies - to observe the impact on results. Table 3-9 demonstrates the corresponding down times for different DG availabilities assuming 1 outage per year.

DER Reliability	99.9%	99%	98%	97%	96%	95%
<i>H [1/a]</i>	1	1	1	1	1	1
<i>T [h]</i>	8,76	87,6	175,2	262,8	350,4	438

Table 3-9 DG Reliability Input Data with constant failure rate

Assuming constant down time (T = 20h) leads to an increased frequency of interruptions with decreasing reliability as shown in Table 3-10.

DER Reliability	99.9%	99%	98%	97%	96%	95%
$H [1/a]$	0.5	4.38	8.76	13.14	17.52	21.9
$T [h]$	20	20	20	20	20	20

Table 3-10 DG Reliability Input Data with constant down time

The values of Table 3-10 are taken for further investigations.

An outage of DG only affects the reliability if the main supply is interrupted in the mean time or vice versa. In other words, the contribution of a DG outage is taken into account by the coexistence of DG failure and any other component failure, which finally causes a failure of the whole system.

The calculation for such 'double and multiple faults' can be expressed by (homogeneous) Markov process [17] (see annex A.2). It must be noted that 'double and multiple faults' are different from not so-called 'common mode fault' (dependent synchronous faults occur in two lines due to a common cause such as the lightning strike), but are defined as 'stochastic double faults' [12] [17]. The impact on each reliability index is shown in Figure 3-19.

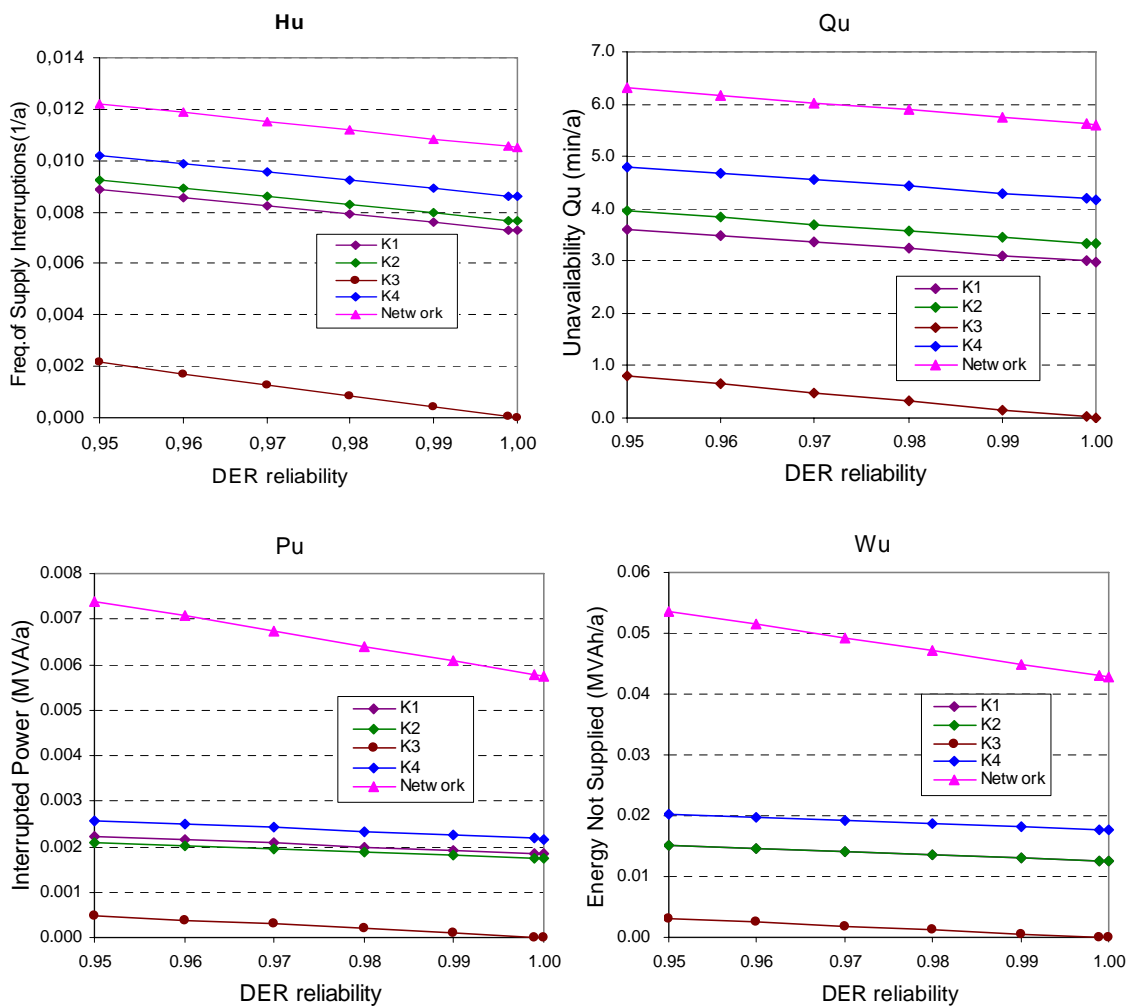


Figure 3-19 Reliability Indices depending on DG reliability

The reliability indices show linear dependency from DG availability. The trend line of node K3 has the largest slope coefficient as it is directly connected to the DG unit, while the trend lines of the other three nodes have the same slope coefficient which is smaller than the one of node K3. The slope coefficient of the network result is dependent on the algorithm of each index (Equation A -8).

The indices in Table 3-11 indicate that a DG availability of 99.99 % has almost the same results as with 100% DG reliability (*Scenario I-T*).

With a considered confidence interval 90 %, the indices are compared in Table 3-11.

90% Confidence Interval	Hu (1/a)		Qu (min/a)		Pu (MVA/a)		Wu (MVAh/a)	
	$E(x)$	Probability	$E(x)$	Probability	$E(x)$	Probability	$E(x)$	Probability
<i>Base Case T</i>	0.0333	(72%) <0.1	19.5183	0-52	0.0280	0-0.075	0.2595	0-0.69
<i>DG Rel.95%</i>	0,0122	(88%) <0.1	6,3083	0-22	0,0074	0-0.034	0,0536	0-0.22
<i>DG Rel.99%</i>	0,0108	(89%) <0.1	5,7521	0-17	0,0061	0-0.018	0,0449	0-0.14
<i>DG Rel.99.9%</i>	0,0105	(90%) <0.1	5,6289	0-13	0,0058	0-0.013	0,0430	0-0.11
<i>Scenario I - T</i>	0.0105	(90%) <0.1	5.6130	0-13	0.0057	0-0.013	0.0428	0-0.11

Table 3-11 Indices Comparison Concerning DG Availability

Compared to *Base Case T* (without DG), there is a much higher reliability with micro-sources even if the units are only 95% reliable, although more failure combinations are considered due to the micro-source outages. The new failure combinations generated by micro-source outages are caused by 'double and multiple faults' which occur with very low probability.

Summary

The impact of the availability of DG on network reliability is not a stand-alone factor. DG outages contribute to system reliability with coexistence of other component failures, which can be presented with the help of (homogenous) Markov Process. Compared to the Base Case T (without DG), the reliability indices are improved significantly anyhow with DG, even if the DG units show a certain unavailability. Moreover, along with the increase of DG outages, i.e. worse DG reliability, both node and network reliability results are getting worse with linear characteristics. The node where the DG unit is connected shows the strongest dependency on DG availability.

1.6 Simple Network Analysis – Time-dependency of Generation and Load Profiles

1.6.1 General Introduction

In most of the literatures related to the field of micro-source reliability, the effect of micro-source on distribution networks is simulated with fixed operating point, rather than considering the actual time-dependent availability of DG units (known from Capacity Factor (CF) and Availability Factor (AF), attached in A.5). Intermittency of the generation is considered in a generally reduced availability of the unit. However, especially for RES, the

actual output is strongly dependent on the intermittency of the primary energy resources at that time, such as sunlight, wind, water and so on, which is normally not controllable. Consequently, the impact of micro-source on system reliability may vary compared with the impact of micro-source units with constant operation.

In this chapter, the time-dependent information of the DG units (PV, WT and CHP in this report) is considered during the simulation. Other network settings stay the same as *Scenario I*, but the input load ADC is rearranged according to different DG types. Three single options PV, WT and CHP are analysed respectively as *Scenario II*, *Scenario III* and *Scenario IV*, where the household load profile is adopted. Different technologies are mixed as well as micro-source allocation is varied to observe the optimum case for reliability improvement. Lastly, the number of DG units are determined that are required to have equivalent reliability in an islanded network operation as in case of a grid connection without micro-source.

As it is currently not possible to simulate actual generation profiles with PSSTMSINCAL (only rated output power and control methods of the injection units are adjustable), new ways had to be found to evaluate this impact approximately. Conditional interruption probabilities $p_{Z,jK}$ are considered to demonstrate the relationship between generation and demand. When the output power is higher than the demand, there will be no interruption, and thus an improvement of reliability.

Thus, it is necessary in a first step to compare the annual load curve (ALC) and the annual generation curve (AGC) and to count the hours per year when the output is higher than the demand (fully supplied hours). In a second step a new ‘virtual’ operating point (rated power) of the DG unit is determined according to both the new input load ADC and the previous determined fully supplied hours of each unit in order to reach similar contribution to the eliminated interruptions during that duration by actual performance of the unit.

1.6.1.1 DG units with household load

In this chapter the impact of the micro-source technologies photovoltaic system (PV), wind turbines (WT), and CHP units (CHP) on the supply of household loads is analysed.

Photovoltaic (PV) generation

PV generation is of highly intermittent nature. A comparison of hourly load profiles of the household load with simultaneous PV generation for the case of a 100 % PV penetration demonstrates that – despite of equal installed capacities – PV generation is able to balance demand locally only for a limited number of hours per year (Figure 3-20). The definition of the *capacity ratio* is similar as the demand ratio in Section 1.4.1.1, with $p_G = P_G / P_{G_{\max}} = P_G / P_{Gr}$.

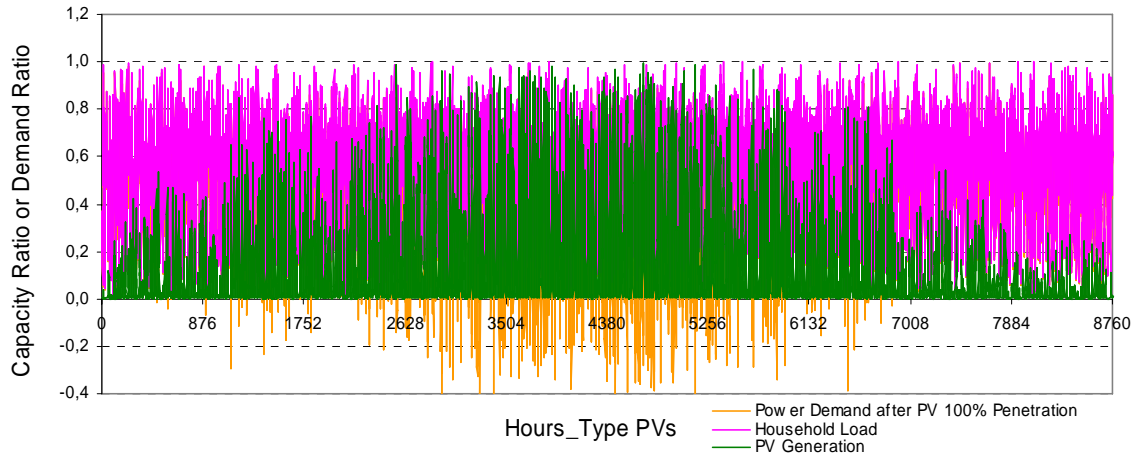


Figure 3-20 Hourly Household Load and PV Generation Profiles

The annual duration curves (ADC) of the corresponding power balances (Figure 3-21) can be calculated as the difference between load and generation. They are taken to determine new input ADC for the simulation of the reliability contribution of PV in PSSTMSINCAL.

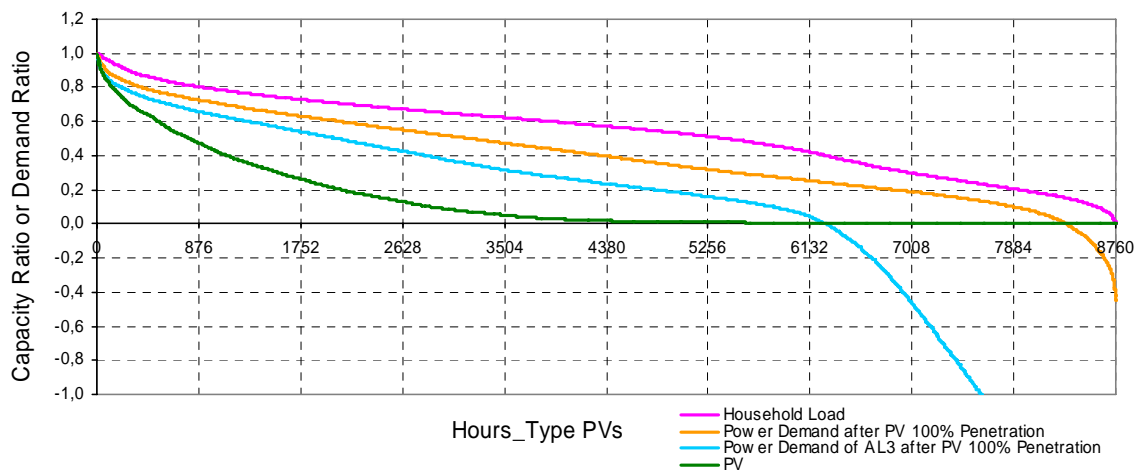


Figure 3-21 ADC of PV and the Household Load

In both figures, the pink and green curves represent the original load (here households) and generation profile; the orange curve is the residual power demand of the whole network in case of 100% penetration with PV units – named as state 1 according to the category 1) (global influence) in section 1.5.2.1. It is calculated from the actual shapes in Figure 3-20, the differences between the total network load and the instantaneous PV generation profile.

The blue curve is the residual power demand of the local load AL3 where PV generation is connected under the same situation that DG size is kept constant (rated power 1.267 MVA equal to 100% penetration that contributes to the supply of the load AL3 with a maximum demand of 300 kW) – named as state 2 (local influence). The negative values represent the surplus power from DG fed to the system when DG output power is higher than the demand. The number of hours with negative values also indicates the fully supplied hours by DG.

The description of the curves will be used throughout the whole chapter.

Wind turbines

Wind power is considered as one of the most important renewable energy sources (RES) worldwide. Besides large wind farms with installed capacities in the range up to GW connected to transmission networks (and therefore out of scope of this report), there are also single wind turbines connected to distribution networks.

Hourly profiles of the household load and simultaneous WT generation are plotted in Figure 3-22; the ADC is plotted in Figure 3-23.

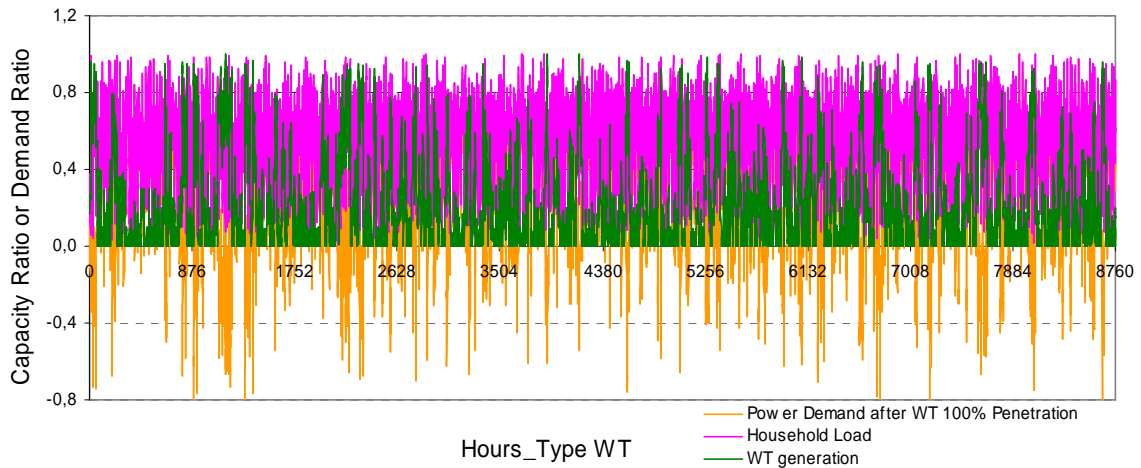


Figure 3-22 Hourly Household Load and WT Generation Profiles

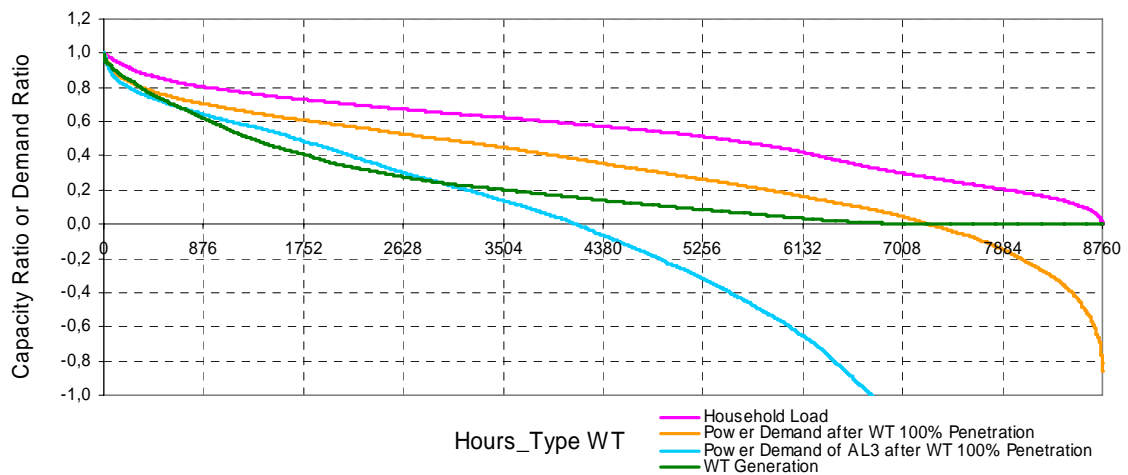


Figure 3-23 ADC of WT and the Household Load

CHP generation

CHP refers to an energy conversion process, where electrical power and useful heat are generated in a single, integrated system, operated either heat-driven or electricity-driven. In this report, heat-driven CHP operation mode is adopted for forming CHP generation curve, which means CHP generates heat as primary product while electricity as by-product, as generally heat-driven CHP is considered to be more efficient and consequently has a large number of applications, although with negative effects concerning reliability improvement.

There might be cases where the operation mode is changed from heat driven to electricity driven in case of failures in the network to enable a local supply in an isolated network (under the precondition that corresponding Microgrid technologies and sufficient (fuel) resources are available to allow this operation). However, this will only have effects on reduction of outage duration; an outage will occur nevertheless if due to limited power gradients the generation unit is not able to cover a suddenly increased demand.

Hourly profiles of the household load and simultaneous CHP generation are plotted in Figure 3-24, the ADC in Figure 3-25. The blue line of state 2 in Figure 3-25 has only negative values, as the CHP unit can fully supply the directly connected load AL3 at any time. In comparison to the generation based on RES, controllable CHP generation has a limited intermittency.

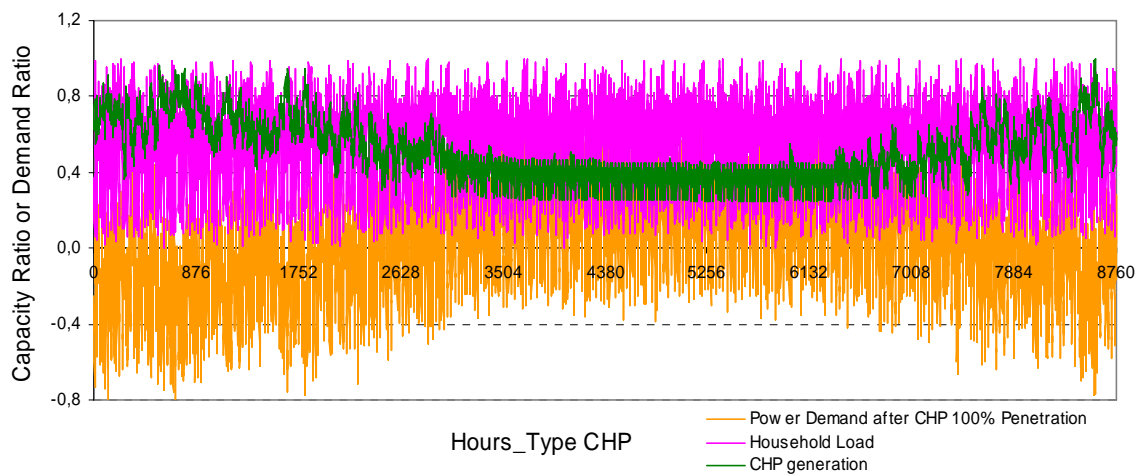


Figure 3-24 Hourly Household Load and CHP Generation Profiles

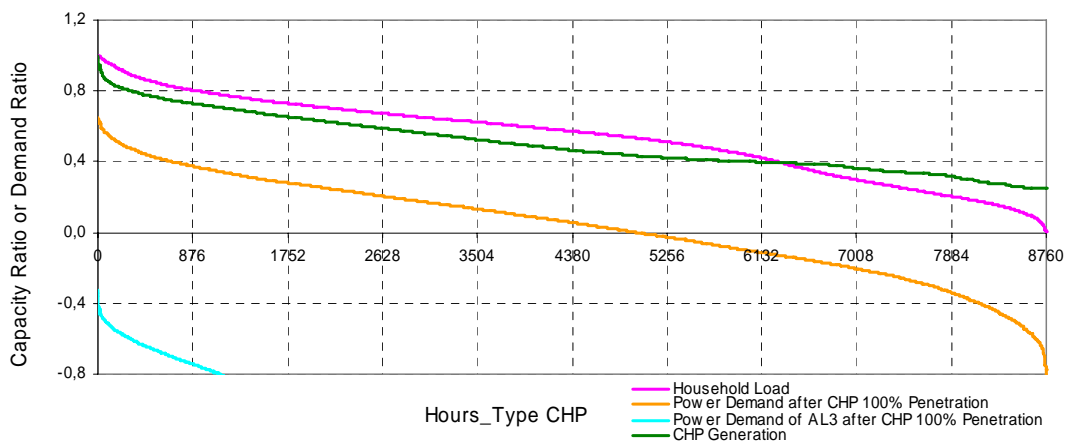


Figure 3-25 ADC of CHP and the Household Load

1.6.2 Probability distribution of Fully Supplied Hours

Figure 3-21, Figure 3-23 and Figure 3-25 indicate the power balance in case of a 100 % penetration of PV, WT or CHP units with household load. The load is only fully supplied by DG if the DG output is higher than the demand ($p_L - p_G < 0$).

The probability distribution of the power balance ($p_L - p_G$) is plotted in Figure 3-26 for all technologies. I.e., the probability of household load p_L lower than the CHP output p_G in one year ($p_L - p_G < 0$) is 0.4325. This indicates that the fully supplied hours in one year equal $0.4325 \cdot 8760h \approx 3788h$.

To have at least equal power balance with a 90 % probability in CHP option, 38 % of the rated power of demand should be covered by an additional supply possibility (such as grid connection or in case of isolated system by battery or other generation units). Concerning PV and WT more than 75 % of the rated power of demand has to be additionally supplied although there is a same installed capacity of generation and demand. Due to the high intermittency and the low output of renewable generation, there is a high probability that the load cannot be covered even if the installed capacities of generation and load are equal.

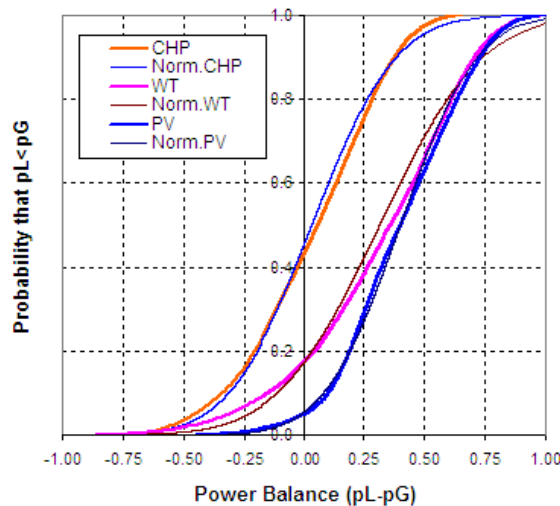


Figure 3-26 Probability of Power Balance $p_L - p_G$ (DER with Household Load)

The bold curves are directly taken from the annual profiles, as frequency distribution of the power balance.

Assuming load and generation to be normally distributed leads also to normal distributions of the power balance (plotted as thin curves in Figure 3-26) that fit quite well to the real distribution in case of a 100% penetration of PV, WT or CHP (Figure 3-26) (for further details see annex A.6).

With the calculation $\mu_z = \mu_x + \mu_y$ for the expected value and $\sigma_z = \sqrt{\sigma_x^2 + \sigma_y^2}$ for the standard deviation of two independent distributions [24], it is easy to calculate the probability of an equal power balance, as long as the parameters of the normal distribution are determined, and thus also the fully supplied hours for different mixtures of DG and different degrees of DG penetration without counting the hours.

1.7 Impact of Single DG Technology

1.7.1 Impact of PV (Scenario II)

The method can be realized in 3 steps:

1. Determining Input load ADC

From Figure 3-21, it can be seen that in state 1 (orange curve), 422 hours are fully supplied by PV while in state 2 (blue curve), 2491 hours are fully supplied by PV. In other words, from system's point of view, $H_{Z,K6}$, $H_{Z,L5}$ and $H_{Z,T1}$ for any of these four loads can be considered as zero during that 422 hours while from load AL3's point of view, $H_{Z,K5}$ and $H_{Z,L3}$ for AL3 can be considered as zero during that 2491 hours.

These fully supplied hours provide the boundaries for the creation of a new resulting input load ADC for the simulation in PSSTMSINCAL that is identified from the ADC of household load (red curve, Figure 3-27). The load factor LF needs to be constant also in case of this discretisation. Segments have to be distinguished for 422 h (step 1) and 2069h (2491h - 422h) (step 2) duration with a demand ratio equal to the mean of the load in each segment.

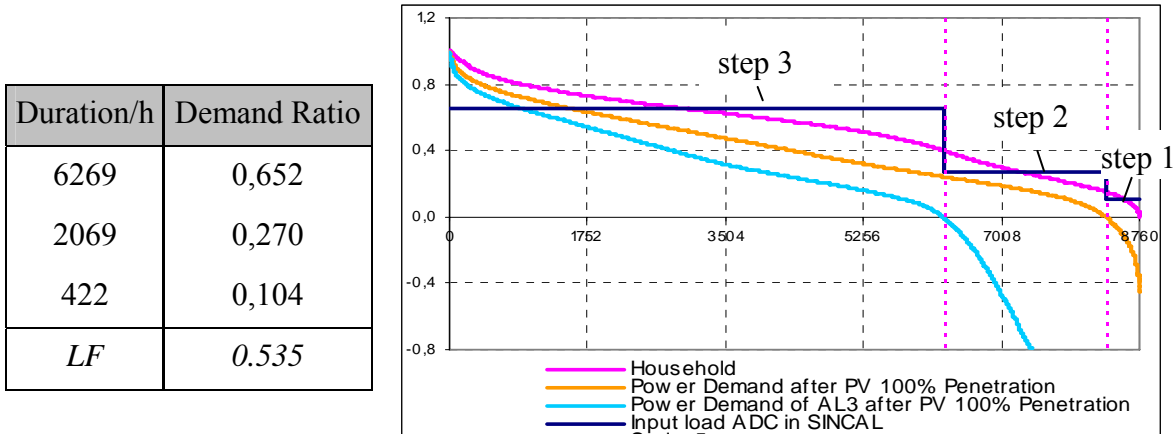


Figure 3-27 Input load ADC for PVs Option (Scenario II)

2. Determining Rated Power of DG

With this new input load ADC, the rated power of DG units can be determined to meet the requirements for both states, the coverage of the total network demand and the local supply. This means in state 1, DG output power is between the demand ratio of the total load between step 1 and 2, while in state 2, DG output power is between the demand ratio of the local load in K3 between step 2 and 3. Consequently, there is

- for state 1: $0.104 \times 1.267MVA < P_{Gr} < 0.27 \times 1.267MVA$,
- for state 2: $0.27 \times 0.3MVA < P_{Gr} < 0.652 \times 0.3MVA$,

and thus $P_{Gr} \in (0.132, 0.196)MVA$. As we have seen in the previous chapter, there is the same effect on reliability as long as generation is within these limits assuming pessimistic power allocation. Therefore, $P_{Gr} = 0.18MVA$ is chosen.

3. Reliability Results

Table 3-12 shows the reliability indices of this PV option according to adopted load ADC and rated PV power of DG units. The improvement of network result in comparison with *Base Case H* is also given.

Node	Hu [1/a]	Qu [min/a]	Tu [h]	Pu [MVA/a]	Wu [MVAh/a]
K1	0,027493	15,05024	9,123577	0,005053	0,046218
K2	0,027871	15,39044	9,203275	0,004608	0,042506
K3	0,025968	14,68843	9,427304	0,004503	0,042158
K4	0,028816	16,24094	9,393373	0,005289	0,049759
Network	0,031818	18,55814	9,720912	0,019453	0,180641
<i>Base Case H</i>	<i>0.033275</i>	<i>19.5183</i>	<i>9.776258</i>	<i>0.01976</i>	<i>0.183309</i>

Table 3-12 Reliability Indices of PV Option

With a considered confidence interval of 90 %, the network indices are compared in Table 3-13 in respect to *Base Case H*.

90% Confidence Interval	Hu (1/a)	Qu (min/a)	Pu (MVA/a)	Wu (MVAh/a)
<i>Base Case H</i>	(72%) <0.1	0-52	0-0.053	0-0.49
<i>Scenario II (PVs)</i>	(73%) <0.1	0-50	0-0.052	0-0.48

Table 3-13 Network Indices Comparison between PV Option and Base Case H

1.7.2 Impact of WT (Scenario III)

Determining Input Load ADC

From Figure 3-23, it can be seen that in state 1 (orange curve), 1527 hours are fully supplied by WT, while in state 2 (blue curve), 4610 hours are fully supplied by WT. Therefore, the input load ADC for WT option can be identified as plotted in Figure 3-28.

Duration/h	Demand Ratio
4150	0,743
3083	0,454
1527	0,135
<i>LF</i>	<i>0.535</i>

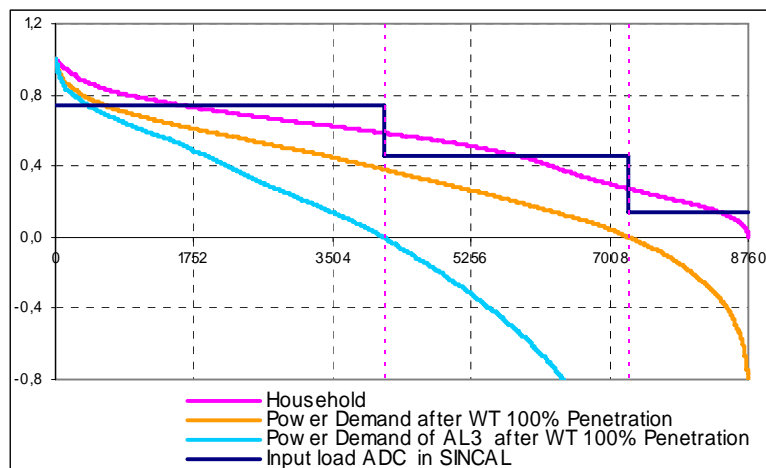


Figure 3-28 Input load ADC for WT Option (Scenario III)

1. Determining Rated Power of DG

From Figure 3-28 it can be derived:

- for state 1: $0.135 \times 1.267 MVA < P_{Gr} < 0.454 \times 1.267 MVA$;
- for state 2: $0.454 \times 0.3 MVA < P_{Gr} < 0.743 \times 0.3 MVA$,

and thus $P_{Gr} \in (0.171, 0.223) MVA$. Therefore, here $P_{Gr} = 0.21 MVA$ is chosen.

2. Reliability Results

The reliability indices of WT option are listed in Table 3-14, compared with the network result of *Base Case H*.

Node	Hu [1/a]	Qu [min/a]	Tu [h]	Pu [MVA/a]	Wu [MVAh/a]
K1	0,024813	13,45125	9,035151	0,004922	0,044917
K2	0,025191	13,79145	9,124657	0,00449	0,041336
K3	0,021347	12,20287	9,52754	0,00411	0,038887
K4	0,026136	14,64195	9,337093	0,005158	0,048458
Network	0,028769	16,66182	9,652543	0,01868	0,173599
<i>Base Case H</i>	<i>0,033275</i>	<i>19,5183</i>	<i>9,776258</i>	<i>0,01976</i>	<i>0.183309</i>
<i>Improvement</i>	<i>13,54%</i>	<i>14,63%</i>	<i>1,27%</i>	<i>5.47%</i>	<i>5.30%</i>

Table 3-14 Reliability Indices of WT Option

With a considered confidence interval 90%, the network indices are compared in Table 3-15. The improvement is with respect to *Base Case H*.

90% Confidence Interval	Hu (1/a)	Qu (min/a)	Pu (MVA/a)	Wu (MVAh/a)
<i>Base Case H</i>	(72%) <0.1	0-52	0-0.053	0-0.49
<i>Scenario III (WT)</i>	(75%) <0.1	0-45	0-0.050	0-0.47
<i>Improvement</i>		0%-13.5%	0%-5.66%	0%-4.08%

Table 3-15 Indices Comparison between WT Option and Base Case H

1.7.3 Impact of CHP (Scenario IV)

1. Determining Input Load ADC

From Figure 3-25, it can be seen that in state 1 (orange curve), 3788 hours are fully supplied by WT, while in state 2 (blue curve), 8760 hours are fully supplied by CHP. Therefore, the input load ADC for CHP option can be identified as plotted in Figure 3-29.

Duration/h	Demand Ratio
4972	0.698
3788	0.322
<i>LF</i>	<i>0.535</i>

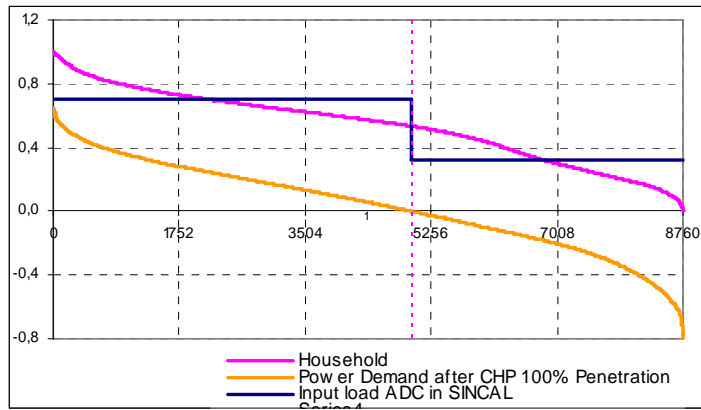


Figure 3-29 Input load ADC for CHP Option (Scenario IV)

CHP units itself, as traditional fuel generators, have – depending on size, manufacturer and technology - an availability between 80% to 99% according to heat- or electricity-driven operation mode. Here it is assumed that the reliability of CHP unit is 90%.

2. Determining Rated Power of DG unit

From Figure 3-28, it can be derived

- for state 1: $0.322 \times 1.267 MVA < P_{Gr} < 0.698 \times 1.267 MVA$;
- for state 2: $P_{Gr} > 0.3 MVA$,

and thus $P_{Gr} \in (0.408, 0.884) MVA$. Therefore, $P_{GR} = 0.6 MVA$ is chosen.

3. Reliability Results

The reliability indices of the CHP option are listed in Table 3-16 (with 100 % availability of CHP unit), and in Table 3-17 (with 90 % availability of CHP unit), each compared with the network result of *Base Case H*.

Node	Hu [1/a]	Qu [min/a]	Tu [h]	Pu [MVA/a]	Wu [MVAh/a]
K1	0,019328	10,17946	8,777781	0,004103	0,036778
K2	0,019706	10,51966	8,897136	0,003754	0,034011
K3	0,012061	7,194757	9,942117	0,002526	0,02511
K4	0,020651	11,37016	9,176404	0,004339	0,04032
Network	0,022563	12,80776	9,460707	0,014722	0,136218
<i>Base Case H</i>	<i>0,033275</i>	<i>19,5183</i>	<i>9,776258</i>	<i>0,01976</i>	<i>0,183309</i>
<i>Improvement</i>	<i>32,19%</i>	<i>34,38%</i>	<i>3,23%</i>	<i>25,50%</i>	<i>25,69%</i>

Table 3-16 Reliability Indices of CHP Option (100 % available)

Node	Hu [1/a]	Qu [min/a]	Tu [h]	Pu [MVA/a]	Wu [MVAh/a]
K1	0,020644	10,68729	8,628437	0,00423	0,037608
K2	0,021022	11,02749	8,743009	0,003868	0,0347578
K3	0,014527	8,069097	9,257273	0,002825	0,0268381
K4	0,021967	11,87799	9,012185	0,004466	0,0411498
Network	0,024148	13,4385	9,275188	0,015389	0,1403537
Base Case H	0,033275	19,5183	9,776258	0.01976	0.183309
Improvement	27,43%	31,15%	5,13%	22,12%	23,43%

Table 3-17 Reliability Indices of CHP Option (90% available)

With a considered confidence interval of 90 %, the reliability indices for the network as well as the improvement with respect to *Base Case H* are compared in Table 3-18.

90% Confidence Interval	Hu (1/a)	Qu (min/a)	Pu (MVA/a)	Wu (MVAh/a)
Base Case H	(72%) <0.1	0-52	0-0.053	0-0.49
Scenario IV (CHP, 100 % available)	(80%) <0.1	0-34	0-0.039	0-0.37
Scenario IV (CHP, 90 % available)	(80%) <0.1	0-35	0-0.041	0-0.38

Table 3-18 Indices Comparison between CHP Option and Base Case H

1.7.4 Consideration of Intermittency with reduced DG availability

The reliability results in previous sections are simulated considering the real time-dependent intermittency of DG units in parallel with given real time-dependent load profiles. A common approach in literature to consider this 'reduced' availability of DG unit due to primary resources unavailability is to assume a constant operation of the units, but, with a reduced availability. This section is dedicated to determine if this approach is valid as such a simulation is much less demanding.

For this, DG unit are modelled with a constant output, but, with only 15% (PV), 22% (WT) or 50% (CHP) availability, with respectively 1314 h/a, 1927 h/a or 4380 h/a in operation. Table 3-19 demonstrates the DG reliability input data (2 schemes with fixed failure rate $H = 100$ 1/a and $H = 10$ 1/a).

DER Reliability	15%	22%	50%	15%	22%	50%
	PV	WT	CHP	PV	WT	CHP
H [1/a]	100	100	100	10	10	10
T [h]	74.46	70.08	43.8	744.6	700.8	438

Table 3-19 Input data of highly unavailable DG Units

The reliability indices achieved in the different simulation modes are compared in Figure 3-30. Different setting of failure rate and down time of DG unit under same unavailability duration impacts only reliability indices H_u and P_u , but shows almost no difference in Q_u and W_u .

Generally, it can be seen that interrupted power and energy not supplied is underestimated by the simulation approach with constant DER operation with a maximum error around 20%.

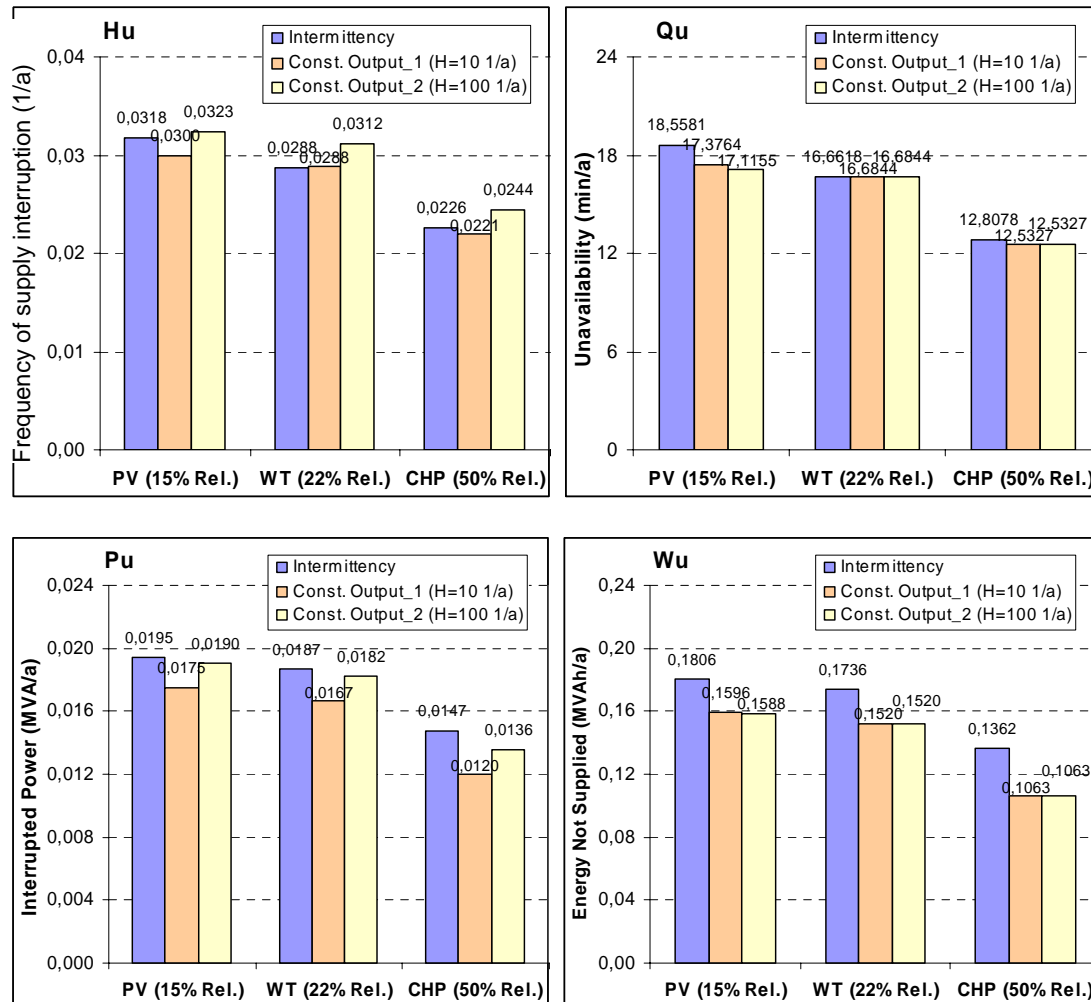


Figure 3-30 Reliability Comparison Concerning Different Simulation Modes

Thus, the simple simulation method is applicable as long as only rough estimates about the impact on reliability are required. For more precise analysis it is necessary to consider time-dependent intermittency.

1.7.5 Comparison of Reliability Impact of Different DG Types

The reliability is obviously improved by the penetration of DG units, but the degree of improvement varies for each DG option. CHP units have the most significant contribution to the improvement of reliability because of the continuous and stable generation. PV units contribute on lowest degree to a reliability improvement due to their relatively low power availability. WT units are in between.

Furthermore, the degree of improvement varies by different indices -- The mean duration of interruption has only a slight improvement as it is mainly dependent on the remedial measures which are almost neglected in this simple network; and other indices are all improved with a considerable degree.

The comparison of reliability indices in each DG option can be easily seen in Figure 3-31 for H_u, Q_u, P_u and W_u respectively. The indices of *Base Case H* and *Scenario I-H* are plotted as well. Furthermore, the reliability improvement of each DG option and *Scenario I-H* in comparison with *Base Case H* are listed in Table 3-20.

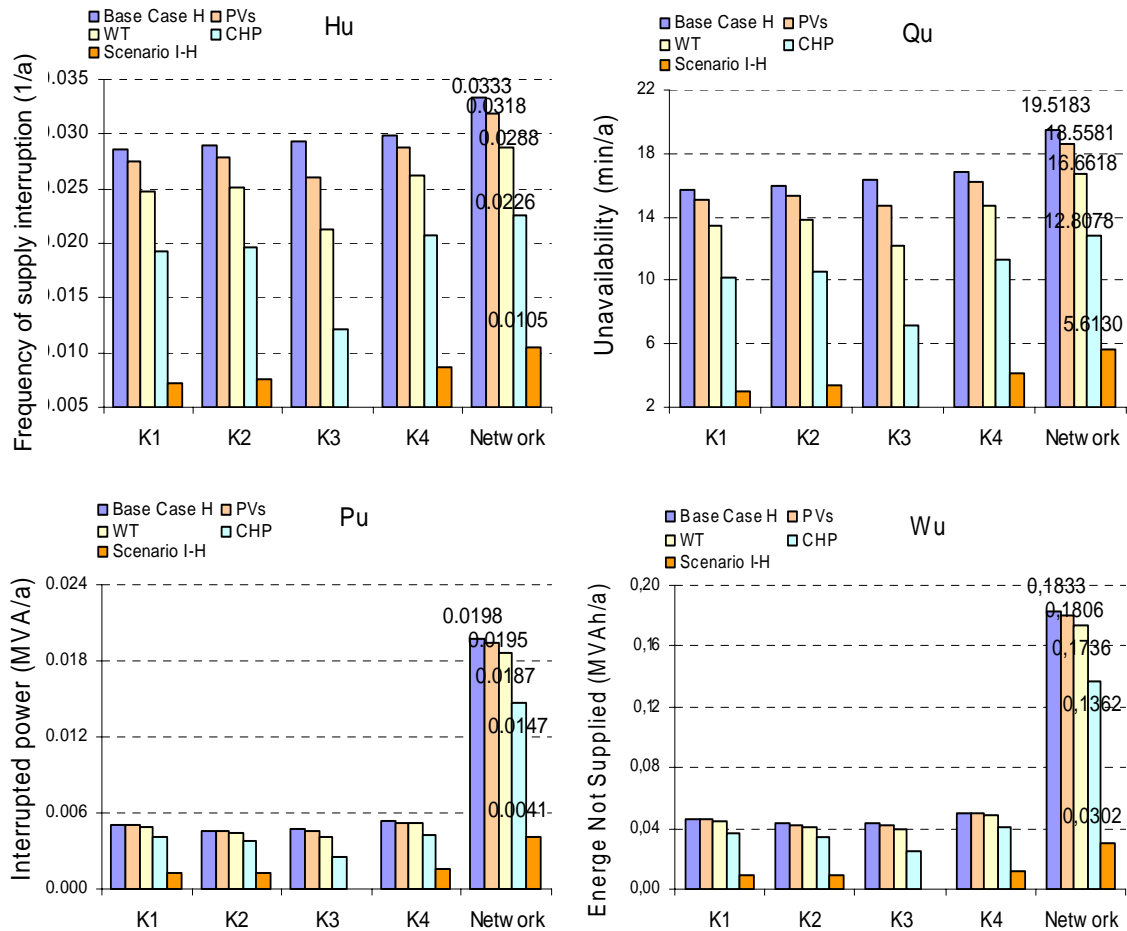


Figure 3-31 Reliability Indices depending on Different DG Types

Improvement (%)	H_u (1/a)		Q_u (min/a)		P_u (MVA/a)		W_u (MVAh/a)	
	$E(x)$	Probability	$E(x)$	Probability	$E(x)$	Probability	$E(x)$	Probability
Base Case H	0.0333	(72%) <0.1	19.5183	0-52	0.0198	0-0.053	0.1832	0-0.49
Scenario I-H	68.4%	(90%) <0.1	71.2%	0%-75%	79.3%	0%-83%	83.5%	0%-85.7%
Scenario II	4,4%	(73%) <0.1	4,9%	0%-3.8%	1.6%	0%-1.9%	1.5%	0%-2.0%
Scenario III	13,5%	(75%) <0.1	14,6%	0%-13.5%	5.5%	0%-5.7%	5.3%	0%-4.1%
Scenario IV	32,2%	(80%) <0.1	34,4%	0%-34.6%	25.5%	0%-26.4%	25.7%	0%-24.5%

Table 3-20 Reliability Improvement by different DG Options, Base Case H and Scenario I-H

The improvement concerning different indices is plotted in Figure 3-32.

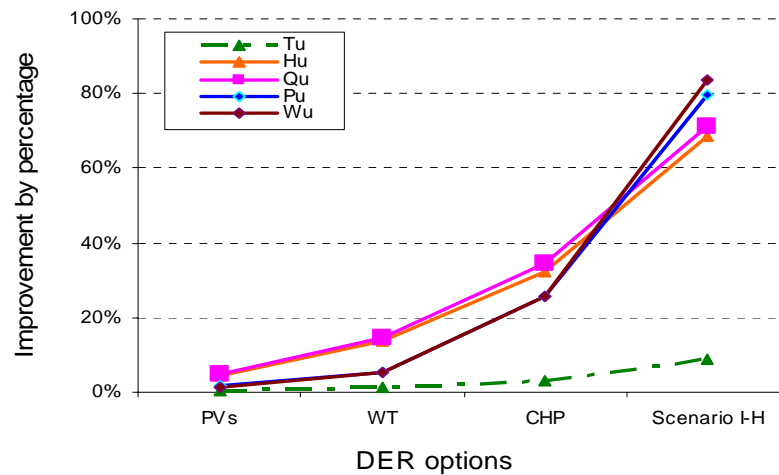


Figure 3-32 Reliability Improvement by Each DG Option Concerning Different Indices

From the comparison between each DG option and *Scenario I-H*, it can be seen that the reliability improvement by actual DG penetration is much less than the scenario with fixed operating point of DER, which proves that it is necessary to consider the correlation of generation profile and load profile rather than using the fixed output power of generation and constant load demand (chapter 1.5), especially for intermittent energy resources.

Furthermore, Figure 3-31 also indicates that reliability of node K3 shows the highest improvement of all three options as the DG unit is directly connected there.

1.8 Reliability Impact of Demand Side Management

There are two possibilities to have an equal power balance locally, increased generation or measures on the demand side such as a general reduction of the demand. This section therefore aims at the question with which approach a higher reliability contribution is achieved: simulation of DG penetration or modelling the load with lower LF, both resulting in equal power flow in the network.

The WT is taken as an example in this study. The orange curves in Figure 3-23 or Figure 3-28 indicate the actual power demand in case of 100% WT penetration (installed capacity equals demand), which is obviously less than the original demand of household load (pink curve). To simulate the equivalent power demand as with WT, one load ADC was identified with same LF as the orange curve in WT option (Scenario LM) (Figure 3-33).

The negative values in orange curve is the surplus power from WT fed back into the network; from the demand point of view, these values can be considered as zero (demand ratio is approximated to be 0.01 as zero is an unacceptable input value in PSSTMSINCAL).

Duration/h	Demand Ratio
4150	0,743
3083	0,454
1527	0,135
LF	0.535

Scenario III (WT penetration)

Duration/h	Demand Ratio
4972	0.593
3083	0.205
1527	0.01
LF	0.355

Scenario LM (Lower LF)

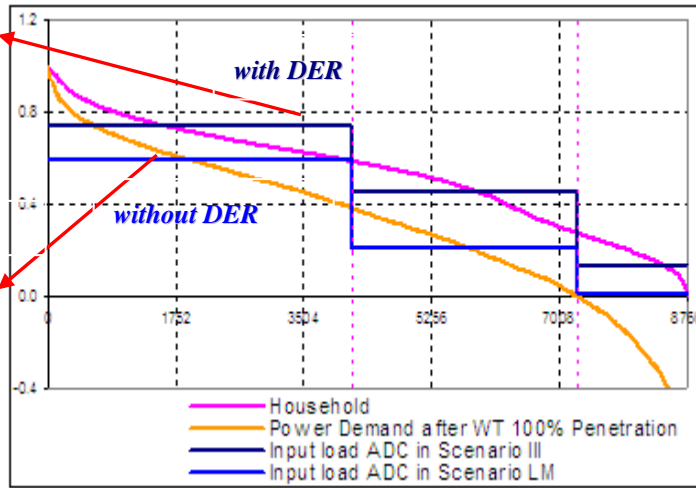


Figure 3-33 Load ADC of Scenario III and Scenario LM

The reliability indices are shown in Figure 3-34. The specific settings of three cases are:

- *Base Case H*: without DER; 3 – states household ADC with LF 0.535
- *Scenario III*: with WT penetration; 3 – states household ADC with LF 0.535
- *Scenario LM*: without DER; 3 – states ADC with LF 0.355 (equivalent power demand as WT penetration)

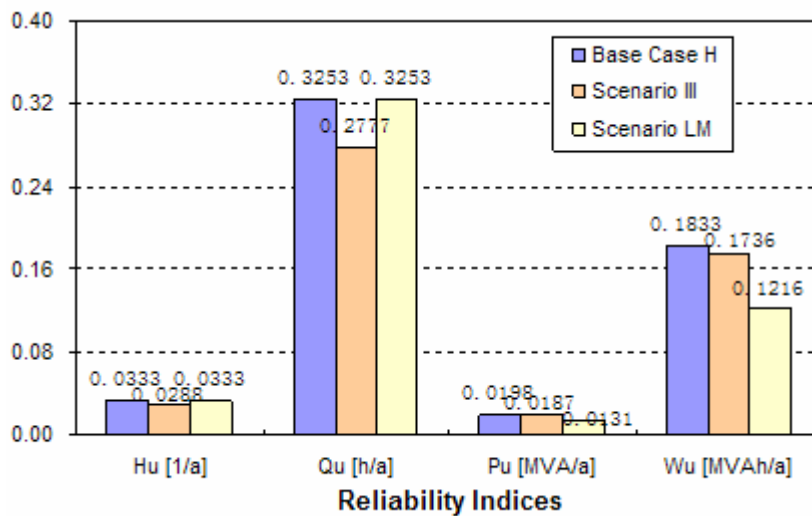


Figure 3-34 Reliability Comparison between Scenario III and Scenario LM

While in *Scenario III with WT* all reliability indices get improved shows *scenario LM* only impact on power related indices P_u and W_u ; H_u and Q_u keep constant as *Base Case H*. As there is less demand to be covered in scenario LM the reduction in P_u and W_u is even higher than in scenario III for pessimistic power allocation mode as restricted power is unacceptable in this case; the improvement of P_u and W_u equals the case of WT installation in optimistic mode (Equation A -7).

1.9 Impact of DG Allocation

1.9.1 General Allocation Options – 100% Penetration Level

With discussions in the last section, impact of each single DG penetration option has been already modelled and compared. This section is primarily focused on the optimization of mixed DG allocation for the attempt of optimum reliability improvement.

Technical analyses based on loss reduction and peak reduction determined optimum allocation for CHP-PV-WT in the network, in radial network ideally from the end-feeder to upstream with such an order.

Furthermore, 7 possible DG options based on the allocation order CHP-PV-WT are checked: single CHP, single PV, single WT (introduced in the last section), CHP-PV, CHP-WT, PV-WT, and CHP-PV-WT. Due to the properties of PV, such as zero power output during night time and relatively low capacity ratio, it is not preferable to apply single PV to the nodes in most of the cases, but is favourable for CHP-PV or PV-WT due to the good compatibility of PV while concerning the contribution to loss reduction.

One of the most important targets of DG penetration is to sustain *system adequacy* in island mode. Thus it is necessary to examine simultaneous generation and load profiles in each allocation option. Intuitively, in other words, the evaluation of the reliability is to count the fully supplied hours in one year of each DG penetration option.

Three typical load profiles (taken from the standard German load profiles) are studied in this section: industry load always need a certain electricity demand to satisfy the ordinary production; in contrast, commercial load demand can be varied in large scale dependent on the time of business activities; and household load is in between (Figure 3-35).

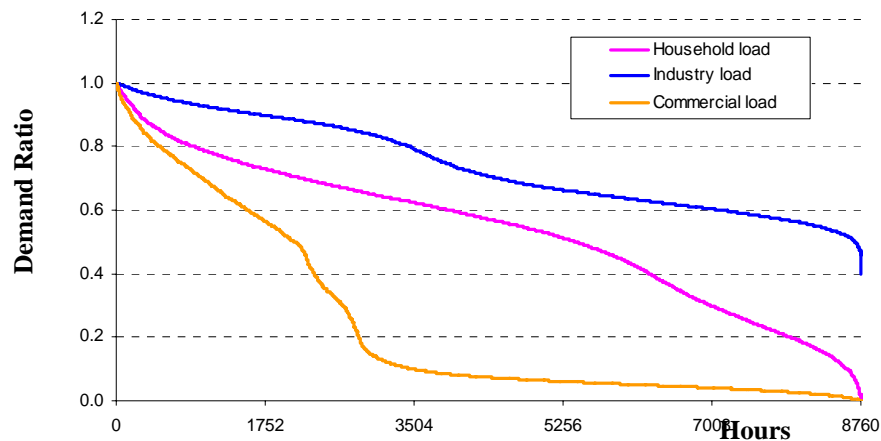


Figure 3-35 ADC of Household Industry and Commercial Load Profile

During computational processes, 1 % allocation rate step for progressive allocation schemes under 100% PL is adopted and the optimum allocation rate, which is in accordance with maximum possible fully supplied hours under this allocation rate in each option, is listed in Table 3-21.

Load profiles	DER options	1	2	3	4	5	6	7
Household	CHP (%)	100			99	99		98
	PV (%)		100		1		1	1
	WT (%)			100		1	99	1
	Fully supplied Hours (h)	3788	422	1527	3747	3758	1506	3718
Industry	CHP (%)	100			99	99		98
	PV (%)		100		1		1	1
	WT (%)			100		1	99	1
	Fully supplied Hours (h)	1258	102	549	1211	1223	529	1161
Commercial	CHP (%)	100			99	99		98
	PV (%)		100		1		14	1
	WT (%)			100		1	86	1
	Fully supplied Hours (h)	6835	1725	4173	6821	6824	4190	6814

Table 3-21 Maximum Possible Fully Supplied Hours of DG Options

CHP units always occupy the most of the percentages during the mixed DG options, in order to achieve the best reliability, i.e. the maximum possible fully supplied hours. It is because CHP units are to a certain extent controllable injection units and hence can provide more stable output power than any other RES.

On the other hand, the reliability could achieve higher improvement with the PV-involved mixed options in comparison with the single PV option. Furthermore, the best cases in PV-involved mixed options always occur with low allocation rate of PV.

The generation of WT is strongly dependent on the complicated geographic and weather conditions which generally have no obvious time or season dependent disciplines. Thus it is hard to find even the rough relationship between the WT output and the load demand. The best case of mixed PV-WT option with industry load shows reliability better than single PV but slightly worse than single WT; but with commercial load, the reliability of this option is better than the both of the single options.

1.9.2 DG is Islanded Operation in Comparison with Grid Connection

As we have seen in last section, 100 % DG penetration is far away from sufficient system adequacy. Considering islanded operation mode, it is necessary to investigate the DG capacity required to achieve a reliability level equivalent to grid connection.

The grid connection is considered as slack node here, having a capacity always equal to the demand. It is assumed to be 100% reliable, and can therefore fully supply all the loads during the whole year. The objective of this section is to observe the DG size (penetration level of assumed 100% reliability DG) of each allocation option that can also fully supply all the loads during one year.

Common approaches only define DG units with an availability factor and demand with a constant value for sake of simplicity. In fact, especially for intermittent RES, the availability factor (taking primary sources availability into account) is very low, such as 0.2 for wind farm or even lower for PV; another unit of the same intermittency type is probably not available either. Therefore, the resulting DG size from the simplicity may make no sense to cope with the intermittency in reality and hence in this section the synergy of generation and load profiles is considered.

Due to their high intermittency it is unfeasible to use only the single technology WT or PV to fully supply the load within the whole year (8760 h), and in a similar way, neither does a combination of both (PV-WT). Only the combination of intermittent generation units based on RES with controllable units or storage units can achieve an equivalent reliability as a grid connection, i.e. usage of single CHP, CHP-PV, CHP-WT and CHP-PV-WT. Table 3-22 shows the minimum PL of the DG in each option that can fully supply the load over 8760 h and one of the possible allocation schemes that was successively computed with 1 % rate step.

It can be seen that in most cases around 300 % DG capacity are required to act as a similar slack node as the main grid and consequently have the equivalent reliability contribution to the network as the main grid normally does when DG is in islanded operating mode.

Load profiles	DER options with allocation rate	1	2	3	4
Household	CHP (%)	100	98	98	98
	PV (%)		2		1
	WT (%)			2	1
	Minimum PL of DG Fully Supplying Loads	2.93	2.99	2.98	2.98
Industry	CHP (%)	100	96	97	96
	PV (%)		4		2
	WT (%)			3	2
	Minimum PL of DG Fully Supplying Loads	2.95	2.99	3	3
Load profiles	DER options with allocation rate	1	2	3	4
Commercial	CHP (%)	100	73	74	73
	PV (%)		27		1
	WT (%)			26	26
	Minimum PL of DG Fully Supplying Loads	2.2	2.98	2.97	2.98

Table 3-22 Equivalent Reliability Contribution between DG Island Mode and Grid Connection

CHP occupies the largest allocation rate in all of the options as the previous studies. But it should be noticed that the allocation rate shown in Table 3-22 is not the unique one. For example, in the option CHP-PV with industry load, the allocation rate appears as $CHP : PVs = 94% : 6%$. It means, to fully supply the load with 8760h, the percentage of CHP is at least 94%, and this option can keep on meeting the target if the percentage of CHP is above 94%. By analogy, in the option CHP-PV-WT with commercial load $CHP : PVs : WT = 73% : 1% : 26%$, once the minimum percentage of CHP 73% with the minimum percentage of PV 1% is achieved, any further larger percentage of PV like 2% with 73% of CHP, or any further larger percentage of CHP like 74% with any rate of PV, can both meet the target of fully supplying the load at any time in one year. All of the other cases in Table 3-22 are in accordance with this analysis.

Figure 3-36 indicates the probability of DG fully supplying loads depending on the PL ranging from 0 % to 300 % (accuracy 1%). With this figure, the DG penetration level required to cover the load with a given probability can easily be derived. Further, the penetration level required to fully supply the load can also be determined; e.g. with a 90% probability of fully supplying household load, 203 % DG penetration is required.

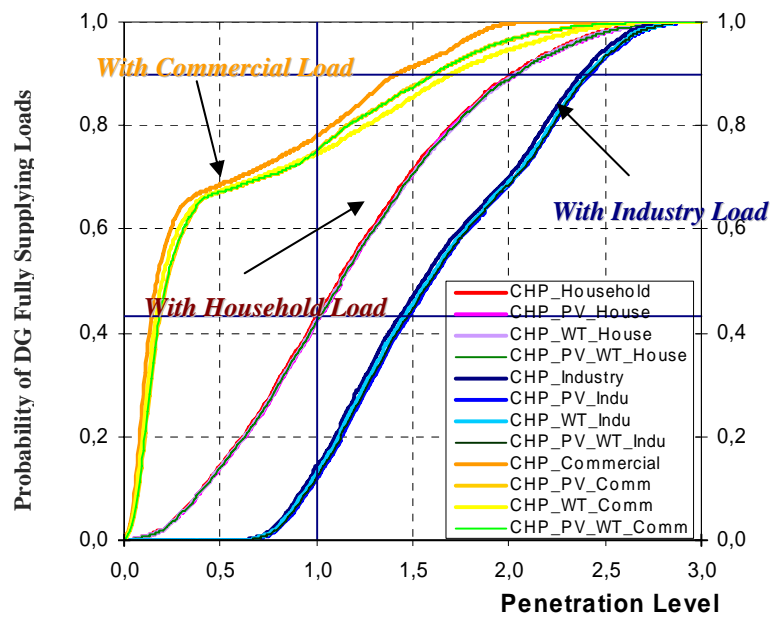


Figure 3-36 Probability of DG Fully Supplying Loads by Different Penetration Level

1.9.3 Summary

Similar as the studies of single DG option in last section, the idea of reliability analysis focused on DG allocation is to count the hours in one year when micro-sources can fully supply the load. Under the same evaluation criteria, the single CHP option is the most effective one to improve the reliability. The best case of any other options together with CHP turns out to be with the allocation rate of CHP as high as possible.

To have equal reliability in islanded mode as in case of grid connection a minimum DG penetration around 300 % is required, but, only in combination with CHP or any further storage units.

The results strongly depend on the yearly shapes of different load segments and of generation units. In this example standard values from Germany were taken.

1.10 Conclusions of Simple Network Analysis

This section summarizes the main observations from the analysis of the simple network. First of all, some limitations of the method applied need to be mentioned:

- The method has a high accuracy in highly meshed networks; however, the errors in radial networks are considerably large.
- Reactive power Q was not considered. Actually Q is assumed to be always balanced with the control method of DG unit in reliability configurations of PSSTMSINCAL. Consequently, all the calculations are based on active power only.
- All the DG units are directly connected to the load nodes, furthermore, for one single node, only one DG type is considered.

The impact of DG on the reliability of the simple network was studied by two general approaches: with constant DG operation and with analysis of time-dependent synergy of generation and load profiles.

Analysis with Constant DG Operation

In this approach, four aspects were observed separately:

- **Impact of DG capacity**

The power allocation mode, either pessimistic or optimistic, contributes only to the power related indices P_u and W_u . Higher reliability improvements are achieved in optimistic mode, continuously with respect to the increasing PL.

Without load priority pessimistic mode: both node and network reliability indices H_u , Q_u , P_u and W_u were improved stepwise and evenly with increasing PL according to the input load ADC.

Without load priority optimistic mode: both node and network reliability indices of P_u and W_u were improved continuously and evenly with the increasing PL.

With load priority pessimistic mode: the node with higher LP had the priority in time sequence to improve all the node reliability indices, with the improving principle to each node the same as the case without LP; network indices of H_u and Q_u were not improved until the reliability of the node with lowest priority is improved, while P_u and W_u would be improved as long as any of the individual node $P_{u,k}$ and $W_{u,k}$ decreased (discretely).

With load priority optimistic mode: the node indices of $P_{u,k}$ and $W_{u,k}$ were improved continuously with the increasing PL, but unevenly due to the varied LP, network indices of P_u and W_u would be improved as long as any of the individual node $P_{u,k}$ and $W_{u,k}$ decreased, but with continuous improving trend.

- **Impact of Numbers of DG Units**

Under the same PL (100 %), one or more DG units were sharing the total DG capacity during simulations. The reliability improvement is dependent on both the capacity of each single DG unit and the location of that unit and hence the best scheme could be obtained when most of the end-customers in DG supply area were fully supplied by the deployment of total DG units.

- **Impact of DG Location**

The most downstream location that DG was connected performs the best reliability as DG can reduce the impact of outages which were in the upstream of the DG location. However, it might not be the optimal choice at the most downstream location in practice due to potentially large amount of surplus power that DG unit produced.

- **Impact of DG Availability**

Several schemes of DG availability, ranging from 95% to 99.9%, were simulated in this aspect. The reliability indices were definitely getting worse compared to 100% DG reliability, however, the difference was not significant as the impact of DG outages contributed to the reliability performance only with coexistence of other component failures, which could result in system deficit. Furthermore, along with decreasing DG reliability, both node and network reliability were getting worse with linear characteristics.

Analysis considering simultaneous Generation and Load Profiles

- **Impact of DG Technology**

The household load profile was chosen to analyse the synergy with each DG generation profile in order to simulate the actual intermittency.

CHP units had the most significant contribution to the improvement of reliability because of their relatively constant output.

To install DG or to cut part of loads could both reduce power demand; under the same criteria, DG reduce all network indices H_u , Q_u , P_u , and W_u , while cutting the load impacts only the power related indices P_u , and W_u .

The reliability improvement considering real intermittency is much less as with assumption of a constant output; DG units only contribute to a reliability improvement when the power output is higher than the demand.

- **Impact of DG Allocation**

Four mixing allocation schemes with allocation order CHP-PV-WT, apart from three single options were observed respectively in accordance with household, industry and commercial load profiles.

A high percentage of total DG penetration should be covered CHP units (or similar controllable technologies with low intermittency) to get the best reliability performance.

With aforementioned findings, following approaches for effectively improving network reliability are recommended (Figure 3-37):

- In order to achieve a considerable reliability improvement, CHP units or other controllable resources should be considered first. With only CHP or in combination with WT or PV technology in which CHP occupies a high percentage, 200% PL can cover nearly 90 % household load.
- After the planned capacity of total DG is determined, it is better to deploy several DG units to different customer nodes, each with relatively small installed capacity (but sufficiently large to supply local demand), than to deploy only one unit to one node with large capacity.
- In radial network, moving the DER units to downstream location could lead to better reliability.
- Load profiles should be concerned attentively while planning DG penetration, as it influences the reliability performance significantly with synergy of DER generation profiles.

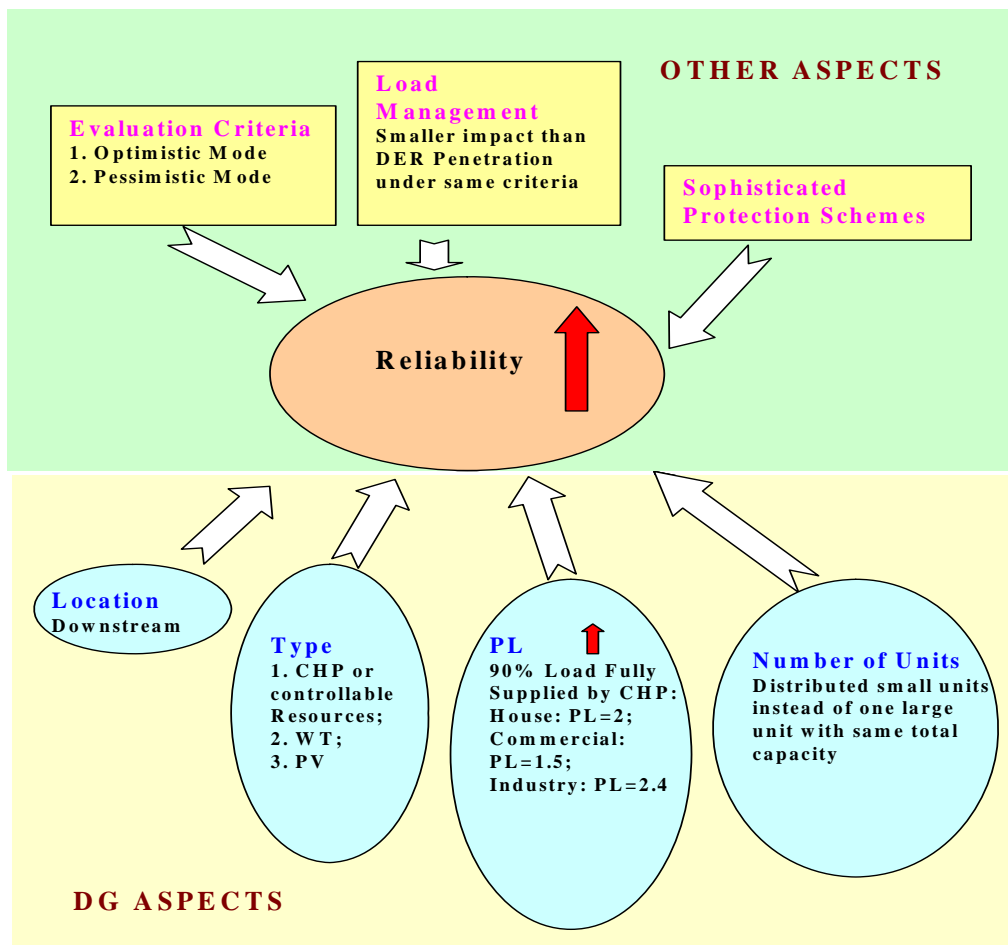


Figure 3-37 Recommendations for Reliability Improvement

4 Analytical reliability analysis directly considering reliability contribution of micro-sources

In this approach, based on the results of ZUBER simulation part, reliability indices are calculated by the analytical method.

1.11 Stochastic load demand and DG generation modelling

For the further analysis of ZUBER simulation result, stochastic load demand and DG generation has to be modelled. Many papers have been published regarding probabilistic load flow computations [54]-[58], taking into account stochastic load demand and DG generation. Different strategies of modelling stochastic property of load and generator are proposed in these papers. In paper [57] DG generation and load demand are modelled by hourly time-series data. Large amounts of time-series data are required to be manipulated by this method, especially when modelling many micro-sources. DG and load can normally be approximated as normal distribution which avoids the time consuming convolution process. In papers [54] and [56] a more accurate strategy of combined cumulants and Gram-Charlier expansion are described to solve this problem. In principle simplified normal distribution is the case that only two orders cumulants are considered by the strategy of combined cumulants and Gram-Charlier expansion, so both methods can be categorized as one strategy. The basic reliability calculation of DG unit and load can be reflected by the following function

$$P_{net} = P_L - P_G \quad \text{Equation 4-1}$$

Where P_L is the load demand, P_G is the DG power; assuming one load and one DG work in island, when P_{net} is higher than 0, end-customer is interrupted. In contrary, when P_{net} is lower than 0, end-customer is fully supplied. Other interruption indices are based on the result of this formula.

This formula is similar with the net flow computation applied in the power flow calculation, so the method of stochastic modelling applied in the power flow calculation can be also used in the reliability calculation.

An advantage of combined cumulant and Gram-Charlier expansion (CGCE) is that the summation of two **independent** variables can be done by the summation of their cumulants, which avoid the time consuming convolution process. This dramatically reduces the computation time. For example when considering only the base order cumulant Gram-Charlie expansion of the stochastic variable, the distribution of these variables are simplified to normal distribution, so the summation of such two variables is still normal distribution ,and the mean value and standard deviation are the corresponding summed mean and deviation of these two variables

$$U = X + Y = Normal(\mu_x + \mu_y, \sigma_x^2 + \sigma_y^2) \quad \text{Equation 4-2}$$

One assumption of this good property is that the variables applied in this method should be independent. However, DG units and loads are interdependent with each other, so before applying the Gram-Charlier expansion (see A.7), these variables have to be decorrelated first.

1.11.1 Decorrelation of interdependent loads and DGs

The property of the cumulant is only valid for independent variables. The generation of many micro-sources depends on natural factors with statistical interdependencies with customer load, so strong correlation exists between DG unit and load. Figure 4-1 describes the correlation of different DGs and loads based on annual German load profiles.

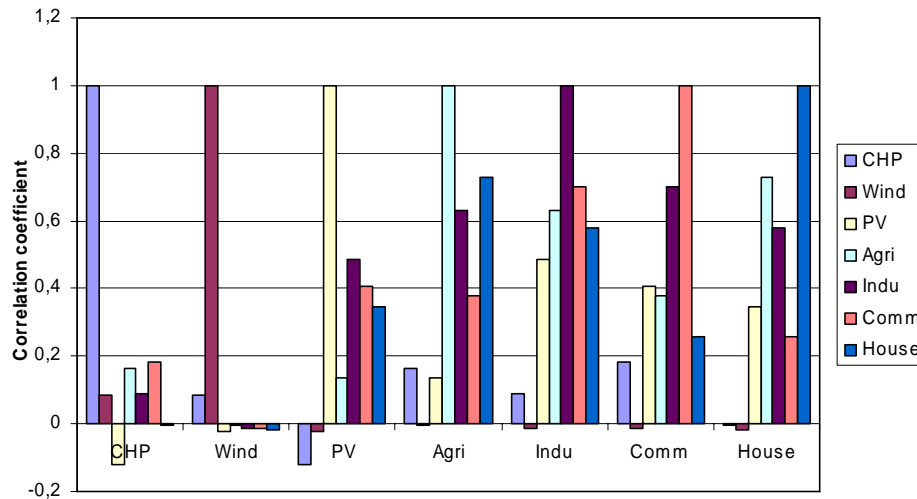


Figure 4-1 Correlation coefficient of German loads and various micro-sources

Correlations exist between DGs, between loads, and also between load and DG. PV and loads show the largest correlation, mainly due to their time interdependence. Three days PV and loads profiles are indicated in Figure 4-2, all with a peak around noon. During the off-peak hours of load at night there is also no PV output. WT generation is mainly influenced by the wind speed, which has small correlation with time, therefore WT have the lowest correlation with loads and other types DG units.

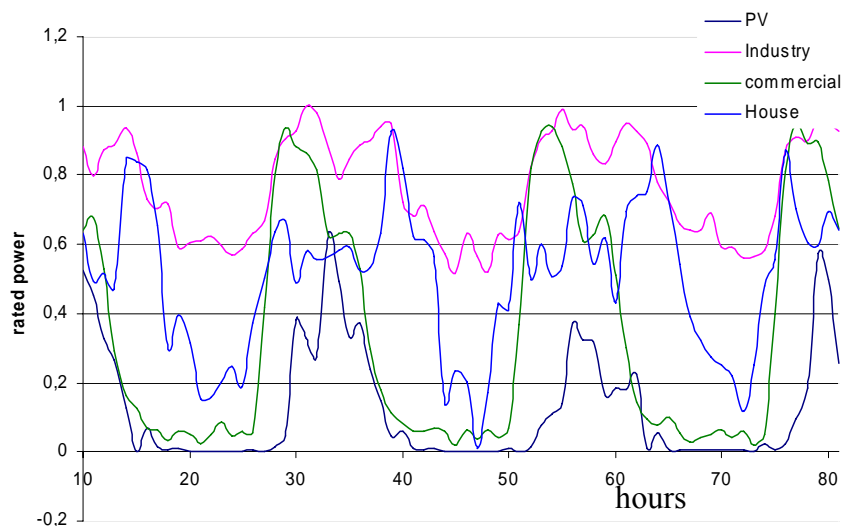


Figure 4-2 PV output power and load demand variation

To eliminate the interdependence of DGs and loads, a decorrelation between load and DGs has to be done as suggested by [56].

Let \vec{S} is a jointly loads and DG variables with mean $\vec{b} = M(\vec{S})$ and a covariance matrix V . The elements of this matrix are given by

$$\begin{aligned} V_{ii} &= \text{Var}(S_i), \\ V_{ij} &= \text{cov}(S_i, S_j) \end{aligned} \quad \text{Equation 4-3}$$

Assume the correlation of elements of \vec{S} is second order. Then a vector of independent random variable \vec{R} is obtained by the transformation

$$\vec{R} = A^{-1}(\vec{S} - \vec{b}) \quad \text{Equation 4-4}$$

where $\vec{V} = AA^T$ is a factorization of the covariance matrix. Matrix \vec{A} is not unique, it is convenient to choose the Cholesky factorization [59]; such an 3*3 matrix looks as

$$\vec{V} = AA^T = \begin{bmatrix} a_{11} & 0 & 0 \\ a_{12} & a_{22} & 0 \\ a_{13} & a_{23} & a_{33} \end{bmatrix} * \begin{bmatrix} a_{11} & a_{12} & a_{13} \\ 0 & a_{22} & a_{23} \\ 0 & 0 & a_{33} \end{bmatrix} = \begin{bmatrix} a_{11}^2 & a_{12}a_{11} & a_{13}a_{11} \\ a_{12}a_{11} & a_{12}^2 + a_{22}^2 & a_{13}a_{12} + a_{23}a_{22} \\ a_{13}a_{11} & a_{13}a_{12} + a_{23}a_{22} & a_{13}^2 + a_{23}^2 + a_{33}^2 \end{bmatrix}$$

Equation 4-5

Assume $v_{i,j}$ is the element of covariance matrix \vec{V} , $a_{i,j}$ is the element of matrix \vec{A}

According to Cholesky factorization, the entries for \vec{A} can be obtained by

$$\begin{aligned} a_{i,j} &= \frac{1}{a_{j,j}} (v_{i,j} - \sum_{k=1}^{j-1} a_{i,k} a_{j,k}) \quad \text{for } i > j \\ a_{i,i} &= \sqrt{v_{i,i} - \sum_{k=1}^{i-1} a_{i,k}^2} \end{aligned} \quad \text{Equation 4-6}$$

Assume only one load and one DG working in the island, which have nationalized power. The most basic calculation of reliability can be reflected by

$$P_{net} = P_L - P_G \quad \text{Equation 4-7}$$

So, if \vec{S} has only two elements (P_L, P_G) then the element of \vec{A} are

$$\begin{aligned} a_{11} &= \sqrt{v_{11}} \quad , \quad a_{12} = 0, \\ a_{21} &= v_{12} / \sqrt{v_{11}} \quad , \quad a_{22} = \sqrt{v_{11}v_{12} - v_{12}^2} / \sqrt{v_{11}} \end{aligned} \quad \text{Equation 4-8}$$

Combined with Equation 4-4

$$\begin{aligned} P_L' &= (P_L - b_1) / a_{11}, \\ P_G' &= -(P_L - b_1)a_{21} / (a_{11}a_{12}) + (P_G - b_2) / a_{22} \end{aligned} \quad \text{Equation 4-9}$$

Where P_L', P_G' are the uncorrelated load demand and DG output variable.

The net power of one island with one DG and one load can be determined by

$$\begin{aligned} P_{net} &= P_L' - P_G' \\ &= (a_{11} - a_{21})R_1 + a_{22}R_2 + b_1 - b_2 \end{aligned} \quad \text{Equation 4-10}$$

as the cumulants of a sum of independent random variables are the sum of their cumulants

$$k_r(P_{net}) = (a_{11} - a_{21})^r k_r(P_L') + a_{22}^r k_r(P_G') \quad \text{Equation 4-11}$$

with

$$\begin{aligned} k_r(P_L) &= a_{11}^r k_r(P_L') \\ k_r(P_G) &= a_{21}^r k_r(P_L') + a_{22}^r k_r(P_G') \end{aligned} \quad \text{Equation 4-12}$$

Therefore,

$$\begin{aligned} k_r(P_L') &= a_{11}^{-r} k_r(P_L) \\ k_r(P_G') &= -(a_{21} / (a_{11}a_{22}))^r k_r(P_L) + a_{22}^{-r} k_r(P_G) \end{aligned} \quad \text{Equation 4-13}$$

And thus,

$$k_r(P_{net}) = ((a_{11} - a_{21})^r - a_{21}^r) / a_{11}^r k_r(P_L) + a_{22}^r k_r(P_G) \quad \text{Equation 4-14}$$

When calculating the sum of any correlated random numbers, it can be done recursively by the following formula. $Y_{i+1} = Y_i + S_i$, Y_i is the summation of first i variables, S_i is the new variable that should be summed.

$$k_r(Y_{i+1}) = \left\{ (1 + \text{cov}(Y_i, S_i) / \text{var}(Y_i)) - (\text{cov}(Y_i, S_k) / \text{var}(Y_i))^r \right\} k_r(Y_i) + (-1)^r k_r(S_i),$$

where

$$\text{var}(Y_{i+1}) = \text{var}(Y_i) + \text{var}(S_i) - 2 \text{cov}(Y_i, S_i),$$

$$\text{cov}(Y_i, S_i) = \text{cov}(Y, S_i) - \sum_{j=1}^{i-1} \text{cov}(S_i, S_j)$$

Equation 4-15

This strategy is applied to micro-sources and all loads in the Microgrid. The covariance coefficients are indicated in Figure 4-3 with a significantly. The correlation between loads and DG units is dramatically reduced after the decorrelation process.

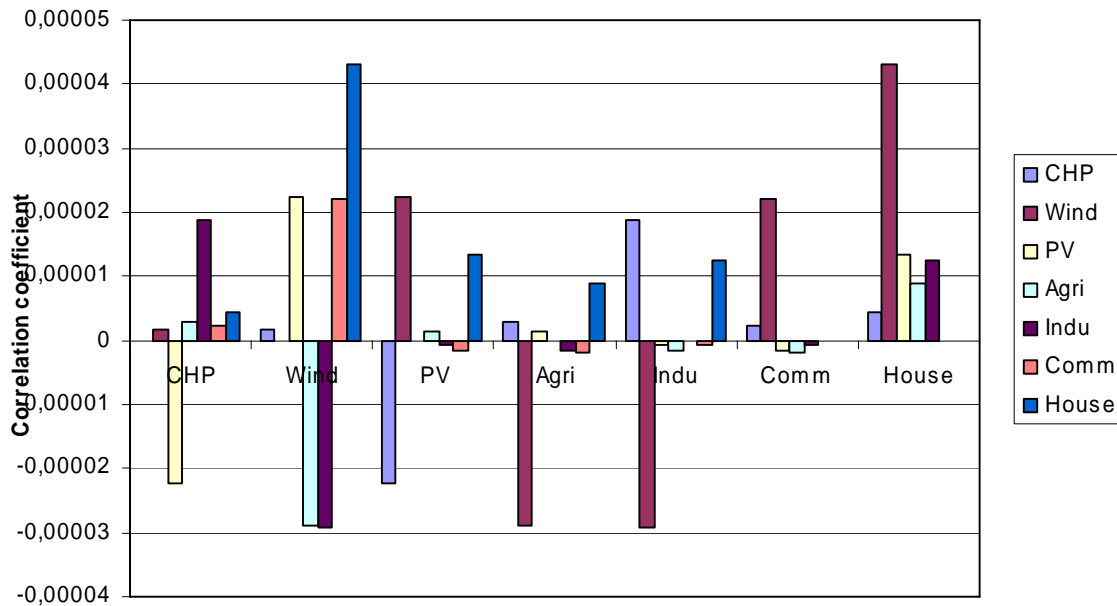


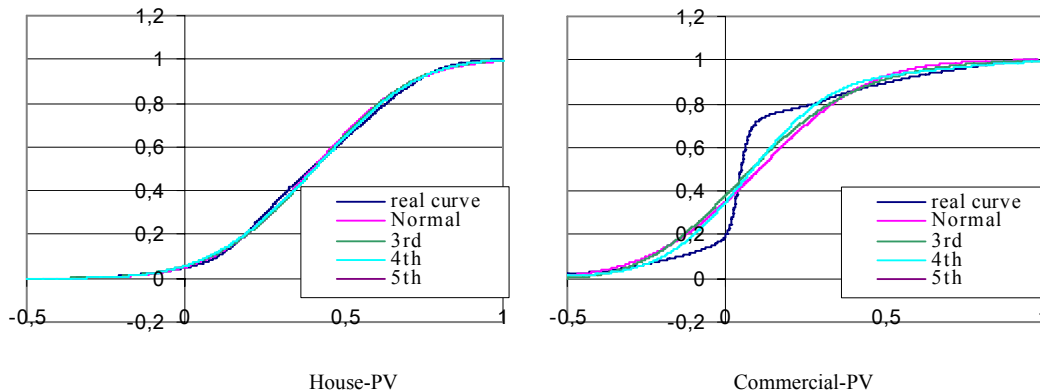
Figure 4-3 Covariance coefficients of DGs and Load

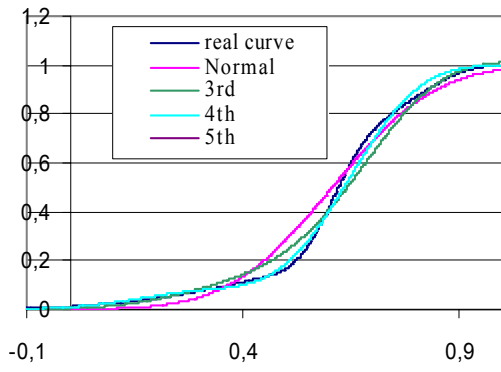
Now non-correlated P'_L and P'_G are obtained, whose cumulants can be directly calculated:

- a) Compute the moment of P_L and P_G according to Equation A -48
- b) Compute the cumulants of P_L and P_G according to Equation A -49
- c) Compute the cumulants of uncorrelated P'_L and P'_G according to Equation 4-14,
- d) Compute the coefficient according to Equation A -56
- e) The probability density function can be calculated by Equation A -57

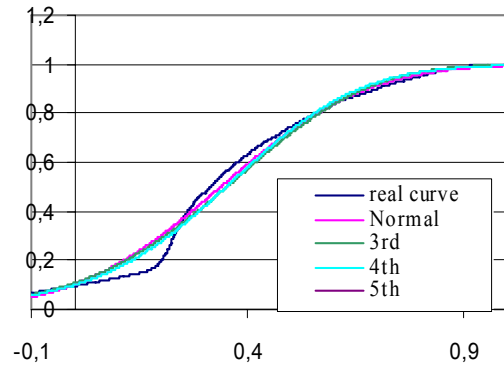
1.12 Comparison of net power PDF based on CGCE model and discrete model

To choose suitable orders of the Gram-Charlier expansion, distinct combinations of DGs and loads with normalized power are applied to the simple island of one DG and one load. Compared subtraction of discrete hourly power generation and load demand, which can be regarded as the real distribution of P_{net} , and the probability distribution of P_{net} based on the expansion of different orders are indicated in figure 3-12.

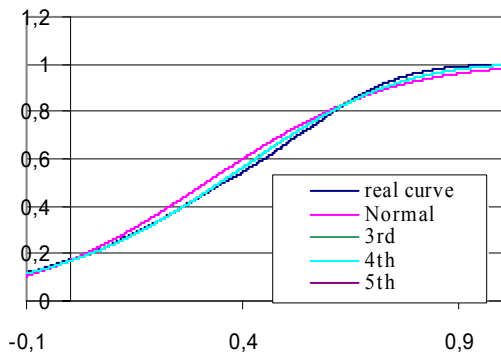




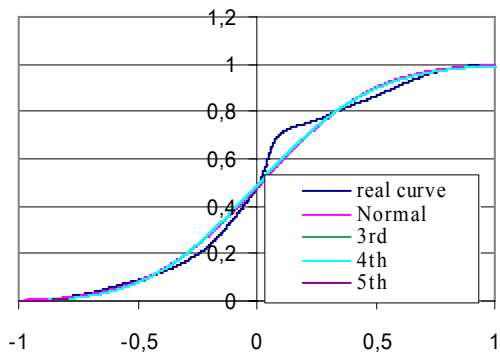
Industry-PV



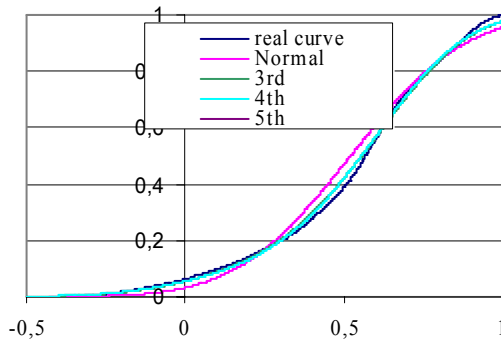
Agriculture-PV



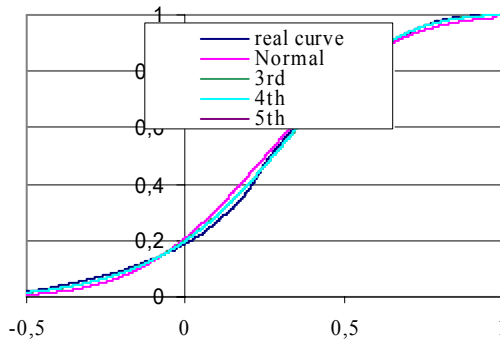
House-Wind



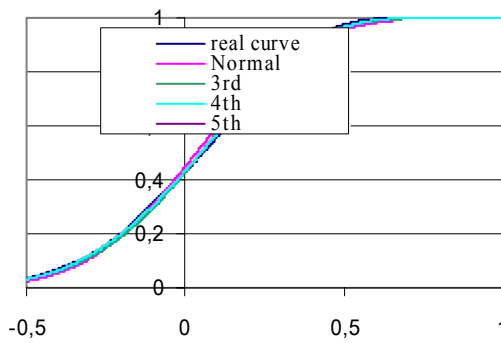
Commercial-Wind



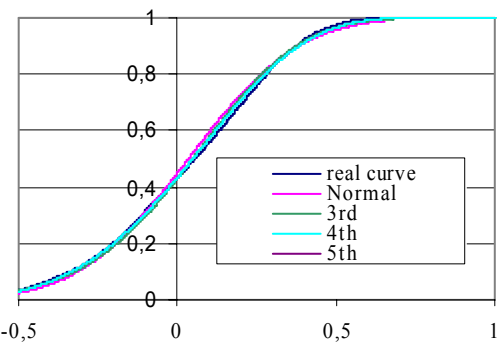
Industry-Wind



Agriculture-Wind



House-CHP



Commercial-CHP

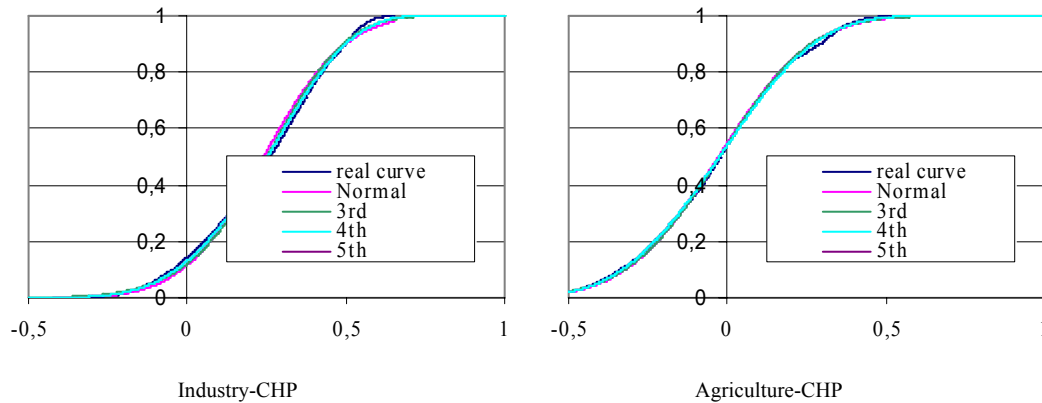


Figure 4-4 Different orders CGCE and real curve comparison

Figure 4-4 indicates that the base order of Gram-Charlier expansion (normal distribution) already offers accurate result of CHP and wind related combination. For PV related combination higher orders Gram-Charlier expansion offer slightly better approximation to the real curve, but the improvement compared with normal distribution is not obvious. Another significant advantage of normal distribution approximation is that, when integrating the interruption power, which is described in the next section, analytical solutions exist, so the time consuming discrete integration can be avoided. This can not be avoided with higher order Gram-Charlier expansion. Therefore in the following analysis part, normal distribution approximation of DGs and loads are used for the reliability indices computation.

1.13 Analysis part

In this section, (system and customer) reliability indices are computed in Excel worksheet by VBA programming based on the simulation result of ZUBER after all failure combinations have been processed

1.13.1 Input of analysis part

Input for the analysis part is the simulation result of ZUBER, which is read from ZUBER generated text file into an Excel worksheet:

- Island information of busbar and upstream infeasible “Tn” directly after failure and after each restoration
- Failure frequency of each failure combination
- Failure duration of each failure combination
- Restoration time of each restoration step

The network element information needs to be entered manually including:

- Busbar parameters including, busbar name, total busbar amount, and total load amount in one busbar
- Load parameters including total load amount in one busbar, load name, load type (House, Industry, Commercial, Agriculture), load priority (very low, low, normal, high, very high), and load rated power
- DG parameters including total DG amount in one busbar, DG name, DG type (CHP, PV, Wind), DG unavailability, and rated power

1.13.2 Reliability indices computation

In this analysis process customer connected with upstream in-feeder is assumed to be fully supplied, so the reliability indices are regarded as 0 in this case. Therefore the reliability indices computation is mainly concentrated on the loads working in island. The computation method is demonstrated by an example with two DGs and two loads working in the island; load and DG settings are indicated in Table 4-1 and 4-2.

Load Name	Load Type	Load Priority	Load Rated Power/kW
Load1	Commercial	High	k_{L1}
Load2	House	Low	k_{L2}
Load3	House	Low	k_{L3}

Table 4-1 Load setting of a example to demonstrate indices computation by SAM

DG Name	DG Type	DG Unavailability	Load Rated Power/ kW
DG1	CHP	20%	k_{DG1}
DG2	PV	20%	k_{DG2}

Table 4-2 DG settings of an example to demonstrate indices computation by SAM

The computation procedures comprise the following steps.

Step 1: Total power generation calculation in island taking into account of DG availability

Compared with conventional generation units, DG units normally have modular structures. Due to economic and technology reasons, micro-sources experience more failure states compared with conventional generation units. Therefore DG unit availability has to be taken into account when total power of DGs is calculated. Two approaches are used to model the DG units with unavailability.

Discrete Model

The distribution function of DG unit of discrete model is described by

$$f(P) = \begin{cases} k\delta(P=0) & P=0 \\ (1-k)\phi(\mu, \sigma^2) & P \neq 0 \end{cases} \quad \text{Equation 4-16}$$

where k is the unavailability of the micro-source unit.

From this model the summed power generation of two DG units, both of which have certain unavailability, can be described by the following distribution

$$f(P_1 + P_2) = \begin{cases} k_1 k_2 \delta(P_{total} = 0) & P_{total} = 0 \\ k_1(1-k_2)\phi(\mu'_1, \sigma_1'^2) + k_2(1-k_1)\phi(\mu'_2, \sigma_2'^2) + \\ (1-k_1)(1-k_2)\phi(\mu'_1 + \mu'_2, \sigma_1'^2 + \sigma_2'^2) & P_{total} \neq 0 \end{cases} \quad \text{Equation 4-17}$$

Where μ'_1 and σ_1' are the uncorrelated mean value and standard deviation.

In this model the probability distribution of total power not equal to 0 is overlapped by three normal distributions. These three parts have to be separately applied to the following

reliability indices calculations. When n DG units work in one island, the probability distribution of the summed power is overlapped by $2^n - 1$ normal distributions, therefore the calculation complexity is dramatically increased.

Adaptation model

Another alternative model to describe the unavailability of DG units is to transform the mean value and standard deviation of each DG unit to a new mean and standard deviation taking into account of unavailability. The micro-source unit is still modelled by an adapted continuous normal distribution instead of a discrete distribution.

$$f(P) = \phi(\mu_{adap}, \sigma_{adap}^2) \quad \text{Equation 4-18}$$

The adaptation can be done by

$$\begin{aligned} \mu_{adap} &= \sum pf(p)\Delta p \\ \sigma_{adap} &= \sqrt{\sum (p - \mu_{adap})^2 f(p)\Delta p} \end{aligned} \quad \text{Equation 4-19}$$

The following formulas derive the relationship between $\mu_{adapt}, \sigma_{adapt}$ and original μ, σ :

$$\begin{aligned} \mu_{adap} &= \sum pf(p)\Delta p = \sum pf(p)k\Delta p + 0(1-k) = k \sum pf(p)\Delta p \\ \therefore \sum pf(p)\Delta p &= \mu_{origin} \\ \text{so } \mu_{adap} &= k\mu_{origin} \\ \sigma_{adap} &= \sqrt{\sum (p - \mu_{adap})^2 f(p)\Delta p} \\ &= \sqrt{\sum (p^2 f(p)\Delta p) + \mu_{adap}^2 \sum f(p)\Delta p - \mu_{adap} \sum 2pf(p)\Delta p} \\ \therefore \begin{cases} \mu_{adap} = k\mu_{origin} \\ \sum f(p)\Delta p = k\mu_{origin} \end{cases} \\ \text{so } \sigma_{adap} &= \sqrt{\sum p^2 f(p)\Delta p + k^2 \mu_{origin}^2 * k - 2k\mu_{origin} k\mu_{origin}} \end{aligned}$$

so in the expanded expression σ_{adap} only the first item is unknown. It can be derived as follows

$$\text{similar as the expansion of } \sigma_{adapt}, \sigma_{origin} = \sqrt{\sum p^2 f(p)\Delta p + k^2 \mu_{origin}^2 * k - 2k\mu_{origin} k\mu_{origin}}$$

For the original distribution function, no adaption is applied, so $k = 1$

so $\sum p^2 f(p)\Delta p = \sigma^2 + \mu^2$ for the unadapted normal distribution

for the adapted normal distribution $\sum p^2 f(p)\Delta p = k(\sigma^2 + \mu^2)$

substitute this expression to σ_{adap}

$$\text{finally } \sigma_{adapt} = \sqrt{(k + k^3 - 2k^2)\mu^2 + k\sigma^2}$$

From the derivation above, we obtain the direct relationship between the adapted mean value, standard deviation and the original mean value, standard deviation.

$$\mu_{adap} = k\mu_{origin} \tag{Equation 4-20}$$

$$\sigma_{adap} = \sqrt{(k + k^3 - 2k^2)\mu_{origin}^2 + k\sigma_{origin}^2}$$

Figure 4-5 indicates the adapted and original PDF of CHP unit with 30% unavailability compared with the CHP unit with 100% availability.

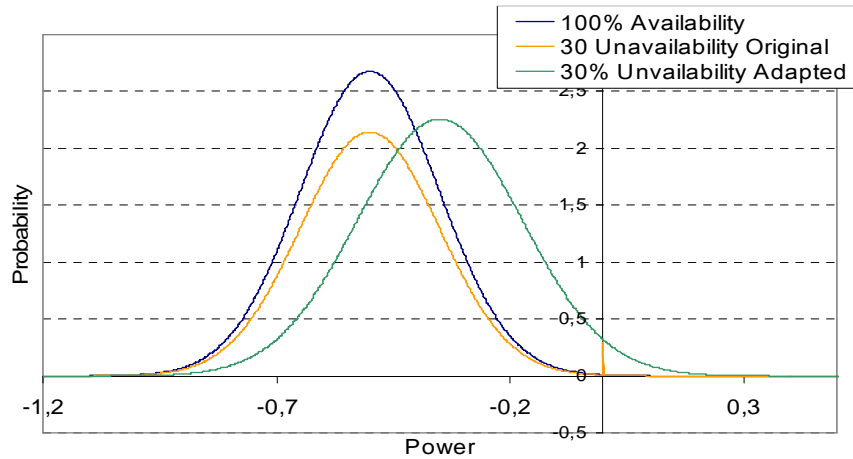


Figure 4-5 PDF of adapted and original CHP unit

Due to the adaptation an error is induced into the calculation; Figure 4-6 compares the interruption frequency and interruption energy based on adaptation model with the discrete, most accurate model. In this test, one CHP unit with an increasing availability from 0% to 100 % and one house load work in island and the reliability indices are calculated based on hourly load and generation.

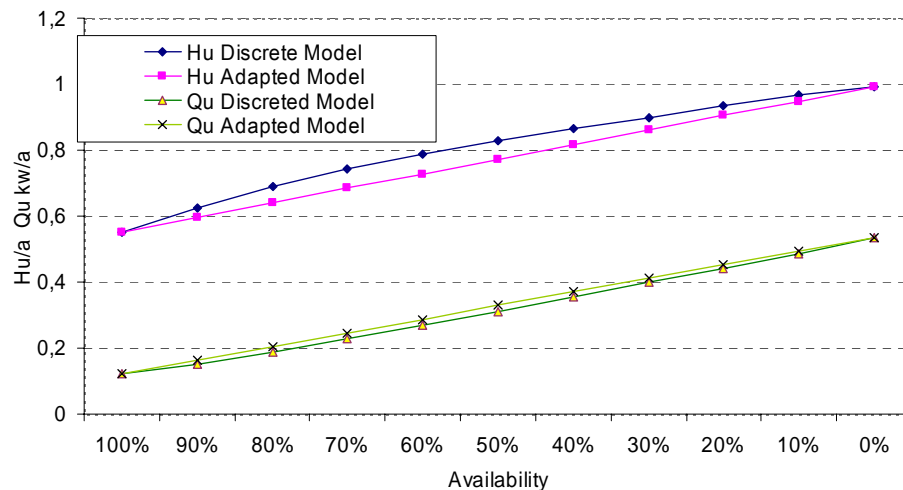


Figure 4-6 Comparison of discrete model and adapted model

Acceptable errors are induced by the adapted model, especially when the unavailability of DG units is lower than 20%. Considering the low computation time investment, in the following analysis adapted model is used to describe DG availability.

Back to the example described at the beginning of this section, the total power distribution applying adapted model is calculated by

$$P_{total} = \phi(\mu'_{total}, \sigma'^2_{total}) \quad \text{Equation 4-21}$$

Where $\mu'_{total} = \mu'_{adap1} + \mu'_{adap2}$, $\sigma'^2_{total} = \sigma'^2_{adap1} + \sigma'^2_{adap2}$

Step 2: Available power computation of end-customer

Load priority is taken into account for the available power calculation of end-customer. Two criteria are considered to calculate the available power of end customer

- a) Load having higher priority level is supplied firstly by DG units
- b) Available power distribution of the loads with the same load priority level is based on the rated power of this load in proportional to the total load.

In the example, load 1 has the first priority of all the loads, the total DG power will supply load 1 first, the available power distribution is indicated by

$$P_{avail1} = \phi(\mu'_{avail1}, \sigma'^2_{avail1}) \quad \text{Equation 4-22}$$

where $\mu'_{avail1} = \mu'_{total}$, $\sigma'_{avail1} = \sigma'_{total}$

The surplus available power after supplying load 1 is distributed to load 2 and load 3 according to criterion b. The available power distribution of both loads is

$$P_{avail2} = \phi(\mu'_{avail2}, \sigma'^2_{avail2})$$

$$\text{where } \mu'_{avail2} = \max(0, (\mu'_{total} - \mu'_{L1}) * \frac{P_{L2}}{P_{L2} + P_{L3}}), \sigma'_{avail2} = \max(0, (\sigma'_{total} - \sigma'_{avail1}) * \frac{P_{L2}}{P_{L2} + P_{L3}})$$

$$P_{avail3} = \phi(\mu'_{avail3}, \sigma'^2_{avail3})$$

$$\text{where } \mu'_{avail3} = \max(0, (\mu'_{total} - \mu'_{L1}) * \frac{P_{L3}}{P_{L2} + P_{L3}}), \sigma'_{avail3} = \max(0, (\sigma'_{total} - \sigma'_{avail1}) * \frac{P_{L3}}{P_{L2} + P_{L3}})$$

Equation 4-23

Step 3: Interruption frequency calculation

With the available power distribution, the net power distribution can be calculated by the subtraction of available power distribution and load distribution:

$$P_{net} = \phi(\mu'_{net}, \sigma'^2_{net}) \quad \text{Equation 4-24}$$

where $\mu'_{net} = \mu'_{avail1} - \mu'_{net}$

Load is assumed to be controllable in Microgrid by load shedding. Thus optimistic allocation mode is applied in the simulation. For each end-customer interruption frequency is calculated by

$$H_{u,0,i} = p_i * p_0 \quad \text{Equation 4-25}$$

Where p_i is the failure frequency of the failure combination i , which is read from the simulation part. p_0 is the cumulative probability of P_{net} less than 0, which represents the interruption probability of end-customer in the case of failure i . This value can be achieved by reading the probability at 0 point from the CDF of P_{net} which is calculated by

$$p_0 = \text{NORMDIST}(0; \mu_{net}; \sigma_{net}; 1) \quad \text{Equation 4-26}$$

Step 4: Interruption Power calculation

The interruption power of end-customer k is calculated as

$$Q_{u,0,i} = p_i * q_0 \quad \text{Equation 4-27}$$

p_i is still the interruption frequency of end-customer. q_0 is the cumulative interruption power of end-customer, which is described by

$$q_0 = \int_{-\infty}^0 pf(p)dp = \int_{-\infty}^0 p * \frac{1}{\sqrt{2\pi}} * e^{-\frac{(p-\mu)^2}{2\sigma^2}} d_p \quad \text{Equation 4-28}$$

By using the method “integration by part”, analytical solution for this integration can be achieved. The following formula derives the analytical solution of this integration:

$$\begin{aligned} \int \left(-\sigma^2 * \frac{1}{\sqrt{2\pi}} * e^{-\frac{(x-\mu)^2}{2\sigma^2}} \right)' * d_x &= \int (x - \mu) * \frac{1}{\sqrt{2\pi}} * e^{-\frac{(x-\mu)^2}{2\sigma^2}} \\ &= \int x * \frac{1}{\sqrt{2\pi}} * e^{-\frac{(x-\mu)^2}{2\sigma^2}} dx - \int \mu * \frac{1}{\sqrt{2\pi}} * e^{-\frac{(x-\mu)^2}{2\sigma^2}} dx \end{aligned}$$

so,

$$\begin{aligned} \int_{-\infty}^0 \left(-\sigma^2 * \frac{1}{\sqrt{2\pi}} * e^{-\frac{(p-\mu)^2}{2\sigma^2}} \right)' d_p &= \int_{-\infty}^0 (p - \mu) * \frac{1}{\sqrt{2\pi}} * e^{-\frac{(p-\mu)^2}{2\sigma^2}} d_p \\ &= \int_{-\infty}^0 p * \frac{1}{\sqrt{2\pi}} * e^{-\frac{(p-\mu)^2}{2\sigma^2}} d_p - \int_{-\infty}^0 \mu * \frac{1}{\sqrt{2\pi}} * e^{-\frac{(p-\mu)^2}{2\sigma^2}} d_p \end{aligned}$$

so

$$\begin{aligned} \int_{-\infty}^0 p * \frac{1}{\sqrt{2\pi}} * e^{-\frac{(p-\mu)^2}{2\sigma^2}} d_p &= \int_{-\infty}^0 \left(-\sigma^2 * \frac{1}{\sqrt{2\pi}} * e^{-\frac{(p-\mu)^2}{2\sigma^2}} \right)' d_p + \int_{-\infty}^0 \mu * \frac{1}{\sqrt{2\pi}} * e^{-\frac{(p-\mu)^2}{2\sigma^2}} d_p \\ &= \left(-\sigma^2 * \frac{1}{\sqrt{2\pi}} * e^{-\frac{(p-\mu)^2}{2\sigma^2}} \right) \Big|_{p=-\infty}^{p=0} + \mu * \int_{-\infty}^0 \frac{1}{\sqrt{2\pi}} * e^{-\frac{(p-\mu)^2}{2\sigma^2}} d_p \end{aligned}$$

The left part of last equation is objective function that should be integrated. The first term of right part is the multiplication of constant value and the value of normal distribution PDF when p is equal to 0, which can be achieved by an Excel-worksheet function

$$\frac{1}{\sqrt{2\pi}} * e^{-\frac{(p-\mu)^2}{2\sigma^2}} \Big|_{p=0}^{p=\infty} = \text{NORMDIST}(0; \mu; \sigma; 0) \quad \text{Equation 4-29}$$

The second part is the multiplication of constant value and the value of normal distribution CDF when p is equal to 0, which can be also obtained by excel function

$$\int_{-\infty}^0 \frac{1}{\sqrt{2\pi}} * e^{-\frac{(p-\mu)^2}{2\sigma^2}} d_p = \text{NORMDIST}(0; \mu; \sigma; 1) \quad \text{Equation 4-30}$$

So finally, interruption power is calculated by

$$Q_{u,0,i} = p_i * q_0 = p_i * (-\sigma^2 * \text{NORMDIST}(0; \mu; \sigma; 0) + \mu * \text{NORMDIST}(0; \mu; \sigma; 1)) \quad \text{Equation 4-31}$$

with $\mu = \mu'_{net}$; $\sigma = \sigma'_{net}$.

Step 5: Interruption Energy and Unavailability calculation

The calculation of interruption energy and unavailability is related the restoration process. After each restoration step is finished, Step 1 and Step 4 have to be repeated to calculate the interruption power $Q_{u,k,i}$ and interruption frequency $H_{u,k,i}$ again.

Interruption Energy and Unavailability is calculated by

$$\begin{aligned} Q_{u,i} &= \sum_k H_{u,k,i} * (T_{u,k+1} - T_{u,k}) \\ W_{u,i} &= \sum_k Q_{u,k,i} * (T_{u,k+1} - T_{u,k}) \end{aligned} \quad \text{Equation 4-32}$$

Where $T_{u,k}$ is the restoration time of step k, a simulation result of ZUBER.

Step 6: Interruption duration and interruption cost calculation

The two reliability indices interruption duration $T_{u,i}$ and interruption cost $C_{u,i}$ depend on $H_{u,i}$, $Q_{u,i}$, $P_{u,i}$, $W_{u,i}$. They are calculated by

$$T_{u,i} = \frac{Q_{u,i}}{H_{u,i}}, \quad C_{u,i} = k_p * P_{u,i} + k_w * W_{u,i} \quad \text{Equation 4-33}$$

Where k_p is power specific interruption cost and k_w is energy specific cost

Step 7: Customer reliability indices calculation

In the previous step, customer reliability indices of each failure combination are calculated. Reliability indices of each customer for all the simulated failure combination are calculated repeating step 1 to step 6. The final customer result is calculated by the summation of result of each failure combination

$$F_u = \sum_i F_{u,i}, \quad T_u = \frac{Q_u}{H_u}, \quad C_u = k_p * P_u + k_w * W_u \quad \text{Equation 4-34}$$

Where $F_{u,i}$ represents the reliability indices $H_{u,i}$, $P_{u,i}$, $Q_{u,i}$, $W_{u,i}$ of failure combination i.

Step 8: System reliability indices calculation

Reliability indices of each customer are calculated by repeating step 1 to step 7. The system reliability indices are based on customer result.

Interruption frequency H and unavailability Q are calculated by

$$F = \frac{\sum F_u}{N} \tag{Equation 4-35}$$

with N as the number of customers

To evaluate the system reliability accumulatively, interruption power P and interruption energy W are calculated by summing all the customer reliability indices

$$F = \sum_u F_u \tag{Equation 4-36}$$

Similar like the customer reliability indices, system reliability result is finally calculated by

$$T = \frac{Q}{H} \tag{Equation 4-37}$$

$$C = k_p * P + k_w * W$$

1.14 Case Study

Two networks collected in task 1 of this work package (TG.1) and described in DG.1 are studied in the following sections: a typical Italian rural (radial) network (Figure 4-7) and a German urban (meshed) LV network (Figure 4-8).

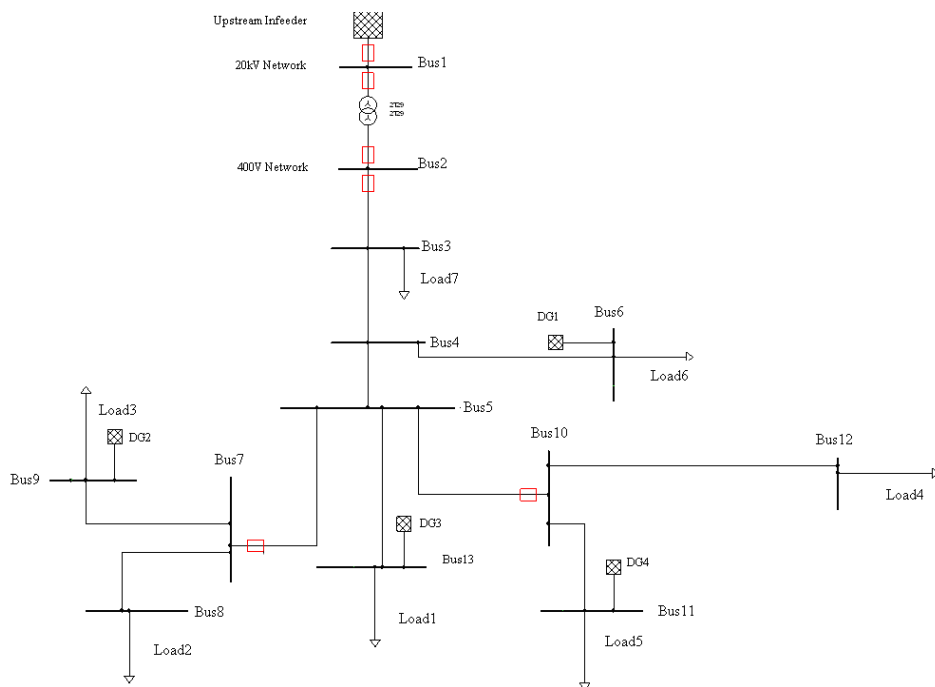


Figure 4-7 Italy rural network topology

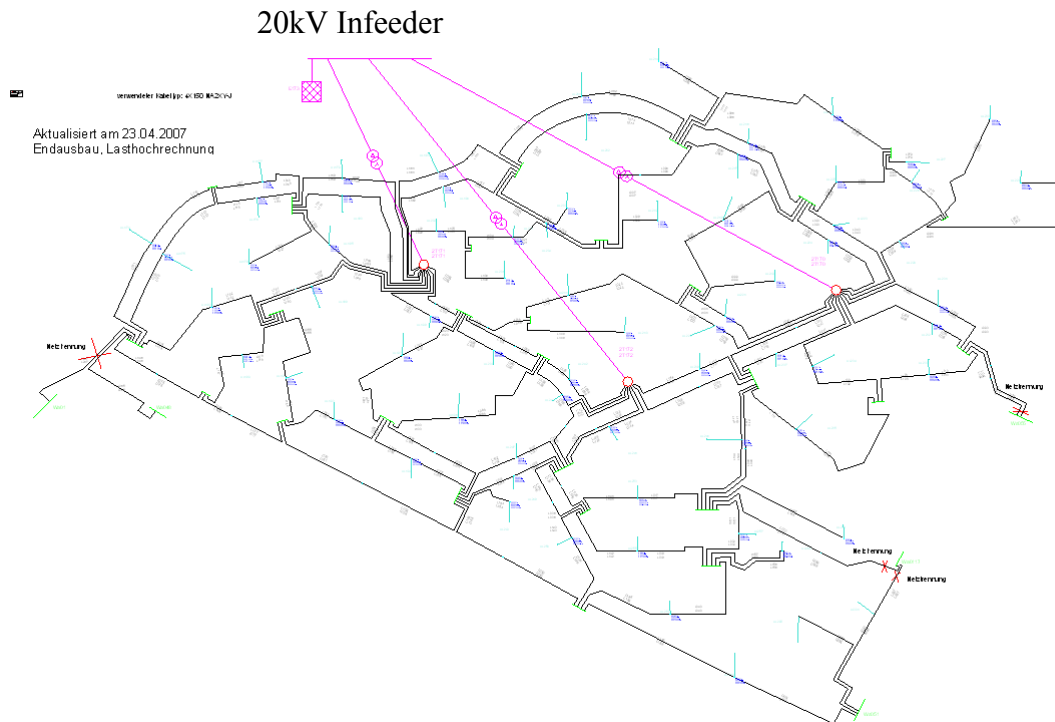


Figure 4-8 German urban LV network topology

1.14.1 Italy Rural network

Basic evaluation

ZUBER provides accurate results when no stochastic processes exist in the network. A simulation with 4 DG units - as shown in Figure 4-7 with constant rated power of 3 kW and constant load of 3 kW - demonstrated identical results for both methods, the analytical analysis by ZUBER and the SAM method. The reliability setting of the 400V network is listed in Table 4-3 .

Network Component	H(1/a)	T(h)
Cable	0,0189	15
Distribution Substation	0,006	6,5
Primary Substation	0,0052	5,5
Switch Bay for Busbar	0,0001	3,2
Switch Bay for Finish per Line	0,0002	3,2

Table 4-3 Reliability setting of LV

As MV and HV network topology doesn't exist in network, the total reliability influence from MV and HV is attributed to upstream in-feeder in the network considering worse system reliability than the rural and urban average indices collected in [60]. Thus, the reliability indices of upstream MV in-feeder are selected as $H = 3.9/a$ and $T = 3h$.

Reliability influence of different type DG penetration

Figure 4-9 presents simulation results for selected scenarios (Table 4-4) with different micro-source types, DG penetration level and DG availability (without considering intermittency).

Scenario2100:	No DG units in the network
Scenario2101:	CHP units are distributed in the network The total penetration level is 150%. DG has 100% availability
Scenario2102:	CHP units are distributed in the network. The total penetration level is 100%. DG has 100% availability.
Scenario2103	CHP is distributed in the network. The total penetration level is 100%. DG has 80% availability.
Scenario2104	PV is distributed in the network. The total penetration level is 80%. DG has 80% availability
Scenario2105	WT is distributed in the network. The total penetration level is 80%. DG has 80% availability.

Table 4-4 Scenario 2100-2105

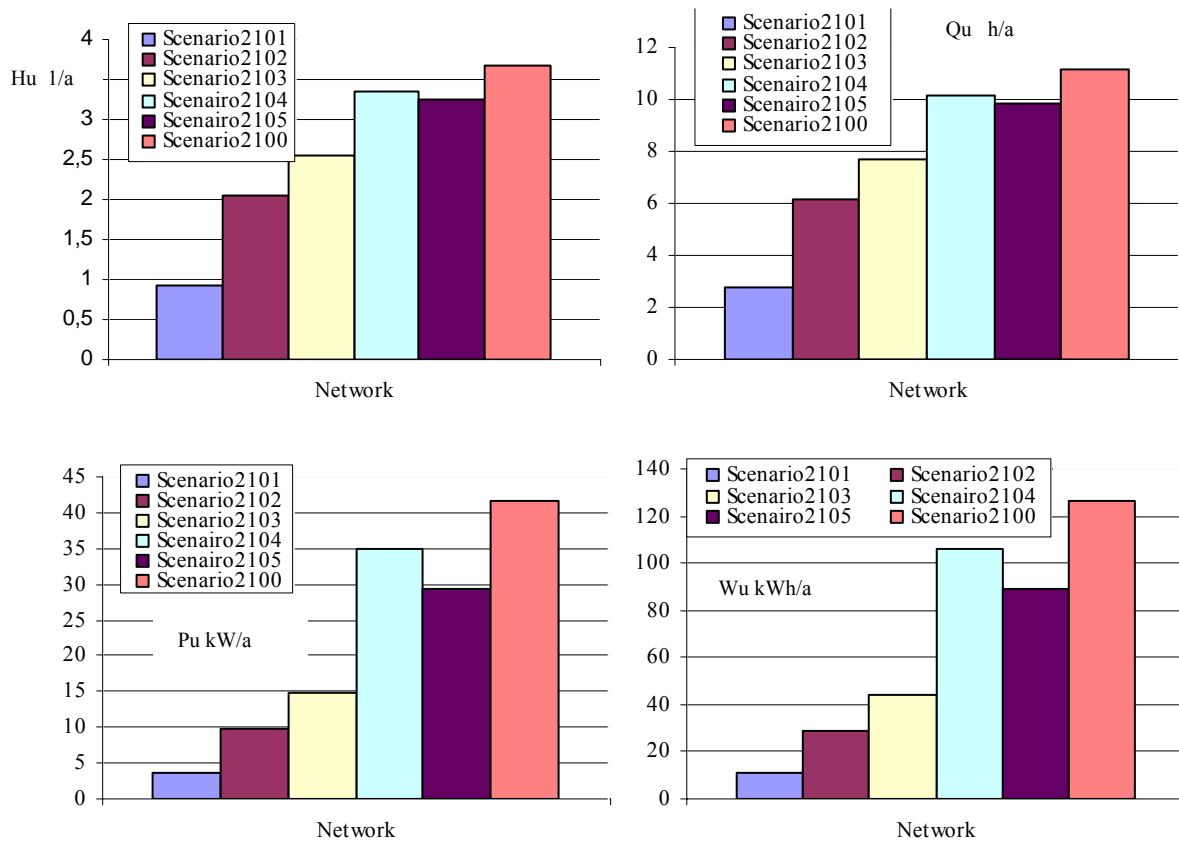


Figure 4-9 Simulation result of scenario 2100-2105

Conclusions that can be easily verified are:

- Microsources with higher availability lead to higher reliability improvement of the network
- Higher penetration levels with micro-sources more improve the reliability of the network
- The reliability improvement of different DG type can be ranked as follows
 $CHP > WT > PV$
- DG availability influence to reliability indices

Figure 4-10 demonstrates the impact of micro-source availability on network reliability with settings as in scenario 2101. Increasing micro-source unavailability decreases network reliability for all types of micro-source. Pu and Wu is linearly dependent on the unavailability while Hu and Qu is non-linear related with DG unavailability.

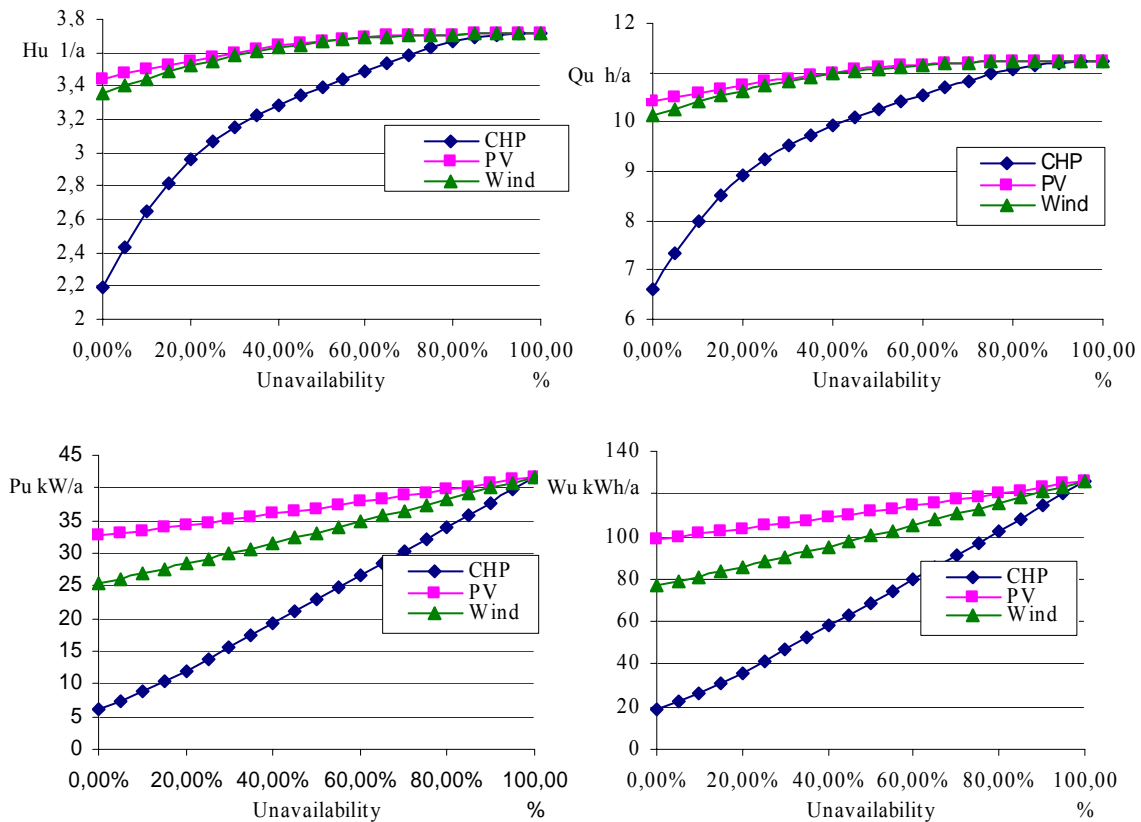


Figure 4-10 Impact of DG unavailability on network reliability

The reason for the different relationship between interruption indices and unavailability of DG unit is due to the different physical background of each index. Hu is calculated by the comparison of load demand and available power. The comparison result can be only “load can be supplied” or “load can not be supplied”. Different available power of the load may have the same comparison result when compared with the same load demand. However Pu is an accumulated value, which is calculated by the arithmetic subtraction of load available

power and load demand. Qu and Wu are determined by Pu and Hu respectively. Therefore Hu and Qu perform different relationship with unavailability compared with Qu and Wu.

1.14.2 German urban LV network

The reliability setting of MV level is selected according German MV and LV network as $H=0, 18/a$, $T=0,8h$. The reliability setting of LV level is selected according to Table 4-3

Again, different scenarios demonstrate the impact of different micro-source technology on reliability as shown in Figure 4-11 for micro-source penetration level of 80%. Highest reliability is achieved when CHP units work in electricity driven mode in case of failure.

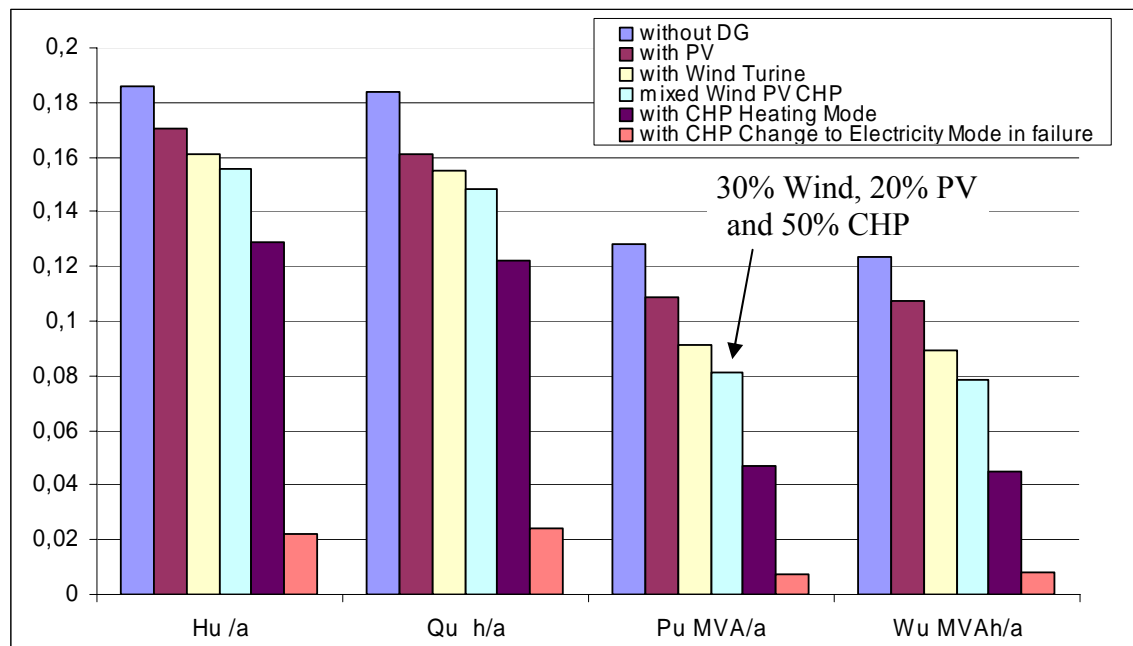


Figure 4-11 Simulation result of German urban LV scenario 2400-2405

5 Time Sequential Monte-Carlo Simulation for Reliability Analysis in Networks with Micro-sources

In chapter 4 a reliability evaluation technique based on analytical method is implemented. The advantage of analytical method is that the computation time is shorter in most cases and the calculation process is more transparent, therefore it can be applied for testing purpose, like determining the optimised location and optimised DG capacity, however, with analytical method the detailed modelling of chronological issues, such as daily load curve or DG generation curve, is only possible with several approximations. In this case, errors will be induced when the distribution network is highly penetrated with DG unit. The analytical method is also restricted to only evaluate the average value of reliability indices, sometimes to a certain range of index distribution [28].

Time sequential Monte-Carlo simulation technique simulates the operational performance of all the equipments chronologically during a certain observation period. Each observation period will be simulated for 1000 times in this application. Because the equipment state is simulated in time, Monte-Carlo simulation is able to model the chronological issues,

especially the past-dependent issues, like charging and discharging process of storage element incorporated in grid, which is impossible to be modelled by analytical method. The operational performance of equipments are achieved by random numbers as well as failure and restoration probabilistic distribution of each equipment, therefore the reliability indices of the system in each simulation period is stochastic and the detailed probabilistic distribution of these indices can be determined by Monte-Carlo method. The disadvantage of this method is large computation time compared with analytical method.

1.15 Monte-Carlo Simulation Procedure

Two basic techniques are utilized in Monte-Carlo applications to power system reliability calculation. These are known as the sequential method and non-sequential method. Non-Sequential methods simulate all the states of the equipment applied in the network. In non-sequential methods the states of all components are simulated and non-chronological system state is obtained. In sequential method, first the failure event and repair event of all equipments are simulated separately by cycle in each observation period and finally the system state in one observation period is obtained by ranking the element state of all the system in one period. The sequential method is able to consider the time dependent issues and therefore applied in the calculation of reliability indices in this chapter.

A general structure of sequential Monte-Carlo simulation process applied in this chapter is described in the Figure 5-1 with two main loops. One loop is to process all observation periods. More observation periods correspond with higher computation time, but, the final calculated result will be more accurate. In this application 1000 simulation periods are selected, high enough to get quasi-accurate results.

Another loop is to process all the failure events in one observation period, which is selected as 50 years. In this loop, each failure event will be processed separately, including fault, restoration and repair processes. Reliability indices will be also calculated in this loop.

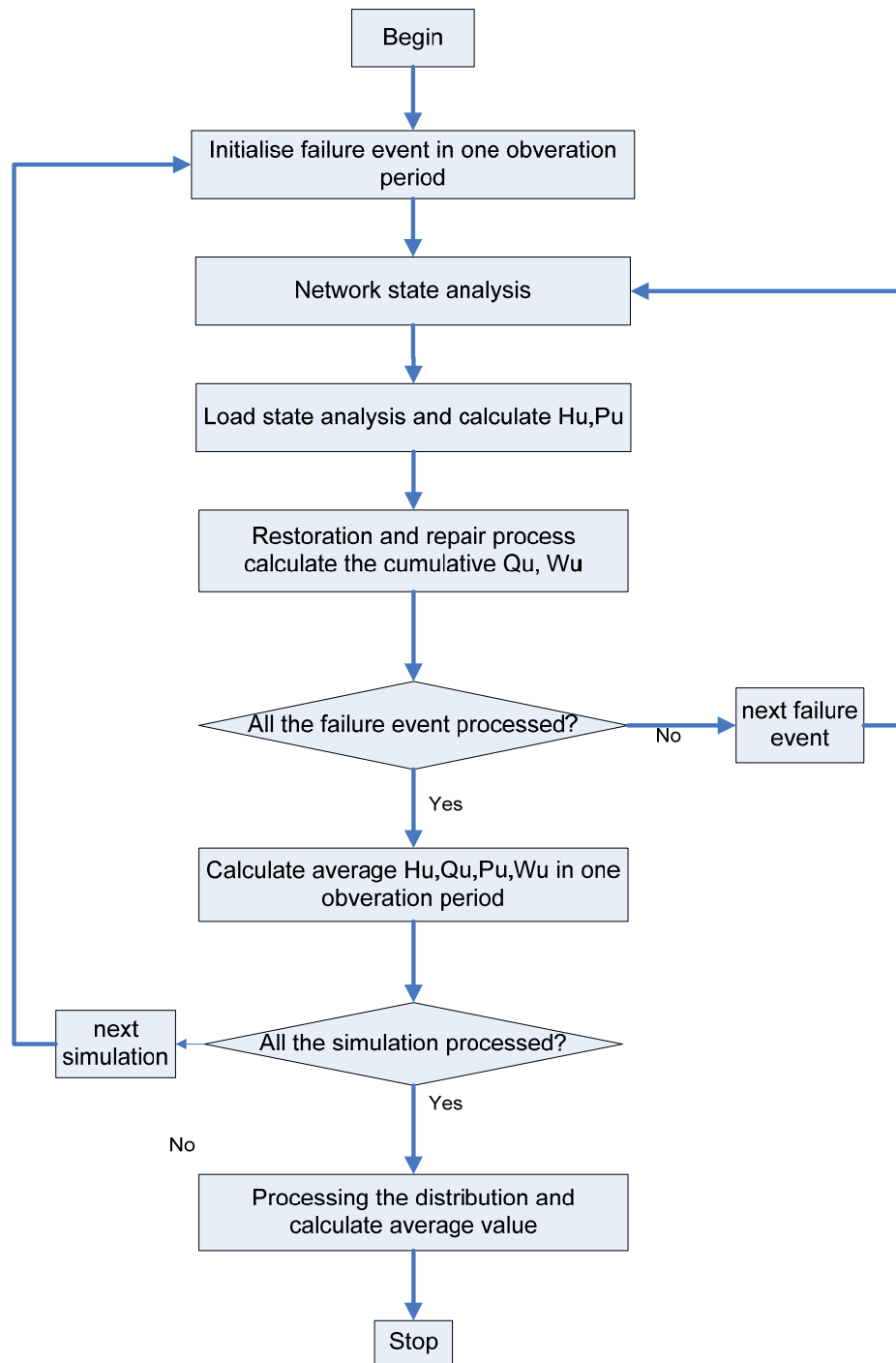


Figure 5-1 Flow chart of time-sequential Monte-Carlo simulation

In the following section, the typical Italian rural network (Figure 4-7), with storage units at each busbar connected with DG, serves as an example to demonstrate the detailed realisation procedure of time sequential Monte-Carlo simulation.

1.15.1 Step 1: Failure event list generation

Time to failure and time to repair statistical distribution for electrical element should be determined in advance. Additionally mean time to failure and mean time to repair statistical distribution for electrical element should be also determined. The mean time to failure and restoration of all electrical elements are chosen as applied in analytical method (Table 4-3).

Only LV failure event is considered in this chapter to clearly observe the reliability difference of different loads.

Time to failure distribution

The most popular used time to failure distribution function for electrical element is exponential distribution. The CDF and PDF for exponential distribution function is

$$\text{CDF: } 1 - e^{-\lambda x} \quad \text{Equation 5-1}$$

$$\text{PDF: } \lambda * e^{-\lambda x}$$

where λ is the rate parameter. The expected value of exponential distribution function is given by

$$E(x) = \frac{1}{\lambda}, \text{ and thus } \lambda = \frac{1}{E(x)} \quad \text{Equation 5-2}$$

Time to restoration distribution

The most popular used time to repair distribution function for electrical element is Weibull distribution. The CDF and PDF for Weibull distribution is given by

$$\text{CDF for Weibull distribution: } 1 - e^{-(x/\lambda)^k} \quad \text{Equation 5-3}$$

$$\text{PDF for Weibull distribution: } \frac{k}{\lambda} * \left(\frac{x}{\lambda}\right)^{k-1} * e^{-(x/\lambda)^k}$$

where k is the shape factor, λ is the scale factor. The expected value of Weibull distribution function is expressed as

$$E(x) = \lambda * \Gamma(1 + 1/k) \quad \text{Equation 5-4}$$

So, the scale factor k for exponential distribution is selected as 4 generally. The scale factor k for each electrical equipment can be determined by

$$\lambda = E(x) / \Gamma(1 + 1/k) = E(x) / \Gamma(4/5) \quad \text{Equation 5-5}$$

After determining the probability distribution function of each electrical equipment, the stochastic failure event can be generated by random number and the distribution function as

$$\text{Time to failure: } T_{fail} = -\ln(1 - P_{rand}) / E(x)_{fail} \quad \text{Equation 5-6}$$

$$\text{Time to restoration: } T_{restor} = (-\ln(1 - P_{rand}))^{1/4} * E(x)_{restor} / \Gamma(5/4)$$

where P_{rand} is the random number generated by random generator, $E(x)_{fail}$ is the mean time to failure, $E(x)_{restor}$ is the mean time to restoration.

An example of failure event generation in one observation period for one busbar is shown as follows to illustrate the event generation process. Assumed failure rate for busbar is 0.006 and restoration time is 5.5 h.

- a) Firstly a random stream for each process must be generated. This can be done by the random generator of excel function.

Stream 1: 0.12133578, 0.15234597, 0.71234589

Stream 2: 0.23458998, 0.52384698, 0.59237468

- b) Calculate the first time to failure according to Equation 5-7.

$$T_{fail} = -\ln(1-0,12133578)/(0,006)=21,30556 \text{ a} = 21 \text{ years}, 4894.6\text{h}$$

- c) Calculate the subsequent restoration time according to Equation 5-7

$$T_{restor} = (-\ln(1-0,2345898))^{1/4} * 6,5 / \Gamma(5/4) = 4.2\text{h}$$

- d) Update calendar

$$T = T_{fail} + T_{restor} = 21\text{year}2678\text{h} + 4,2\text{h} = 21\text{year}4898,8\text{h}$$

- e) Repeat step a) with the second random number in stream 1 generate

$$T_{fail} = 27 \text{ year } 4792\text{h}$$

- f) Repeat step b) with the second random number in stream 2 generate

$$T_{restor} = 5,5\text{h}$$

- g) Updating the calendar

$$T = 49 \text{ years } 935,9\text{h}$$

This process is stopped after the calendar is exceeding 50 years observation period. In this example the third random number will bring the calendar exceeding 50 years, so in this simulation period, there two failure events for busbar 1 in total.

The failure event of other electrical elements in the network can be obtained by repeating the process above.

Finally the failure events of the whole system can be merged and sorted into one list according to the time sequence. Each failure event will be processed separately as described in the following sections.

1.15.2 Step 2: Network State Analysis

After failure events are generated, the network state must be analyzed to detect the existing island due to the failure event.

a) Network topology information

Network topology information includes the following information:

- **Terminal Information**

Terminal is the connection point of electrical elements in the network. Disconnectors are mounted on each terminal. Failure current interruption device, which are most cases fuses in LV, can be chosen to be mounted on terminals according to the protection concept.

Figure 5-2 shows a simple illustration of terminal position in the network. One example of required terminal information is listed in Table 5-1.

Terminal ID	Terminal Name	Connected Element 1 Type	Connected Element 1 ID	Connected Element 2 Type	Connected Element 2 ID	Protection ID
4	Terminal 4	Busbar	2	Line	1	1

Table 5-1 Terminal information required for Monte-Carlo simulation

Each terminal connects two elements, so in this table the two elements connected by terminal are distinguished. Protection ID represents whether fuse is mounted on the terminal. ID “1” represents fuse is mounted on terminal and ID “0” represents no fuse is mounted on terminal

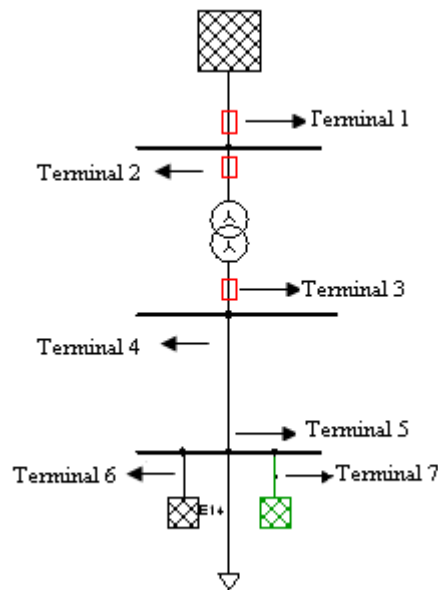


Figure 5-2 Terminal positions in the network

- **Infeeder Information**

Infeeder should be distinguished by upstream infeder or DG, i.e.:

Infeeder ID	Connected Terminal ID	Infeeder Type	DG Type	Unavailability	Rated Power /kW
1	1	Upstream			
2	6	DG	CHP	%0	3

Table 5-2 Infeeder information required for Monte-Carlo simulation

- **Busbar Information**

An example of busbar information is listed in Table 5-3

Busbar ID	Busbar Name	Connected Terminal Amount	Connected Terminal 1	Connected Terminal 3	Connected Terminal 2
1	Busbar 1	2	1	2	
2	Busbar 2	2	3	4	
3	Busbar 3	3	5	6	7

Table 5-3 Busbar information required for Monte-Carlo simulation

It should be noted here that, the amount of terminals that connected by each busbar can be different; so the terminal amount should be specified.

- **Line information**

An example of Line information is listed in Table 5-4

Line ID	Line Name	Connected Terminal 1 ID	Connected Terminal 2 ID	Line Length /m
1	Line 1	4	5	100

Table 5-4 Line information required for Monte-Carlo simulation

- **Transformer Information**

An example of transformer information is listed in Table 5-5

Transformer ID	Transformer Name	Connected Terminal 1 ID	Connected Terminal 2 ID
1	Trafo1	2	3

Table 5-5 Transformer information required for Monte-Carlo simulation

- **Load Information**

Load is directly connected with busbar, so there is no terminal information for load, only the connected busbar should be specified. In Monte Carlo simulation, similar as in the analytical method, the load type varies between Industry, Household, or Agriculture. Load Priority is categorized as “Very High”, “High”, “Normal”, “Low”, “Very Low”, in total five stages.

Load ID	Load Name	Connected Bus ID	Load Priority	Load Type	Rated Power/kW
1	Load 1	3	Normal	House	3

Table 5-6 Load information required for Monte-Carlo simulation

It can be seen from elements information, except loads, that all the electrical elements have the “terminal” information and all the terminals have the information, that with which electrical elements are terminals connected the following analysis are based on the relations between electrical element and terminals.

b) Network topology analysis

After failure happens on one element, disconnectors at all terminals of this element will be triggered, then it should be judged whether a fuse is mounted on these terminals. If a fuse is mounted on this terminal, a failure will be not extended to another element connected with this terminal, otherwise all terminals of the element connected with the failure element are

also triggered to isolate this failure. The similar trigger will proceed until the fuse interrupts the failure current.

After the failure is isolated, connected elements is categorized into one island, which is marked by the same number.

In the example shown in Figure 5-3 , after failure happens on the line, which is marked by “red”, all the elements inside this protection zone are triggered, which is marked by “blue”

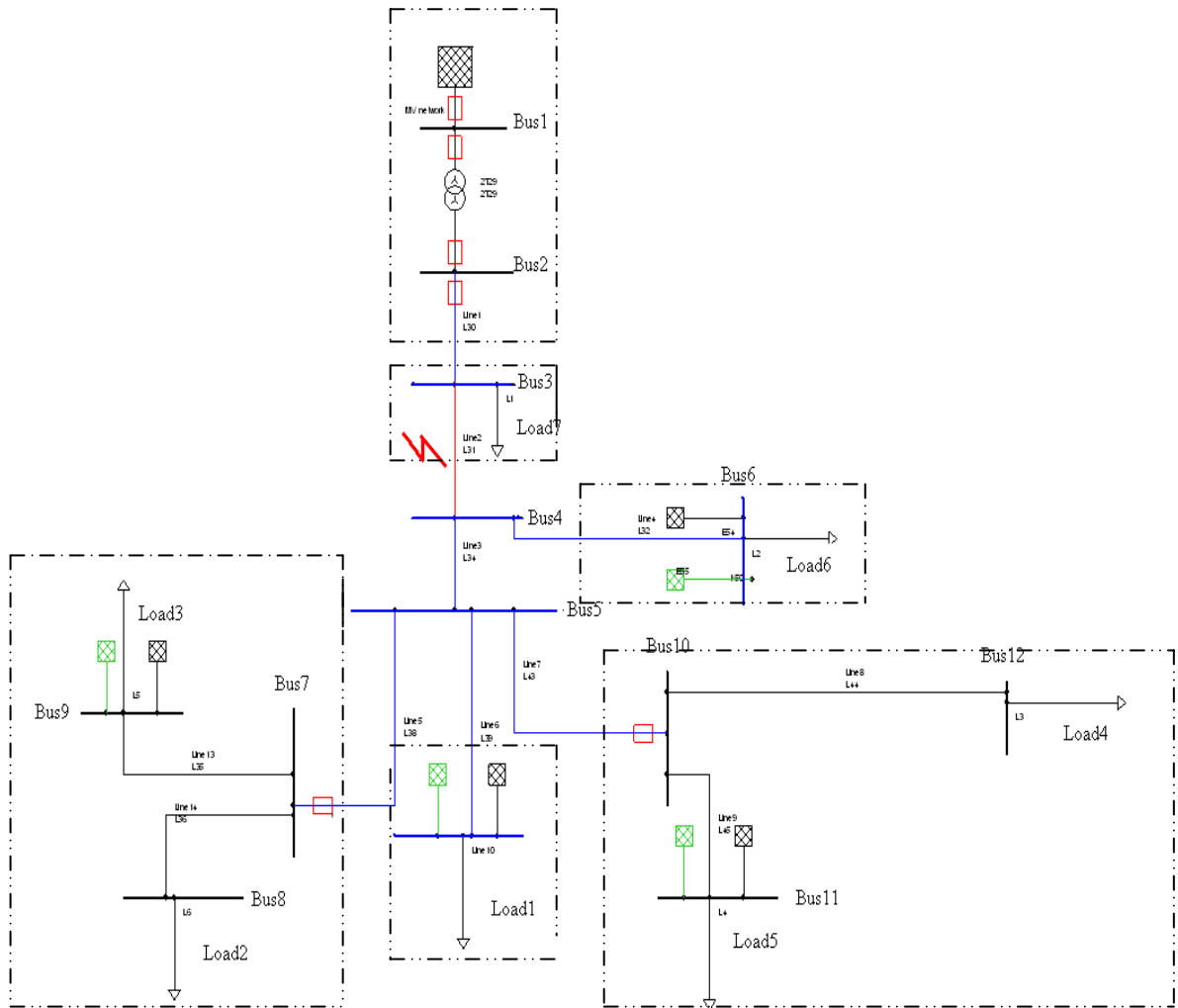


Figure 5-3 Islanding topology of Italy rural network

After network analysis, all networks marked by the same island ID are categorized in the same island, i.e.:

Island ID	Infeeder	Load	
0	Upstream Infeeder		
2		Load 7	
3	DG 4	Load 6	
4	DG 3	Load 4, Load 5	
5	DG 2	Load 2, Load 3	
6	DG 1	Load 1	

Table 5-7 Island categorization for network topology analysis

1.15.3 Step 3: Load State Analysis

After the network analysis load state is analysed to calculate the interruption frequency and interruption power. Load state analysis can be performed in three different cases

a) Load is connected with upstream infeeder

In this case, load can be fully supplied by upstream infeeder, so interruption frequency and interruption power are both 0

b) Load is disconnected from upstream infeeder and no DG work in the same island with this load

In case b, no infeeder supplies this load, so load is interrupted and interruption power equal to instantaneous load demand at the failure time.

c) Load is disconnected from upstream infeeder and there are DGs working in the same island with this load.

In case c, two cases should be separately processed.

Loads working in the same island have the same load priority

For instance, in island 5 of last example, load 2, load 3 and DG 2 work in the same island.

Assume at the failure time, instantaneous DG power is P_{DG} , instantaneous load demand of load 2 is P_{Load2} , instantaneous load demand of load 3 is P_{Load3} , load 2 and load 3 have the same priority, then the available power of load 2 is

$$P_{Avail,2} = P_{DG} * \frac{P_{Load2}}{P_{Load2} + P_{Load3}} \quad \text{Equation 5-7}$$

In Microgrid load can be shed to instantaneous power at the failure time, so the interrupted power corresponds to

$$P_{loss} = \max(P_{Avail,2} - P_{DG}, 0) \quad \text{Equation 5-8}$$

Load is regarded to be interrupted when

$$P_{load1} - P_{Avail1} < 0 \quad \text{Equation 5-9}$$

Loads working in the same island have different load priority

Assume load 2 having higher load priority than load 3, then

$$P_{Avail,2} = P_{DG} \quad \text{Equation 5-10}$$

$$P_{Avail,3} = \max((P_{Avail,2} - P_{Load2}), 0)$$

When more loads are available in one island with different priorities, the same iteration can be done to calculate the available power

$$P_{Avail,i} = \max((P_{Avail,i-1} - P_{Load,i-1}), 0) \quad \text{Equation 5-11}$$

Where $P_{Avail,i-1}$ and $P_{Load,i-1}$ are the available power and load demand of the load in the last priority stage. Then the same calculation can be done to calculate the interruption power and interruption frequency according to Equation 5-8.

1.15.4 Step 4: Restoration and repair process

After the failure is isolated, the restoration process starts. All the triggered elements are restored. Finally the failure elements are repaired and system work in normal state again. After each restoration of electrical elements, system state is analyzed again according to step 2. During the period between current restoration and next restoration, load state is analyzed chronologically as in step 3 according to the instantaneous load demand and DG output power of each step. It can be seen from here intermittent micro-source output is considered. Interrupted energy and interruption duration during this period are calculated. After the failure element is repaired, the calculated interruption duration and interruption energy during each restoration step is summed to obtain the total interruption energy and interruption duration of one failure event. The flow chart of restoration and repair process is shown in Figure 5-4.

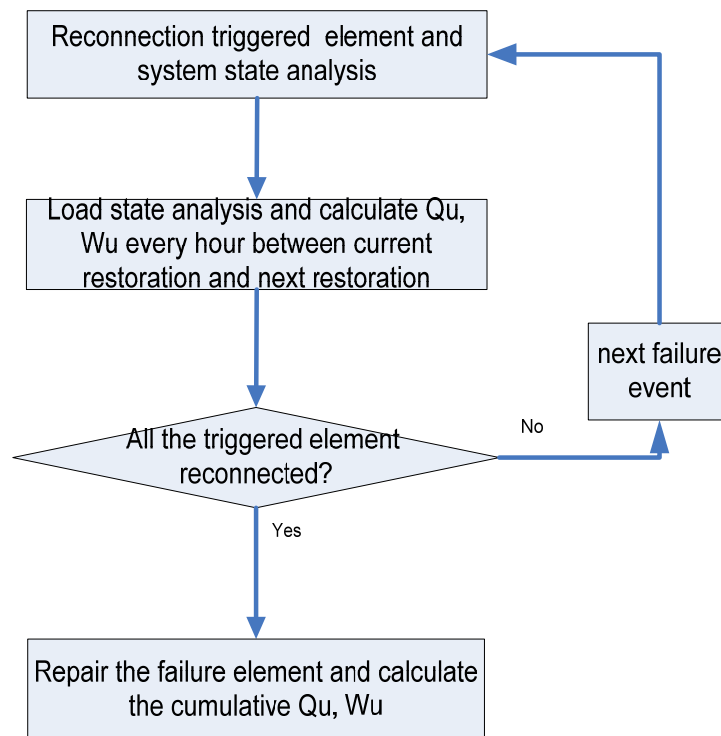


Figure 5-4 Flow chart of restoration process

After one observation period is finished, system reliability indices H_u , Q_u are calculated according to

$$F_k = \frac{\sum_i \sum_j F_{u,i,j}}{OP} \tag{Equation 5-12}$$

Where OP means observation period, which is chosen as 50 year, F_k is the system reliability of the k^{th} observation period. $F_{u,i,j}$ is the reliability index for the end load customer i of failure event j .

System reliability indices are P_u , W_u are cumulative values, which can be calculated by

$$F_k = \sum_i \sum_j F_{u,i,j} \quad \text{Equation 5-13}$$

The final reliability indices after can be calculated by

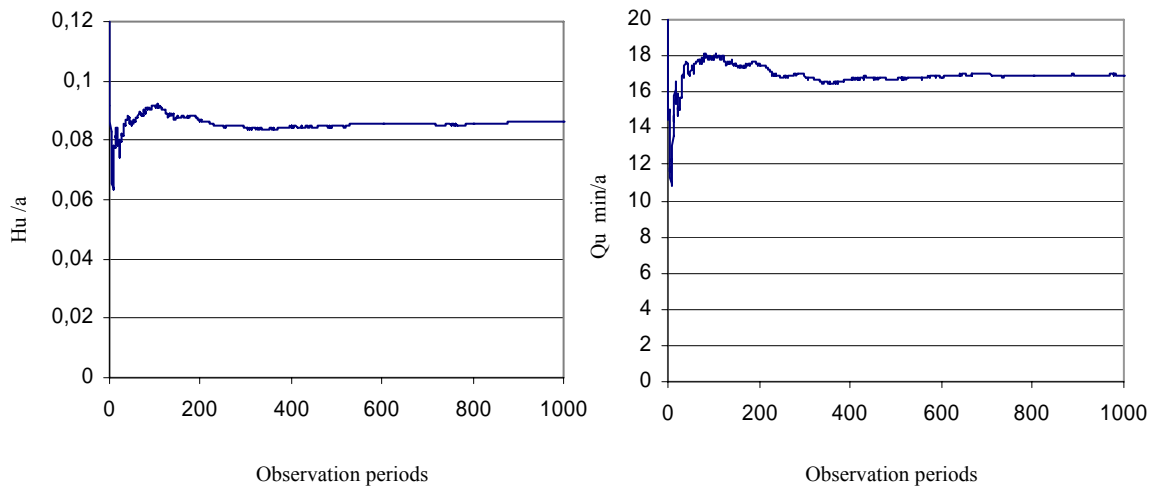
$$F_N = \frac{\sum_1^{NS} F_k}{NS}, \quad F_N = \sum_1^{NS} F_k \quad \text{Equation 5-14}$$

where NS means the number of observation periods, which is chosen as 1000 times.

1.16 Case study- Italy rural network

1.16.1 Convergence progress of system reliability after applying micro-sources

Italy rural network topology is indicated in Figure 5-3 with load and DG power both rated 3kW. The convergence process of system reliability without battery is shown in Figure 5-5. In theory, Monte-Carlo simulation achieves most accurate result after infinite observation periods; however as it can be seen, after 300 observation periods system reliability indices already begin to converge, so it is possible to get quasi-accurate result after sufficient, but limited observation periods.



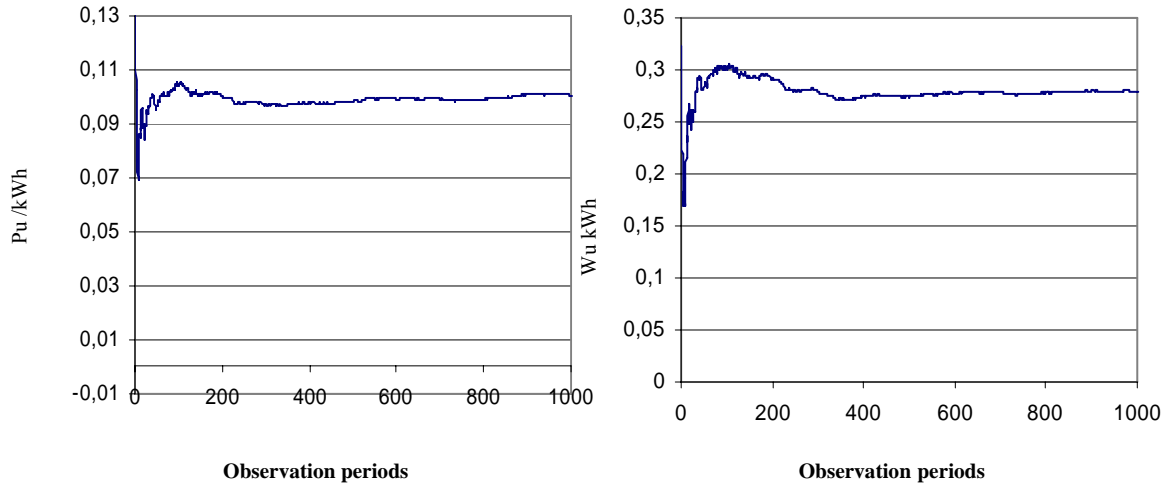


Figure 5-5 Convergence process of system reliability

1.16.2 Comparison between Monte-Carlo simulation and analytical method

To compare system reliability indices, Figure 5-6 presents the simulation result for both analytical and Monte-Carlo simulation for CHP penetration of Italian network, Figure 5-7 presents the results for wind turbine penetration, Figure 5-8 that for PV.

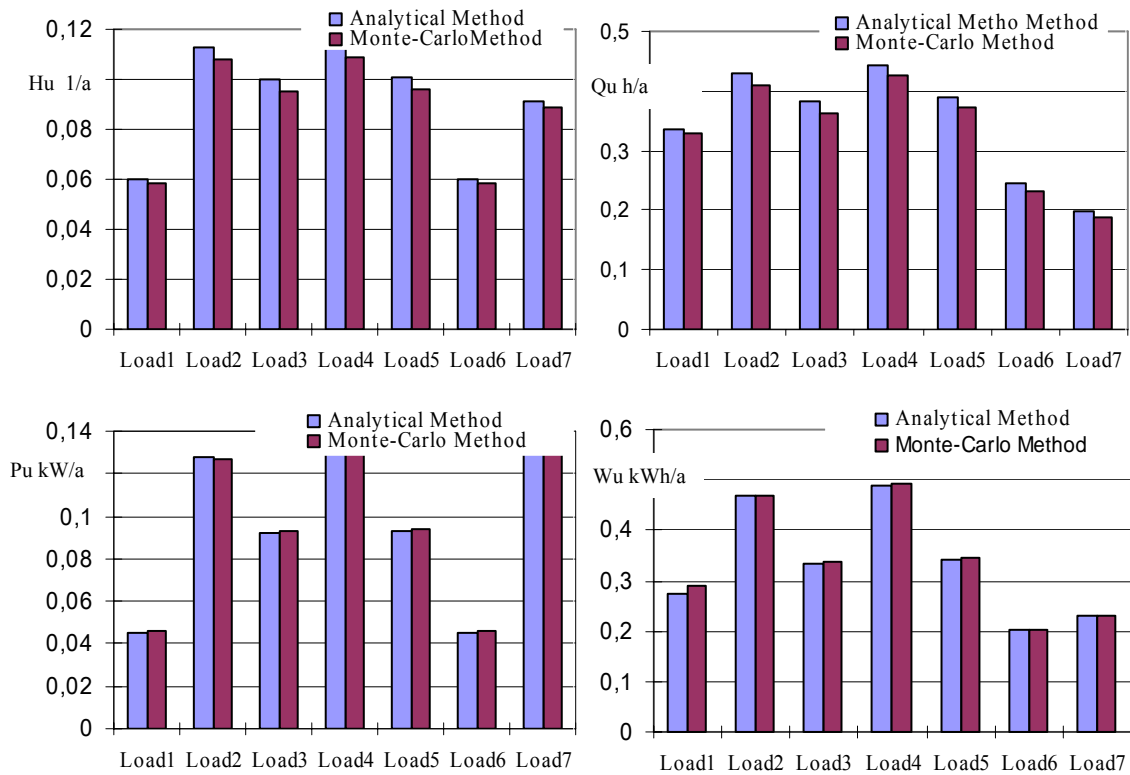


Figure 5-6 Reliability indices comparison for CHP scenario

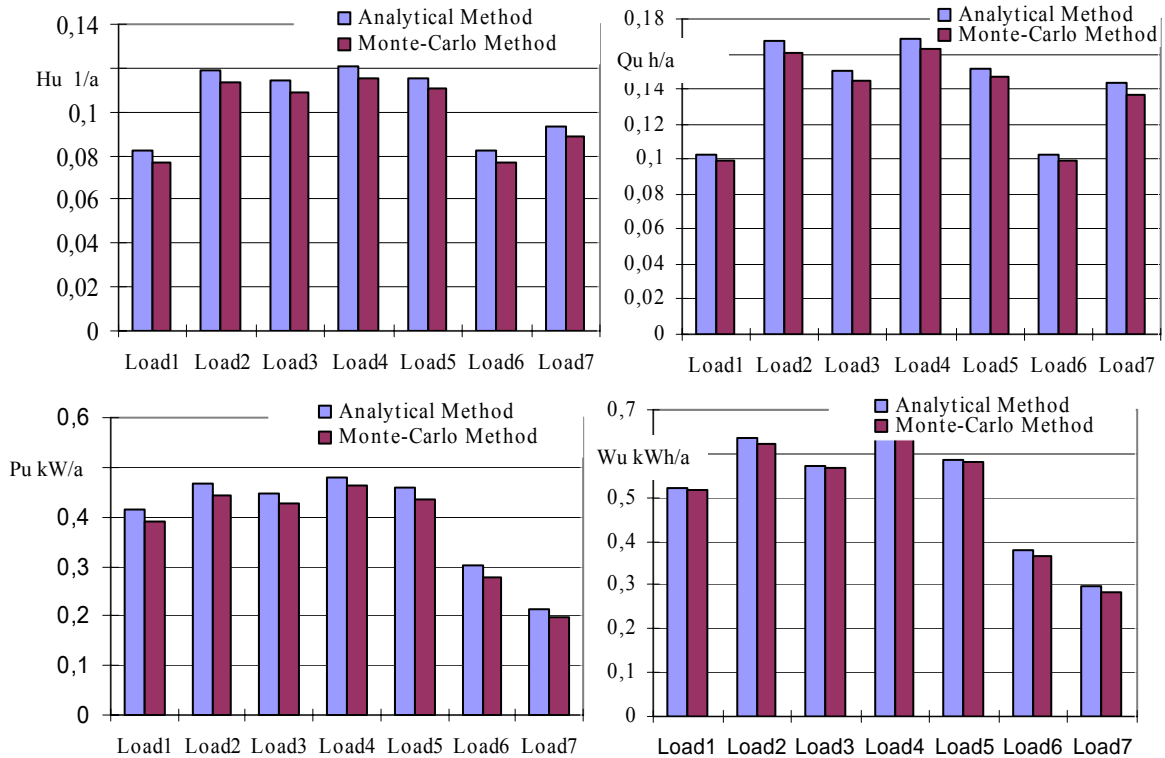


Figure 5-7 System reliability indices comparison for WT scenario

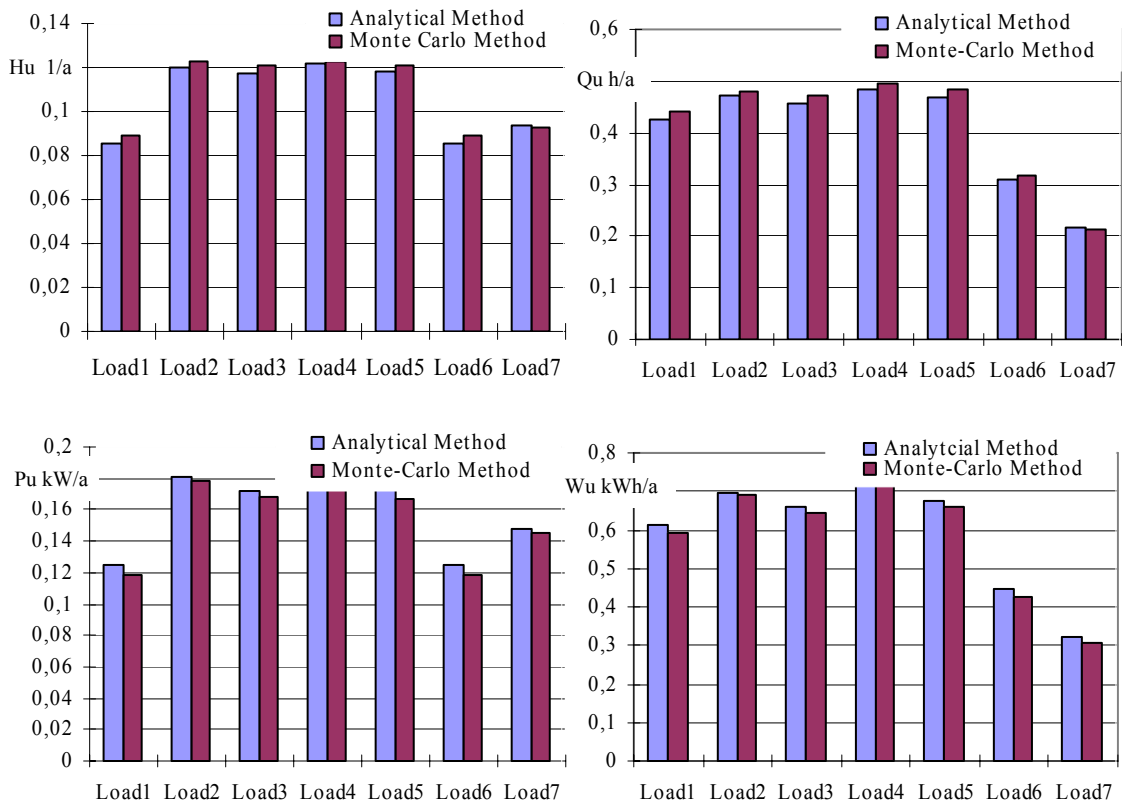


Figure 5-8 System reliability indices comparison of scenario 4120

Deviations up to 5% exist between both methods. Generally Monte-Carlo simulation results are quasi-accurate after enough times simulation periods. As already analyzed in the previous

chapter, due to the normal distribution approximation, error of analytical result can not be avoided. It is also interesting to see that the errors for H_u , Q_u and P_u , W_u have different trends, which is caused by different calculation methods for H_u , Q_u and P_u , W_u respectively. Nevertheless, this error is acceptable, which proves again SAM and Monte-Carlo simulation being successful.

1.16.3 Comparison of probability distribution of reliability indices

Up to now, the reliability assessment is limited in the range of expected value. With regards to reliability aspects, the risk is mainly derived from the stochastic nature of failure event. Especially power generation from PV and Wind turbine depend on intermittent weather conditions; therefore the reliability indices generally possess a very wide probability distribution. From the aspect of network planning, the rarely happened failure event is also very important and should be considered during this period, therefore the evaluation of reliability expected value is not sufficient to have a complete assessment of system reliability. Probability distributions of reliability indices are required that are generally calculated by Monte-Carlo method, due to the simulation property of this method. Paper [28] demonstrates a method to determine the distribution also for the analytical method, however this works only for the case without micro-sources and is limited to a specific distribution of failure event. Monte-Carlo simulation is the only possible method to correctly evaluate the reliability distribution indices due to fluctuation renewable generation.

The cumulative probability density function (CDF) of system reliability indices for CHP penetration is presented in Figure 5-9, the PDF is shown in Figure 5-10.

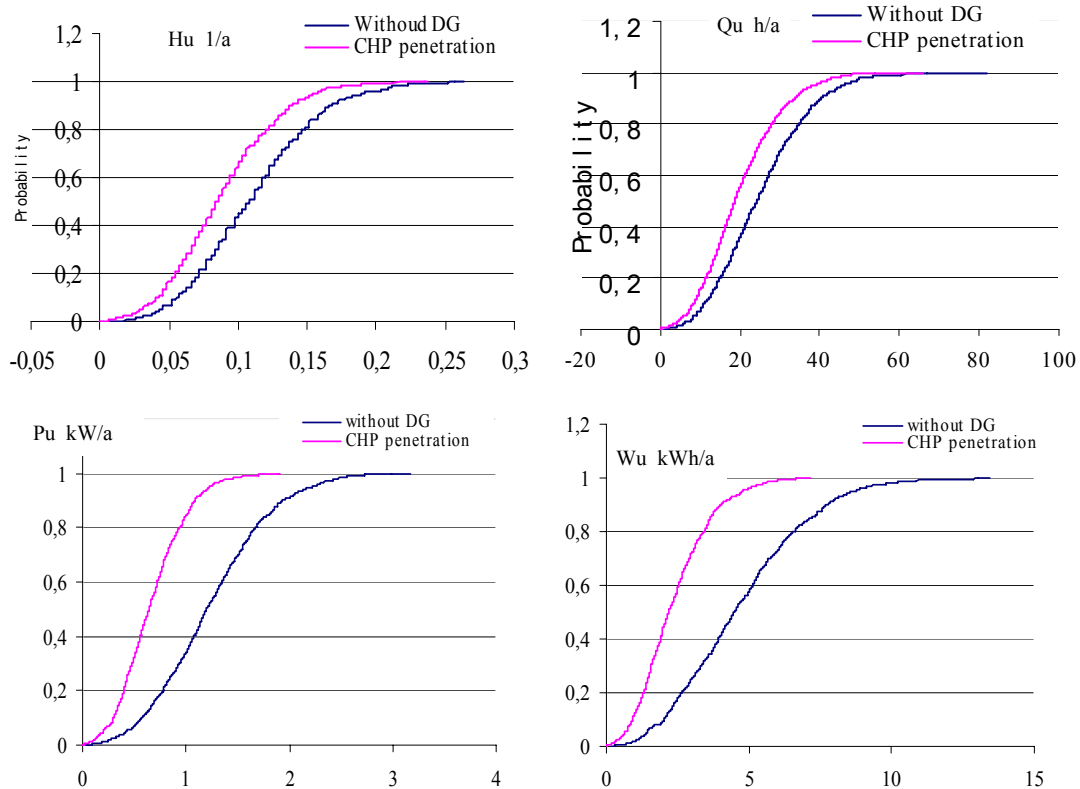


Figure 5-9 Cumulative distribution function (CDF) for Italian rural network with CHP penetration

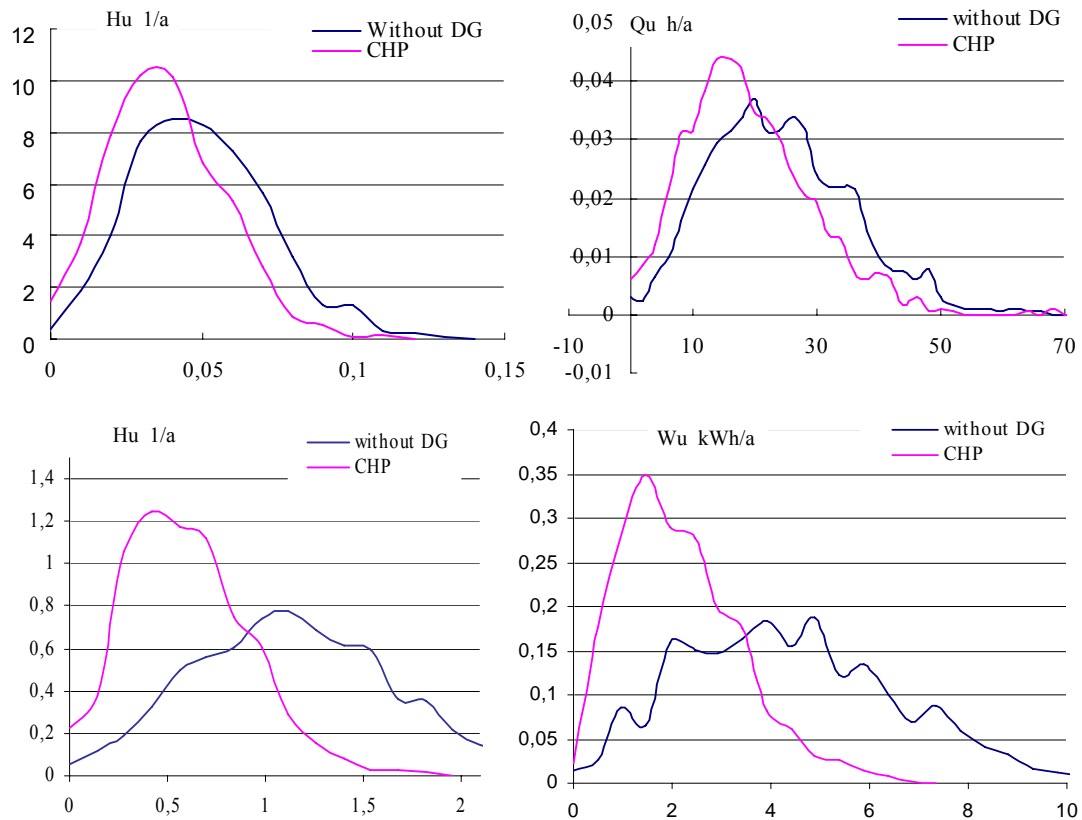


Figure 5-10 Probability density function (PDF) for Italian rural network with CHP penetration

All the reliability indices have a wide distribution that provides more detailed assessment of system reliability. It can also be derived that from perspective of distribution, that system reliability is improved by micro-sources.

1.17 Battery Modelling

Wind and solar generation is intermittent, therefore energy storage units are required to be incorporated into network in order to match the power balance of instantaneous power generation and load demand. Traditional energy storage elements that may be applied in Microgrids are battery, flywheel and pump storage. New solutions such as electric vehicles with distributed storage in the network are out of scope of this report.

Available power of energy storage elements is relevant with charging and discharging process. As this is strongly time dependent, analytical method is not applicable. In contrary, Monte-Carlo method simulates the system performance chronologically, so with good modelling of battery charging and discharging process, Monte-Carlo method is the most suitable method to simulate reliability impact of storage elements.

1.17.1 Battery charging and discharging modelling

The basic function of the battery is to smooth the fluctuating of power generation. Whenever instantaneous power generation is higher than instantaneous load demand, surplus power will be stored into the battery. When instantaneous power generation is lower than load demand, battery is discharged to supply the load.

Because of limited volume and weight, all batteries have a limited storage capacity, which is rated by “Ah”. For instance a battery, which is rated at 100 Ah will deliver 5 A over a 20 h period at room temperature. From the aspect of battery life time, deep discharging of a battery should be avoided. Repeated deep discharge will result in capacity loss and even failure, when the electrode disintegrate due to mechanical stresses, therefore maximal discharging capacity should be limited in advance. After exceeding this value, control unit of battery shuts down discharging circuit. Available capacity of a battery is dependent on the rate at which it is discharged, if a battery is discharged at a relative high rate, the available capacity will be lower than expected, for instance, if a battery rated at 100 Ah is discharged at 50 A, it will run out of charge before the theoretically expected 2 hours, therefore to make use of battery available capacity maximal discharging rate should be limited. In the following application, maximal battery discharging rate is 20 % of battery storage capacity. The maximal storage capacity is set as the rated capacity and minimal storage capacity is set as 40 % of battery rated capacity.

The chronological battery storage state can be achieved from the load state and power generation state, taking into account of maximal charging/discharging rate and minimal battery storage capacity [61]. Here, it is calculated using the following model:

- a. **Determine the surplus generation $SG(t)$, which can be either a positive or a negative value time series from the instantaneous load demand $L(t)$ and the power generation $RG(t)$ using**

$$SG(t) = RG(t) - L(t) \quad \text{Equation 5-15}$$

The instantaneous battery charging/discharging power $CG(t)$ is determined by:

If $CG(t) \geq 0$, which means battery is charged

$$CG(t) = \begin{cases} CG_{\max} & SG(t) \geq CG_{\max} \text{ and } ES(t) < ES_{\max} \\ SG(t) & .SG(t) < CG_{\max} \text{ and } ES(t) < ES_{\max} \\ 0 & ES(t) = ES_{\max} \end{cases} \quad \text{Equation 5-16}$$

If $CG(t) < 0$, which means battery is discharged

$$CG(t) = \begin{cases} -CG_{\max} & SG(t) \leq -CG_{\max} \text{ and } ES(t) > ES_{\min} \\ SG(t) & .SG(t) > -CG_{\min} \text{ and } ES(t) > ES_{\min} \\ 0 & ES(t) = ES_{\min} \end{cases} \quad \text{Equation 5-17}$$

with $ES(t)$ as instantaneous battery storage capacity, which is determined by charging /discharging process in the previous hour, CG_{\max} as the maximal charging/discharging power, ES_{\max} as maximal battery storage capacity, and ES_{\min} as minimal battery storage capacity.

b. Compute the instantaneous energy storage of battery next hour $ES(t+1)$, using the following equation

$$ES(t+1) = \begin{cases} ES_{\min} & ES(t) + SG(t) \leq ES_{\min} \\ ES_{\max} & ES(t) + SG(t) \geq ES_{\max} \\ ES(t) + CG(t) & ES_{\min} < ES(t) + SG(t) < ES_{\max} \end{cases} \quad \text{Equation 5-18}$$

Assume one household load with 3 kW rated power, one PV unit with 3 kW rated and battery with 3 kWh rated capacity work in one island, Figure 5-11 indicates the charging and discharging process of battery.

When instantaneous DG output is higher than load demand, the battery is charged by the surplus power with limited charging rate. When DG output is lower than load demand, the battery is discharged to supply the load with limited discharge rate. Battery storage capacity is not possible to be charged and discharged infinite. They are limited by the minimal and maximal storage capacity.

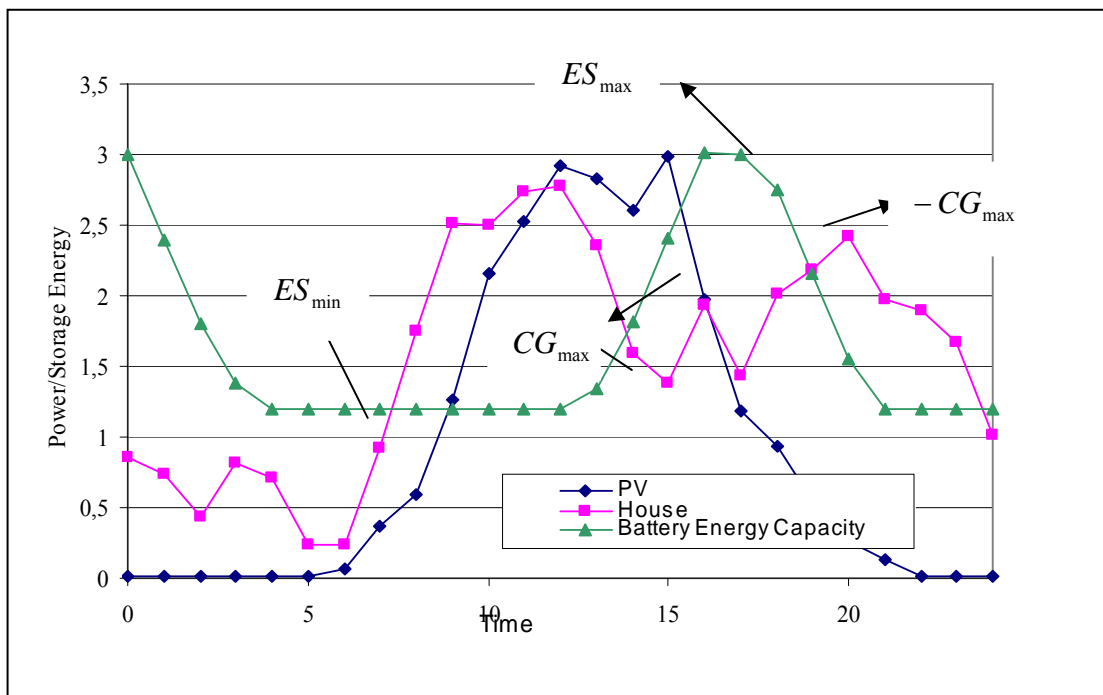


Figure 5-11 Operation state of battery

1.17.2 Battery impact on reliability performance

When instantaneous power generation is lower than load demand, battery is discharged and able to supply part of loads what increases system reliability.

Scenario a: 6 kWh battery and 3 kW CHP unit in network as indicated in Figure 5-12

Probability distribution of simulation results with battery is compared to the case without in Figure 5-13 and Figure 5-14 for PDF and CDF of reliability indices.

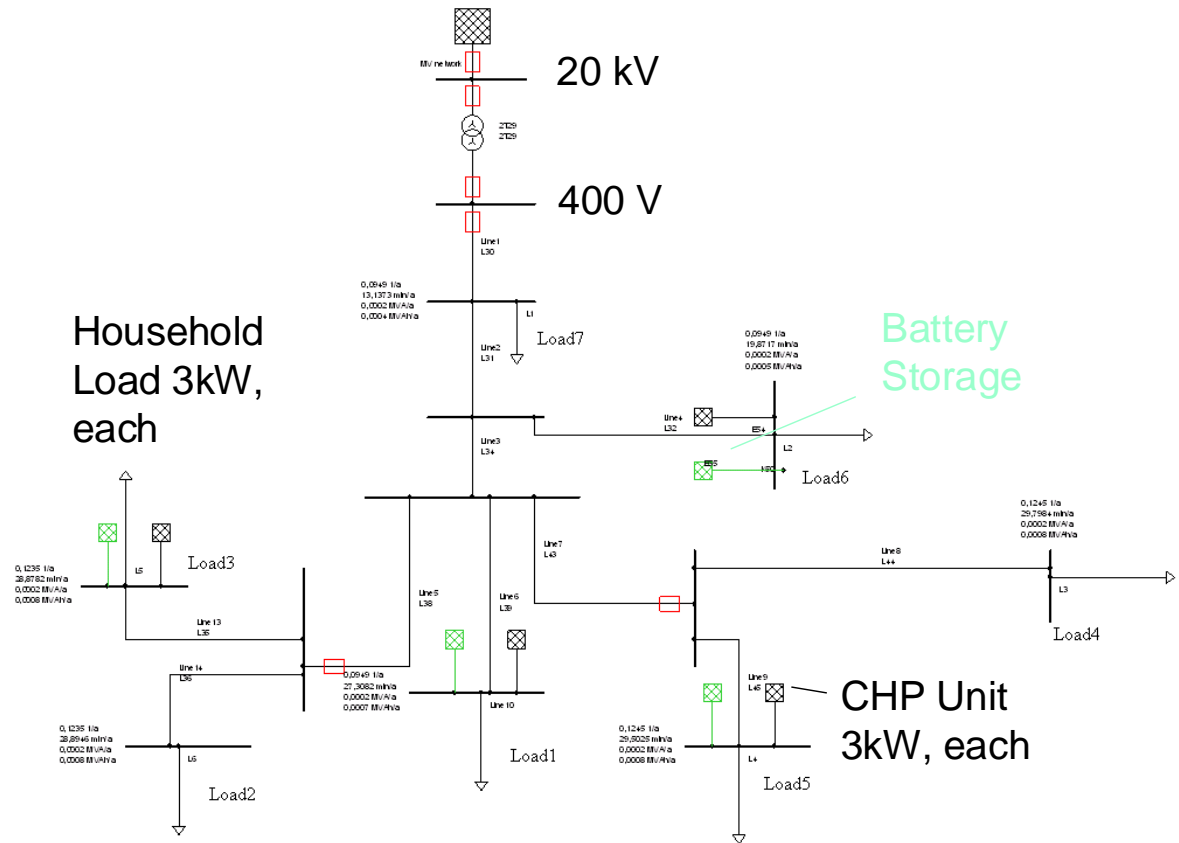


Figure 5-12 Location of battery storage in Italian rural network

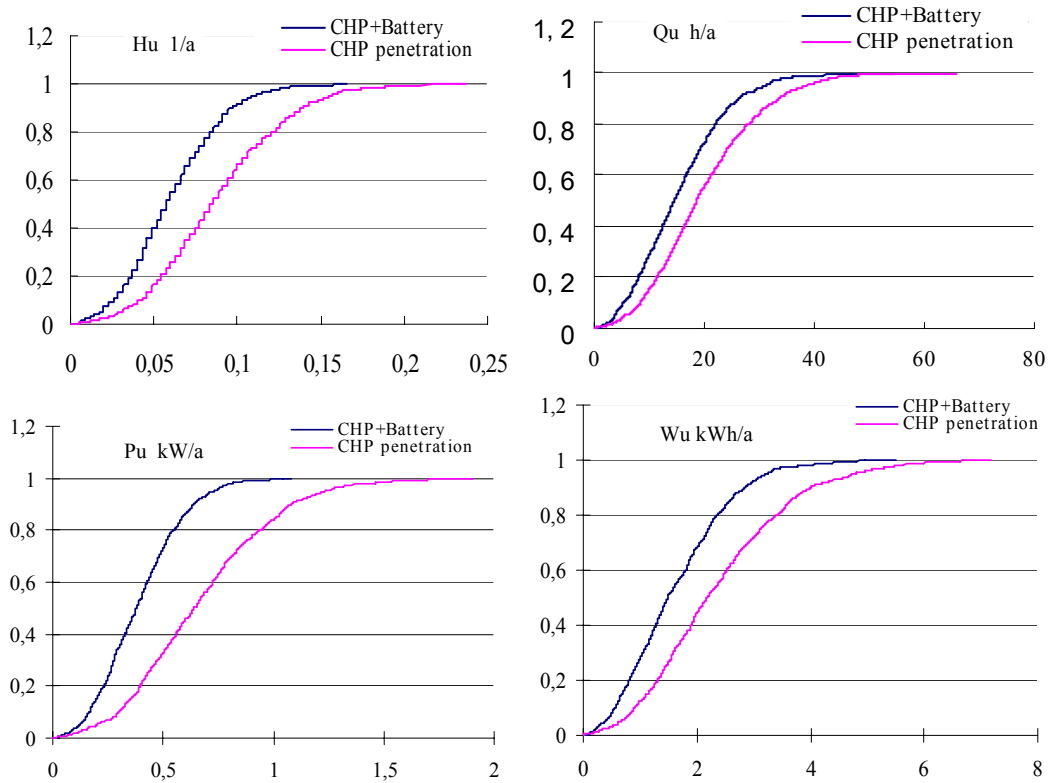


Figure 5-13 PDF system reliability improvement by battery

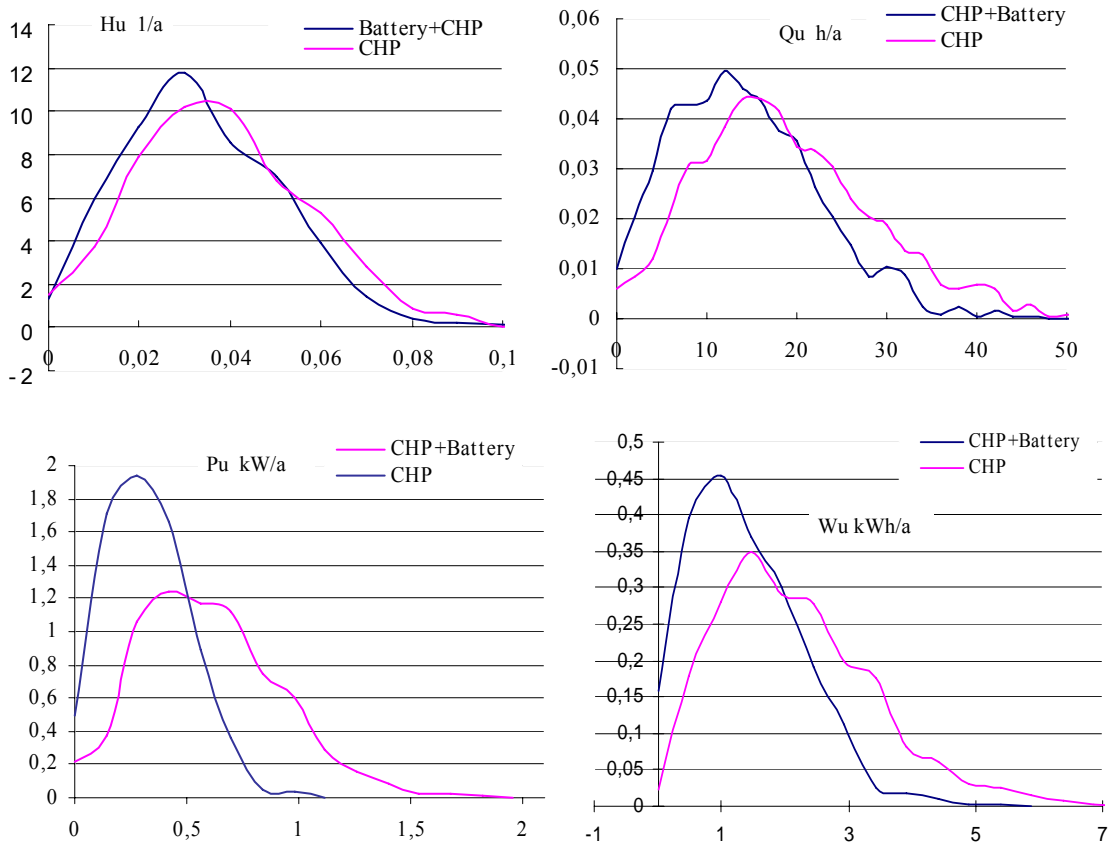
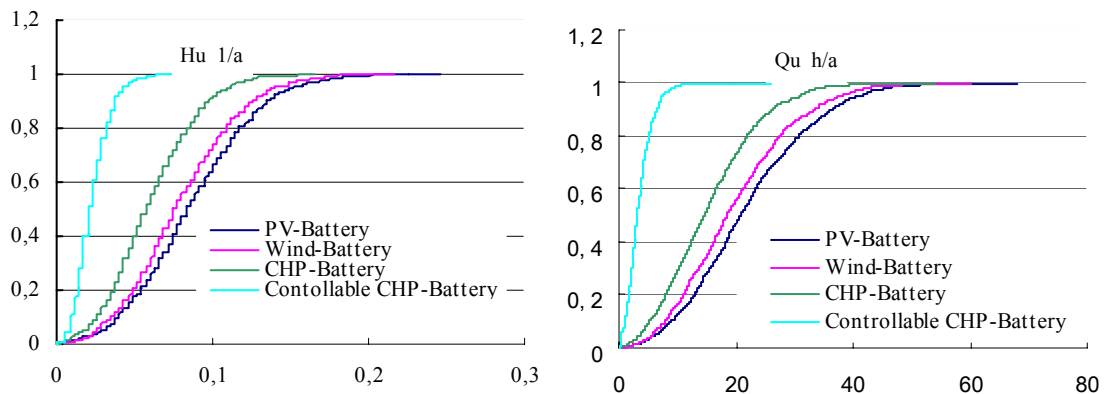


Figure 5-14 CDF System reliability improvement by battery

To quantify reliability improvement by battery with different combinations of micro-sources, the following scenarios are investigated (Figure 5-15):

- a: 6 kWh battery and 3 kW PV unit
- b: 6 kWh battery and 3 kW Wind generation
- c: 6 kWh battery and 3 kW CHP operated heat-driven
- d: 6 kWh battery and 3 kW controllable CHP



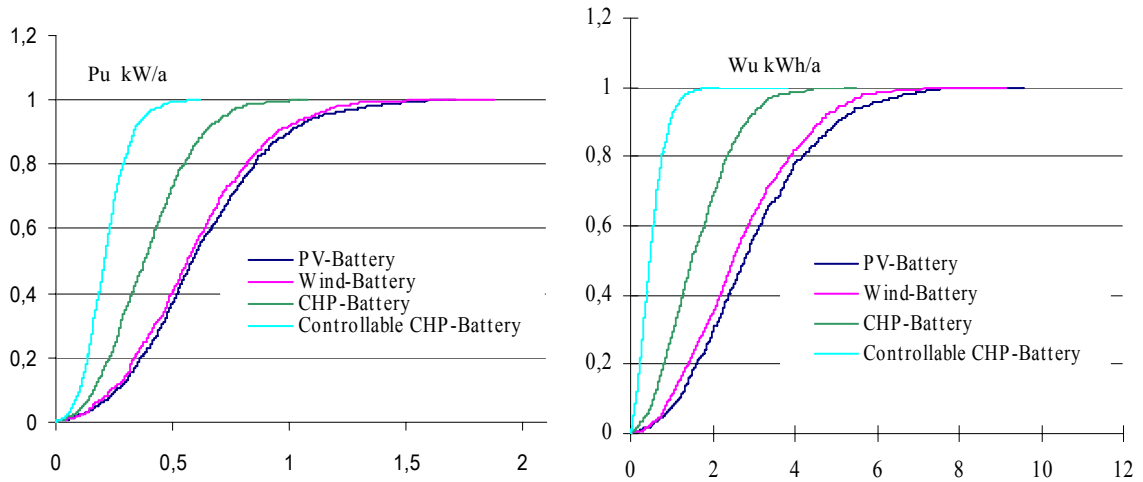


Figure 5-15 CDF System reliability indices with battery and different micro-sources

Similar to the case without batteries in the network reliability is improved with increasing controllability and full-load hours of the micro-sources (Figure 5-16). As shown, best results are achieved with CHP and battery (6 kWh).

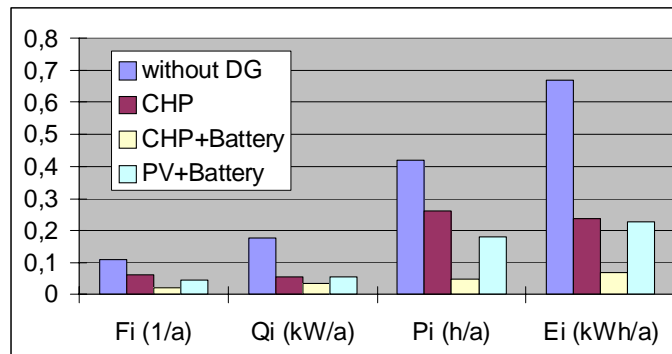


Figure 5-16 Comparison of micro-source technology impact on reliability

Figure 5-17 demonstrates the impact of the battery capacity on the reliability improvement, together with 3 kW CHP units. Reliability indices decrease up to battery capacity around 20 kWh; a further increase of battery capacity has no further influence of reliability. In this case battery and micro-sources are already able to supply most of the load in island mode. So, for each network and load configuration there is always an optimum battery size with limited capacity (and thus optimum costs).

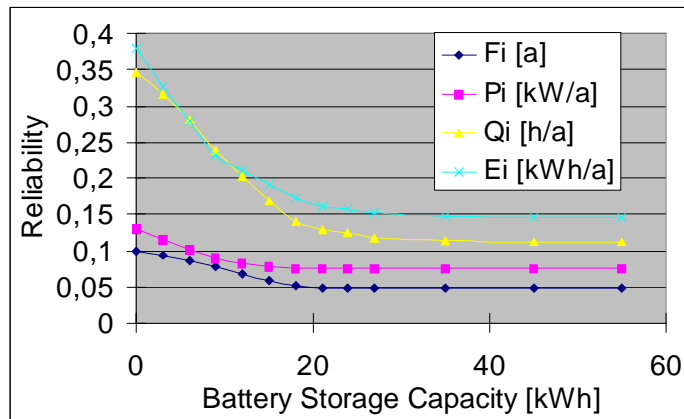


Figure 5-17 Battery storage capacity influence to system reliability

1.18 Impact of Microgrid Control on Reliability

Immediate transition to island mode mainly improves frequency dependent reliability indices as shown in Figure 5-18 and Figure 5-19 for CHP 3 kW and Battery 6 kWh.

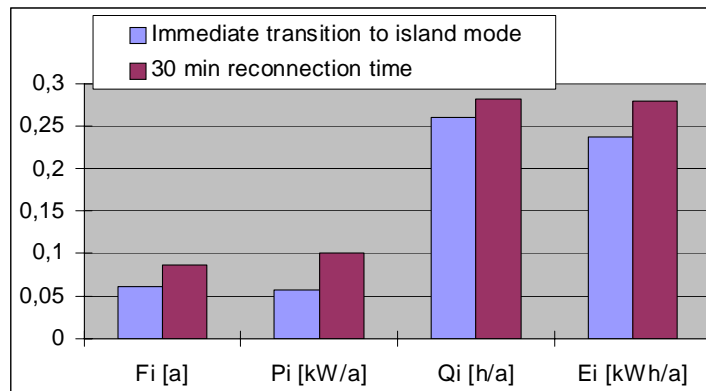


Figure 5-18 Battery storage capacity influence to system reliability

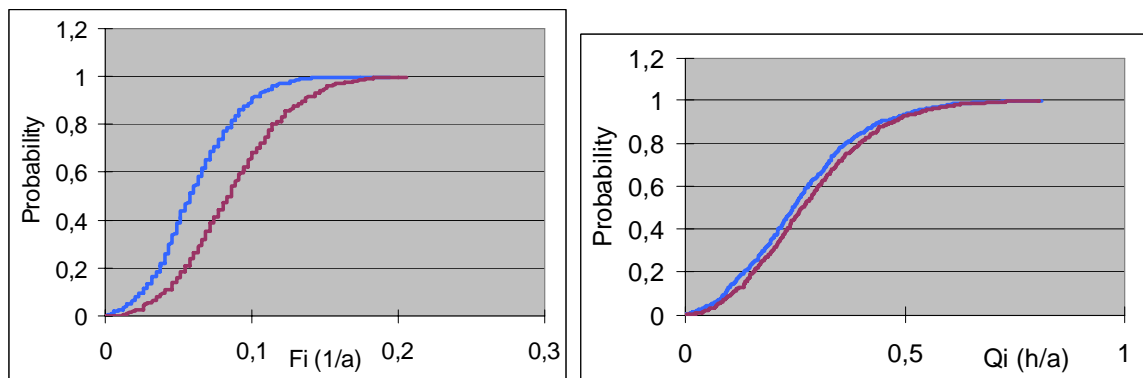


Figure 5-19 Probability distribution of technology dependent reliability indices

1.19 Comparison of Sequential Monte-Carlo Simulation and Analytical Method

Table 5-8 compares both simulation methods as already described in the previous chapters.

It can be seen that Monte-Carlo method is most suitable to simulate micro-sources located in the network. However, due to the enormous reduction of simulation time the analytical method is applied to detect the optimised penetration with micro-sources, which is described in the next chapter.

Table 5-8 Comparison of Monte-Carlo method and analytical method

	Analytical simulation	Monte-Carlo simulation
Accuracy without DG	Most accurate result	Quasi-accurate after enough time simulation
Accuracy after applying DG	Certain error exists due to the normal distribution approximation of DG unit	Quasi-accurate after enough time simulation(1000 times in this experiment, 50 years observe duration)
Simulation Speed	Fast	Slow
Possibility to get probability distribution function	Possible before applying DG (after applying DG will be further studied)	Possible
Possibility to simulate battery	Not possible	Possible
Applying area in the reliability studies	Test the optimization result of DG position, and DG power	Simulate the battery get the distribution function

6 Optimum micro-source planning strategy considering their impact on reliability

Two different planning strategies are investigated in this chapter - the technical reliability improvement, which means achieving the best reliability improvement with limited micro-source number and capacity and the economic benefit caused by reliability improvement.

1.20 Optimum micro-source planning strategy for technical reliability improvement

1.20.1 Micro-source location

In previous reliability studies [51], it is concluded that

- DG located in downstream has better reliability improvement than located upstream.
- Decentralized micro-sources achieve higher improvement than centralized generation.

LV networks – which form Microgrids - are already the most downstream network. From average German reliability indices [60] it can be seen that most of failures of the network are caused by MV and HV level; therefore when failures from MV level are taken into account, failures from LV doesn't have significant influence.

Italy rural network (as from Figure 4-7) with load and reliability settings as above is studied for the optimization purpose.

Downstream planning strategy

According to the downstream level bus9>bus7>bus4>bus2, different micro-source locations (with 100 % CHP penetration) are compared in Figure 6-1 without considering MV and HV. The simulation result considering MV and HV is plotted in Figure 6-2

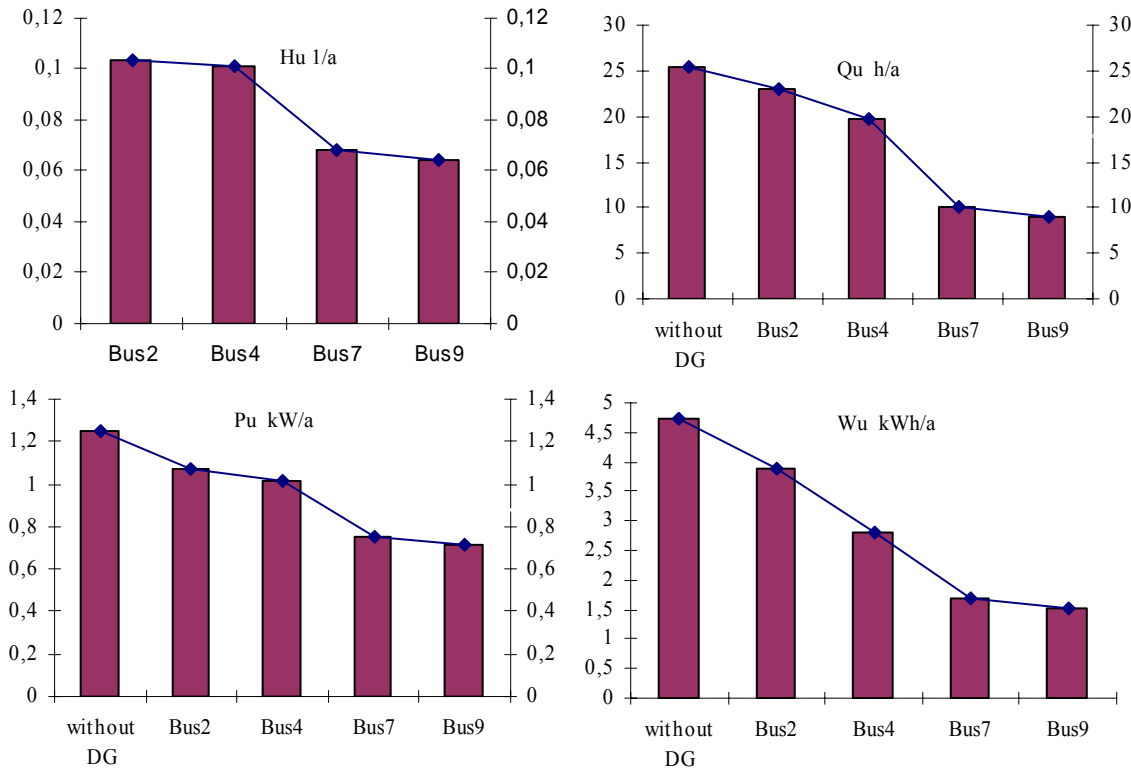


Figure 6-1 Reliability depending on CHP location neglecting HV and MV influence

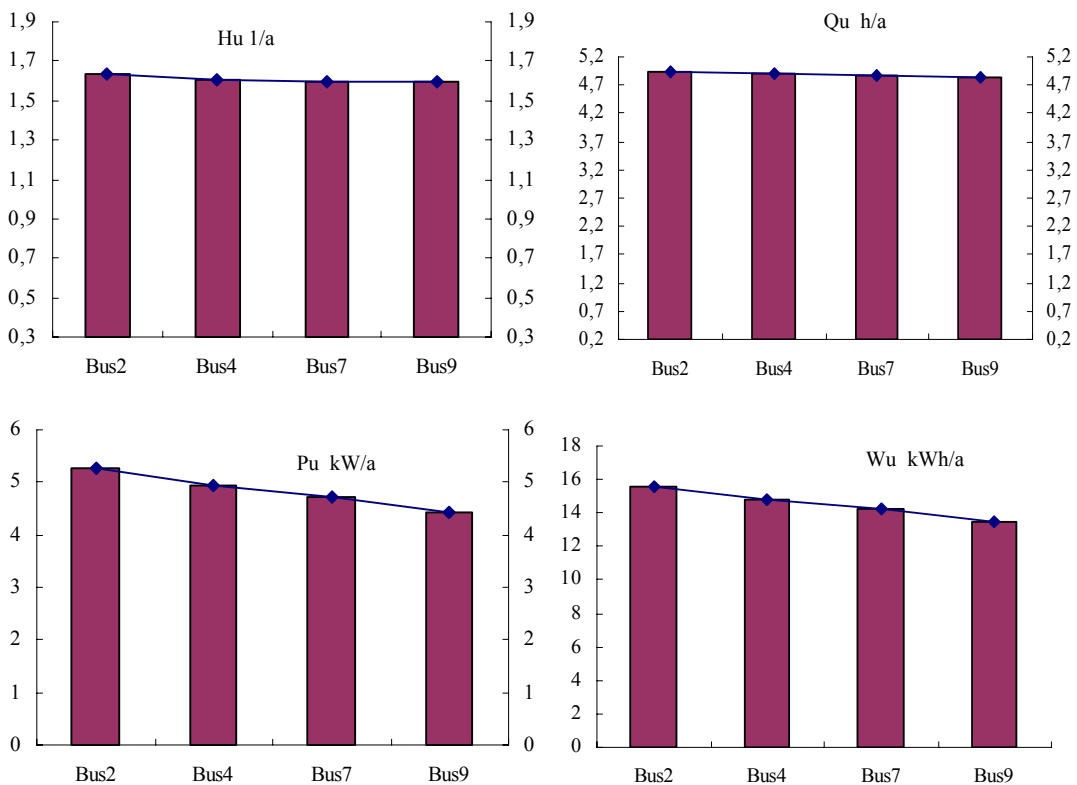


Figure 6-2 Reliability depending on CHP location considering HV and MV influence

All the indices are obviously improved the more downstream CHP units are connected, because DG located most downstream is able to supply the load in more failure cases.

In Figure 6-2 reliability indices are slightly improved, however the improvement is not obvious, because when failure is from HV and MV, all the DG units and load work in one island, so micro-source location in LV has no difference for the reliability improvement.

Centralisation planning strategy

The following scenarios, each with 100 % penetration level, are simulated with and without considering HV and MV influence separately (Figure 6-3 and Figure 6-4). The reliability setting of LV is still same as before.

- a: 1 CHP units are concentrated to bus4
- b: 4 CHP units are dispersed to bus6, bus9, bus11 and bus13
- c: 5 CHP units are dispersed to bus6, bus8, bus9, bus11 and bus13
- d: 7 CHP units are dispersed to bus 3, bus6, bus11, bus12, bus8, bus9 and bus13

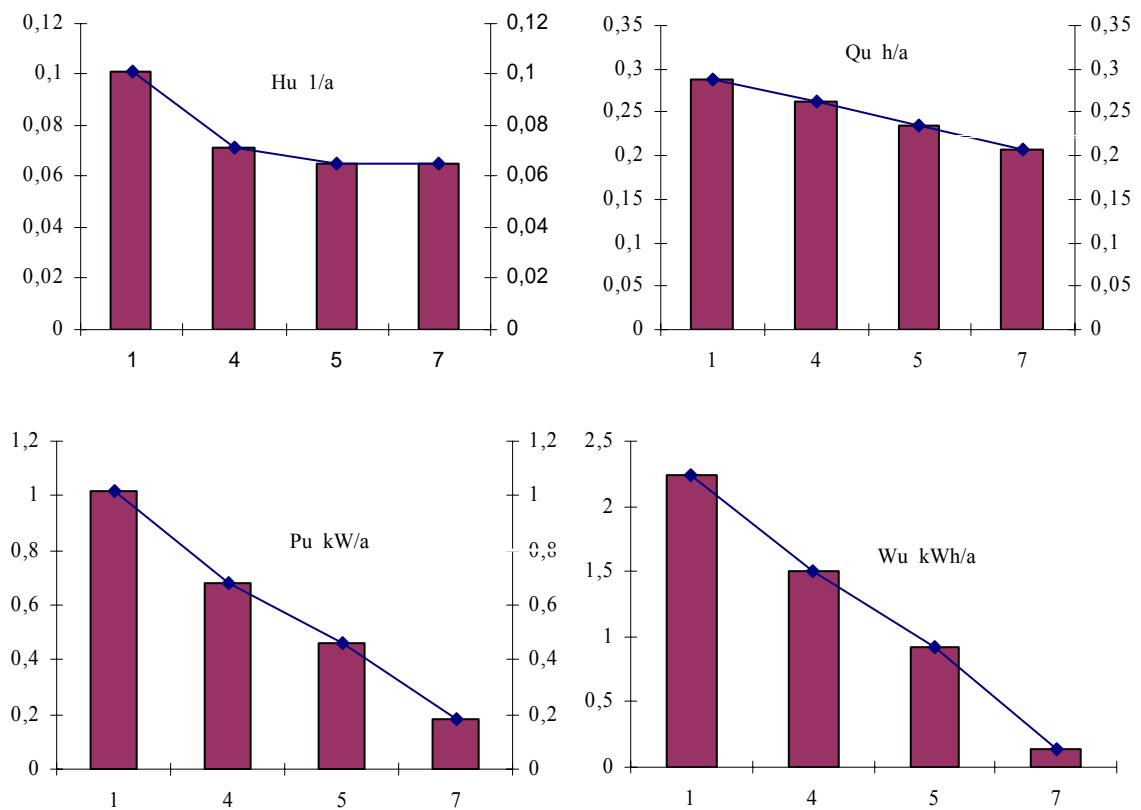


Figure 6-3 Reliability depending on number of micro-sources neglecting HV/ MV influence

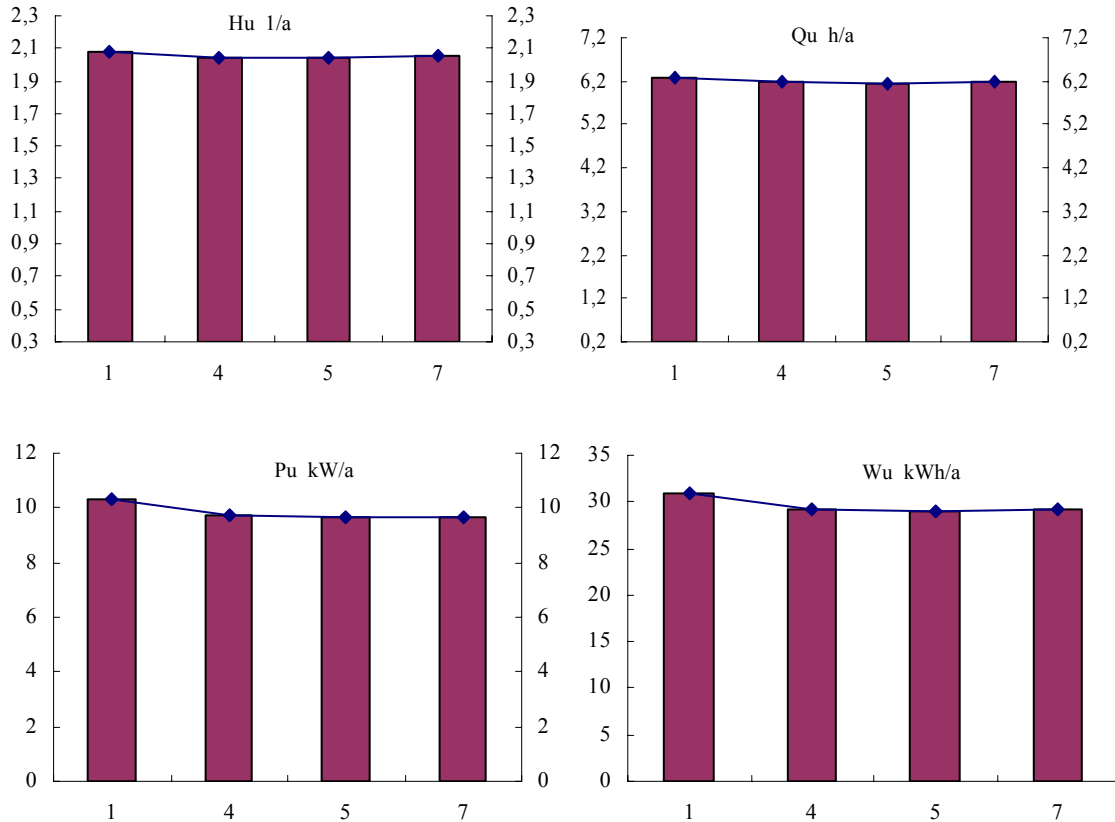


Figure 6-4 Reliability depending on number of micro-sources considering HV and MV influence

System reliability indices are obviously improved when CHP is increasingly dispersed in the network. In case of failure, CHP is able to locate at more islands, so more loads are able to be supplied by CHP units, and thus reliability is improved. In Figure 6-4 due to the overlap of failures from MV and LV, the reliability improvement due to local generation is not obvious to system reliability.

Penetration strategy in the same downstream level

A further problem for micro-source location is when several loads are connected to the same downstream level of the network but available generation is not sufficient to cover all loads. In this case the micro-source unit has to supply that load with highest reliability benefit. Figure 6-5 compares the interruption costs for the following scenarios:

- a: One 25 kW CHP unit is connected to load5 with 5 kW rated power
- b: One 25 kW CHP unit is connected to load4 with 10 kW rated power
- c: One 25 kW CHP unit is connected to load3 with 15 kW rated power
- d: One 25 kW CHP unit is connected to load2 with 20 kW rated power

Load3, load2, load5 and load4 have the same downstream level. In the first step LV and HV influence is not taken into account.

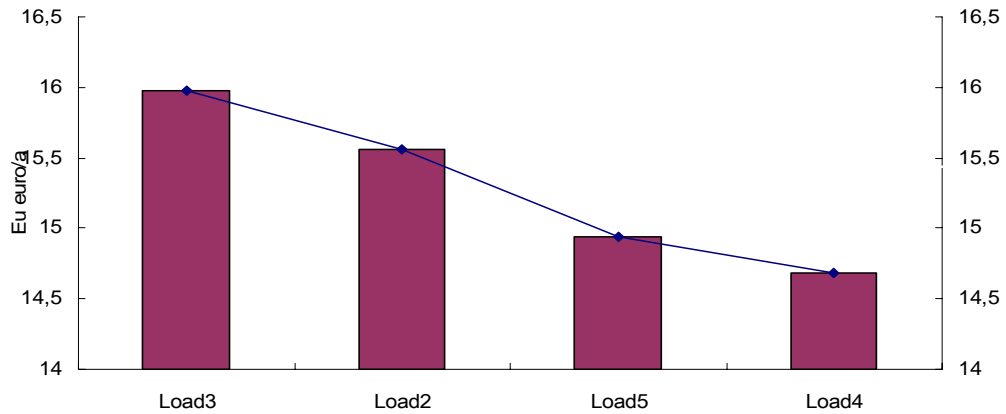


Figure 6-5 Reliability depending on load size neglecting MV and HV influence

The reliability increases with increasing rated power of the load that was selected for connection. As already verified above different micro-source location achieves no obvious improvement of system reliability when only considering the failure from MV and HV.

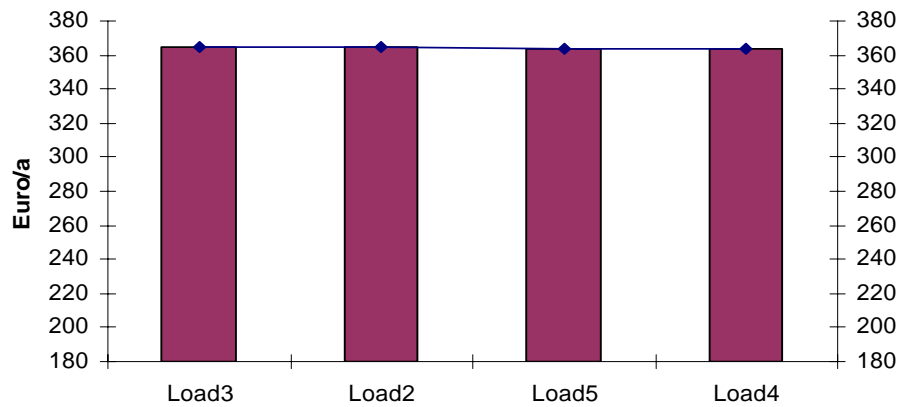


Figure 6-6 Reliability depending on load size considering MV and HV influence

In the previous studies all the loads located in the network have the same load priority. However in the real case, several types of load segments such as household, agriculture, industry or commercial load face different interruption costs, which is listed in Table 6-1 according to the assumptions from the data collection task TG.1 (see deliverable DG.1); supply of the loads should thus be attempted with different priorities.

	€kW	Minimum €kWh	Average €kWh	Maximum €kWh
Residential	0	0.5	1.5	5
Agriculture	0.5	2	5	10
Industry	3	5	10	25
Commercial	2	5	10	30

Table 6-1 Interruption cost of different types of load

In the following scenario loads in Italy rural network are categorized by two groups:

- Group1: Load1, Load3, Load4, Load6
- Group2: Load2, Load5, Load7

Group1 is assumed to be commercial load with higher priority with rated power is 10 kW. Group2 is household load with normal priority with rated power 3 kW.

Figure 6-7 compares different connections of 4 DG units (each scenario equal to a total penetration level of 40 %) with the following variations:

- a: 4 CHP units are connected to loads of group1
- b: 3 CHP units are connected to loads of group1, one unit to loads of group2
- c: 2 CHP units are connected to loads of group1, two units to loads of group2
- d: 1 CHP unit is connected to loads of group1, three units to loads of group2

Interruptions caused by MV and HV are not taken into account.

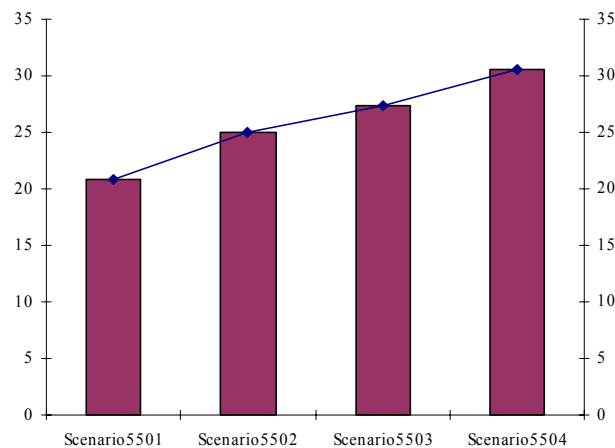


Figure 6-7 Interruption costs depending on location of CHP units close to loads with different priority
The interruption cost decreases when more microsources are directly connected to industrial loads. This strong decrease is caused by higher interruption costs of commercial loads compared with that of household loads.

1.20.2 Micro-source operation

Figure 6-8 demonstrates the impact of micro-source operation mode on reliability where 4 CHP units with identical output power are applied to bus6, bus9, bus11, and bus13 with a total penetration level from 0% to 400% CHP in electricity driven mode and heating driven mode, respectively.

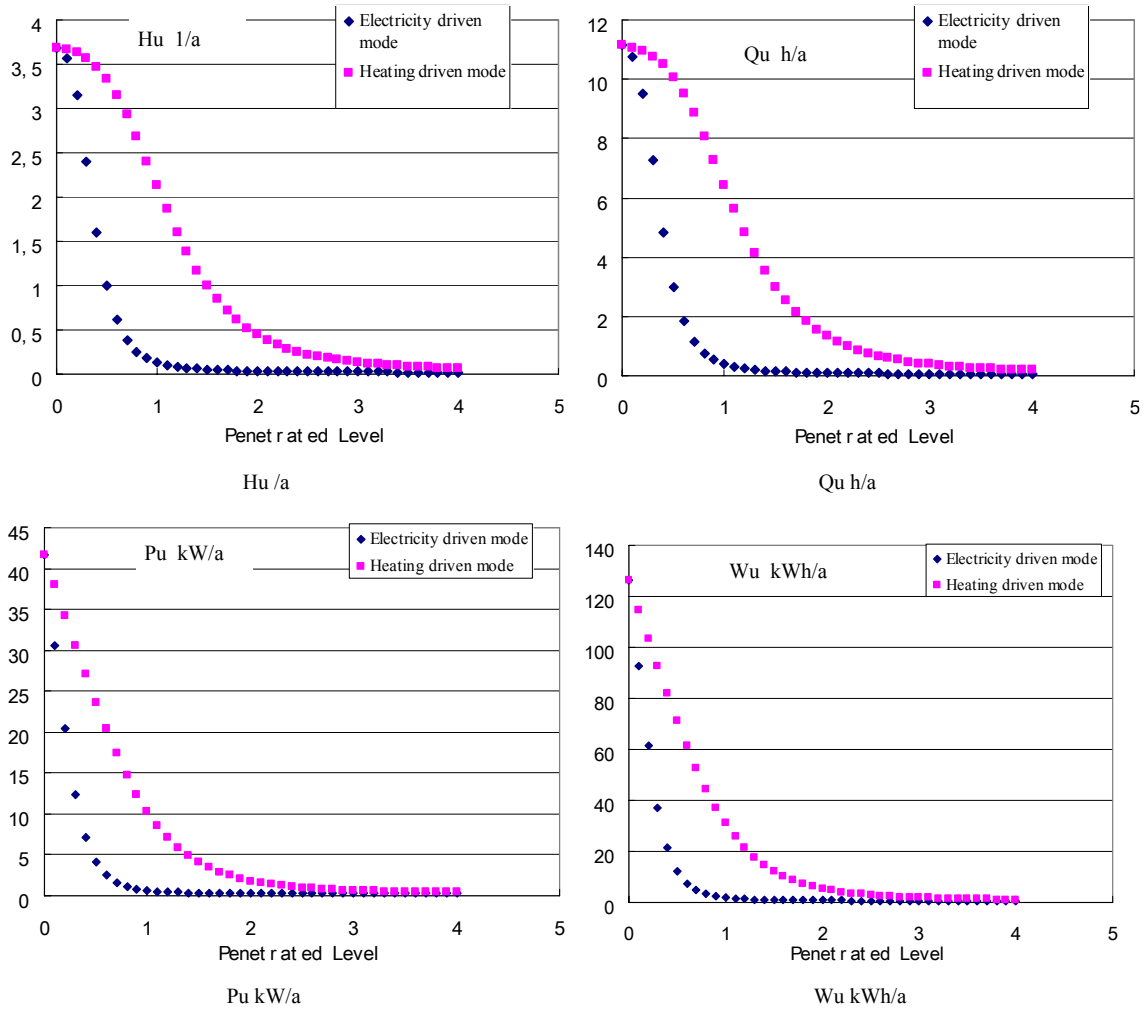


Figure 6-8 CHP reliability indices improvement with the increase of CHP penetration level

After CHP in heating driven mode exceeding approximate 200% penetration level and in electricity driven mode exceeding approximate 80% penetration level, the further increasing of CHP penetration level doesn't have significant improvement for reliability indices, in this case, CHP unit is already able to supply most of load. Therefore from technical reliability improvement point of view, it can be assumed in these cases these penetration levels are optimised.

1.21 Optimal planning strategy considering economic benefit

Investment costs have not been taken into account for the optimal planning strategy in the previous section. The objective function of the previous section was to achieve the highest reliability improvement with a minimum number of micro-sources. However with such objective function over-investment is still possible.

This section considers also investment costs; the best results should however first fulfil technical reliability aspects.

1.21.1 Economic benefit model of micro-sources

Micro-sources contribute to reliability when they are able to supply the load in island mode in case of failures. However additional micro-source control (including more complicated network protection as i.e. developed in WPC) is required to work in island mode; so the investment cost regarding reliability improvement is mainly the control unit cost and the operation cost of the micro-source in island mode. Investment cost in the installation of the micro-source are not considered here assuming they will operate anyway due to other reasons providing technical, economic or ecologic benefits to different stakeholders. Additionally, the period of island working is relatively short compared to the normal operation of the unit, also justifying that their investment costs are neglected.

The economic benefit EB regarding reliability improvement achieved by micro-sources as objective function is the difference between the interruption cost per year when no DG is applied (C) and the costs with DG (C_a)

$$EB = C - C_a \quad \text{Equation 6-1}$$

Interruption cost C can be calculated by simulation without any micro-sources depending on load type specific interruption costs as defined in Table 6-1.

The total cost C_a after the DG application can be calculated by

$$C_a = C_u + C_w + C_c \quad \text{Equation 6-2}$$

C_u is the interrupted cost per year after specified DG application

C_w is the operation cost in island mode per year after DG application

C_c is the control unit cost per year

Interruption cost per year C_u after DG application can be achieved by reliability indices.

Energy cost C_w in island mode per year after DG application is calculated by

$$C_w = c_w * W \quad \text{Equation 6-3}$$

with W as the energy supplied by DG in island mode, and c_w as specific energy cost of the unit. It is assumed to be 40 €/MWh for CHP, while wind and PV are free.

Control unit cost C_c is calculated by

$$C_c = N * c_c, \quad \text{Equation 6-4}$$

with c_c as specific control cost per unit and year and N as the number of control units.

To calculate the investment cost for control unit per year, annuity method is applied:

$$\text{equivalent cash flow } A = \frac{q^N (q-1)}{q^N - 1} * B \quad \text{Equation 6-5}$$

with B as the initial capital, q , the discount rate and N the lifetime

Based on this method specific control unit cost is indicated in Table 6-2.

	initial capital Euro	Life time	discount rate	investment cost per unit per year
DG control unit	500	15	5%	40,12

Table 6-2 Specific control unit cost

with

Operational costs DG: CHP: 4 Ct/kWh,
 PV: 0 Ct/kWh,
 Wind: 0 Ct/kWh

The final objective function is now

$$EB = K - (c_w * W + N * c_c + C_u) \quad \text{Equation 6-6}$$

Two cases must be distinguished concerning the transition into islanding:

- immediate (direct) islanding without any supply interruption
- islanding after a short switching period causing a short interruption of supply (indirect islanding)

Generally, direct islanding requires more investment. The definition of EB in equation 9-6 applies for indirect islanding. As for household load, interruption power cost is 0, and considering that even without directly islanding, the duration of re-supplying the load within the Microgrid is relative short compared to the total islanding duration, there is almost no difference in the interruption cost between direct and indirect islanding for household load.

It can be seen from the definition of variables in this equation that interruption cost C without micro-sources is a relative constant value in the case of fixed network topology and load type that only change with the per unit interruption cost value. c_w and c_c , are also relative constant values depending only on the micro-source and the control unit market price respectively .

Thus, to achieve highest economic benefit, the target of optimization is to reduce interruption cost C_u by micro-source, operation time of CHP units with energy W and/or the number N of micro-sources required for islanding.

It is important to note that the investment cost regarding the reliability is only the investment of control unit and operation of DG in island, which is not influenced by micro-source capacity. The higher the DG unit rated power, the lower the interruption cost. The extreme case is that the micro-source unit can cover the whole load operated in one island, so it is better to choose the DG unit with higher rated power. However the rated power of DG unit is restricted by the other technical requirements of the micro-sources in the island. For the following optimisation we choose a maximum DG power of 140 kW per unit. The influence to the optimised result by maximum DG rated power is described at the end of this section.

1.21.2 German LV network optimisation

The German LV network (Figure 4-8) with household loads is studied in this section; the simplified network topology is indicated in Figure 6-9. The network is highly meshed, therefore two types of load can be found in the network, one feeder load and two feeders

load. Technically same micro-sources connected to one feeder loads achieve higher reliability improvements than these connected to two feeders load.

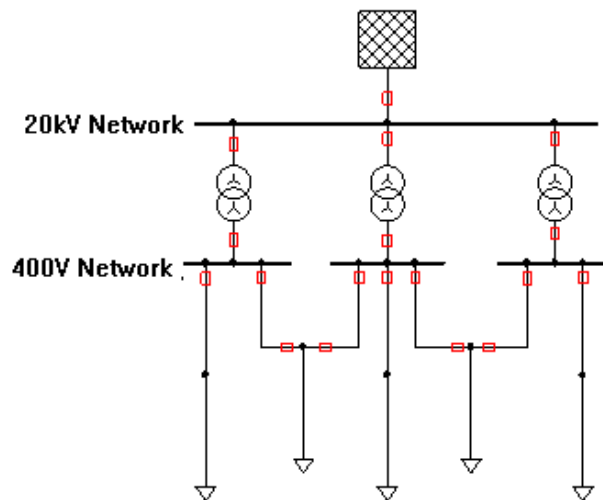


Figure 6-9 Simplified topology of German LV network

Optimised result considering average cost model

Based on technical optimisation results from the previous section, micro-sources are connected to the network according to the following criterion

- DG is distributed to different protection zones
- DG is located to most downstream
- DG is connected with one feeder load
- DG is connected with the load with higher rated power

Different scenarios with increasing number of DG units according to Table 6-3 were analysed.

Figure 6-10a shows the relation between economic cost and DG unit amount. Replacing DG amount by reliability, part b) of the figure is achieved, with a definition of reliability derived from unavailability assuming the unit of Q_u is h/a as:

$$\text{Reliability} = 1 - Q_u / 8760$$

Investment costs increase with an increasing number of DG units. The more DG units are dispersed in the network, the more interruption cost is reduced, but investment cost is increased. The lowest total cost can be achieved when 4 DG units are distributed in the network. In this case, the system reliability is increased to 99.9982 %.

According to the technical optimum result, 200 % CHP penetration achieves already best system reliability indices, a further increase of micro-sources obviously doesn't have an impact on the system reliability.

Applied DG units	Load connected with DG	Interruption cost without DG (Euro/a)	Interruption cost after DG application (Euro/a)	Investment cost after DG application Euro/a	Total Cost after DG application Euro/a	Economic Benefit Euro/a	Reliability
1*140kW	L227	369,9	369.9	0	369.9	0	99.9957%
2*140 kW	L227, L212		262,61	43.34	305.95	63.95	99.9959%
3*140kW	L227, L212, L230		168.58	86.28	254.86	115.04	99.9964%
4*140kW	L227, L212, L230, L210		99.9987	128.46	228.46	141.44	99.9973%
5*140kW	L227, L212, L230, L210, L228		58.59732	169.82	228.42	141.48	99.9982%
6*140kW	L227, L212, L230, L210, L228, L301		37.0203	210.59	247.61	122.29	99.9988%
7*140kW	L227, L212, L230, L210, L228 L301, L295		21.72027	251.16	272.89	97.01	99.9993%
8*140kW	L227, L212, L230, L210, L228 L301, L295, L256		14.62722	291.49	306.13	63.77	99.9996%
9*140kW	L227, L212, L230, L210, L228, L301, L295, L256, L219		11.45404	331.71	343.17	26.73	99.9997%
1*140kW	L227		9.470686	371.89	381.36	-11.46	99.9997%

Table 6-3 DG setting of scenarios for German LV network

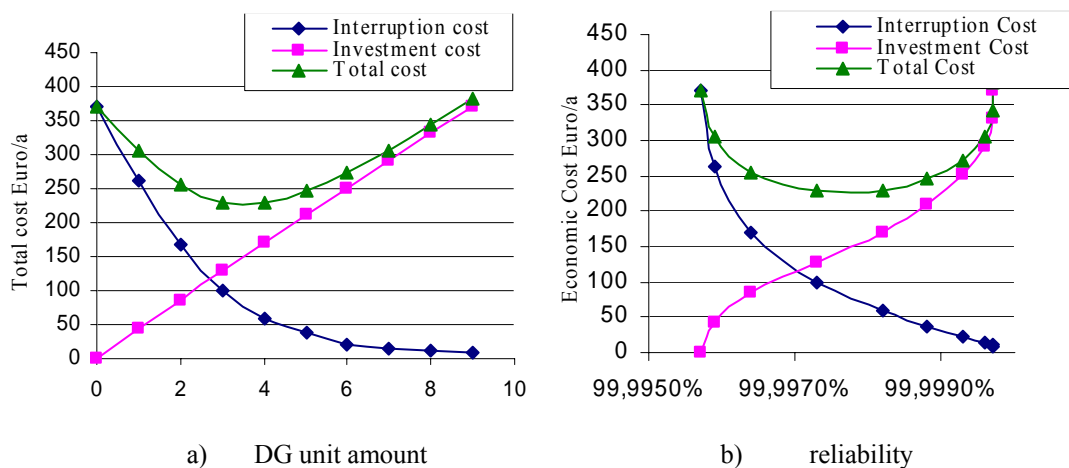


Figure 6-10 Impact on economic cost regarding DG unit and reliability

The total load in this network is 1084 kW, so technically the optimum number of DG units amount can be calculated by

$$N = \frac{1084kW * 200\%}{140kW} \approx 12$$

By comparing the technical optimization result and economical optimization result, the optimum number of micro-sources based on economical requirement is considerably lower than the result based on technical requirement.

Maximum cost model

With settings as of Table 6-3, maximum cost model is applied to calculate the optimisation result according to Table 6-4 as shown in Figure 6-11.

DG amount	Interruption cost without DG (Euro/a)	Interruption cost after DG application (Euro/a)	Investment cost after DG application Euro/a	Total Cost after DG application Euro/a	Economic Benefit Euro/a	Reliability
0	1233	1233	0	1233	0	99,9957%
1*140 kW		875,38	43,33858	918,72	314,28	99,9959%
2*140 kW		561,94	86,27956	648,22	584,78	99,9964%
3*140 kW		333,33	128,457	461,79	771,21	99,9973%
4*140 kW		195,32	169,8191	365,14	867,86	99,9982%
5*140 kW		123,4	210,5864	333,99	899,01	99,9988%
6*140 kW		72,4	251,1654	323,57	909,43	99,9993%
7*140 kW		48,76	291,4982	340,26	892,74	99,9996%
8*140 kW		38,18	331,7134	369,89	863,11	99,9997%
9*140 kW		31,57	371,8929	403,46	829,54	99,9997%

Table 6-4 Economic cost in case of maximum outage costs

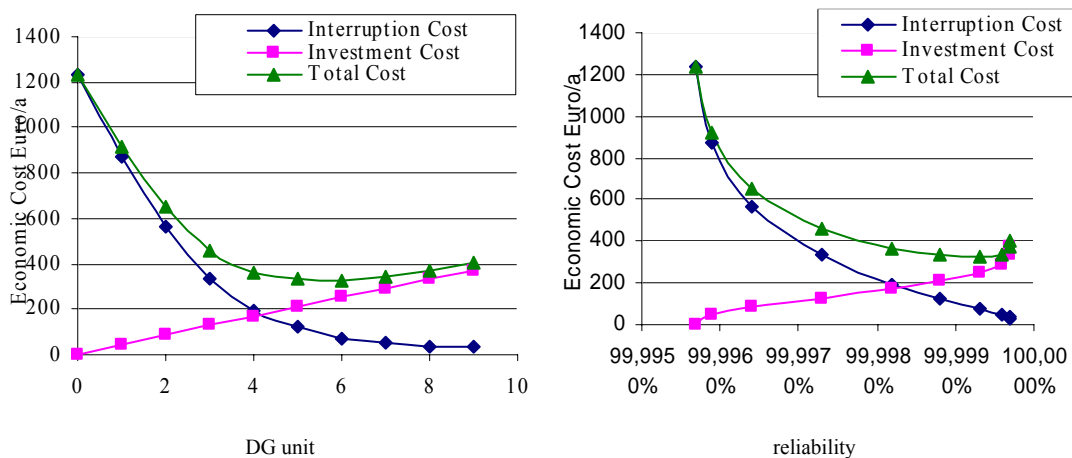


Figure 6-11 Economic cost regarding DG unit and reliability in case of maximum outage costs

If maximum cost model is applied in the calculation, the optimised number of micro-sources is increased to 6 with an increased reliability of 99.993 %.

Minimum cost model

The simulation result for minimum outage cost model with costs from Table 6-5 is shown in Figure 6-12. Due to minimum cost model the interruption cost is relatively low, so it is not advantageous to invest in any micro-source.

DG amount	Interruption cost without DG (Euro/a)	Interruption cost after DG application (Euro/a)	Investment cost after DG application Euro/a	Total Cost after DG application Euro/a	Economic Benefit Euro/a	Reliability
0	123,3	123,3	0	123,3	0	99,9957%
1*140 kW	123,3	87,54	43,338583	130,88	-7,58	99,9959%
2*140 kW	123,3	56,19	86,279561	142,47	-19,17	99,9964%
3*140 kW	123,3	33,23	128,457039	161,69	-38,39	99,9973%
4*140 kW	123,3	19,53	169,8190804	189,35	-66,05	99,9982%
5*140 kW	123,3	12,34	210,586391	222,93	-99,63	99,9988%
6*140 kW	123,3	7,24	251,1653919	258,41	-135,11	99,9993%
7*140 kW	123,3	4,88	291,4981834	296,37	-173,07	99,9996%
8*140 kW	123,3	3,82	331,7133788	335,53	-212,23	99,9997%
9*140 kW	123,3	3,16	371,8928794	375,05	-251,75	99,9997%

Table 6-5 Economic cost in case of minimum outage costs

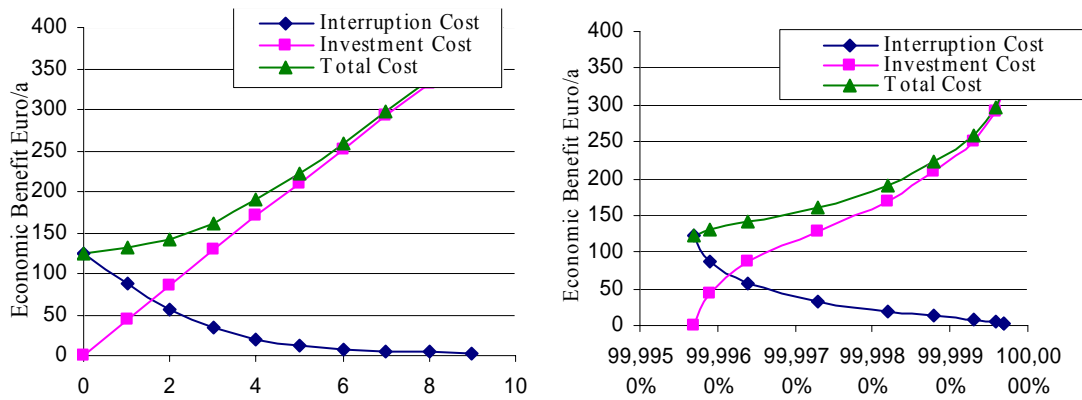


Figure 6-12 Economic cost regarding DG unit and reliability in case of minimum outage costs

Economic benefit of all three cost models is compared in Figure 6-13. With increasing outage costs it becomes beneficial to install a higher number of micro-sources for island operation.

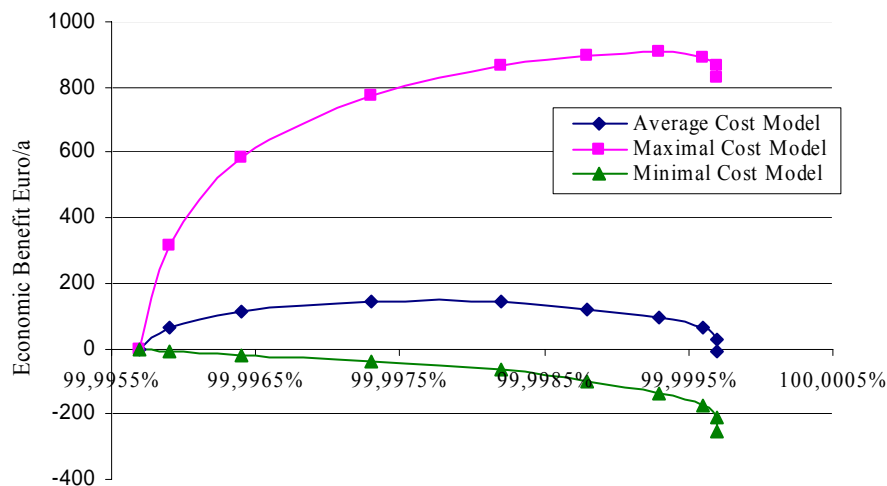


Figure 6-13 Economic benefit depending on outage costs

While in the previous studies DG capacity was limited to 140 kW. Figure 6-14 compares the optimum results caused by different maximum rated power of per DG units, for capacities of 210 kW, 300 kW, 350 kW, 420 kW and respectively, as shown in Table 6-6.

Maximum Power kW	Economic benefit Euro/a	Reliability	Penetrated DG unit power	Penetration Level
140	141,48	99.9982%	140*4	32.3%
210	194,66	99.9985%	210*3	48.6%
300	232,39	99.9985%	300*2	46.2%
350	242,15	99.9987%	350*2	53.9%
420	252,09	99.9992%	420*2	64.6%

Table 6-6 Optimised DG penetration based on maximum DG output power

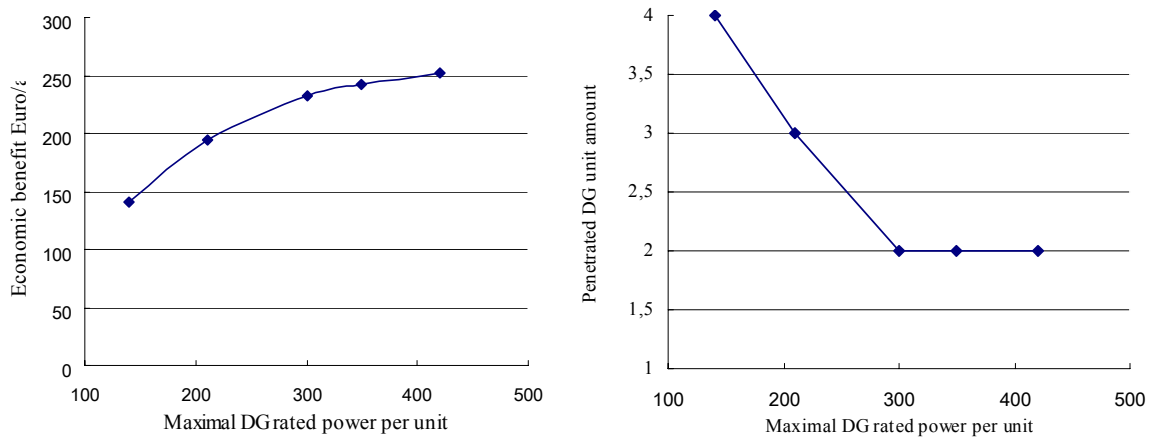


Figure 6-14 Optimised DG penetration based on maximal DG rated power per unit

It can be seen from Figure 6-14 that the optimised economic benefit and reliability is nearly positive related with maximum micro-source rated power which is limited in each simulation. Also the number of the optimally selected micro-source is reduced from 4 to 2 units with increasing maximum DG rated power.

With the increase of the DG rated power, less DG unit are required to be installed in network to reduce the interruption costs; therefore, investment costs caused by DG control unit are also reduced and more economic benefit is achieved. The most extreme case is that the rated power of DG unit is not limited. In this case it is obviously only one DG unit needed to achieve maximum economic benefit. This situation is due to the fact that installation costs for micro-sources were not considered when calculating the economic benefit of Microgrid-operation. To calculate the added value of Microgrids explicitly additional costs for enabling island operation, i.e. the difference between normal networks with various dispersed generation units was only determined.

Due to further technical reasons, DG unit rated power is always limited. The maximum value of DG rated power must be predefined for all scenarios in order to compare the optimised economic benefit of micro-sources which is influenced by other factors, such as the network reliability degree without micro-sources.

Impact of Micro-source availability

The benefits achieved also depend on the availability of the micro-sources. Figure 6-14 demonstrates that the benefit decreases with decreasing micro-source availability.

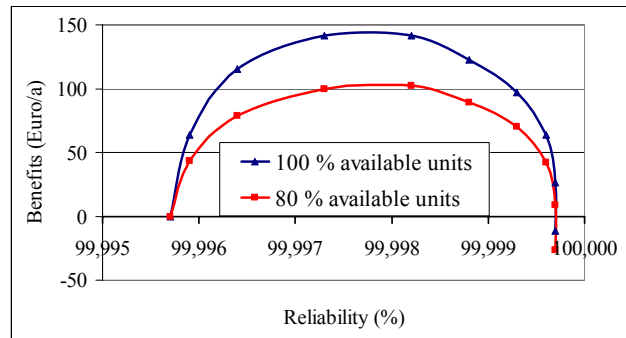


Figure 6-15 Cost impact of micro-source availability with average outage cost model

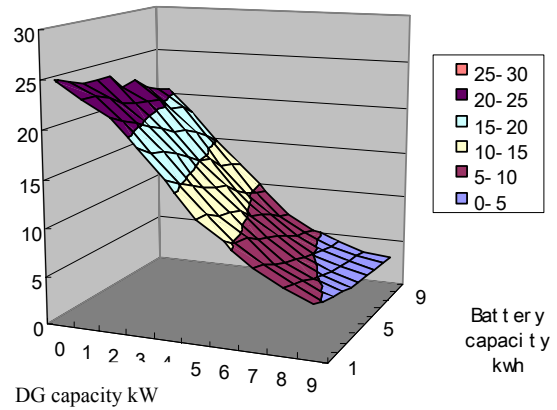
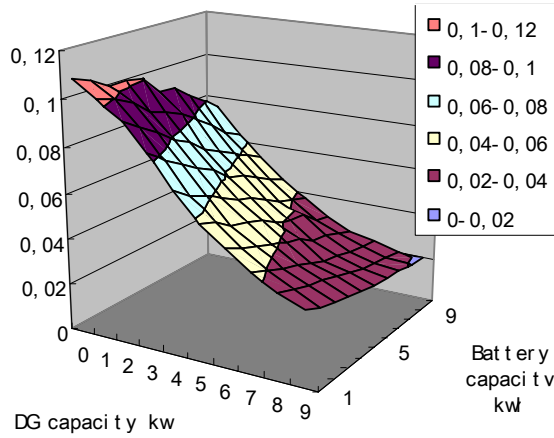
1.22 Optimum battery planning strategy

In the previous sections, analytical method was applied for the optimization purpose, therefore only DG units can be applied to the network, due to the limitation of analytical method.

In the cost model battery installation cost is neglected and only control unit cost and operation cost is applied to battery, therefore battery performs like a micro-source during the discharging process. The micro-source location criterion for DG units can be still applied to battery and battery can be analyzed as one micro-source when the cost model is applied. However the optimum micro-source penetration level changes with batteries; with the contribution of battery output power, optimum micro-source penetration level should be lower than the case without batteries.

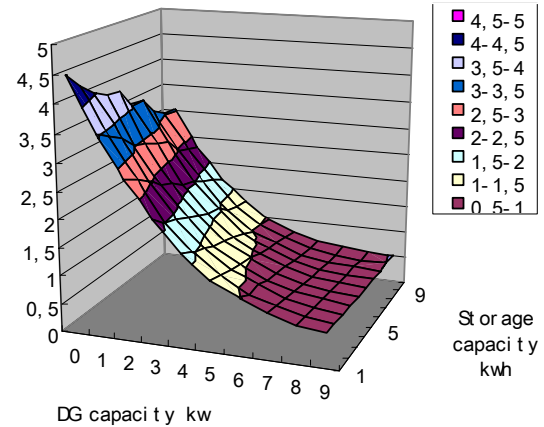
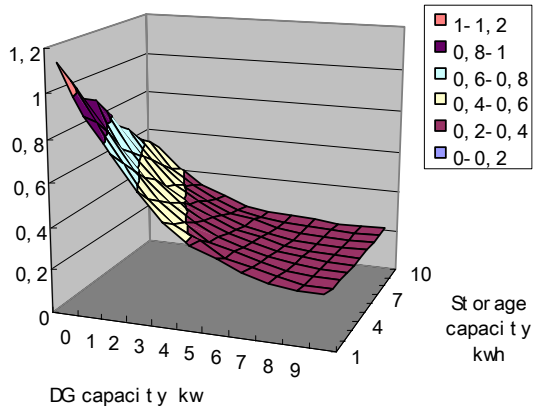
System reliability of Italy rural network is calculated based on the different combinations of CHP unit capacity and battery storage capacity (Figure 5-12). From Figure 6-14 it is possible to derive the combination of DG unit rated power and battery storage capacity which has the same reliability impact with the case when battery is not installed in the network.

With this method, the optimisation procedure can be done by analytical method without battery penetration, which is generally quite fast. Similar results are achieved by the Monte-Carlo method. The combination of DG rated power and battery storage capacity which has the same reliability impact can be achieved from this curve. This curve is valid to any optimisation result obtained by analytical method, therefore Monte-Carlo simulation is only done once during the whole optimization procedures and the optimisation speed is quite reduced.



H_u/a

$Q_u \text{ min/a}$

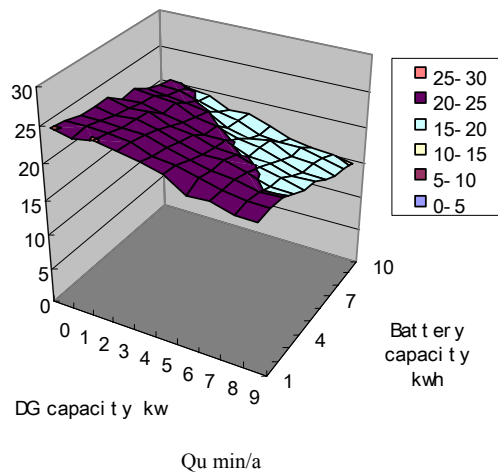
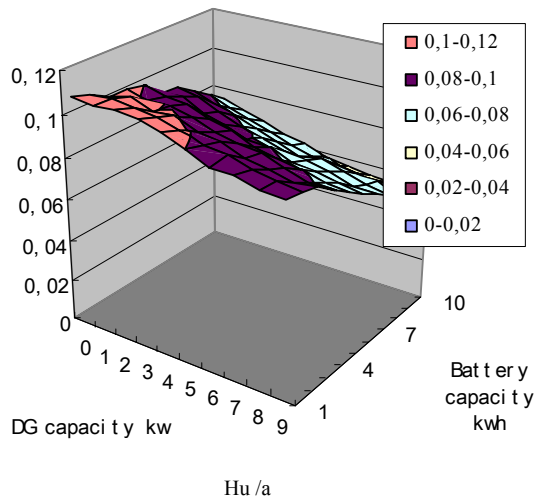


$W_u \text{ kWh/a}$

$P_u \text{ kW/a}$

Figure 6-16 System reliability indices regarding CHP capacity and battery capacity

The similar curves for PV unit, WT and battery combination are demonstrated in Figure 6-17 and Figure 6-18.



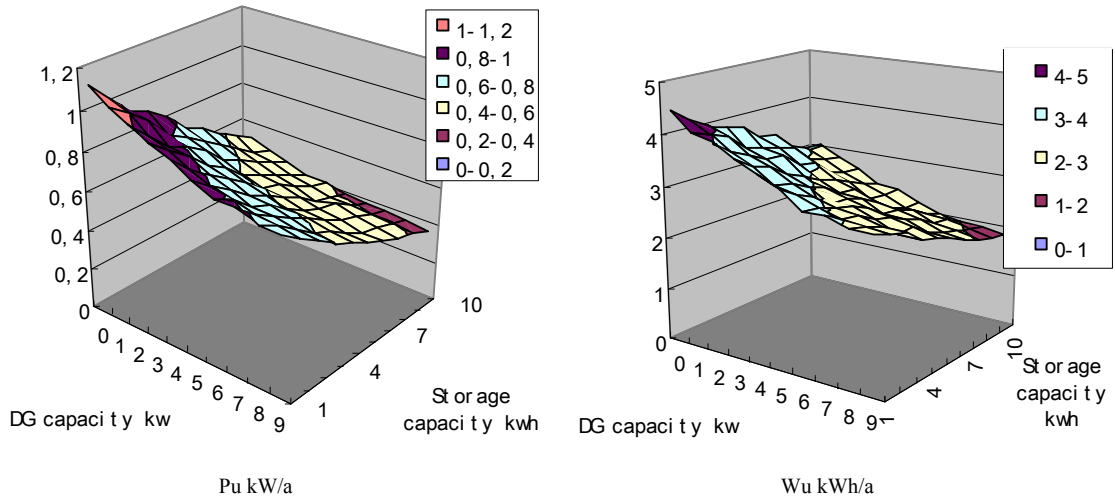


Figure 6-17 System reliability indices regarding WT capacity and battery capacity

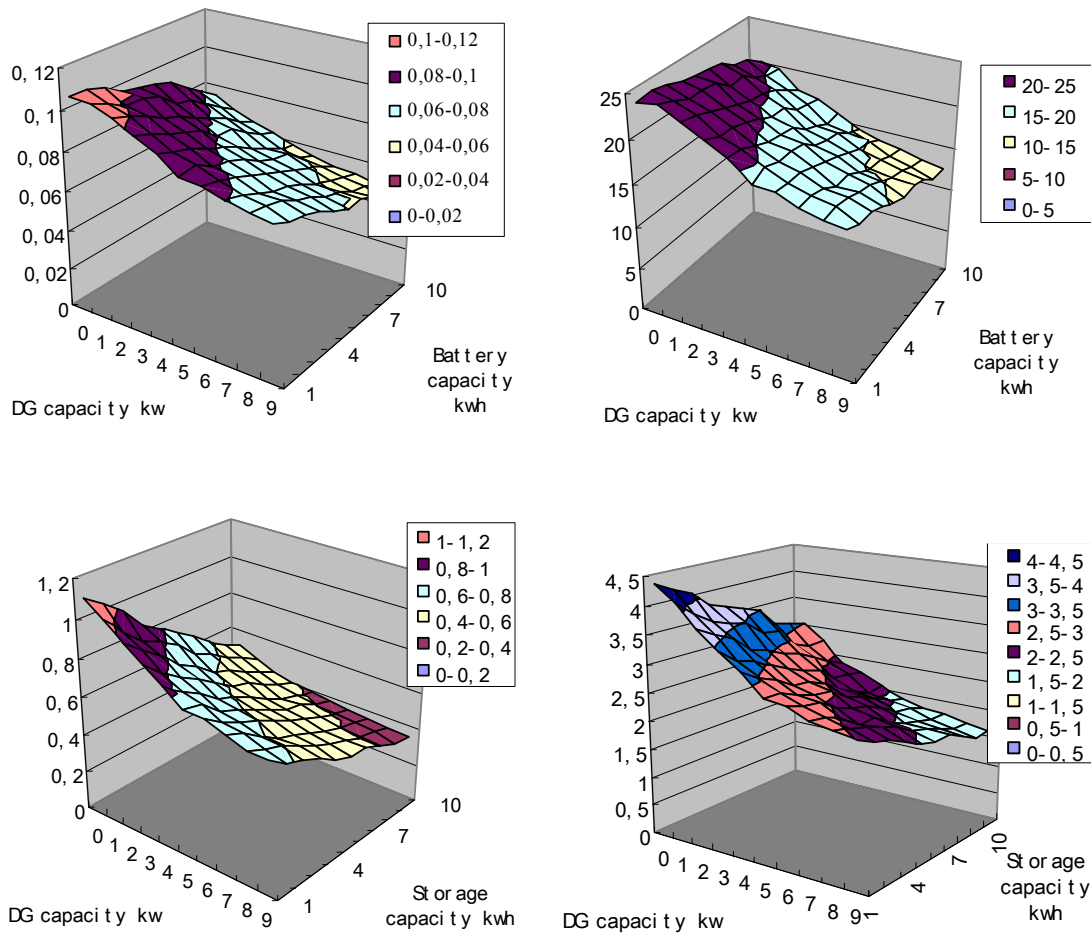


Figure 6-18 System reliability indices regarding PV capacity and battery capacity

1.23 Conclusions

Technically, optimum micro-source location can be obtained based on the following criteria:

- micro-source is distributed to different protection zones
- micro-source is located most downstream
- micro-source is connected to the load with highest demand
- micro-source is prioritised to connect with the most sensitive load

LV networks building Microgrids are already the most downstream; as most failures are caused in the upstream MV and HV networks, there is only a slight improvement compared with other planning strategy.

The most important criterion that influences system reliability is the total micro-source penetration level in the Microgrid. When micro-sources are able to cover most of the load demand, a further increasing of micro-source installed capacity doesn't have obvious improvement of system reliability. With batteries in the network, the optimum DG capacity decreases. The optimum combination of DG unit rated power and battery capacity can be achieved by the reliability equivalent curve regarding DG rated power and battery storage capacity simulated by Monte-Carlo method.

7 European Network Simulation

In this chapter, European networks collected in WPG task 1 are studied [60]. The reliability setting of LV level is still same as the previous scenario. The setting of HV and MV network is taken from average values collected. Generally, urban networks have better reliability performance than rural networks, therefore reliability setting of rural network is selected worse than the average value and reliability setting of urban network is selected better the average value as shown in Table 7-1

	Italy		Germany		Holland		Portugal	
	Rural	urban	Rural	Urban	Rural	Urban	Rural	Urban
Frequency of Supply Interruption 1/a	3,6	1,3	0,54	0,18	0,6	0,22	5,4	1,8
Interruption duration h	3	1	1,2	0,8	1,4	1	5	2,5

Table 7-1 HV and MV Reliability setting of European network

Network parameters are attributed by average values to each network although not fully reflecting the realistic operation performance:

- The line length of rural network is 60 m between 2 busbars. The line length of urban network is 20 m between 2 busbars
- The load of the network is selected as house load with rated power 15 kW
- The protection device is assumed to be a fuse. The assumed protection scheme can be found in the figure of each network topology.

It should be also noted that the following optimization is focused on DG units. When battery is also applied in the network, the optimum combination of DG unit and battery can be achieved by the equivalent curve which is similar as Figure 6-16 to Figure 6-18.

1.24 German urban LV network

German urban LV network was studied in the last chapter to demonstrate the reliability calculation method.

1.25 Italy rural network

Technical optimum result

Italy rural network (Figure 4-7) – as also studied in previous chapters – yields best results if CHP units with in total 200% penetration level are dispersed to different protection zones. The detailed DG setting and load setting can be found in A 8. The simulation result of 200% Table 7-2 compares CHP penetration with the PV, WT with the same penetration level.

	Hu /a	Qu h	Tu h/a	Pu kW/a	Wu kWh/a	Cu Euro/a
No DG	3,68512217	11,14238	3,023613	208,6264	630,80552	946,2082856
PV	2,48306655	7,492861	3,017584	161,3352	487,58678	731,3801758
Wind	2,06450591	6,222647	3,01411	102,676	309,57573	464,3635943
CHP	0,36513039	1,07588	2,946563	7,930956	22,492679	33,73901925

Table 7-2 Italy rural network reliability indices of different DG penetration

System reliability indices are significantly improved by micro-source operation, especially by CHP units.

DG optimisation taking into account economic benefit

Similar as the optimization procedure described in the last chapter, to achieve the best economic benefit, the following scenarios are simulated.

The simulation results are listed in Table 7-3 for average cost model, Table 7-4 for maximum cost model and Table 7-5 for minimum cost model. The detailed DG location can be found by referring the DG connected busbar name of the corresponding optimised scenario to the network topology indicated in A8.

applied DG	DG connected busbar	Interruption Cost Euro/a	Investment Cost Euro/a	Total Cost Euro/a	Economic Benefit Euro/a	Reliability	Unavailability h/a
0	Without DG	946,2083	0	946,2083	0	99,873%	11,14238
1*140 kW	Bus13	131,7429	61,83908	193,582	752,6263	99,954%	3,994135
2*140 kW	Bus13, Bus9	23,01617	104,8585	127,8746	818,3337	99,993%	0,597349
3*140 kW	Bus13, Bus9, Bus11	9,784235	145,3313	155,1155	791,0927	99,998%	0,197306

Table 7-3 Simulation result with average outage costs

DG connected busbar	Interruption Cost Euro/a	Investment Cost Euro/a	Total Cost Euro/a	Economic Benefit Euro/a	Reliability	Unavailability h/a	Applied DG unit
Without DG	3154,028	0	3154,028	0	99,873%	11,14238	0
Bus13	439,1429	61,83908	500,982	2653,046	99,954%	3,994135	1*140 kW
Bus13, Bus9	76,72057	104,8585	181,579	2972,449	99,993%	0,597349	2*140 kW
Bus13, Bus9, Bus11	32,61412	145,3313	177,9454	2976,082	99,998%	0,197306	3*140 kW

Table 7-4 Simulation result with maximum outage costs

DG connected busbar	Interruption Cost Euro/a	Investment Cost Euro/a	Total Cost Euro/a	Economic Benefit Euro/a	Reliability	Unavailability h/a	Applied DG unit
Without DG	315,4028	0	315,4028	0	99,873%	11,14238	0
Bus13	43,91429	61,83908	105,7534	209,6494	99,954%	3,994135	1*140 kW
Bus13, Bus9	7,672057	104,8585	112,5305	202,8722	99,993%	0,597349	2*140 kW
Bus13, Bus9, Bus11	3,261412	145,3313	148,5927	166,81	99,998%	0,197306	3*140 kW

Table 7-5 Simulation result with minimum

For each cost model there is a optimum number of micro-sources, as demonstrated in Table 7-6.

Model	Applied unit	DG	Economic benefit Euro/a	Reliability	Unavailability h/a
Average cost	2		818,33	99,993%	0,5973
Maximal cost	3		2976,25	99,998%	0,1973
Minimal cost	1		209,65	99,954%	3,9941

Table 7-6 Optimised DG penetration of Italy rural network considering economic benefit

1.26 Italy urban network

The Italy urban network topology is indicated in Figure 7-1

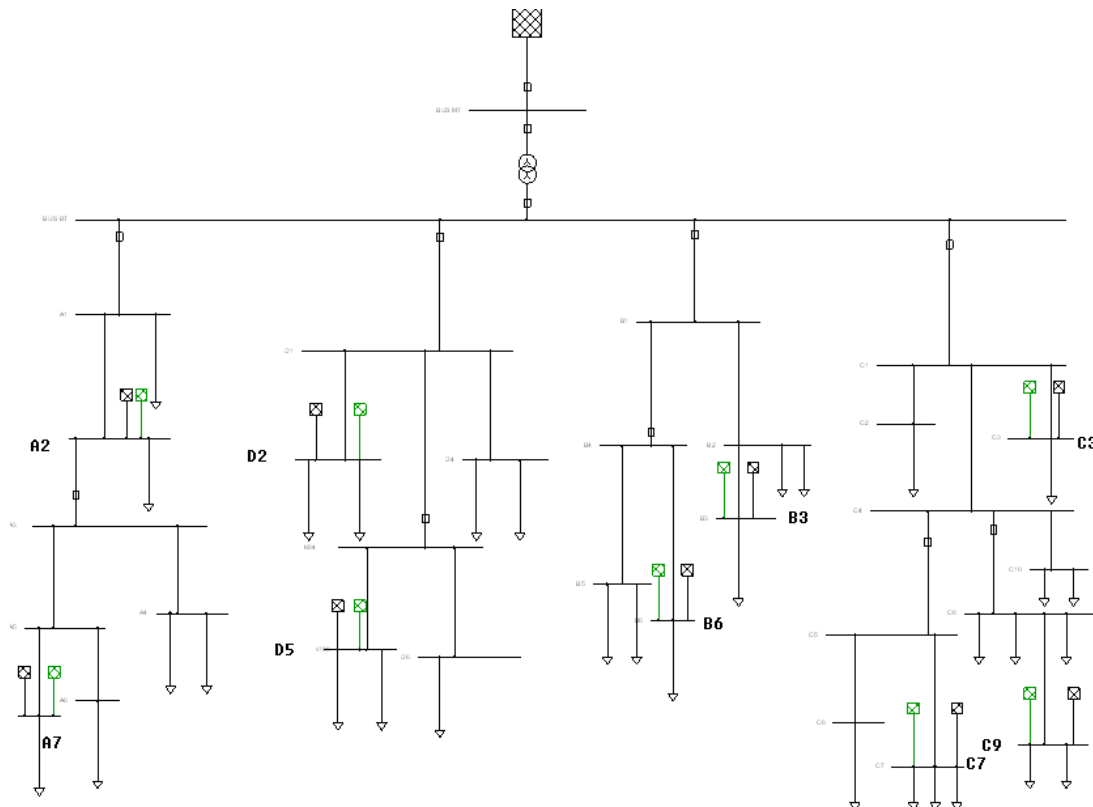


Figure 7-1 Italy urban network topology

Technical optimised result

According to the technical optimization criterion, DG units are decentralized to each protection zone, which is indicated in Figure 7-1 . Detailed load and DG setting are listed in A8.

The technically optimised penetration level for CHP unit is equal to 200% dispersed to each protection zone. Table 7-7 compares that case with 200% PV, Wind penetration and without DG units.

	Hu /a	Qu h/a	Tu h	Pu kW/a	Wu kWh/a	Eu Euro/a
No DG	1,375602	1,576622	1,146132	361,3652	414,6824	622,0236
PV	0,955391	1,097345	1,148582	279,582	323,9442	485,9163
Wind	0,811065	0,933773	1,151292	183,5892	214,3273	321,491
CHP	0,0248	0,060123	2,424333	5,594	13,38722	20,08084

Table 7-7 Italy network reliability indices of different DG penetration

Compared to the case without micro-sources, 200 % CHP penetration enormously increases system reliability indices nearly approaching 0. The system reliability indices are also improved after PV and WT penetration.

DG optimization taking into account economic benefit

In order to achieve the best economic benefit, based on the technical optimization result, the following scenarios are investigated for CHP penetration in Table 7-8 to Table 7-10

DG connected busbar	Interruption Cost Euro/a	Investment Cost Euro/a	Total Cost Euro/a	Economic Benefit Euro/a	Reliability	Unavailability h/a	Applied DG unit
Without DG	2073,4119	0	2073,412	0	99,9820%	1,5766219	0
C9	1569,4458	44,1517	1613,597	459,8144	99,9828%	1,505075	1*140kW
C9,A7	1112,9895	87,9234	1200,913	872,499	99,9848%	1,3330359	2*140kW
C9,A7,D2	751,28228	130,937	882,2193	1191,193	99,9878%	1,0730575	3*140kW
C9,A7,D2, C3	504,82811	173,029	677,8568	1395,555	99,9912%	0,7739352	4*140kW
C9,A7,D2, C3,C7	331,4045	214,536	545,9406	1527,471	99,9941%	0,5209789	5*140kW
C9,A7,D2, C3,C7,B3	231,89127	255,452	487,3434	1586,068	99,9960%	0,3506321	6*140kW
C9,A7,D2, C3,C7,B3, D5	163,57347	296,119	459,6922	1613,72	99,9973%	0,2388202	7*140kW
C9,A7,D2, C3,C7,B3, D5,A2	136,24764	336,457	472,705	1600,707	99,9980%	0,1770506	8*140kW 8

Table 7-8 Simulation result with maximum outage cost model

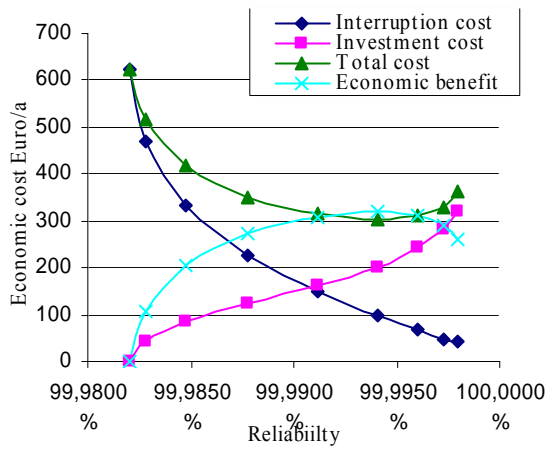
Interruption Cost Euro/a	Investment Cost .Euro/a	Total Cost Euro/a	Economic Benefit Euro/a	Reliability	Unavailability h/a	Applied DG unit
622,02356	0	622,0236	0	99,9820%	1,5766219	0
470,83373	44,1517	514,9855	107,0381	99,9828%	1,505075	1
333,89686	87,9234	421,8202	200,2033	99,9848%	1,3330359	2
225,38468	130,937	356,3217	265,7018	99,9878%	1,0730575	3
151,44843	173,029	324,4771	297,5465	99,9912%	0,7739352	4
99,421349	214,536	313,9574	308,0662	99,9941%	0,5209789	5
69,56738	255,452	325,0195	297,004	99,9960%	0,3506321	6
49,072041	296,119	345,1907	276,8328	99,9973%	0,2388202	7
40,874291	336,457	377,3316	244,692	99,9980%	0,1770506	8

Table 7-9 Simulation result with minimum cost model

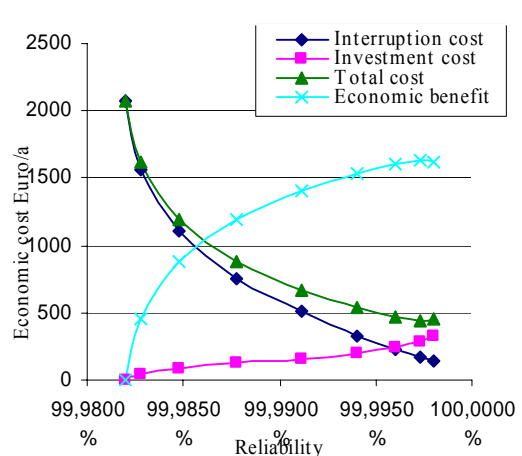
Interruption Cost Euro/a	Investment Cost .Euro/a	Total Cost Euro/a	Economic Benefit Euro/a	Reliability	Unavailability h/a	Applied DG unit
207,34119	0	207,3412	0	99,9820%	1,5766219	0
156,94458	44,1517	201,0963	6,244883	99,9828%	1,505075	1
111,29895	87,9234	199,2223	8,118855	99,9848%	1,3330359	2
75,128228	130,937	206,0653	1,275923	99,9878%	1,0730575	3
50,482811	173,029	223,5115	-16,17029	99,9912%	0,7739352	4
33,14045	214,536	247,6765	-40,33532	99,9941%	0,5209789	5
23,189127	255,452	278,6413	-71,3001	99,9960%	0,3506321	6
16,357347	296,119	312,4761	-105,1349	99,9973%	0,2388202	7
13,624764	336,457	350,0821	-142,7409	99,9980%	0,1770506	8

Table 7-10 Simulation result with average cost model

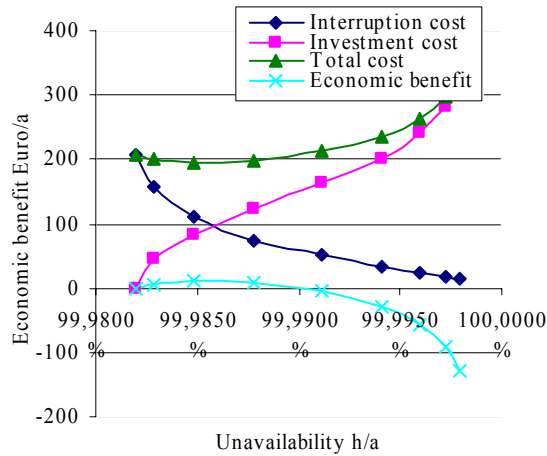
The economic cost regarding reliability are more clearly indicated in Figure 7-2



Average cost model



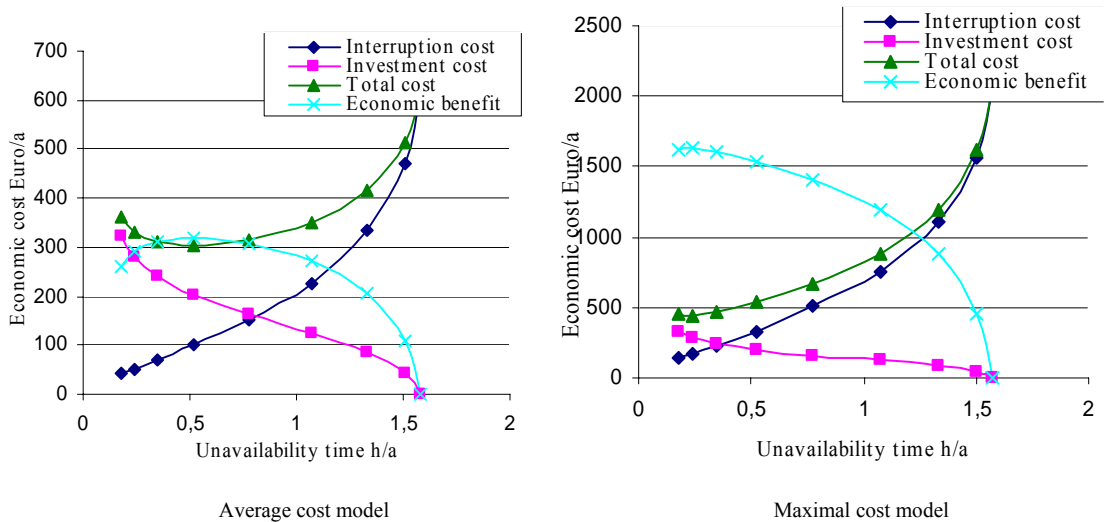
Maximal cost model



Minimal cost model

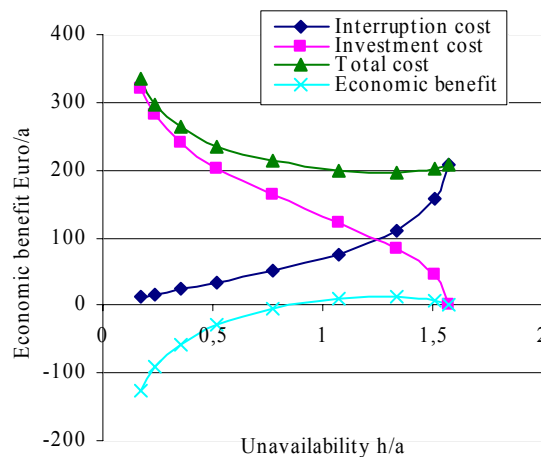
Figure 7-2 Economic cost regarding reliability

By changing the x-axis to the unavailability time of one year for each scenario Figure 7-3 can be obtained.



Average cost model

Maximal cost model



Minimal cost model

Figure 7-3 Economic cost of scenario regarding unavailability

Table 7-11 indicates the optimum number of micro-sources depending on cost model.

Model	Applied unit	DG	Economic benefit Euro/a	Reliability	Unavailability h/a
Minimal cost	2		8,118855	99,9848%	1,3330359
Average cost	5		308,0662	99,9941%	0,5209789
Maximal cost	7		1613,72	99,9973%	0,2388202

Table 7-11 Optimised DG penetration of Italy rural network considering economic benefit

1.27 Portugal urban network

Portugal urban network is listed in Figure 7-4

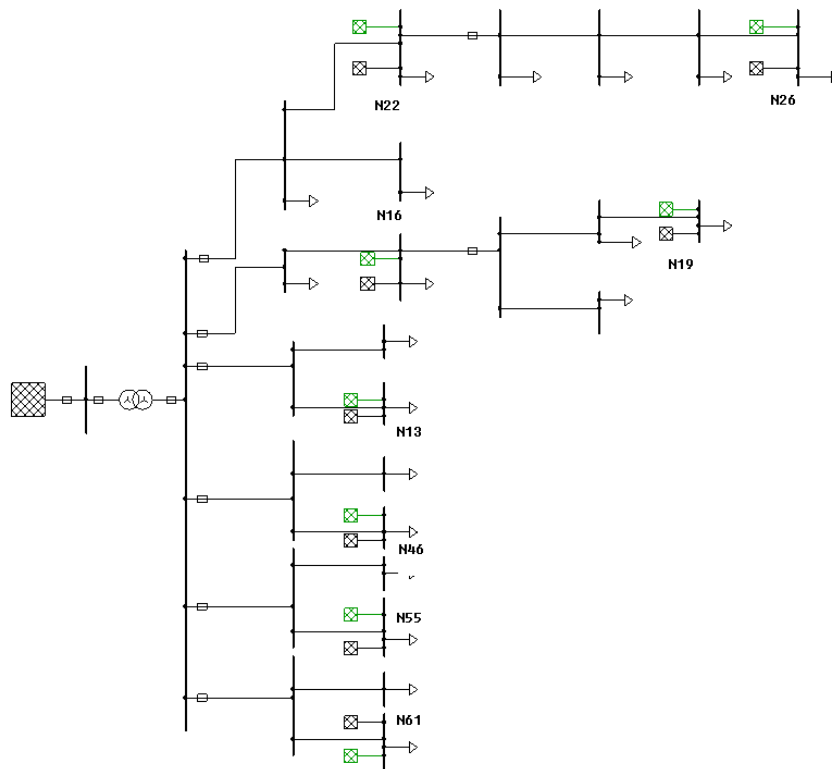


Figure 7-4 Portugal urban network

Technical optimised result

Similar as the previous network optimization, the optimised position of DER units are indicated in Figure 7-4 . The optimised result of CHP penetration is again achieved with 200% CHP penetration in the network. Compared with 200% PV and wind penetration simulation results are listed in Table 7-12 . The detailed load and DG setting can be found in A8.

	Hu /a	Qu h/a	T h	Pu kW/a	Wu kWh/a	Eu euro/a
Without DG	1,82328	4,642385	2,546172	294,919	750,9145	1126,372
PV	1,233311	3,13735	2,543843	227,9334	581,1775	871,7663
Wind	1,027599	2,613168	2,542983	145,4853	370,8238	556,2357
CHP	0,185568	0,475224	2,560911	11,46706	30,03396	45,05094

Table 7-12 Technical optimised result of Portugal urban network

DG optimization taking into account economic benefit

The following scenario is simulated to detect the optimised DG penetration taking into account the economic benefit for different cost models as listed in Table 7-13 to Table 7-15 .

DG connected busbar	Interruption Cost Euro/a	Investment Cost Euro/a	Total Cost Euro/a	Economic Benefit Euro/a	Reliability	Unavailability h/a	Applied DG unit
Without DG	1126,372	0	1126,372	0	99,9470%	4,642385	0
N26	672,6312	52,21975	724,8509	401,5209	99,9517%	4,232491	1*140kW
N26,N22	329,1009	101,5006	430,6014	695,7704	99,9666%	2,928806	2*140kW
N26,N22,N19	142,7401	146,5902	289,3303	837,0415	99,9829%	1,497004	3*140kW
N26,N22,N19,N46	70,28396	188,6423	258,9263	867,4455	99,9917%	0,725051	4*140kW
N26,N22,N19,N46,N13	41,24876	229,5366	270,7854	855,5864	99,9956%	0,38419	5*140kW
N26,N22,N19,N46,N13,N61	27,83431	270,0143	297,8486	828,5232	99,9974%	0,230454	6*140kW
N26,N22,N19,N46,N13,N61,N16	21,88547	310,293	332,1784	794,1934	99,9982%	0,157924	7*140kW

Table 7-13 Simulation result with average cost model

Interruption Cost Euro/a	Investment Cost Euro/a	Total Cost Euro/a	Economic Benefit Euro/a	Reliability	Unavailability h/a	Applied DG unit
3754,573	0	3754,573	0	99,9470%	4,642385	0
2242,104	52,21975	2294,324	1460,249	99,9517%	4,232491	1*140kW
1097,003	101,5006	1198,503	2556,069	99,9666%	2,928806	2*140kW
475,8004	146,5902	622,3906	3132,182	99,9829%	1,497004	3*140kW
234,2799	188,6423	422,9222	3331,65	99,9917%	0,725051	4*140kW
137,4959	229,5366	367,0325	3387,54	99,9956%	0,38419	5*140kW
92,78103	270,0143	362,7954	3391,777	99,9974%	0,230454	6*140kW
72,95157	310,293	383,2445	3371,328	99,9982%	0,157924	7*140kW

Table 7-14 Simulation result with maximum cost model

Interruption Cost Euro/a	Investment Cost Euro/a	Total Cost Euro/a	Economic Benefit Euro/a	Reliability	Unavailability h/a	Applied DG unit
375,4573	0	375,4573	0	99,9470%	4,642385	0
224,2104	52,21975	276,4301	99,02713	99,9517%	4,232491	1
109,7003	101,5006	211,2008	164,2564	99,9666%	2,928806	2
47,58004	146,5902	194,1702	181,287	99,9829%	1,497004	3
23,42799	188,6423	212,0703	163,3869	99,9917%	0,725051	4
13,74959	229,5366	243,2862	132,1711	99,9956%	0,38419	5
9,278103	270,0143	279,2924	96,16483	99,9974%	0,230454	6
7,295157	310,293	317,5881	57,86914	99,9982%	0,157924	7

Table 7-15 Simulation result with minimum cost model

The economic benefit can be more clearly seen from Figure 7-5

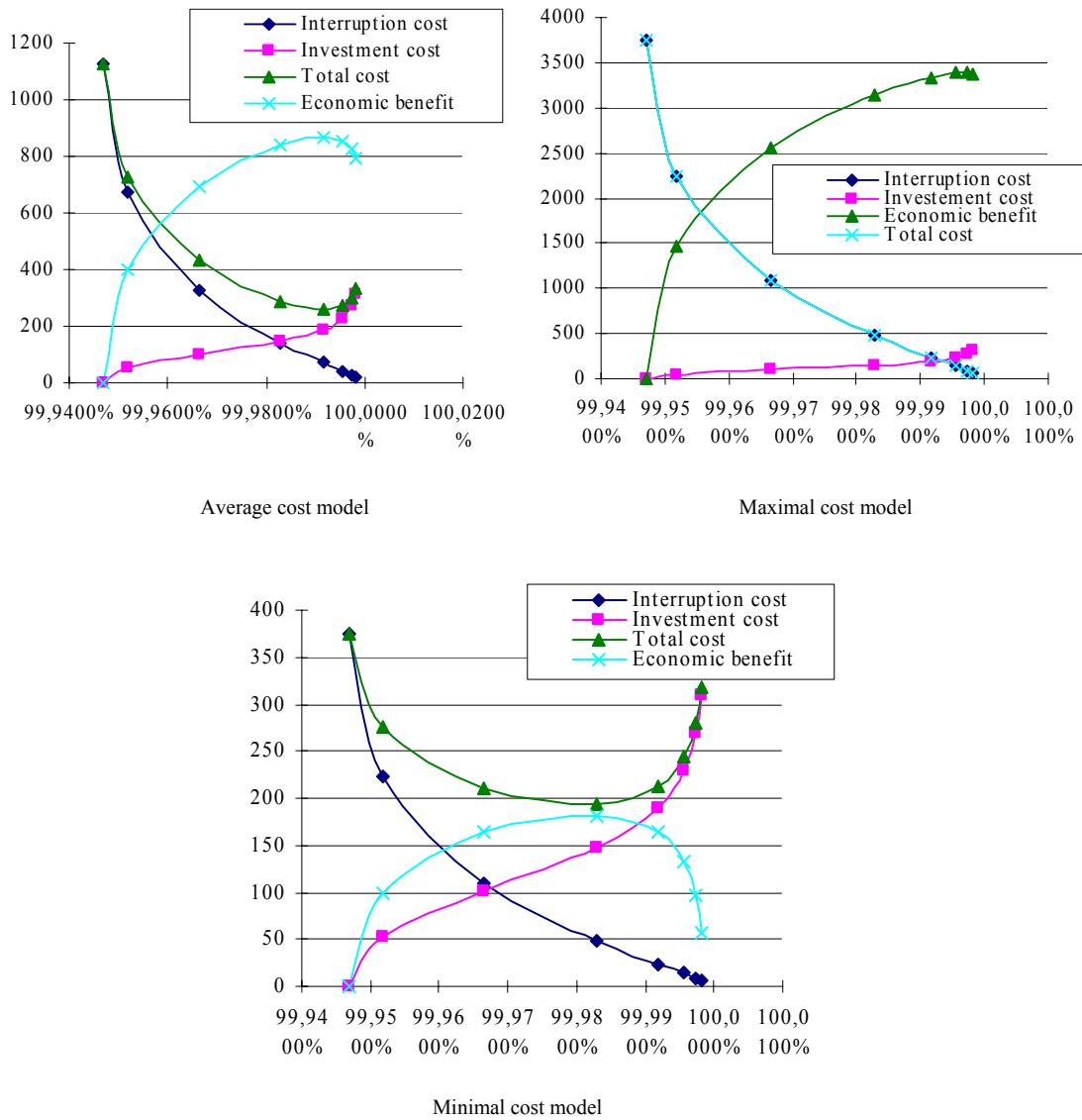


Figure 7-5 Economic cost of Portugal urban network after DG penetration with different cost models

Again, there are different numbers of micro-sources depending on outage costs.

Model	Applied unit DG	Economic benefit Euro/a	Reliability	Unavailability h/a
Minimal cost	3	181,287	99,9829%	1,497004
Average cost	4	867,4455	99,9917%	0,725051
Maximal cost	6	3391,777	99,9974%	0,230454

Table 7-16 Optimised DG penetration of Portugal urban network considering economic benefit

1.28 Portugal rural network

Portugal rural network topology is indicated in Figure 7-6 with DG locations marked in green.

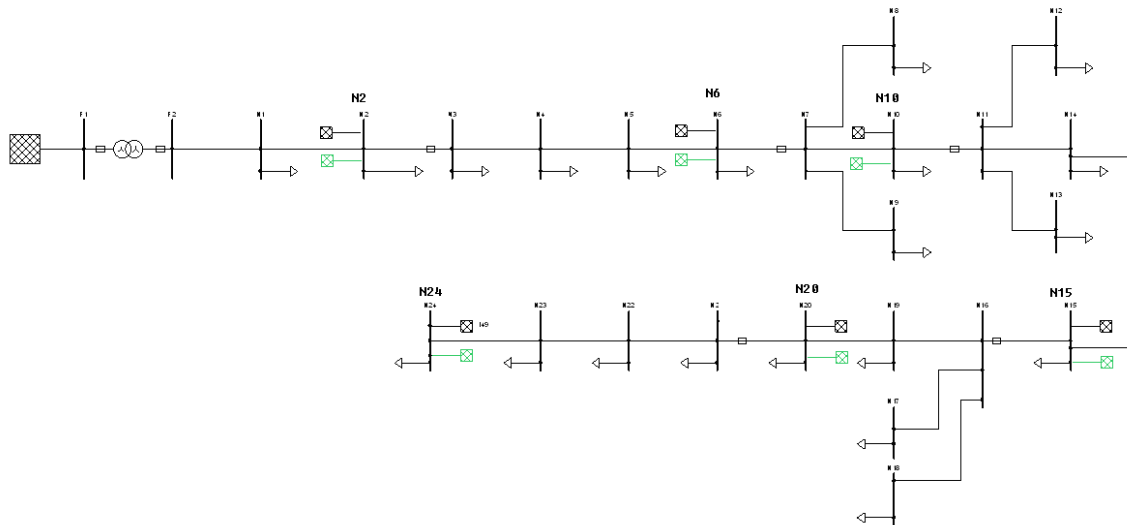


Figure 7-6 Portugal rural network topology

Technical optimised result

Table 7-17 compares the technical optimised CHP penetration with wind, PV penetration as well as without DG unit penetration.

	Hu /a	Qu h/a	T h	Pu kW/a	Wu kWh/a	Eu euro/a
Without DG	5,543361	27,62476	4,983396	941,4816	4691,775	7037,663
PV	3,80061	18,90254	4,973556	725,9518	3611,219	5416,828
Wind	3,189996	15,84585	4,967357	467,959	2321,635	3482,452
CHP	0,615663	2,966719	4,818739	38,72589	175,5425	263,3138

Table 7-17 Portugal rural network reliability indices of different DG penetration

DG optimisation taking into account economic benefit

Simulation results for average, maximum and minimum outage cost model are listed in Table 7-18- Table 7-20.

DG connected busbar	Interruption Cost Euro/a	Investment Cost Euro/a	Total Cost Euro/a	Economic Benefit Euro/a	Reliability	Unavailability h/a	Applied DG unit
Without DG	7037,663	0	7037,663	0	99,6846%	27,62476	0
N24	4276,176	113,7597	4389,936	2647,727	99,7092%	25,47525	1*140kW
N24,N20	2105,025	211,777	2316,802	4720,861	99,7930%	18,1323	2*140kW
N24,N20,N15	912,4312	283,6995	1196,131	5841,532	99,8897%	9,658576	3*140kW
N24,N20,N15, N10	411,4246	337,1797	748,6043	6289,059	99,9469%	4,650255	4*140kW
N24,N20,N15, N10,N6	212,5278	382,6036	595,1314	6442,532	99,9731%	2,352999	5*140kW
N24,N20,N15, N10,N6,N2	166,4074	423,9535	590,3608	6447,302	99,9795%	1,7987	6*140kW
N24,N20,N15, N10,N6,N2,N 23	105,0873	465,7087	570,796	6466,867	99,9880%	1,049141	7*140kW

N24,N20,N15, N10,N6,N2,N 23,N19	64,32267	506,9157	571,2384	6466,425	99,9937%	0,555563	8*140kW
N24,N20,N15, N10,N6,N2,N 23,N19,N14	51,20067	547,3857	598,5863	6439,077	99,9954%	0,405802	9*140kW

Table 7-18 Simulation result for average outage cost model

Interruption Cost Euro/a	Investment Cost .Euro/a	Total Cost Euro/a	Economic Benefit Euro/a	Reliability	Unavailability h/a	Applied DG unit
23458,88	0	23458,88	0	99,6846%	27,62476	0
14253,92	113,7597	14367,68	9091,197	99,7092%	25,47525	1*140kW
7016,748	211,777	7228,526	16230,35	99,7930%	18,1323	2*140kW
3041,437	283,6995	3325,137	20133,74	99,8897%	9,658576	3*140kW
1371,415	337,1797	1708,595	21750,28	99,9469%	4,650255	4*140kW
708,4259	382,6036	1091,03	22367,85	99,9731%	2,352999	5*140kW
554,6912	423,9535	978,6447	22480,23	99,9795%	1,7987	6*140kW
350,2909	465,7087	815,9996	22642,88	99,9880%	1,049141	7*140kW
214,4089	506,9157	721,3247	22737,55	99,9937%	0,555563	8*140kW
170,6689	547,3857	718,0546	22740,82	99,9954%	0,405802	9*140kW

Table 7-19 Simulation result for maximum cost model

Interruption Cost Euro/a	Investment Cost .Euro/a	Total Cost Euro/a	Economic Benefit Euro/a	Reliability	Unavailability h/a	Applied DG unit
2345,888	0	2345,888	0	99,6846%	27,62476	0
1425,392	113,7597	1539,152	806,736	99,7092%	25,47525	1*140kW
701,6748	211,777	913,4519	1432,436	99,7930%	18,1323	2*140kW
304,1437	283,6995	587,8433	1758,044	99,8897%	9,658576	3*140kW
137,1415	337,1797	474,3212	1871,566	99,9469%	4,650255	4*140kW
70,84259	382,6036	453,4462	1892,441	99,9731%	2,352999	5*140kW
55,46912	423,9535	479,4226	1866,465	99,9795%	1,7987	6*140kW
35,02909	465,7087	500,7378	1845,15	99,9880%	1,049141	7*140kW
21,44089	506,9157	528,3566	1817,531	99,9937%	0,555563	8*140kW
17,06689	547,3857	564,4526	1781,435	99,9954%	0,405802	9*140kW

Table 7-20 Simulation result for minimum cost model

The simulation result is more clearly indicated in Figure 7-7.

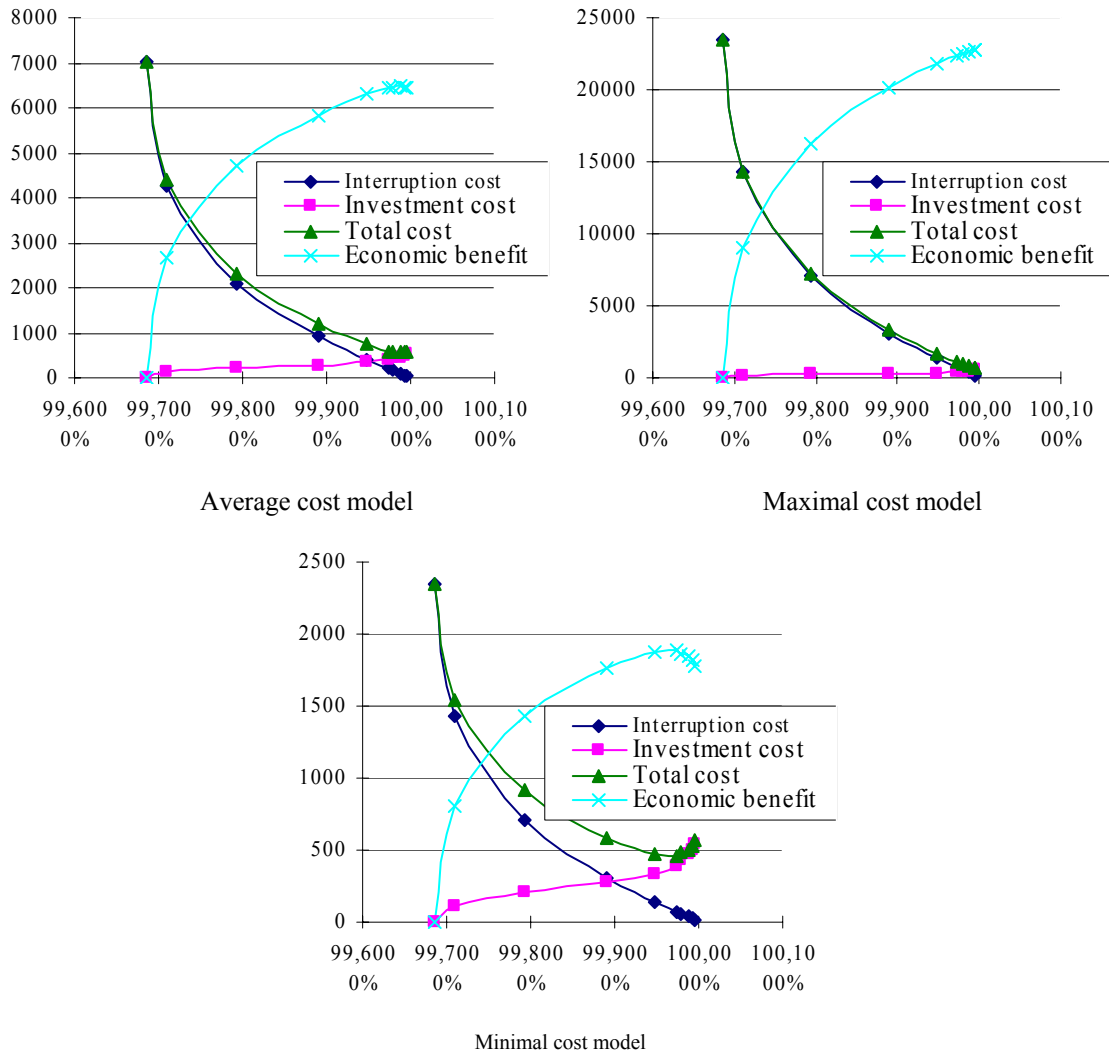


Figure 7-7 Economic cost of Portugal rural network after DG penetration with different cost model

The system reliability of Portugal rural network is quite low; thus more micro-source units are worthwhile to be located into the network with a relative high economic benefit. The optimised DG units are listed in Table 7-21

Model	Applied unit	DG	Economic benefit Euro/a	Reliability	Unavailability h/a
Minimal cost	5		1892,441	99,9731%	2,352999
Average cost	7		6466,867	99,9880%	1,049141
Maximal cost	9		22740,82	99,9954%	0,405802

Table 7-21 Optimised DG penetration of Portugal rural network considering economic benefit

1.29 The Netherlands network

Holland network topology is indicated in Figure 7-8 with DG location marked in green.

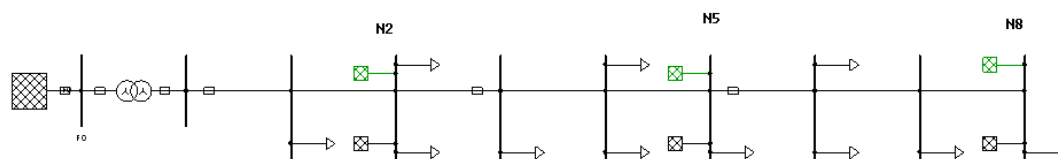


Figure 7-8 Holland network topology

Technically optimised result

Simulation result of optimised 200 % CHP penetration compared with PV and WT is indicated in Table 7-22.

	Hu /a	Qu h/a	Tu h	Pu kW/a	Wu kWh/a	Eu euro/a
Without DG	0,380492	0,690739	1,815383	33,75924	60,74887	91,1233
PV	0,260548	0,462805	1,776276	26,68533	48,53649	72,80473
Wind	0,219087	0,385139	1,757932	17,43767	31,18001	46,77002
CHP	0,052227	0,087163	1,668918	2,695282	4,555123	6,832684

Table 7-22 Holland network reliability indices of different DG penetration

DG penetration taking into account economic benefit

The simulation results for different cost models are listed in Table 7-23 -Table 7-25

DG connected busbar	Interruption Cost Euro/a	Investment Cost .Euro/a	Total Cost Euro/a	Economic Benefit Euro/a	Reliability	Unavailability h/a	Applied DG unit
Without DG	91,12330388	0	91,123304	0,00	99,53%	0,69073927	0
N8	28,76049094	41,783008	70,543499	20,58	99,71%	0,41618403	1*140kW
N8,N5	10,03396019	80,739374	90,773334	0,35	99,91%	0,1363425	2*140kW
N8,N5,N2	5,864099683	120,4712	126,3353	-35,21	99,96%	0,06471482	3*140kW

Table 7-23 Reliability indices for average cost model

Interruption Cost Euro/a	Investment Cost .Euro/a	Total Cost Euro/a	Economic Benefit Euro/a	Reliability	Unavailability h/a	Applied DG unit
303,7443463	0	303,74435	0,00	99,53%	0,69073927	0
95,86830315	41,783008	137,65131	166,09	99,71%	0,41618403	1
33,44653396	80,739374	114,18591	189,56	99,91%	0,1363425	2
19,54699894	120,4712	140,0182	163,73	99,96%	0,06471482	3

Table 7-24 Reliability indices for maximum cost model

Interruption Cost Euro/a	Investment Cost .Euro/a	Total Cost Euro/a	Economic Benefit Euro/a	Reliability	Unavailability h/a	Applied DG unit
30,37443463	0	30,374435	0,00	99,53%	0,69073927	0
9,586830315	41,783008	51,369839	-21,00	99,71%	0,41618403	1
3,344653396	80,739374	84,084028	-53,71	99,91%	0,1363425	2
1,954699894	120,4712	122,4259	-92,05	99,96%	0,06471482	3

Table 7-25 Reliability indices for minimum cost model

Due to the relatively reliable network topology of Holland network, there is no benefit for DG penetration based on minimum cost model. The largest benefit can be achieved by 1 DG unit for average cost model and 2 DG units for maximum cost model.

1.30 Germany MV network

An existing German MV network as shown in Figure 7-9 ($P_{\text{load}} = 3.8 \text{ MW}$) with high DG penetration ($P_{\text{WT}} \sim 39 \text{ MW}$, $P_{\text{CHP}} \sim 4 \text{ MW}$, $P_{\text{PV}} \sim 3 \text{ MW}$) is evaluated in this section. Load and DG scheme is listed in A8. The red points in the network topology indicates load while the blue points show DER locations.

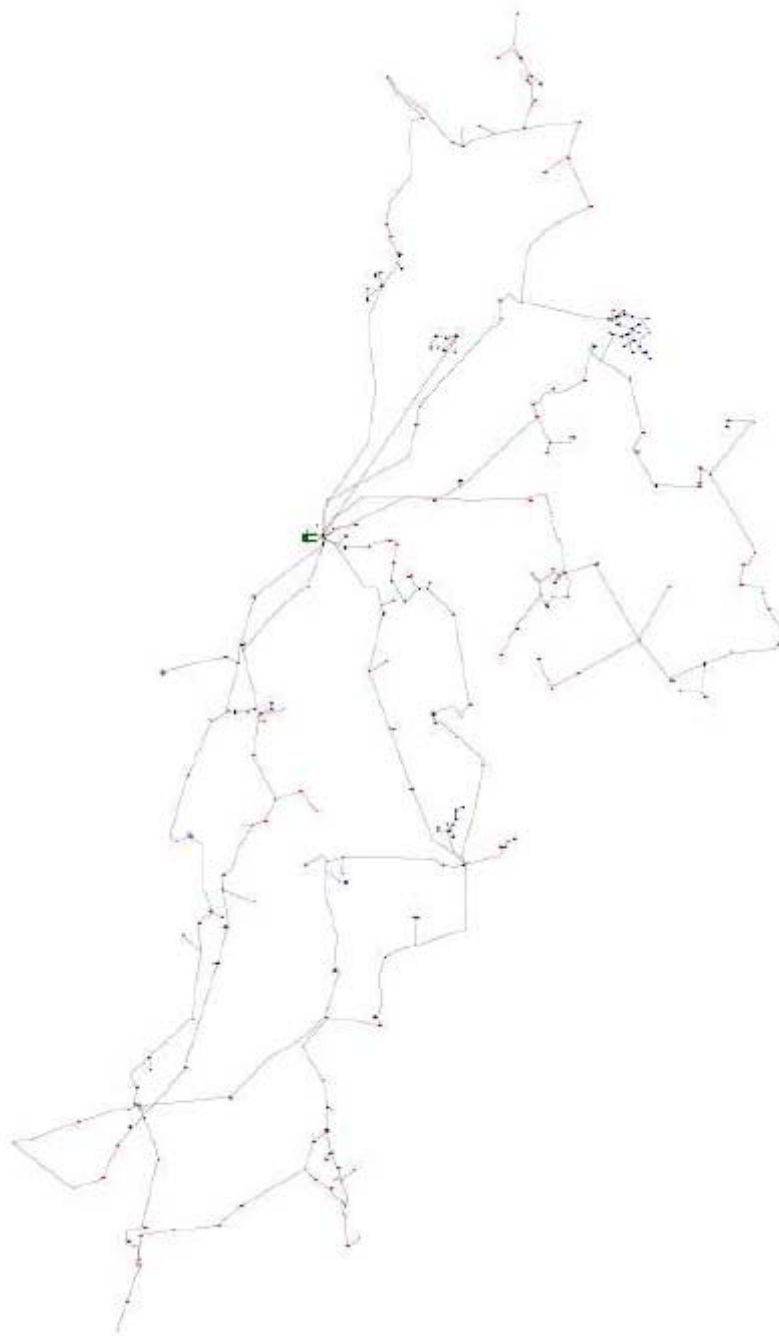


Figure 7-9 German MV network topology

Two scenarios are simulated separately, a network with and one without micro-sources. Simulation results are shown in Table 7-26.

	Hu/a	Qu min/a	Tu h	Pu kVA/a	Wu kVAh/a	Ku Euro/a
with micro-sources	1,321464	631,9198	7,969949	18,44611	172,7341	259,1011
without micro-sources	2,56993	1352,341	8,77028	73,20997	543,8626	815,7938

Table 7-26 Simulation result with and without micro-sources in German MV network

It can be seen the reliability improvement by micro-sources is significant.

1.31 Comparison of simulation results on European Level

Economic benefit

The optimised economic benefits of different networks are compared in Figure 7-10 . The x-axis is the multiplication of the total load of the network and the unavailability of this network in each year, which is symbolized by PQ. Y-axis is the economic benefit.

It can be seen that the optimised economic benefit of each country is almost linear related with PQ. The reason is obvious. Interruption costs without DG increase with increasing total demand and unavailability, leading to higher benefits of Microgrid operation.

The optimised economic benefit regarding different cost models ranks as follows,

Maximal cost model > Average Cost Model > Minimal Cost Model

The reason for such ranking is similar as the relationship between economic benefit and PQ: With increasing per unit energy and power interruption costs, the total network interruption cost increases in case without DG penetration; the benefit of micro-sources increases with higher per unit energy and power cost.

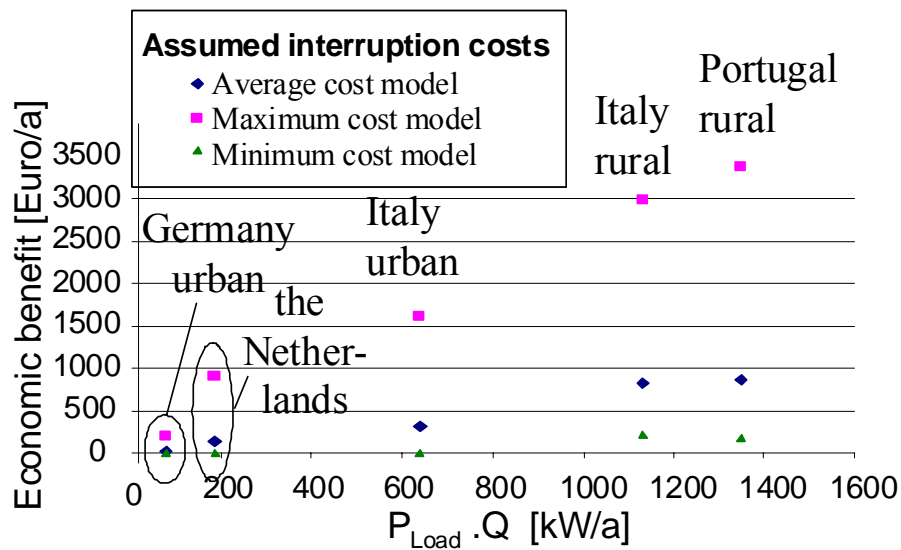


Figure 7-10 Economic benefit comparison of Microgrids on European Level

System reliability index

A reduction of System unavailability Q , as one example for system reliability indices, by the installation of micro-sources that enable (partial) island operation is demonstrated in Figure 7-11.

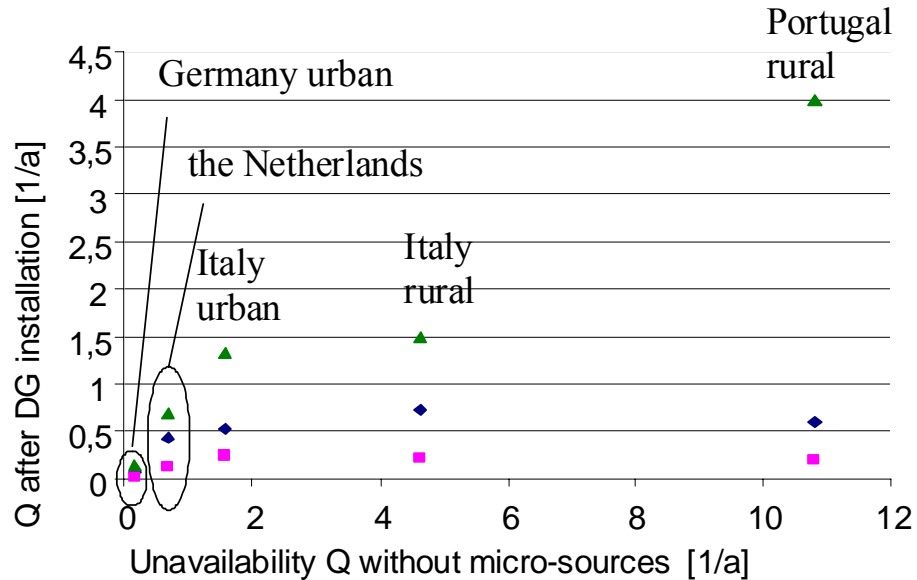


Figure 7-11 System unavailability comparison of different countries

System unavailability Q is improved for all countries analysed by the installation of micro-sources compared with the compared to the case without DG.

The countries which have worse system reliability achieve higher improvements than the countries with high system reliabilities also without DG. For instance, in Portugal rural network the system unavailability decreases from more than 10 h/a to the value of below 1 h/a with maximal and average cost model; even with average cost model yearly unavailability is also reduced to approximate 4h/a. However, the improvement for German urban network and Holland network, which have already good system reliability without micro-sources, is not obvious, although system reliability is also improved to a certain extent for both networks.

With higher interruption cost model, system reliability can be better improved. Higher interruption costs justify higher micro-source investment, thus achieving higher system reliability improvements.

Microgrid operation from reliability point of view is thus most beneficial in countries with lower power quality or in regions or for customer segments with comparably high outage costs.

Optimised DG penetration level

One question that most system operators are concerned with is the optimised DG penetration level. Relationship regarding different cost models between optimised DG penetration level and interruption frequency is indicated in Figure 7-12.

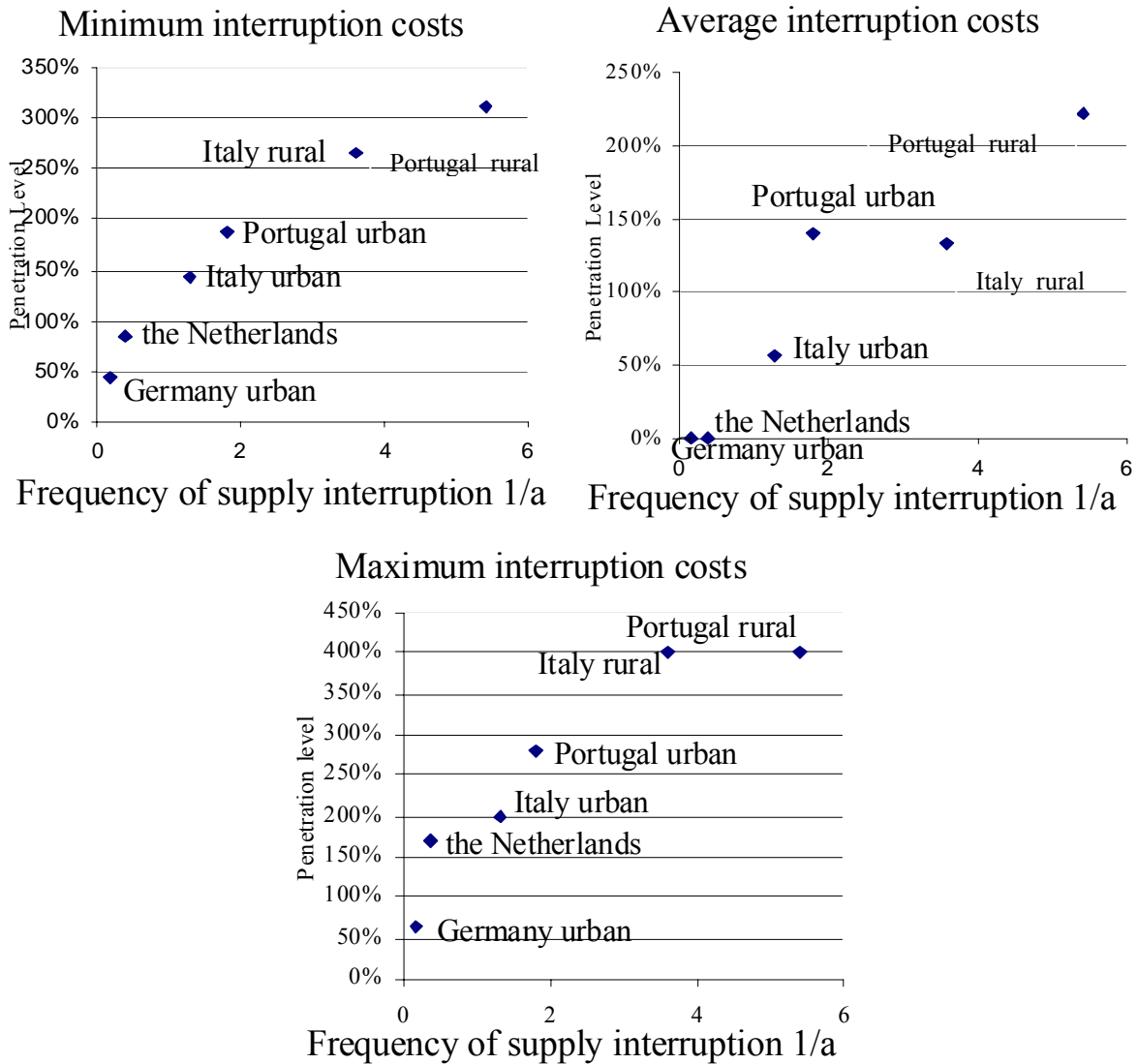


Figure 7-12 Optimised penetration level regarding interruption frequency without micro-sources

Optimum micro-source penetration level is positive related with the interruption frequency without DG penetration; especially for average interruption costs, the relationship is almost linear. This relationship is important for system planning; as the system interruption frequency without DG penetration is generally known, the system operator is able to roughly determine of the optimum DG penetration level from reliability point of view

Optimum micro-source location

As already described, when only failures caused by LV network are considered, optimum micro-source location should take into account the following criteria:

- DG is distributed to different protection zone
- DG is located most downstream in the network
- DG is connected to the load with higher demand
- DG is prioritised to connect with the sensitive load

When MV and HV level failures are considered (as is the reason for most outages), different micro-source locations have the same effect to the reduction of load interruption caused by this failure; micro-sources improve system reliability independent from their location.

8 References

- [1] Endrenyi, J. 1978, *Reliability Modelling in Electric Power Systems*, John Wiley & Sons, New York, NY
- [2] I. Jimenez Lerma, *Application of Monte Carlo Method to Power System Reliability Calculations*, Subdireccion de Programacion Comision Federal de Electricidad, Mexico, 1999
- [3] R.E. Brown, J.R. Ochoa, *Distribution System Reliability: Default Data and Model Validation*, IEEE Transactions on Power System, Vol.13, No.2, May 1998
- [4] R. Billington and R. Allan, *Reliability Evaluation of Power Systems 2nd Edition*, Plenum Press, New York, 1996
- [5] Chris Marnay, Giri Venkataramanan, *Microgrids in the Evolving Electricity Generation and Delivery Infrastructure*, the 2006 IEEE power engineering society general meeting, February 2006
- [6] *IEEE Guide for Electric Power Distribution Reliability Indices*, the Institute of Electrical and Electronics Engineers. Inc. May 2004
- [7] M. Henderson, *Reliability Indices*, Power Engineering Society Summer Meeting, 2000. IEEE, Volume 1, Issue , 2000 Page(s):623 - 624 vol. 1, 2000
- [8] Haß, P, *Das (n-1)-Kriterium bei DG Planung von Übertragungsnetzen*, Elektrizitätswirtschaft 80, 1981
- [9] M. Schwan, *Aspekte DG Zuverlässigkeitsberechnung elektrische Energieversorgungsnetze im liberalisierten Markt*, Dissertation, DG Naturwissenschaftlich-Technischen Fakultät II DG Universität des Saarlandes, Saarbrücken, 2003
- [10] R. Bilinton and R. Allan, *Reliability Evaluation of Power Systems: Concepts and techniques*, Pitman Publishing, London, Marshfield 1983
- [11] M. Schwan, Wolfram H. Wellssow, Hans-Juergen Koglin, *Identification of Probability Distributions of Probabilistic Reliability Indices for Monetary Evaluation and Risk Assessment*, 14th PSCC, Sevilla, 24-28 June 2002
- [12] M. Schwan, A. Slupinski, *ZUBER Manual*, FGH e.V. Mannheim, August 2004

- [13] A. Pregelj, M. Begovic, A. Rohatgi, D. Novosel, *On Optimization of Reliability of Distributed Generator-Enhanced Feeders*, Proceedings of the 36th Hawaii International Conference on System Sciences, 6-9 Jan. 2003
- [14] Lj. A. Kojovic, R. D. Willoughby, *Integration of Distributed Generation in a Typical USA System*, Proceedings of the 16th CIRED, pp. 5, Vol. 4, 2001
- [15] Lina Bertling, *Reliability Centered Maintenance for Electric Power Distribution Systems*, Ph.D. dissertation, Dept. Elect. Power Engineering, KTH, Stockholm, Sweden, 2002
- [16] Enrico Carpanet, Alessandra Mosso, Andrea Ponta, Emiliano Roggero, "Comparison of Reliability and Availability Evaluation Techniques for Distribution Network Systems", IEEE Proceedings Annual Reliability and Maintainability Symposium, 2002
- [17] C. Matheus, *Power System II—Reliability Calculation*, Lecture notes, IAEW Aachen, summer term 2003
- [18] Schwan, M., Schwaegerl, C., Wellßow, W. H., Connor, T., *Generation System Reliability in a Market Environment*, Probabilistic Methods Applied to Power Systems, 2006. PMAPS 2006, International Conference, June 2006
- [19] Gebler, H. *Berechnung von Zuverlässigkeitskenngrößen für Elektrische Energieversorgungsnetz*, Dissertation, TH Darmstadt, Darmstadt 1981
- [20] Wellßow, W.H. *Ein Beitrag zur Zuverlässigkeitsberechnung in DG Netzplanung*, Dissertation, TH Darmstadt, Darmstadt 1986
- [21] Smirnow, N. W., Dunin-Barkowski, I. W.: *Mathematische Statistik in DG Technik. Kurzer Lehrgang*. Deutscher Verlag DG Wissenschaften Berlin, 1963
- [22] Weber, H.: *Einführung in die Wahrscheinlichkeitsrechnung und Statistik für Ingenieure*. B. G. Teubner Stuttgart, 1992
- [23] Bartsch, H.-J.: *Taschenbuch DG Mathematik*. Fachbuchverlag Leipzig, 1991
- [24] Beyer, O., u. a.: *Wahrscheinlichkeitsrechnung und mathematische Statistik. Mathematik für Ingenieure, Naturwissenschaftler, Ökonomen und Landwirte (MINÖL)*, Band 17, Teubner Verlagsgesellschaft, Leipzig, 1976
- [25] Bronstein, I. N., Semendjajew, K. A.: *Taschenbuch DG Mathematik*. 25. Auflage, B. G. Teubner Verlagsgesellschaft, Stuttgart, Leipzig, Verlag Nauka Moskau, 1991
- [26] Grosche, G., Ziegler, V., Ziegler, D., Zeidler, E. (Hrsg.): *Teubner Taschenbuch DG Mathematik. Teil II. (7. Auflage, vollständig überarbeitete und wesentlich erweiterte Neufassung DG 6. Auflage DG „Ergänzenden Kapitel zum Taschenbuch DG Mathematik von I. N. Bronstein und K. A. Semendjajew“*, B. G. Teubner Verlagsgesellschaft Leipzig, 1995
- [27] R. Billinton and R. Allan, *Reliability Evaluation of Power System 2nd Edition*, Plenum Press, New York, 1996
- [28] Michael Schwan, Wofram H. Wellssow, Hans-Jürgen Koglin, 14th PSCC, Sevilla, 24-28 June 2002
- [29] Märtel, D, Wellßow, W. H., *Die Qualität der Versorgung mit elektrischer Energie. Elektrizitätswirtschaft 95(1996)*, Vol. 25
- [30] *Comprehensive Power System Reliability Assessment*. Project report. Power Systems Engineer Research Center, April 2005

- [31] Fotuhi-Firuzabad, M; Rajabi-Ghahnavie, A, An Analytical Method to Consider DG Impacts on Distribution System Reliability, Transmission and Distribution Conference and Exhibition: Asia and Pacific, 2005 IEEE/PES
- [32] Nguyen Hoang Viet, MA. Pham Hong Thanh, Power System Reliability Analysis with Distributed Generators, International Symposium on Electrical & Electronics Engineering 2007-Oct24, 25 2007-HCM City, Vietnam
- [33] Billinton, R., Wenyuan, L., "Hybrid Approach for Reliability Evaluation of Composite Generation and Transmission Systems Using Monte Carlo Simulation and Enumeration Technique", IEEE Proceedings-C, Vol.138, No.3, May 1991
- [34] Ubeda, R., Allan, R.N., "Sequential Simulation Applied To Composite System Reliability Evaluation", IEE Proceedings-C, Vol.139, No.2, March 1992
- [35] Cunha, S.H.F., Pereira, M.V.F., Pinto, L.M.V.G., Olivera, G.C., "Composite Generation and Transmission Reliability Evaluation in Large Hydroelectric Systems", IEEE Transaction on Power Apparatus and Systems, VOL.PAS-104, No.10, Oct.1985, pp.2657-2663
- [36] R. Billinton, A. Jonnavithula, Application of sequential Monte Carlo simulation to evaluation of distributions of composite system indices, IEE Proceedings-Gener. Transm. Distrib., Vol. 144, No.2, March 1997
- [37] A. Sankarakrishnan, R. Billinton, Sequential Monte Carlo Simulations for Composite Power System Reliability Analysis with Time Varying Loads, IEEE Transactions on Power Systems, Vol.10, No.3, August 1995
- [38] Math, Bollen. Different Views on Reliability – Reliability and reliability indices in the viewpoint of the network operator and in the viewpoint of the customer, EU-DEEP Project Contribution, internal document, July 7, 2007
- [39] R. Lasseter et al, The CERTS Microgrid Concept, White paper on Integration of Distributed Energy Resources, April 2002
- [40] N. Hatziaryiou, G. Strbac, Microgrids – A Possible Future Energy Configuration, IEA Workshop "Distributed Generation: Key issues, Challenges, Roles", Paris, 1 March 2004
- [41] MICROGRIDS – Advanced Architectures and Control Concepts for More Microgrids, contract no. PL019864, Technical Annex, June 2005
- [42] A.G. Tsikalakis, N.D. Hatziaryiou, Aghia Pelagia Crete, Environmental Benefits of Microgrids Operation, the 19th ECOS 06 Conference, Greece, July 2006
- [43] Julija Vasiljevska, Antonis Tsikalakis, Nikos Hatziaryiou, Report on the Economic Benefits of Microgrids, internal document Project More Microgrids, July 2007
- [44] Brown, R. E, Freeman, L.A.A. Analyzing the reliability impact of distributed generation. Power Engineering Society Summer Meeting, 2001 .IEEE
- [45] Sun, Y., Bollen, M.H.J., Ault, G. W. Probabilistic Reliability Evaluation for Distribution Systems with DER and Microgrids, Probabilistic Methods Applied to Power Systems, 2006. PMAPS 2006.
- [46] In-Su Bae, Jin-O Kim, Jae-Chul Kim, C. Singh, Optimal Operating Strategy for Distributed Generation Considering Hourly Reliability Worth. IEEE Transactions on Power Systems Vol.19, No.1, February 2004

- [47] A.A.Chowdhury, S.K.Agarwal, D.O.Koval, Reliability Modelling of Distributed Generation in Conventional Distribution Systems Planning and Analysis, Industry Applications, IEEE Transactions on Volume 39, Issue 5, Sep-Oct. 2003, Page1013-1018
- [48] Mahmud Fotuhi.Firuzabad, Abbas Rajabi-Ghahnavie, An Analytical Method to Consider DG Impacts on Distribution System Reliability IEEE/PES Transmission and Distribution Conference & Exhibition : Asia and Pacific Dalian, China
- [49] David Robinson, Christopher Atcitty, Jason Zuffranieri, Doug Arent, Impact of Distributed Energy Resources on the Reliability of a Critical Telecommunications Facility. Technical Report. Sandia National Laboratory.
- [50] G. Celli, S. Mocci, F. Pilo, R. Cicoria, Probabilistic Optimization of MV Distribution Network in Presence of Distributed Generation. 14th PSCC, Sevilla, 24-28th June 2002
- [51] Ryan Firestone, Chris Marnay, Energy Manager Design for Microgrids, California Energy Commission, Jan. 2005
- [52] R. Walawalkar, Vaidyanathiyer, Distribution Generation for Power Quality and Reliability
- [53] Olimpo Anaya-lara, Ahmed Shafiu, Rachel Li, Coordinated Voltage Support and Flow Control, Microgrid Contribution Contract No. SES6-019864, July 2007
- [54] Pei Zhang, Stephen T.Lee, Probabilistic Load Flow Computation Using the Method of Combined Cumulants and Gram-Charlier Expansion. IEEE Transaction on power systems, VOL19, No.1,February 2004
- [55] P.W.Sauer and G.T.Heydt,"A generalized stochastic power flow algorithms" presented at the IEEE Summer Meeting, Los Angeles, CA, July 1978
- [56] Jeremy A. Bloom, Probabilistic Production Costing with Dependent Generation Source, IEEE Transactions on Power Apparatus and Systems, Vol. PAS-104, No.8, August 1985
- [57] J. F. Dopazo, O A. Klitin, and A. M. Sasson, "Stochastic load flow" Proceedings International Electrical Engineer 121, pp. 1551-1556,1974
- [58] R. N. Allan, A. M. L. Da Silva, and R. C. Burchett, "Evaluation methods and accuracy in probabilistic load flow solutions", IEEE Transactions on Power Apparatus and Systems, Vol.PAS-94, pp. 299-309, Mar/Apr.1975
- [59] Stewart, G. W., 1973, Introduction to Matrix Computations, Academic Press (New York)
- [60] More Microgrids, WPG, deliverable DG.1, Definition of future Microgrid scenarios and performance indices, 2008
- [61] Bagen R. Billinton, Impacts of energy storage on power system reliability performance, Electrical and computer engineering conference, Canadian conference, 2005

9 Appendix

A.1 General Scenario Overview

Scenarios	Description	
<i>Base Case T</i>	Original simple network without DER units; Failure Model: only Independent Single Failure; Rate Power of Demand: 1.267 MVA (without LP); Unavailability Threshold: E-10; Power Allocation Mode: pessimistic mode; Load Profile: 2 states Testing load ADC	
<i>Scenario I – T</i>	Simple network with DER penetration; DER Characteristics: one DER unit, 100% penetration level, connected to node K3, 100% DER reliability; Supplementary DER Settings; Islanded Operating Mode allowed; DER reacting immediately after interruptions; Other Settings: the same as <i>Base Case T</i>	
DER Size	Based On <i>Scenario I–T</i>	Without LP $\begin{cases} \text{Pessimistic} \\ \text{Optimistic} \end{cases}$ / With LP $\begin{cases} \text{Pessimistic} \\ \text{Optimistic} \end{cases}$ Different PL schemes
DER Number		1 unit connected to K3; 2 units connected to K3 and K1; 3 units connected to K1, K2 and K3; 4 units connected to K1, K2, K3 and K4
DER Location		DER unit connected to K3; K5 and K7 respectively
DER Reliability		DER reliability ranging from 95% to 100%
<i>Base Case H</i>	Original simple network without DER units; Load Profile: 2 states Household load ADC; Other Network Settings: the same as <i>Base Case T</i>	
<i>Scenario I – H</i>	Simple network with DER penetration; Load Profile: 2 states Household load ADC; Other Network Settings: the same as <i>Scenario I–T</i>	
Scenario II	Based On <i>Scenario I–H</i>	PV option: synergy of PV and Household profiles
Scenario III		WT option: synergy of WT and Household profiles
Scenario IV		CHP option: synergy of CHP and Household profiles
Scenario LM	Based on <i>Base Case H</i>	Load Profile: 3 states load ADC (the same LF as the curve of power demand after 100% WT penetration)

Table A -1 Descriptions of Scenarios analysed in this report

A.2 Homogeneous Markov Process

A2.1 General Description

Markov Process is a process with the *Markov property*. In probability theory, a stochastic process has the Markov property if it is given the present state with conditionally independent of the past states (the path of the process). It is generally comprised with *Markov chain (discrete-time Markov process)* and *Continuous-time Markov process*.

Mathematically, if $X(t)$, $t > 0$, is a stochastic process, the Markov property states that

$$\Pr[X(t+h) = y \mid X(s) = x(s), \forall s \leq t] = \Pr[X(t+h) = y \mid X(t) = x(t)],$$

Markov process are typically termed *homogeneous* if

$$\Pr[X(t+h) = y \mid X(t) = x] = \Pr[X(h) = y \mid X(0) = x], \forall t, h > 0,$$

Homogeneous Markov Process is the most important class of Markov process.

Markov chain

The most famous Markov processes are *Markov chains*. Markov chains are often described by a *directed graph*, where the edges are labelled by the probabilities with p_{ij} of going from one state i to the other states j . And the probability p_{ij} does not depend on which states the chain was in before the current state. p_{ij} is defined as *transition probability* while the process could remain in the state it is in, with the probability p_{ii} .

For the *single-step transition*, it is expressed as

$$p_{ij} = \Pr(X_1 = j \mid X_0 = i), \text{ and } p_{ii} = 1 - \sum_{j \neq i} p_{ij},$$

The probability of going from state i to state j in n time state is expressed as

$$p_{ij}^{(n)} = \Pr(X_n = j \mid X_0 = i),$$

The n -step transition satisfies the Chapman-Kolmogorov equation, that for any $k \in (0, n)$,

$$P_{ij}^{(n)} = \sum_{r \in S} p_{ir}^{(k)} p_{rj}^{(n-k)}, \text{ with } S: \text{state space of the chain}$$

The marginal distribution $\Pr(X_n = x)$ is the distribution over states at time n . The initial distribution is $\Pr(X_0 = x)$. The evolution of the process through one time step is described by

$$\Pr(X_n = j) = \sum_{r \in S} p_{rj} \Pr(X_{n-1} = r) = \sum_{r \in S} p_{rj}^{(n)} \Pr(X_0 = r), \text{ with } n \text{ of integer-value only}$$

If the state space S is finite, the transition probability distribution can be represented by a matrix named transition matrix, with the element (i, j) of \mathbf{P} equal to

$$p_{ij} = \Pr(X_{n+1} = j \mid X_n = i).$$

\mathbf{P} is a stochastic matrix. It is independent of the label n with *homogeneous Markov chain*, and then the k -step transition probability can be computed as \mathbf{P}^k .

Continuous-time Markov process

A *continuous-time Markov process* is a stochastic process $\{X(t) : t \geq 0\}$, which satisfies the *Markov property* and takes values from state space. It is declared that the state of the process at any time $s > t > 0$ is conditionally independent of the history of the process before time t , given the state of the process at time t .

Mathematically, with the definition of some small increment of time t to $t + h$ as well as the start state $X(t) = i$ and a transition to current state $X(t + h) = j$, a *continuous-time homogeneous Markov process* can be expressed as

$$\Pr(X(t + h) = j | X(t) = i) = q_{ij}h + o(h),$$

Where $o(h)$ is an infinitesimal asymptotic describing the error term while $h \rightarrow 0$. Thus the probability of a particular transition over a sufficient small interval of time is roughly proportional to the duration of that interval. And q_{ij} is the *transition rate*, which is the ij -th element to the *transition rate matrix Q*.

The most intuitive *continuous-time Markov process* has the following two characteristic:

- **Conservative** – the i -th diagonal element q_{ii} of **Q** is given by

$$q_{ii} = -q_i = -\sum_{j \neq i} q_{ij},$$

- **Stable** – for any given state i , all elements q_{ij} (and q_{ii}) are finite.

A3.2 Consideration of Microsource Availability

With the consideration of DG outages, the failure combination order is maximum 2 due to considering only one DG unit and one failure model ISF, which means only two components can suffer interruptions at the same time. Therefore, 4-state transition diagram is sufficient to describe the Markov process.

Figure A-1 describes a 4-state transition prototype as the fundamental to build the Markov model in case the DG and L5 both are in failure state (state number 4). The reliability indices of state 4 are the variables that need to be known. $\alpha_{1,2}$ is the repair rate, and $\alpha_{2,1}$ is the failure rate.

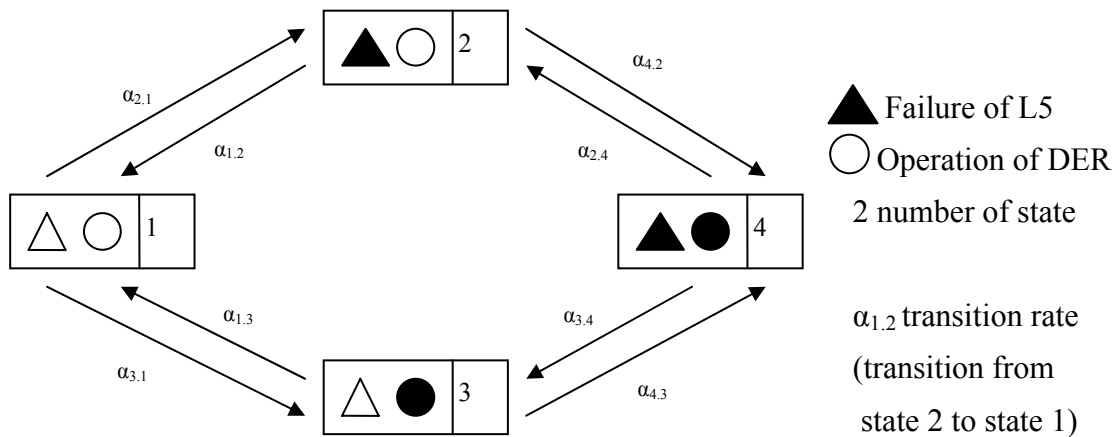


Figure A-1 State Transition Diagram

The relation between transition rate and reliability input data (failure rate and down time) is expressed in the following equations. 99.9 % reliability is taken as an example.

$$\begin{aligned}\alpha_{1,2} = \alpha_{3,4} &= \frac{1}{T_{Z,L5}} = \frac{1}{15h} = 584a^{-1} \\ \alpha_{1,3} = \alpha_{2,4} &= \frac{1}{T_{Z,DER}} = \frac{1}{20h} = 438a^{-1} \\ \alpha_{2,1} = \alpha_{4,3} &= H_{Z,L5} = 9.45 \times 10^{-3} a^{-1} \\ \alpha_{3,1} = \alpha_{4,2} &= H_{Z,DER} = 0.5a^{-1}\end{aligned}$$

Equation A-1

So the Markov model equation can be drawn as

$$\begin{pmatrix} 0 \\ 0 \\ 0 \\ 0 \end{pmatrix} = \begin{pmatrix} -(\alpha_{2,1} + \alpha_{3,1}) & \alpha_{1,2} & \alpha_{1,3} & 0 \\ \alpha_{2,1} & -(\alpha_{1,2} + \alpha_{4,2}) & 0 & \alpha_{2,4} \\ \alpha_{3,1} & 0 & -(\alpha_{1,3} + \alpha_{4,3}) & 0 \\ 0 & \alpha_{4,2} & \alpha_{4,3} & -(\alpha_{2,4} + \alpha_{3,4}) \end{pmatrix} \times \begin{pmatrix} P_{r(S1)} \\ P_{r(S2)} \\ P_{r(S3)} \\ P_{r(S4)} \end{pmatrix}$$

$P_{r(Si)}$ is the probability of each state

Equation A -2

With

$$\sum_{i=1}^4 P_{r(Si)} = 1$$

Equation A -3

The Markov matrix can be solved with 4 variables and 4 linear independence equations. The results that we need are

$$P_{r(S4)} = 1.86e-008, \quad H_{Z,S4} = 1.91e-005 a^{-1}.$$

Alternatively, in an easy-to-understand way, the frequency of supply interruption in state 4 is the probability of the both L5 and DG out of operation. Two possibility lead to such multiple faults: L5 fails during the unavailable time of DER; or DG is out of operation during the time that L5 is in the failure state as well. And thus it can be calculated with the thought of the occurrence probability of such event in the following way.

$$H_{Z,S4} = H_{Z,L5} \times \frac{T_{Z,L5}}{8760h} \times H_{Z,DER} + H_{Z,DER} \times \frac{T_{Z,DER}}{8760h} \times H_{Z,L5}$$

Equation A -4

The result is $1.93e-005 a^{-1}$, the error is so slight that can be neglected. However, it is only a thought to understand clearly in this simple network, in real large network, it is too complicate to calculate it manually. Other results of multiple faults are presented in Table A-2.

Event	DER&K6	DER&L5	DER&T1	DER&L3	DER&K5
$H_Z[1/a]$	9.34e-006	1.91e-005	7.83e-006	2.91e-006	9.74e-006
$Q_Z[\text{min}/a]$	2.72e-003	9.78e-003	2.00e-003	1.40e-003	2.78e-003

Table A-2 Failure Combinations of Multiple Faults

As introduced in the first part, the reliability results of the end-customers are the enumerative sum of all the related failure combinations. Node K3 is the most reliable node as it is directly connected to the DG, therefore failure in busbar K5 or line L3, only coexistence with failure in DG can affect the result (See Eq. A-5). In contrast to node K3, at other 3 nodes K1, K2 and K4, no matter the DG is on operation or not, once K5 or the line which is connected to the end-customers fails, the supply will be interrupted (See Eq. A-6).

$$H_{u,K3} = H_{Z,DER\&K1} + H_{Z,DER\&T1} + H_{Z,DER\&L5} + H_{Z,DER\&K5} + H_{Z,DER\&L3} \quad \text{Equation A -5}$$

$$H_{u,K2} = H_{Z,DER\&K1} + H_{Z,DER\&T1} + H_{Z,DER\&L5} + H_{Z,K5} + H_{Z,L2} \quad \text{Equation A -6}$$

A.3 Node Result and Network Result of Simple Network

The failure combination of each network component i , which may suffer from supply interruption, is the fundamental of the reliability indices calculation. For example, Table A-3 lists the failure combinations i of the original simple network.

i	Element	Network Level	$H_Z [1/a]$	$Q_Z [\text{min}/a]$	$T_Z [h]$	$P_Z [\text{MVA}/a]$	$W_Z [\text{MVAh}/a]$
0	K6	20KV	0,006200	2,3784	6,39	0,0059528	0,0380598
1	T1	20KV	0,005400	1,7544	5,41	0,0051847	0,0280744
2	L5	20KV	0,009650	8,5434	14,76	0,0092653	0,1367137
3	K5	0,4KV	0,006500	2,4360	6,25	0,0062409	0,0389815
4	L1	0,4KV	0,000767	0,5487	11,92	0,0001938	0,0023107
5	L2	0,4KV	0,001145	0,8889	12,94	0,0002604	0,0033689
6	L3	0,4KV	0,001523	1,2291	13,45	0,0003463	0,0046583
7	L4	0,4KV	0,002090	1,7394	13,87	0,0005281	0,0073248

Table A-3 Failure Combinations in the Original Simple Network

To explain the formula of the reliability indices, several indices need to be considered [9]:

- $H_{Z,i}$ Frequency of supply interruption of failure combination i ;
- $H_{u,ik}$ Frequency of supply interruption of end-customer k in failure combination i ;
- $H_{u,k}$ Frequency of supply interruption of end-customer k ;
- H_u Frequency of supply interruption of the network;
- T_{ikr} Duration from outage to the r^{th} sequence of the restoration measurement of end-customer k in failure combination i ;
- S_{kmax} Peak load demand of end-customer k ;
- S_{ikr} Available power of end-customer k during the time $T_{ik(r-1)}$;

- $p_{Z,ik}$ Conditional interruption probability of end-customer k in failure combination i . If the available power is higher than the demand of end-customer k , it will not cause that customer suffering supply interruption. It can be calculated as ratio of the duration, when the available power is higher than demand, and the total considered duration (1 year).

Now the formula for both node result and network result can be derived [9][19][20].

Node Result

$$H_{u,k} = \sum_i H_{u,ik} \quad \text{with } H_{u,ik} = p_{Z,ik} \cdot H_{Z,i}$$

$$Q_{u,k} = \sum_i Q_{u,ik} \quad \text{with } Q_{u,ik} = H_{Z,i} \cdot \sum_r p_{S,ikr} \cdot T_{ikr}$$

$p_{S,ikr}$: the probability of the load demand between S_{ikr} and $S_{ik(r+1)}$ in the r^{th} step of the restoration measurement, it can be determined from ADC

$$T_{u,k} = \frac{Q_{u,k}}{H_{u,k}} \quad \text{with } T_{u,ik} = \frac{Q_{u,ik}}{H_{u,ik}} = \frac{1}{p_{Z,ik}} \cdot \sum_r p_{S,ikr} \cdot T_{ikr}$$

$$S_{u,k} = \sum_i S_{u,ik} \quad \text{with } S_{u,ik} = H_{Z,i} \cdot S_{Z,ik}^* = H_{Z,i} \cdot \sum_d p_d \cdot (S_{kd} - S_{ik1})$$

(optimistic mode) d : the step from ADC with $S_{kd} > S_{ik1}$
 p_d : probability of step d in 1 year from ADC
 S_{kd} : load demand of end – customer k in step d
 $S_{Z,ik}^*$: with pessimistic mode $S_{Z,ik}^* = \sum_d p_d \cdot S_{kd}$

$$W_{u,k} = \sum_i W_{u,ik} \quad \text{with } W_{u,ik} = H_{Z,i} \cdot \sum_r p_{S,ikr} \cdot S_{Z,ikr} \cdot [T_{ikr} - T_{ik(r-1)}] \text{ and}$$

$$S_{Z,ikr} = \sum_d p_{d|r} \cdot (S_{kd} - S_{ikr})$$

d : the step from ADC with $S_{kd} > S_{ikr}$
 $p_{d|r}$: conditional probability of step d from ADC, under the condition $S_{ikr} < S_{kd} < S_{ik(r+1)}$

Equation A -7

Network Result

$$\begin{aligned}
H_u &= \sum_i H_{u,ij} && \text{with } H_{u,ij} = \text{Max}_k(H_{u,ik}) \\
Q_u &= \sum_i Q_{u,ij} && \text{with } Q_{u,ij} = \text{Max}_k(Q_{u,ik}) \\
T_u &= \frac{Q_u}{H_u} && \text{with } T_{u,ij} = \text{Max}_k(T_{u,ik}) \\
S_u &= \sum_i S_{u,i} && \text{with } S_{u,i} = \sum_k S_{u,ik} \\
W_u &= \sum_i W_{u,i} && \text{with } W_{u,i} = \sum_k W_{u,ik}
\end{aligned}$$

Equation A -8**A.4 Probability Distributions of Reliability Indices***A4.1 General Description*

Probability distribution can be characterized with its probability density function (PDF) and cumulative distribution function (CDF).

- PDF is denoted as $f(x)$, which assigns a probability to each value of a random variable x . The probability in an infinitely small interval $[x_0, x_0 + dx]$ is $f(x_0)dx$, thus leading to:

$$f(x_0) = P(x_0 < x < x_0 + dx) / dx$$

- CDF is denoted as $F(x)$, which represents the probability of variable x that is smaller than or equal to each value, like e.g. x_0 , with the description:

$$F(x_0) = P(x \leq x_0)$$

The relationship between PDF and CDF can be described with the following equation:

$$\frac{d}{dx} F(x) = f(x) \quad \text{or} \quad F(b) - F(a) = \int_a^b f(x) dx = P(a \leq x \leq b)$$

The probability of occurrence for a difference between two variants of at least Δx in the expected value of a reliability index x can be calculated as follows [20],

$$\begin{aligned}
P(x_2 \geq x_1 + \Delta x) &= 1 - \int_0^{\infty} f_1(x) \cdot F_2(x + \Delta x) dx \\
F_2(x + \Delta x) &= \int_0^{x + \Delta x} f_2(x) dx
\end{aligned}$$

with $f_1(x)$ PDF of reliability index x for variant 1
 $F_2(x)$ CDF of reliability index x for variant 2

A4.1 Poisson Distribution for Frequency of Supply Interruptions

The discrete Poisson distribution gives the probability $f(x = k)$ for the occurrence of k events in the time interval (o, t) :

$$f(x = k) = \frac{\lambda^k e^{-\lambda}}{k!} \text{ with the unique parameter } \lambda = E(x).$$

The frequency of supply interruptions is described by this Poisson distribution [10]. The expected value $E(x)$ of the frequency is provided by ZUBER, with which the unique parameter of Poisson distribution λ can be determined.

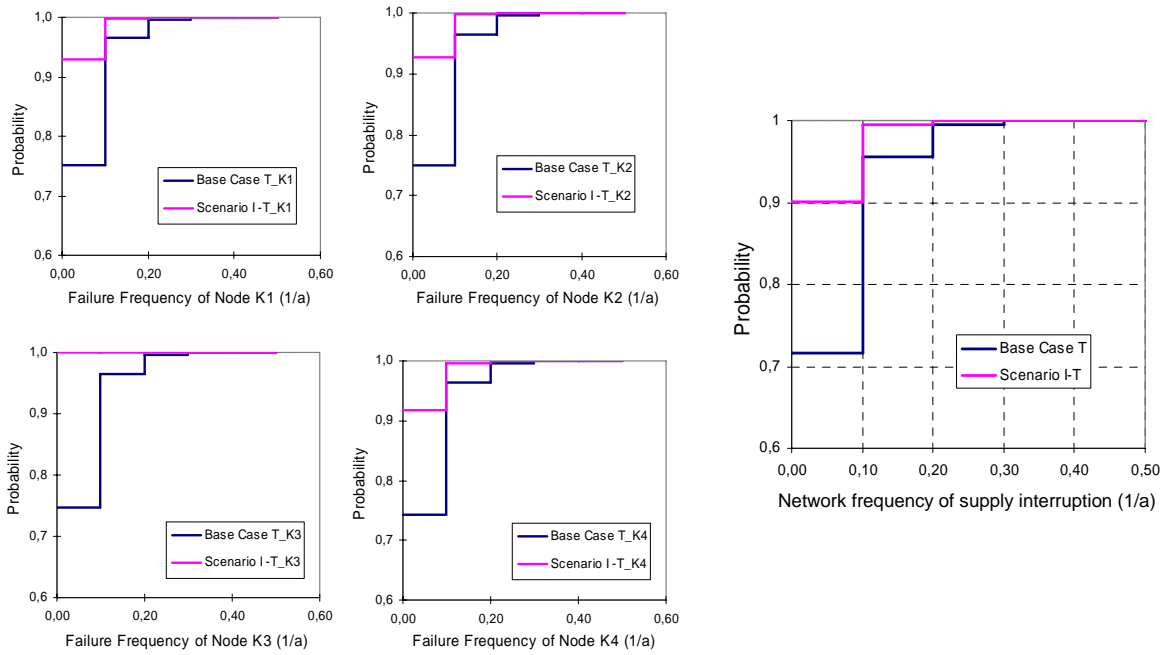


Figure A-2 Poisson Distribution of Frequency of Supply Interruption

A4.2 Weibull Distribution of Other Indices

The Weibull distribution is a continuous, nonnegative distribution with the random variable distributed over the interval $[0, \infty]$, and characterized by two parameters a and b . The PDF $f(x)$ and CDF $F(x)$ of Weibull distribution are given in Equation A -9:

$$f(x) = \frac{b}{a} \cdot \left(\frac{x}{a}\right)^{b-1} \cdot \exp\left[-\left(\frac{x}{a}\right)^b\right]$$

$$F(x) = 1 - \exp\left[-\left(\frac{x}{a}\right)^b\right]$$

Equation A -9

With the known $E(x)$ and $\sigma^2(x)$ from ZUBER, the parameters of Weibull distribution a and b can be estimated.

$$E(x) = a \cdot \Gamma\left(1 + \frac{1}{b}\right)$$

$$\sigma^2(x) = a^2 \cdot \left[\Gamma\left(1 + \frac{2}{b}\right) - \Gamma^2\left(1 + \frac{1}{b}\right) \right]$$

with the Gamma function : $\Gamma(x) = \int_0^\infty e^{-u} u^{x-1} du$

Equation A -10

For estimation of the two parameters, the following approximated approach can be realized using the programming of VBA based on Excel.

$$\begin{cases} E^2 = a^2 \cdot \Gamma^2\left(1 + \frac{1}{b}\right) \\ E^2 + \sigma^2 = a^2 \cdot \Gamma\left(1 + \frac{2}{b}\right) \end{cases} \Rightarrow \frac{\Gamma\left(1 + \frac{2}{b}\right)}{\Gamma^2\left(1 + \frac{1}{b}\right)} = 1 + \left(\frac{\sigma}{E}\right)^2 = 1 + \sigma_r^2$$

Equation A -11

The distributions of Q_u, P_u and W_u of two Base Cases with and without DG (*Base Case T and Scenario I - T*) are plotted in Figure A-3 to Figure A-5.

It should be noted that the real probability distribution of the reliability indices is a discrete distribution, as the events contribution to the reliability indices are discrete. However, in practical large network, the discrete steps of the distribution are so small that the distribution becomes quasi-continuous [9].

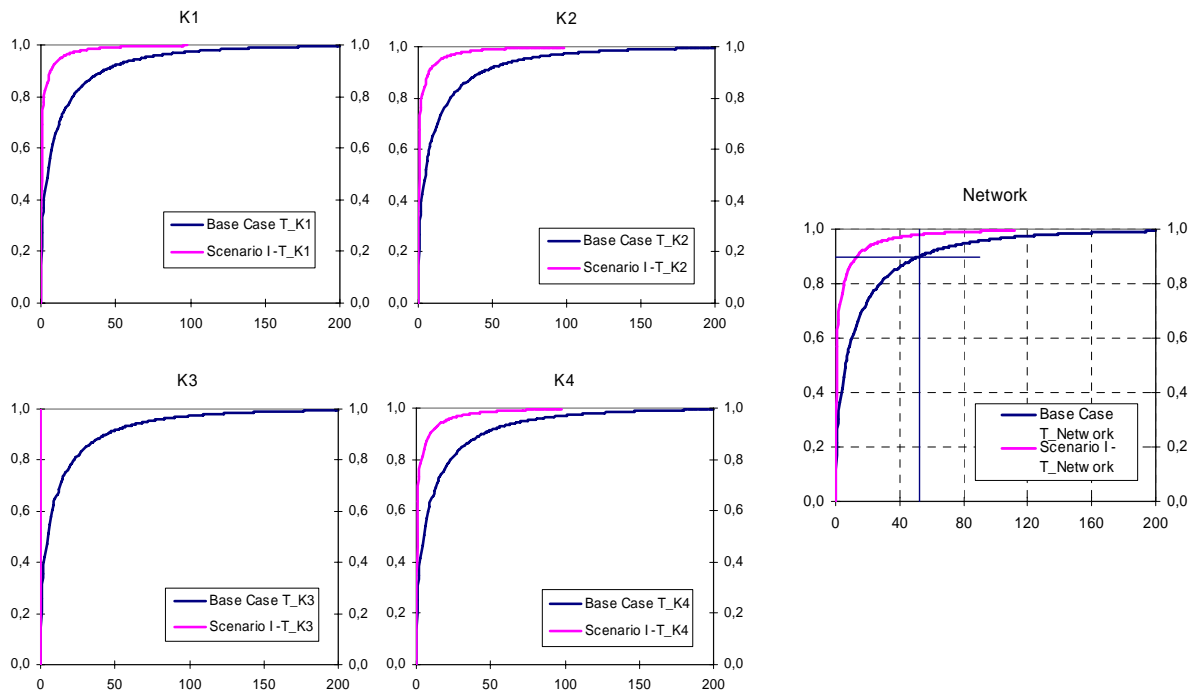


Figure A-3 Weibull Distribution of Unavailability (min/a)

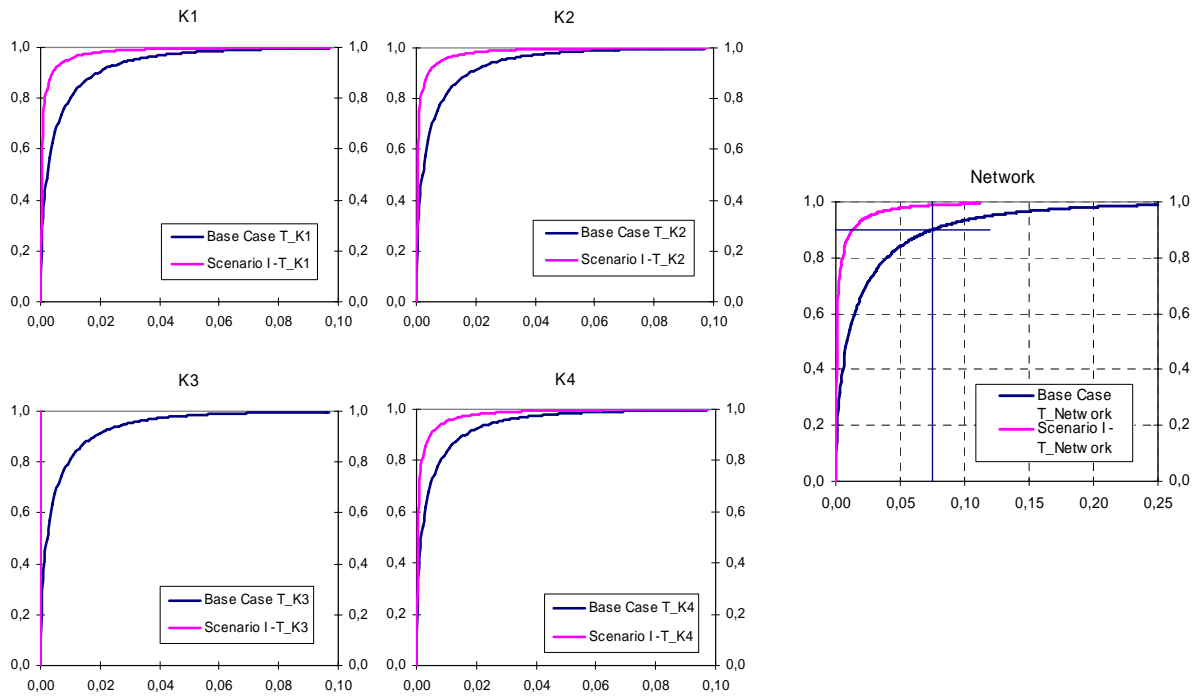


Figure A-4 Weibull Distribution of Interrupted Power (MVA/a)

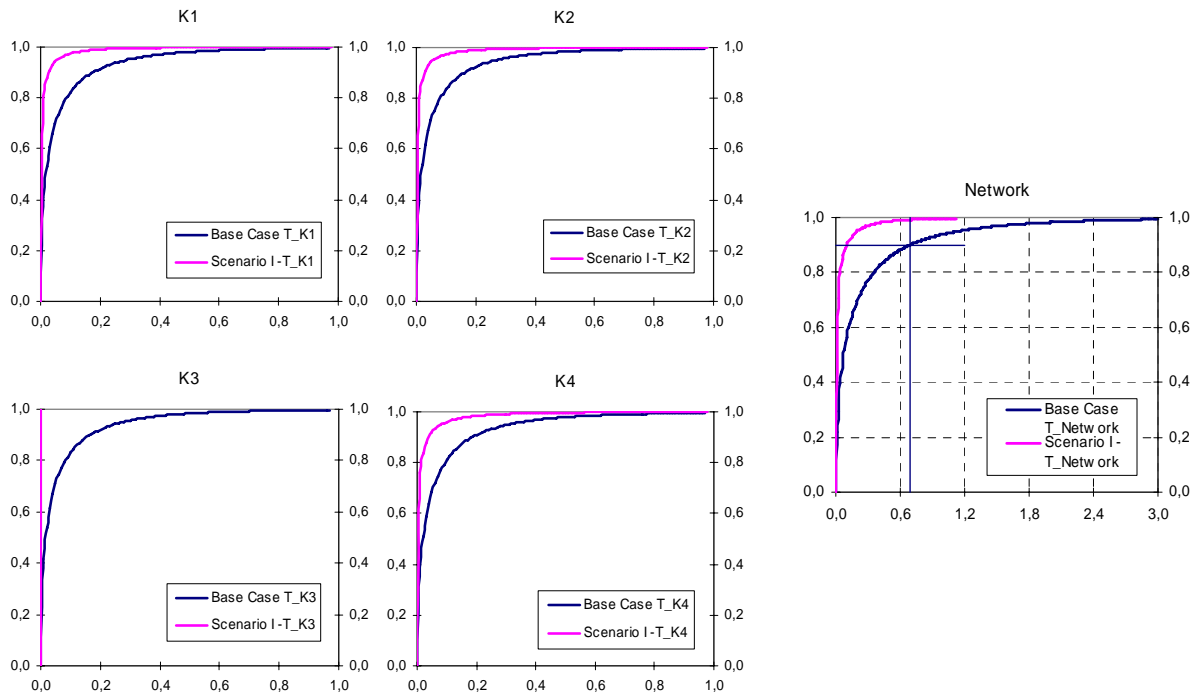


Figure A-5 Weibull Distribution of Energy Not Supplied (MVAh/a)

A.5 Capacity Factor and Availability Factor

Capacity Factor

The *Capacity Factor* CF is the ratio of the actual output power and fully operated capacity of a power plant over a considered period. It can be calculated as the quotient of actual total energy that the power plant produces and the energy it would have produced at full capacity.

Capacity factors vary strongly dependent on the type and design of the power plant.

- *A base load power plant* normally has a large capacity factor as it is designed for maximum efficiency and operated continuously at high output, which is in most economical operating. The general reason of not 100% capacity factor for such plants is out of service due to equipment failures or routine maintenance.
- *Peaking power plants* may operate only several hours up to days per year by curtailed output due to the uneconomical operation and hence have much lower capacity factors. Therefore, their electricity is relatively expensive compared to the price of base load plants produced electricity due to the relatively high equipment costs with respect to their efficiency.
- *Load following power plants* are in between these two extremes in terms of capacity factor, efficiency and cost. They keep high efficiency during the day, when prices and demand are highest, and shut down or reduce the output during nights.
- *DER units, focused on RES*, probably have very low capacity factors. Although the plants may be capable of producing electricity (high *Availability Factor*), their primary sources such as wind, sunlight or water may not be available.

Availability Factor

The *Availability Factor* (AF) is the ratio of the amount of the time that it is capable of producing electricity over a certain period and the amount of the time in that period.

The availability factor varies strongly dependent on the type of fuel, the design and operating characteristic of the plant. Generally, less maintenance of the power plant means higher availability factor.

The availability factor of RES power plants such as solar and wind power plants is depending on whether periods when the plant is operational, but there is no sunlight or wind, are considered as available, unavailable or disregarded. If these times are counted as available, the availability factor of PV is almost equal to 100% while WT is also about 98%. However, if these times are considered as not available, the availability factor could be much lower.

A.6 Probability Distribution of Power Balance Provided by DG

A6.1 Power Balance of Different Loads and Generation Units

The intermittent output of renewable generation units only contributes to reliability in intervals when the generated power is higher than the load. The local time dependent power balance is the sum of all loads and simultaneous generation:

$$P_{Balance} = \sum_{i=1}^n P_i(t) \tag{Equation A -12}$$

with n – number of generation units

$P_i(t)$ – power output of unit j at time t , resp. power demand (with sign)

A6.2 Theory of Probability Distributions

In a first approximation, load and generation can be considered to be normally distributed as demonstrated in Figure A-6 for different load and generation profiles.

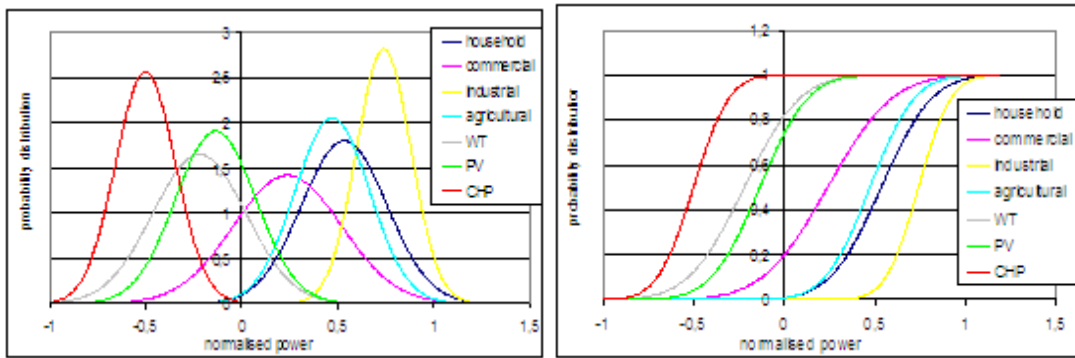


Figure A-6 Probability Distributions of Normalized Generation and Load

The sum of distributions of independent probability values equals the convolution of their density functions ([21][22]):

$$\begin{aligned} f_Z(z) &= \int_{x=-\infty}^{\infty} f_X(x) \cdot f_Y(z-x) dx \\ &= f_X(x) * f_Y(y) \end{aligned} \tag{Equation A -13}$$

with

$$Z = X + Y \tag{Equation A -14}$$

This leads to the probability function:

$$\begin{aligned} F_Z(K) &= W(Z < K) \\ &= \int_{z=-\infty}^K \left[\int_{x=-\infty}^{\infty} [f_X(x) \cdot f_Y(z-x)] dx \right] dz \\ &= \int_{z=-\infty}^K [f_X(x) * f_Y(y)] dz. \end{aligned} \tag{Equation A -15}$$

For the sum of n independent probability values there is:

$$W((Z = X_1 + X_2 + \dots + X_n) < K) = \int_{z=-\infty}^K [f_{X_1}(x_1) * f_{X_2}(x_2) * \dots * f_{X_n}(x_n)] dz \quad \text{Equation A -16}$$

A convolution is only possible with probability functions. If there are exact values such as fixed operation point of a non- renewable unit or a demand known as constant, these values have to be considered as a distribution as well that equals a step-function at the expected value Figure A-7.

$$F_{\mu}(P) = W(\mu < P) = \begin{cases} 0 & \text{for } P < \mu \\ 1 & \text{for } P > \mu \end{cases} \quad \text{Equation A -17}$$

Their density is defined by a dirac impulse at the expected value.

$$f_{\mu}(P) = \frac{dF_{\mu}(P)}{dP} = \delta(\mu = P) \quad \text{Equation A -18}$$

With

$$\delta(\mu = P) = \begin{cases} 0 & \text{for } P < \mu \\ \infty & \text{for } P = \mu \\ 0 & \text{for } P > \mu \end{cases} \quad \text{Equation A -19}$$

and

$$\int_{P=-\infty}^{\infty} \delta(\mu = P) dP = 1 \quad \text{Equation A -20}$$

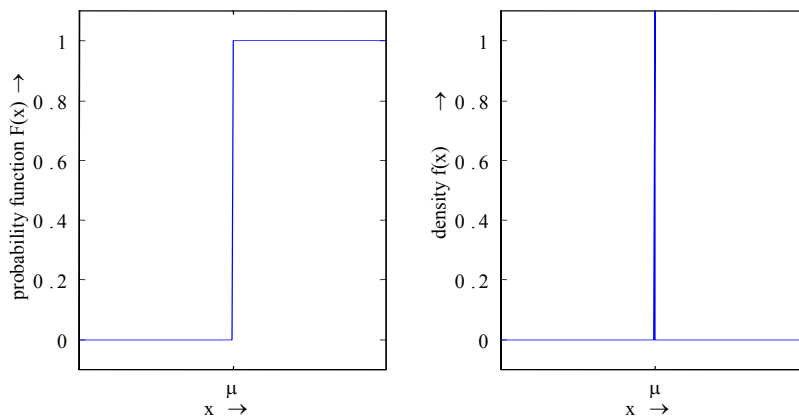


Figure A-7 Distribution of Step Function

In a first approximation renewable generation, heat driven CHP generation as well as load can be assumed to be normally distributed with density function

$$f(x) = \frac{1}{\sqrt{2\pi\sigma^2}} \cdot e^{-\frac{(x-\mu)^2}{2\sigma^2}} \quad \text{Equation A -21}$$

A6.3 Probability Distributions with Power Limits

Equation A -22 is defined from $-\infty$ to $+\infty$ with values ≥ 0 . However, power output can be only in range $[P_{min}; P_{max}]$ due to known constraints. This means that the density function is always zero outside the limits for power output with steps in the probability distribution function for these values (Figure A-8). The probability that power is outside $[P_{min}; P_{max}]$ cumulates on these limits:

$$f(P) = \begin{cases} 0 & \text{for } P < P_{min} \\ K_1 \cdot \delta(P = P_{min}) & \text{for } P = P_{min} \\ \frac{1}{\sqrt{2\pi\sigma^2}} \cdot e^{-\frac{(P-\mu)^2}{2\sigma^2}} & \text{for } P_{min} < P < P_{max} \\ K_2 \cdot \delta(P = P_{max}) & \text{for } P = P_{max} \\ 0 & \text{for } P > P_{max} \end{cases} \quad \text{Equation A -22}$$

With the corresponding probability function

$$F(X < P) = \int_{P'=-\infty}^P f(P') dP' \quad \text{Equation A -23}$$

Within $P_{min} < P < P_{max}$ the probability function has the shape of the normal distribution. On both limits there is a step from 0 to the value of the normal distribution respectively from this value to 1. For the lower limit there is

$$\begin{aligned} F(X \leq P_{min}) &= \int_{P'=-\infty}^{P_{min}} \left[\frac{1}{\sqrt{2\pi\sigma^2}} \cdot e^{-\frac{(P'-\mu)^2}{2\sigma^2}} \right] dP' \\ &= \int_{P'=-\infty}^{P_{min}} [K_1 \cdot \delta(P' = P_{min})] dP' \end{aligned} \quad \text{Equation A -24}$$

As

$$\int_{P'=-\infty}^{P_{min}} \delta(P = P_{min}) dP' = 1 \quad \text{Equation A -25}$$

And

$$f(P) = 0 \text{ for } P < P_{min} \quad \text{Equation A -26}$$

K_1 and K_2 are calculated as

$$K_1 = \int_{P'=-\infty}^{P_{min}} \left[\frac{1}{\sqrt{2\pi\sigma^2}} \cdot e^{-\frac{(P'-\mu)^2}{2\sigma^2}} \right] dP' \quad \text{Equation A -27}$$

$$\begin{aligned} K_2 &= \int_{P'=P_{max}}^{\infty} \left[\frac{1}{\sqrt{2\pi\sigma^2}} \cdot e^{-\frac{(P'-\mu)^2}{2\sigma^2}} \right] dP' \\ &= 1 - \int_{P'=-\infty}^{P_{max}} \left[\frac{1}{\sqrt{2\pi\sigma^2}} \cdot e^{-\frac{(P'-\mu)^2}{2\sigma^2}} \right] dP' \end{aligned} \quad \text{Equation A -28}$$

The probability density of the truncated normal distribution is therefore:

$$\begin{aligned}
 f(P) = & \frac{e^{-\frac{(P-\mu)^2}{2\sigma^2}}}{\sqrt{2\pi\sigma^2}} \cdot H(P - P_{\min}) \cdot H(P_{\max} - P) \\
 & + \int_{P'=-\infty}^{P_{\min}} \left[\frac{e^{-\frac{(P'-\mu)^2}{2\sigma^2}}}{\sqrt{2\pi\sigma^2}} \right] dP' \cdot \delta(P = P_{\min}) \\
 & + \int_{P'=P_{\max}}^{\infty} \left[\frac{e^{-\frac{(P'-\mu)^2}{2\sigma^2}}}{\sqrt{2\pi\sigma^2}} \right] dP' \cdot \delta(P = P_{\max})
 \end{aligned}
 \tag{Equation A -29}$$

With

$$H(x) = \begin{cases} 0 & \text{for } x < 0 \\ 1 & \text{for } x > 0 \end{cases} \quad (\text{Heaviside-function, step function}) \tag{Equation A -30}$$

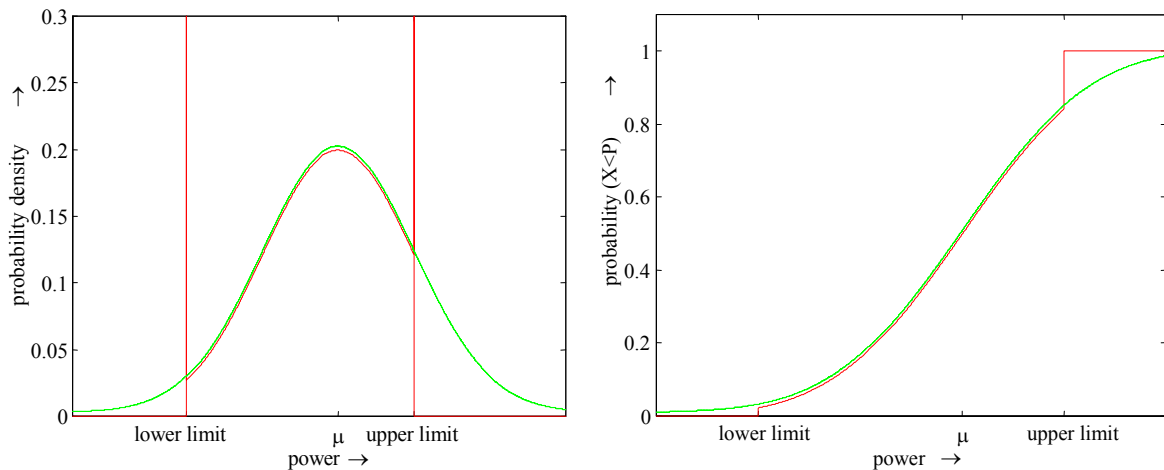


Figure A-8 Probability Density and Probability Function with Given Power Limits

There are three possibilities to handle these truncated distributions:

- calculate with normal distribution nevertheless
- calculate with adapted normal distribution
- calculate with adapted distribution

A6.4 Calculation with Normal Distribution

If the expected values are far from the limits of the units/demand ($>2\sigma$) the truncated part of the normal distribution can be neglected. Everything can be calculated as if the units would have no limits.

The convolution of two independent normal distributions is a new normal distribution with $\mu_z = \mu_x + \mu_y$ and $\sigma_z = \sqrt{\sigma_x^2 + \sigma_y^2}$ ([24]). Average power that is available on each node is:

$$P_{ges}(t) = \sum_{i=1}^n P_i(t)$$

$$\sigma_{ges}(t) = \sqrt{\sum_{i=1}^n \sigma_i^2(t)}$$

Equation A -31

The probability W that the power balance is positive (no missing power to supply the loads) is:

$$W(P_{Balance}(t) > 0) = 1 - \int_{P'=-\infty}^0 \left[\frac{1}{\sqrt{2\pi\sigma_{ges}^2(t)}} \cdot e^{-\frac{(P'-P_{ges}(t))^2}{2\sigma_{ges}^2(t)}} \right] dP'$$

Equation A -32

There is a non acceptable error in this method if the expected value of the power is close to any limit.

In case there is a correlation between the normal distributions expected value and standard deviation have to be calculated as a bivariate normal distribution (x1: load; x2: DER):

$$P(x_1, x_2) = \frac{1}{2\pi\sigma_1\sigma_2\sqrt{1-\rho^2}} \exp\left[-\frac{z}{2(1-\rho^2)}\right]$$

where $z \equiv \frac{(x_1 - \mu_1)^2}{\sigma_1^2} - \frac{2\rho(x_1 - \mu_1)(x_2 - \mu_2)}{\sigma_1\sigma_2} + \frac{(x_2 - \mu_2)^2}{\sigma_2^2}$

With

$$\sigma^2 = \frac{\sum (x - \bar{x})^2}{n-1} \Rightarrow \sigma^2 \cdot (n-1) = \sum (x - \bar{x})^2 = \sum x^2 - n \cdot \bar{x}^2$$

$$\text{and } \bar{x} = \frac{\sum x}{n} \quad \bar{x} = a \cdot \bar{x}_1 - b \cdot \bar{x}_2 \quad (x_1 : \text{load demand}; x_2 : \text{DER output})$$

$$\begin{aligned} \therefore \sigma'^2 \cdot (n-1) &= \sum (a \cdot x_1 - b \cdot x_2)^2 - n \cdot (a \cdot \bar{x}_1 - b \cdot \bar{x}_2)^2 \\ &= a^2 \cdot \sum x_1^2 + b^2 \cdot \sum x_2^2 - 2ab \cdot \sum (x_1 \cdot x_2) - n \cdot (a \cdot \bar{x}_1 - b \cdot \bar{x}_2)^2 \\ &= a^2 \cdot [\sigma_1^2 \cdot (n-1) + n \cdot \bar{x}_1^2] + b^2 \cdot [\sigma_2^2 \cdot (n-1) + n \cdot \bar{x}_2^2] - n \cdot a^2 \cdot \bar{x}_1^2 \\ &\quad - n \cdot b^2 \cdot \bar{x}_2^2 - 2ab \cdot [\sum (x_1 \cdot x_2) - n \cdot \bar{x}_1 \cdot \bar{x}_2] \end{aligned}$$

$$\therefore \sigma'^2 = a^2 \cdot \sigma_1^2 + b^2 \cdot \sigma_2^2 - 2ab \cdot \sigma_1 \sigma_2 \rho$$

ρ : correlation coefficient between two random var iate x_1 and x_2

$$\text{with } \rho = \frac{E((x_1 - \bar{x}_1) \cdot (x_2 - \bar{x}_2))}{\sigma_1 \cdot \sigma_2}$$

Equation A -33

A 6.5 Calculation with Adapted Normal Distribution

Cutting of a part of a normal distribution leads to a new distribution. In a first approximation this new function can again be considered to be normally distributed with a new expected value and a new standard deviation. These new parameters are calculated corresponding to the laws to determine the moments of distribution functions according to Equation A -34 to Equation A -40.

$$\mu' = \int_{x=-\infty}^{+\infty} [x \cdot f(x)] dx \quad \text{Equation A -34}$$

And

$$\sigma' = \sqrt{\int_{x=-\infty}^{+\infty} [(x - \mu')^2 \cdot f(x)] dx} \quad \text{Equation A -35}$$

For discrete density functions there is

$$\mu' = \sum_{x=-\infty}^{+\infty} [x \cdot f(x)] \Delta x \quad \text{Equation A -36}$$

and

$$\sigma' = \sqrt{\sum_{x=-\infty}^{+\infty} [(x - \mu')^2 \cdot f(x)] \Delta x} \quad \text{Equation A -37}$$

As the density function is 0 outside the limits of each unit the summation can be limited to the domain within the limits with

$$\mu' = \sum_{P=\text{Lower power limit}}^{\text{Upper power limit}} [P \cdot f(P)] \Delta P \quad \text{Equation A -38}$$

and

$$\sigma' = \sqrt{\sum_{P=\text{lower power limit}}^{\text{upper power limit}} [(P - \mu')^2 \cdot f(P)] \Delta P} \quad \text{Equation A -39}$$

The parameter of the distribution function of the power balance now can be determined as

$$P_{ges}(t) = \sum_{i=1}^n \mu'_{P_i}(t) \quad \text{Equation A -40}$$

$$\sigma_{ges}(t) = \sqrt{\sum_{i=1}^n \sigma_{P_i}^2(t)}$$

Although there may be quite a deviation of this adapted normal distribution from the original distribution (Figure A-9) trials have shown a good approximation to the distribution that resulted from the convolution (Figure A-12).

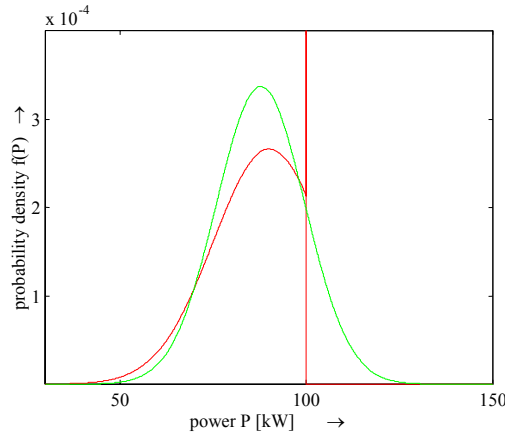


Figure A-9 Comparison of Truncated and Adapted Normal Distribution

A6.6 Calculation the Power Balance by Convolution of Probability Functions

There will always be a small error if a truncated normal distribution is approximated by another normal distribution.

In case it is necessary to calculate with the real functions it is not further possible to simply add expected values as in Equation A -20 for normal distribution. Calculating the real convolution means

$$f(z) = \int_{P_1=-\infty}^{\infty} \left[\begin{aligned} & \frac{e^{-\frac{(P_1-\mu_1)^2}{2\sigma_1^2}}}{\sqrt{2\pi\sigma_1^2}} \cdot H(P_1 - P_{\min_1}) \cdot H(P_{\max_1} - P_1) \\ & + \int_{P_1'=-\infty}^{P_{\min_1}} \frac{e^{-\frac{(P_1'-\mu_1)^2}{2\sigma_1^2}}}{\sqrt{2\pi\sigma_1^2}} dP_1' \cdot \delta(P_1 = P_{\min_1}) \\ & + \int_{P_1'=P_{\max_1}}^{\infty} \frac{e^{-\frac{(P_1'-\mu_1)^2}{2\sigma_1^2}}}{\sqrt{2\pi\sigma_1^2}} dP_1' \cdot \delta(P_1 = P_{\max_1}) \end{aligned} \right] \cdot \left[\begin{aligned} & \frac{e^{-\frac{((z-P_1)-\mu_2)^2}{2\sigma_2^2}}}{\sqrt{2\pi\sigma_2^2}} \cdot H((z - P_1) - P_{\min_2}) \cdot H(P_{\max_2} - (z - P_1)) \\ & + \int_{P_2'=-\infty}^{P_{\min_2}} \frac{e^{-\frac{(P_2'-\mu_2)^2}{2\sigma_2^2}}}{\sqrt{2\pi\sigma_2^2}} dP_2' \cdot \delta((z - P_1) = P_{\min_2}) \\ & + \int_{P_2'=P_{\max_2}}^{\infty} \frac{e^{-\frac{(P_2'-\mu_2)^2}{2\sigma_2^2}}}{\sqrt{2\pi\sigma_2^2}} dP_2' \cdot \delta((z - P_1) = P_{\max_2}) \end{aligned} \right] dP_1 \quad \text{Equation A -41}$$

It is not possible to solve this analytically as is shown in the following. A replacement of all terms independent from z by constants simplifies the equation to

$$f(z) = \int_{P_1'=-\infty}^{\infty} \left\{ \begin{aligned} & \left[\frac{e^{-\frac{(P_1'-\mu_1)^2}{2\sigma_1^2}}}{\sqrt{2\pi\sigma_1^2}} \cdot H(P_1'-P_{\min_1}) \cdot H(P_{\max_1} - P_1') \right. \\ & \quad + K_{\min_1} \cdot \delta(P_1' = P_{\min_1}) \\ & \quad \left. + K_{\max_1} \cdot \delta(P_1' = P_{\max_1}) \right] \\ & \cdot \left[\frac{e^{-\frac{((z-P_1')-\mu_2)^2}{2\sigma_2^2}}}{\sqrt{2\pi\sigma_2^2}} \cdot H((z-P_1')-P_{\min_2}) \cdot H(P_{\max_2} - (z-P_1')) \right. \\ & \quad + K_{\min_2} \cdot \delta((z-P_1') = P_{\min_2}) \\ & \quad \left. + K_{\max_2} \cdot \delta((z-P_1') = P_{\max_2}) \right] \end{aligned} \right\} dP_1 \quad \text{Equation A -42}$$

being multiplied

$$f(z) = \int_{P_1'=-\infty}^{\infty} \left\{ \begin{aligned} & \frac{e^{-\frac{(P_1'-\mu_1)^2}{2\sigma_1^2}} \cdot e^{-\frac{((z-P_1')-\mu_2)^2}{2\sigma_2^2}}}{2\pi\sigma_1\sigma_2} \\ & \cdot H(P_1'-P_{\min_1}) \cdot H(P_{\max_1} - P_1') \\ & \cdot H((z-P_1')-P_{\min_2}) \cdot H(P_{\max_2} - (z-P_1')) \\ & + \text{terms with dirac impulses} \end{aligned} \right\} dP_1 \quad \text{Equation A -43}$$

Solving this equation requires the calculation to the integral

$$y = \int e^{ax^2+bx+c} dx \quad \text{Equation A -44}$$

what is not possible analytically. Other solutions have to be found such as transformations of power series expansions that are not easily applicable.

The only solution is the perform the convolution numerically with the integral

$$f_z(z) = \int_{x=-\infty}^{\infty} [f_x(x) \cdot f_y(z-x)] dx \quad \text{Equation A -45}$$

being approximated by the sum

$$f_z(z) = \sum_{x=-\infty}^{\infty} [f_x(x) \cdot f_y(z-x)] \Delta x \tag{Equation A -46}$$

The range can be limited according the requirements on accuracy. Empirical investigations have shown that the error is lower than 1 % for

$$f_z(z) = \sum_{x=\min(\mu_x-3\sigma_x, \mu_y-3\sigma_y)}^{\max(\mu_x+3\sigma_x, \mu_y+3\sigma_y)} [f_x(x) \cdot f_y(z-x)] \cdot \left[\frac{|\max(\mu_x + 3\sigma_x, \mu_y + 3\sigma_y) - \min(\mu_x - 3\sigma_x, \mu_y - 3\sigma_y)|}{1000} \right] \tag{Equation A -47}$$

$$\text{for } \min(\mu_x, \mu_y) < z < \max(\mu_x, \mu_y)$$

A6.7 Comparison of the Variants

A comparison has to consider calculation time and accuracy. The calculation time raises some decades (depending on accuracy) applying the convolution. Judging the accuracy is not generally possible. As all methods are approximations the accuracy depends on the error due to simplification. Tests with a simple system with truncated WT and PV generation, one load and diesel engine and battery with fixed operating point have shown preferences for the adapted normal distribution as shown in an example in Figure A-10 to Figure A-12.

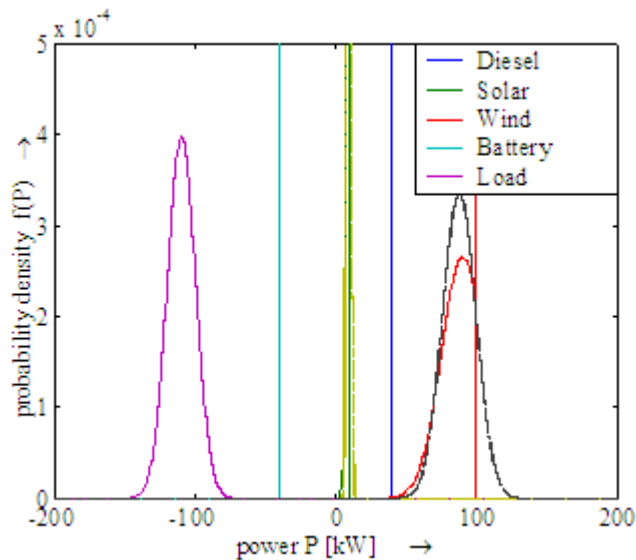


Figure A-10 Example for Limited Power Distribution

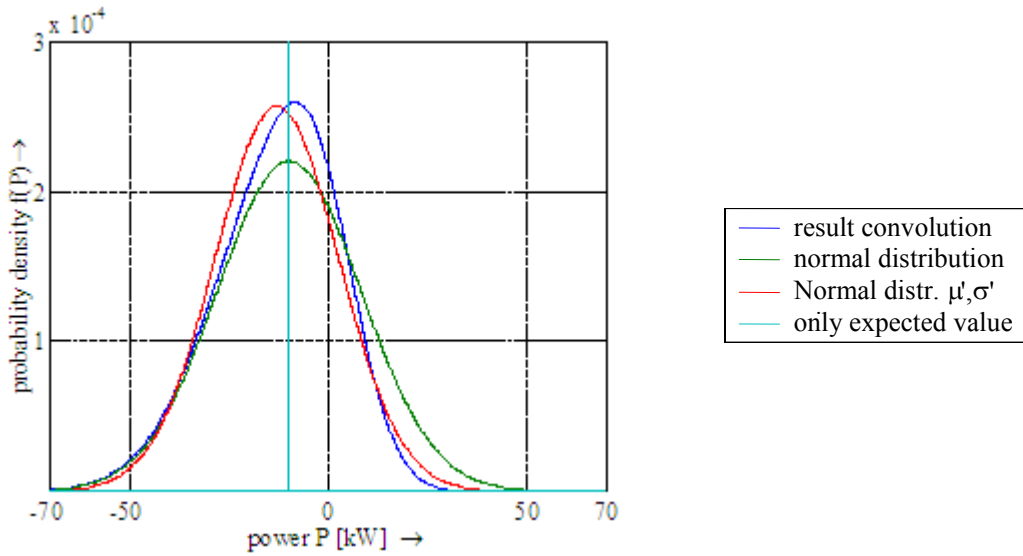


Figure A-11 Comparison of Probability Density Functions

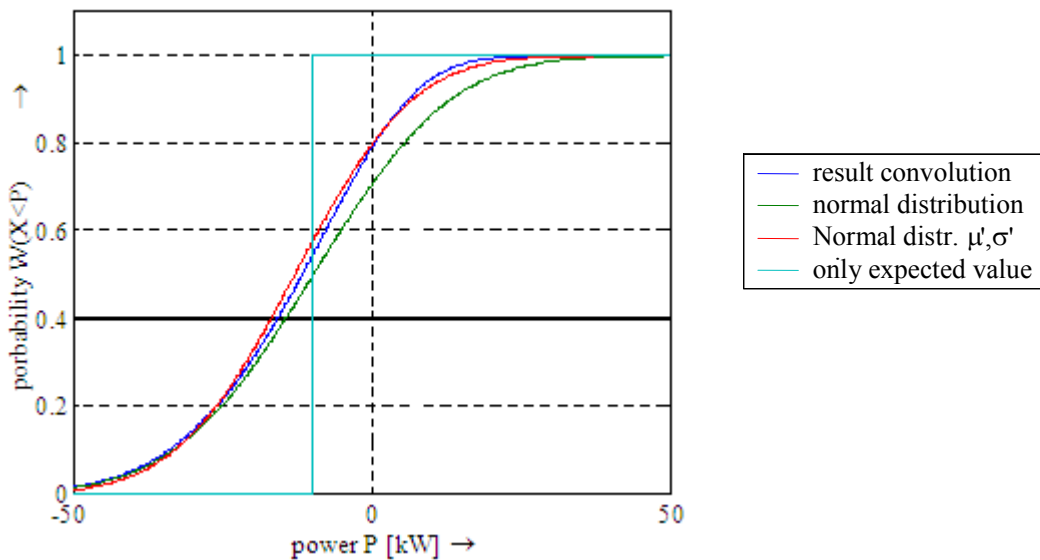


Figure A-12 Comparison of Probability Functions

Although there are some deviations between the methods, the adapted normal distribution gives nearly equal results as the convolution concerning an equal power balance.

A6.8 Application for Calculation of Fully Supplied Hours

Figure A-13 and Figure A-14 show a comparison of the real shape of generation and different load segments with their normal distribution.

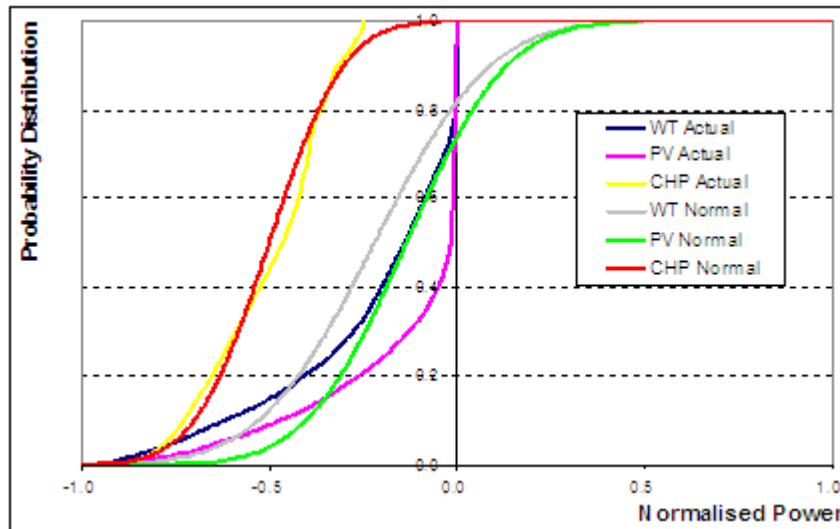


Figure A-13 Comparison of Probability Functions of Generation

A comparison of the distribution of actual shapes with the calculated ones showed similar values for both methods only for CHP generation as well as household, industrial and agricultural load segments.

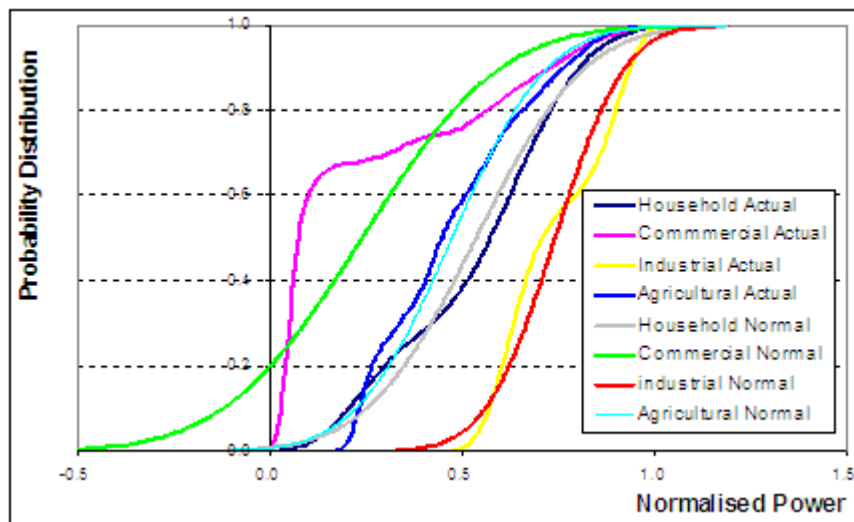


Figure A-14 Comparison of Probability Functions of Load

High deviations occur for commercial load as well as the PV and WT generation. Generation units can only have negative values, while loads demand only positive power what is not considered in the normal distribution with expected values close to limits.

However, the approximated normal distributions are within limits for CHP generation, household, agriculture and industrial load.

Limits	House	Commercial	Industry	Agriculture	WT	PV	CHP
Min.	0.001991	0	0.400024	0.139035	0	1.23E-06	0.249709
Max.	0.999641	0.996818	0.999612	0.997455	0.998475	0.992946	0.999981

Table A-4 Power Limits of Load and DER Generation Profiles

For the truncated distributions of commercial load, WT and PV generation adapted normal distributions have to be taken as presented in Figure A-15, Figure A-16 and Figure A-17 respectively.

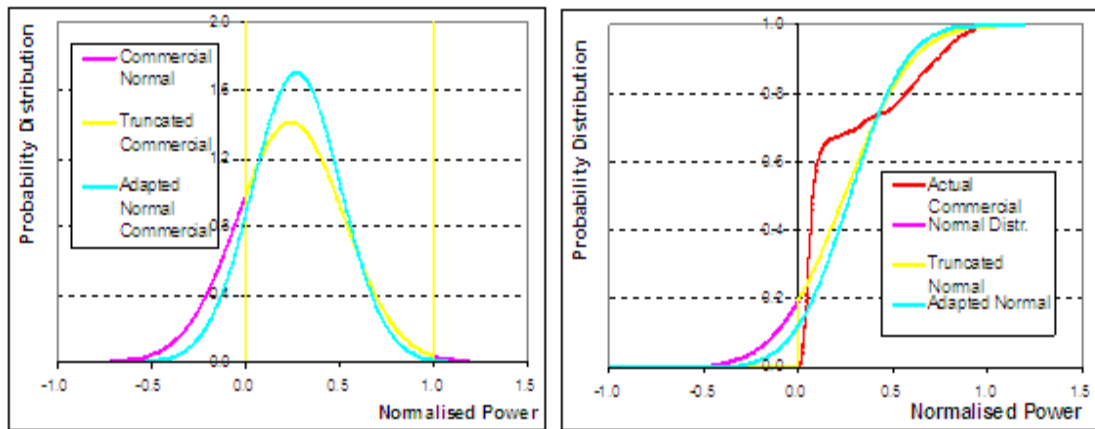


Figure A-15 Truncated and Adapted Normal Distribution for Commercial Load

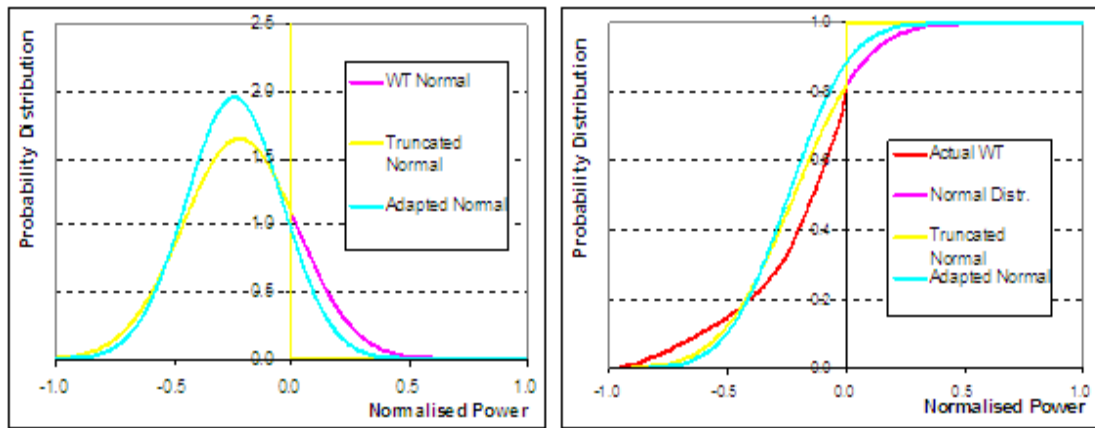


Figure A-16 Truncated and Adapted Normal Distribution for WT Generation

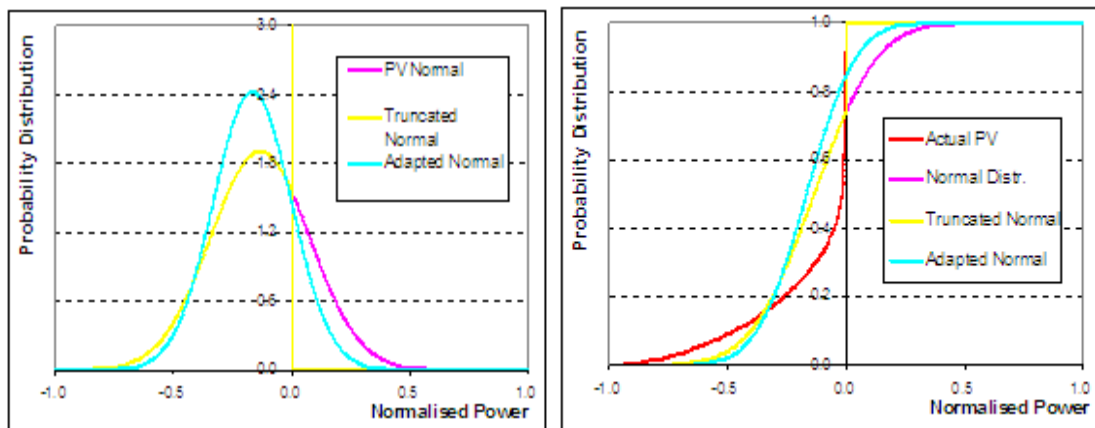


Figure A-17 Truncated and Adapted Normal Distribution for PV Generation

The method works in general, although commercial load is not normally distributed at all.

Synergy of Household Load and Generation (100% PL)

Considering Equation A -12, the actual distributions of power balance can be determined by calculating the difference between instantaneous demand and generation. The approximated normal distribution and adapted normal distribution are realized from the aforementioned theory and then compared with the actual distributions.

WT & Household	Calculated from Normal Distr.	Calculated from Adapted Normal Distr.	Calculated from Actual Difference
	$\mu_Z = \mu_X + \mu_Y$ $\sigma_Z = \sqrt{\sigma_X^2 + \sigma_Y^2}$	$\mu'_Z = \mu'_X + \mu'_Y$ $\sigma'_Z = \sqrt{\sigma'^2_X + \sigma'^2_Y}$	$\mu_{Z0} = E(\rho_L - \rho_G)$ $\sigma_{Z0} = \sigma(\rho_L - \rho_G)$
μ	0,315136	0,291964	0,315136
σ	0,32853	0,30168	0,331393

Table A-5 Distribution Parameters from Different Methods (WT Option)

PV & Household	Calculated from Normal Distr.	Calculated from Adapted Normal Distr.	Calculated from Actual Difference
	$\mu_Z = \mu_X + \mu_Y$ $\sigma_Z = \sqrt{\sigma_X^2 + \sigma_Y^2}$	$\mu'_Z = \mu'_X + \mu'_Y$ $\sigma'_Z = \sqrt{\sigma'^2_X + \sigma'^2_Y}$	$\mu_{Z0} = E(\rho_L - \rho_G)$ $\sigma_{Z0} = \sigma(\rho_L - \rho_G)$
μ	0,400241	0,367497	0,400241
σ	0,305272	0,276168	0,247298

Table A-6 Distribution Parameters from Different Methods (PV Option)

CHP & Household	Calculated from Normal Distr.	Calculated from Actual Difference
	$\mu_Z = \mu_X + \mu_Y$ $\sigma_Z = \sqrt{\sigma_X^2 + \sigma_Y^2}$	$\mu_{Z0} = E(\rho_L - \rho_G)$ $\sigma_{Z0} = \sigma(\rho_L - \rho_G)$
μ	0,034526	0,034526
σ	0,271211	0,271729

Table A-7 Distribution Parameters from Different Methods (CHP Option)

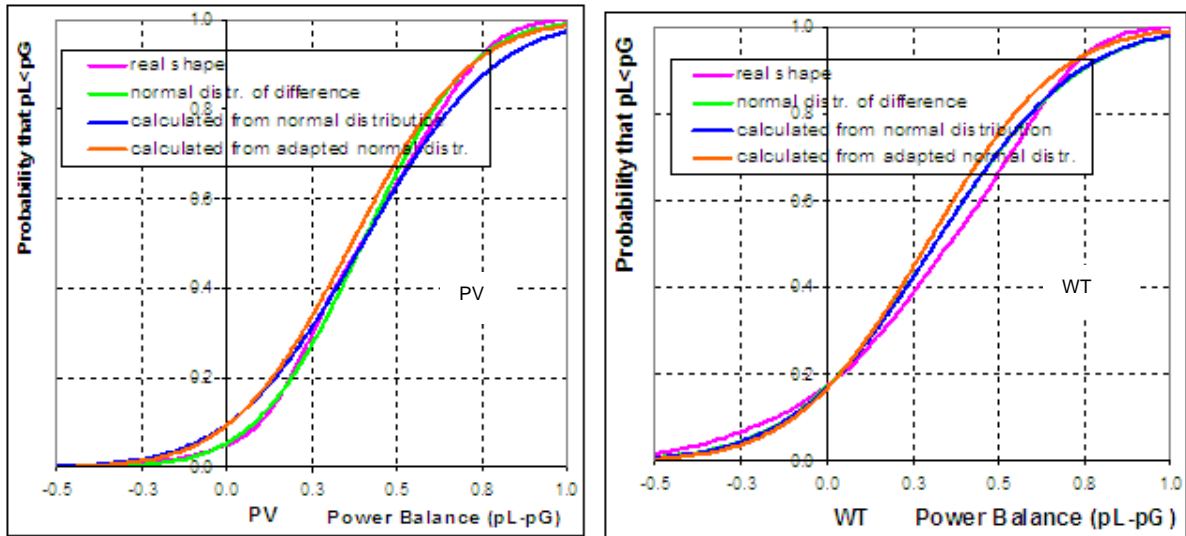


Figure A-18 Distributions of Power Balance between PV/WT and Household

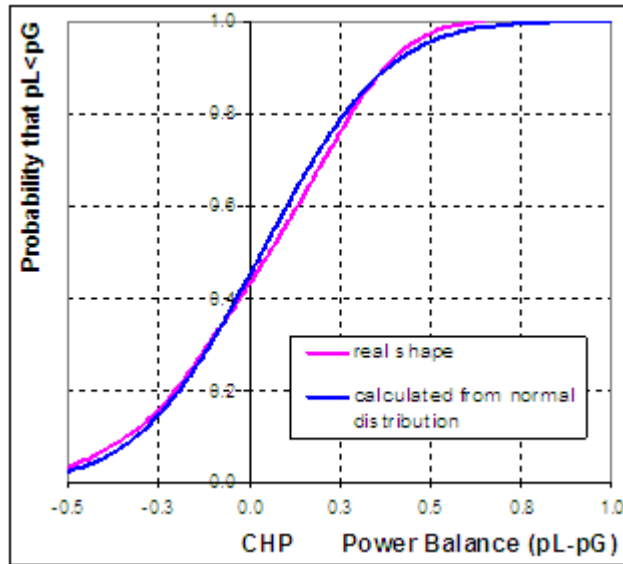


Figure A-19 Distributions of Power Balance between CHP and Household

The probability of fully supplied hours is indicated in figures,

$$P_{\text{fully supplied hours}} = f(p_L - p_G = 0)$$

which proves that the manually calculated results are correct.

PV generation exceeds load with a probability of 9.49% (9.16% for adapted distribution), while only 5.28 % probability which is determined from real distribution. From these values also the full load hours can be calculated. Values for WT vary from all methods between 16.59 % and 17.02 %, and for CHP it is 44.83 %.

Interestingly there is almost no difference between the real shape of the difference and a normal distribution while the PL of DER is 100%.

A.7 Gram-Charlier expansion

This explanation is based on [54].

Definition of moment

Assume a positive integer n and the function X^n is integrable with respect to $F(x)$ over $(-\infty, \infty)$, the integral

$$\mu_n = E(x^n) = \int_{-\infty}^{+\infty} x^n dF(x) \tag{Equation A -48}$$

is called the n th moment about 0.

Definition of cumulant

The cumulants c_n is defined by the cumulant-generating function which is the $g(t)$.

$$g(t) = \log(E(e^{tX})) = \sum_{n=1}^{\infty} c_n \frac{t^n}{n!} = c_1 t + c_2 \frac{t^2}{2} + \dots \tag{Equation A -49}$$

Relationship between cumulant and moment

The relationship between cumulant and moment are expressed by

$$\begin{aligned} c_1 &= \mu_1, c_2 = \mu_2 - \mu_1^2, c_3 = \mu_3 - 3\mu_1\mu_2 + 2\mu_1^3. \\ c_4 &= \mu_4 - 4\mu_1\mu_3 - 3\mu_2^2 + 12\mu_1^2\mu_2 - 6\mu_1^4 \\ &\dots \end{aligned} \tag{Equation A -50}$$

It can be seen from this relationship and moment definition,

$$c_1 = m, c_2 = \sigma^2 \tag{Equation A -51}$$

Where m is the mean value of variable X , σ is the standard deviation of variable X .

Cumulant has a very good property. For two independent variables X, Y

$$g_{X+Y}(t) = \log(E(e^{tX})) = \log(E(e^{tX}) * E(e^{tY})) = \log(E(e^{tX})) + \log(E(e^{tY})) = g_X(t) + g_Y(t)$$

Equation A -52

That means the summation of two **independent** variables can be done by the summation of their cumulants, which avoid the time consuming convolution process. This dramatically reduces the computation time.

Gram-Charlier expansion

Assume that a random variable Y has the density function f and the cumulants $C_k (k \geq 1)$, all of which are finite and known, then, f is expanded as follows:

$$f(x) = \sum_{n=0}^{\infty} \frac{q_n}{\sqrt{c_2}} H_n\left(\frac{x-c_1}{\sqrt{c_2}}\right) \phi\left(\frac{x-c_1}{\sqrt{c_2}}\right) \tag{Equation A -53}$$

Where $\phi\left(\frac{x-c_1}{\sqrt{c_2}}\right)$ is the standard normal distribution, c_2 is the standard deviation of Y,

$H_n\left(\frac{x-c_1}{\sqrt{c_2}}\right)$ is the Chebyshev-hermite polynomial. The first 7 orders Chebyshev-hermite polynomial are

$$\begin{aligned} H_0(x) &= 1, H_1(x) = x, H_2(x) = x^2 - 1, H_3(x) = x^3 - 3x \\ H_4(x) &= x^4 - 6x^2 + 3, H_5(x) = x^5 - 10x^3 + 15x, \\ H_6(x) &= x^6 - 15x^4 + 45x^2 - 15, H_7(x) = x^7 - 21x^5 + 105x^3 - 105x \end{aligned} \tag{Equation A -54}$$

q_n is expressed by the given cumulants as

$$\begin{aligned} q_0 &= 1, q_1 = q_2 = 0, q_3 = \frac{c_3}{3!c_2^{3/2}}, q_4 = \frac{c_4}{4!c_2^2} \\ q_5 &= \frac{c_5}{5!c_2^{5/2}}, q_6 = \frac{c_6 + 10c_3^2}{6!c_2^3}, q_7 = \frac{c_7 + 35c_3c_4}{7!c_2^{7/2}} \end{aligned} \tag{Equation A -55}$$

After expansion $f(x)$ can be expressed by

$$f(x) = \phi\left(\frac{x-c_1}{\sqrt{c_2}}\right) \left(1 + \frac{q_3}{\sqrt{c_2}}(x^3 - 3x) + \frac{q_4}{\sqrt{c_2}}(x^4 - 6x^2 + 3) + \frac{q_5}{\sqrt{c_2}}(x^5 - 10x^3 + 15x) + \dots\right)$$

Equation A -56

Back to the beginning simple case of one DG and one load working in island, to calculate the variable $P_{net} = P_L - P_G$, it can be done by the following step.

- Compute the moment of P_L and P_G according to Equation A -48
- Compute the cumulants of P_L and P_G according to Equation A -49
- Compute the cumulants of net power P_{net} (Equation A -52)
- Compute the coefficient (Equation A -55)
- The probability density function can be calculated by Equation A -56

Especially when only the 1st order is considered, that means both of load and DG are regarded normal distribution, the net power of load and DG is still the normal distribution:

$$P_{net} = P_L - P_G = Normal(\mu_{L_i} - \mu_G, \sigma_L^2 + \sigma_G^2) \tag{Equation A -57}$$

A.8 Load settings for European network simulation

A8.1 Load setting of German urban LV network

Busbar Name	Total Load Num	Load Name	Load Type	Load Priority	Rated Power /kW
N194	1	L194	House	Normal	26,44014
N215	1	L215	House	normal	29,05251
N232	1	L232	House	normal	23,83789
N256	1	L256	House	normal	8,431158
N174	1	L174	House	normal	6,928421
N196	1	L196	House	normal	3,442021
N216	1	L216	House	normal	1,390316
N233	1	L233	House	normal	15,53684
N257	1	L257	House	normal	15,43242
N175	1	L175	House	normal	16,03536
N197	1	L197	House	normal	11,41642
N217	1	L217	House	normal	17,50189
N234	1	L234	House	normal	32,7992
N259	1	L259	House	normal	28,42695
N176	1	L176	House	normal	22,10526
N198	1	L198	House	normal	18,29305
N218	1	L218	House	normal	33,76242
N235	1	L235	House	normal	39,39727
N260	1	L260	House	normal	93,35368
N177	1	L177	House	normal	21,97558
N200	1	L200	House	normal	7,45789
N219	1	L219	House	normal	12,27663
N237	1	L237	House	normal	23,15789
N261	1	L261	House	normal	7,614737
N178	1	L178	House	normal	9,139
N201	1	L201	House	normal	9,744
N221	1	L221	House	normal	6,598
N238	1	L238	House	normal	4,918
N295	1	L295	House	normal	8,80298
N179	1	L179	House	normal	11,93853
N202	1	L202	House	normal	49,61432
N222	1	L222	House	normal	14,35158
N241	1	L241	House	normal	17,3795
N301	1	L301	House	normal	9,13305
N180	1	L180	House	normal	8,413
N203	1	L303	House	normal	6,552
N223	1	L223	House	normal	3,947
N242	1	L242	House	normal	6,116
N182	1	L182	House	normal	28,495
N204	1	L204	House	normal	22,105
N224	1	L224	House	normal	17,379
N243	1	L243	House	normal	13,025
N183	1	L183	House	normal	18,8129
N205	1	L205	House	normal	19,499221
N225	1	L225	House	normal	6,008842
N246	1	L246	House	normal	23,15789

N184	1	L184	House	normal	11,5785
N206	1	L206	House	normal	7,615579
N226	1	L226	House	normal	4,552105
N247	1	L247	House	normal	8,355769
N185	1	L185	House	normal	2,301
N208	1	L208	House	normal	22,38
N227	1	L227	House	normal	140
N248	1	L248	House	normal	9,2539
N188	1	L188	House	normal	5,1053
N210	1	L210	House	normal	12,19342
N228	1	L228	House	normal	11,31598
N249	1	L249	House	normal	9,473684
N189	1	L189	House	normal	15,26316
N211	1	L211	House	normal	30,52632
N229	1	L229	House	normal	18,8905
N253	1	L253	House	normal	19,39747
N190	1	L190	House	normal	20,75453
N212	1	L212	House	normal	50
N230	1	L230	House	normal	10
N254	1	L254	House	normal	21,95179
N193	1	L193	House	normal	16,88295
N214	1	L214	House	normal	6,316789
N231	1	L231	House	normal	11,39832
N255	1	L255	House	normal	6,008842

A8.2 Load setting of Italian urban LV network

Busbar Name	Load Type	Load Priority	Rated Power /kW	Total DG Num	DG Type	Rated Power/kW	Unavailability
A4	House	normal	30	0			
B3	House	normal	15	1	CHP	32	3%
C9	House	normal	30	1	CHP	75	3%
A6	House	normal	15	0			
B5	House	normal	30	0			
D2	House	normal	30	1	CHP	22	3%
A7	House	normal	15	1	CHP	42	3%
B6	House	normal	30	1	CHP	75	3%
D4	House	normal	30	0			
D5	House	normal	30	1	CHP	32	3%
D6	House	normal	15	0			
C10	House	normal	30	0			
C2	House	normal	15	0			
C3	House	normal	15	1	CHP	12	3%
A1	House	normal	15	0			
C6	House	normal	15	0			
A2	House	normal	15	1	CHP	12	3%
C7	House	normal	45	1	CHP	32	3%
B2	House	normal	30	0			
C8	House	normal	45	0			

A8.3 Settings of Italian rural network

Busbar Name	Load Type	Load Priority	Rated Power kW	Total DG Num	DG Type and Capacity	Unavailability
Bus13	House	normal	15	1	CHP, 32 kW	3%
Bus3	House	normal	15	0		
Bus6	House	normal	15	0		
Bus12	House	Normal	15	1	CHP, 32 kW	3%
Bus11	House	Normal	15	1	CHP, 32 kW	3%
Bus9	House	Normal	15	0		
Bus8	House	Normal	15	1	CHP, 32 kW	3%

A8.4 Setting of Portuguese rural network

Busbar Name	Load Type	Load Priority	Load rated power	DG Type	Rated Power/kW
N18	House	normal	15	0	
N60	House	normal	15	0	
N19	House	normal	15	1 CHP	96
N61	House	normal	15	1 CHP	64
N20	House	normal	15	0	
N21	House	normal	15	0	
N22	House	normal	15	1 CHP	96
N23	House	normal	15	0	
N24	House	normal	15	0	
N25	House	normal	15	0	
N26	House	normal	15	1 CHP	128
N27	House	normal	15	0	
N45	House	normal	15	0	
N13	House	normal	15	1 CHP	64
N46	House	normal	15	1 CHP	64
N14	House	normal	15	0	
N15	House	normal	15	0	
N54	House	normal	15	0	
N16	House	normal	15	1 CHP	64
N55	House	normal	15	0	64

A8.4 Settings of the Netherlands rural network

Busbar Name	Load Type	Load Priority	Rated Power /kW	DG Type	Rated Power/kW	Unavailability
N8	House	normal	15	CHP	128	3%
N1	House	normal	15			
N2	House	normal	30	CHP	96	3%
N3	House	normal	15			
N4	House	normal	30			
N5	House	normal	15	CHP	128	3%
N6	House	normal	30			
N7	House	normal	15			

A8.4 Settings of German MV network

Busbar Name	Load Type	Load Priority	Rated Power /kW	Total DG Num	DG Type	Rated Power/kW	Unavailability
N1	House	normal	214				
N2	House	normal	6				
N3	House	normal	33	1	PV	465	0%
N4	House	normal	24				
N5	House	normal	35				
N6	House	normal	6				
N7	House	normal	36				
N8	House	normal	17	1	PV	203	0%
N9	House	normal	21				
N10	House	normal	35	1	PV	150	
N11	House	normal	10	1	CHP	347	0%
N12	House	normal	68	1	Mix	209	0%
N13	House	normal	6				
N14	House	normal	6				
N15	House	normal	4				
N16	House	normal	13				
N17	House	normal	6				
N18	House	normal	47	1	CHP	15	0%
N19	House	normal	46				
N20	House	normal	19				
N21	House	normal	24				
N22	House	normal	40				
N23	House	normal	14	1	PV	44	0%
N24	House	normal	6				
N25	House	normal	15				
N26	House	normal	24				
N27	House	normal	8	1	WT	23	0%
N28	House	normal	13				
N29	House	normal	3				
N30	House	normal	7				
N31	House	normal	8				
N32	House	normal	21	1	Mix	454	0%
N33	House	normal	7				
N34	House	normal	7				
N35	House	normal	67				
N36	House	normal	10				
N37	House	normal	6	1	WT	150	0%
N38	House	normal	32				
N39	House	normal	33	1	PV	158	0%
N40	House	normal	54				
N41	House	normal	14	1	CHP	300	0%
N42	House	normal	14	1	CHP	500	0%
N43	House	normal	48				
N44	House	normal	63	1	PV	84	0%
N45	House	normal	85				
N46	House	normal	26	1	PV	234	0%
N47	House	normal	6	1	WT	600	0%
N48	House	normal	24				

More Microgrids

TG2

N49	House	normal	46				
N50	House	normal	82				
N51	House	normal	35	1	PV	69	0%
N52	House	normal	46	1	PV	124	0%
N53	House	normal	4				
N54	House	normal	33				
N55	House	normal	3				
N56	House	normal	24	1	PV	24	0%
N57	House	normal	10				
N58	House	normal	6				
N59	House	normal	17				
N60	House	normal	24				
N61	House	normal	33	1	CHP	250	0%
N62	House	normal	4				
N63	House	normal	14				
N64	House	normal	31	1	PV	131	0%
N65	House	normal	7	1	Mix	826	0%
N66	House	normal	26	1	Mix	76	0%
N67	House	normal	4				
N68	House	normal	24				
N69	House	normal	7	1	CHP	200	0%
N70	House	normal	1	1	CHP	526	0%
N71	House	normal	8				
N72	House	normal	21				
N73	House	normal	46				
N74	House	normal	26	1	Mix	166	0%
N75	House	normal	7	1	WT	2250	0%
N76	House	normal	0,001				
N77	House	normal	26				
N78	House	normal	8				
N79	House	normal	24	1	CHP	24	0%
N80	House	normal	29				
N81	House	normal	4				
N82	House	normal	4				
N83	House	normal	1				
N84	House	normal	7	1	WT	4080	0%
N85	House	normal	28				
N86	House	normal	6				
N87	House	normal	3				
N88	House	normal	17	1	PV	16	0%
N89	House	normal	7	1	WT	225	0%
N90	House	normal	7	1	WT	4080	0%
N91	House	normal	17				
N92	House	normal	15				
N93	House	normal	28	1	PV	75	0%
N94	House	normal	21				